Optimal Design of Advanced Engineering Modular Systems through a New Genetic Approach

Marco Montemurro

THÈSE DE DOCTORAT DE L'UNIVERSITÉ PIERRE ET MARIE CURIE

Spécialité: MÉCANIQUE

présentée par :
Marco MONTEMURRO

pour obtenir le titre de
DOCTEUR DE L'UNIVERSITÉ PIERRE ET MARIE CURIE

Optimal Design of Advanced Engineering Modular Systems through a New Genetic Approach

28 Novembre 2012
Composition du jury :

Rapporteur	Pr.	L. Gallimard	Université Paris X
Rapporteur	Pr.	L. Dumas	Université de Versailles-St-Quentin
	Pr.	E. M. Daya	Université de Lorraine
	DR INRIA	M. Schoenauer	INRIA Saclay-Ile-de-France
	DR CNRS	J. Pouget	Université UPMC Paris VI
	MdC HDR	M. Gigliotti	IUT et ENSMA de Poitiers
Directeur de Thèse	Pr.	P. Vannucci	Université de Versailles-St-Quentin
Co-directrice de Thèse	MdC	A. Vincenti	Université UPMC Paris VI

Institut Jean Le Rond d'Alembert
Université U.P.M.C. Paris VI / C.N.R.S. – UMR 7190

To my wife for all of her love and
to my parents, as an example of determination and constancy.

A mia moglie per tutto il suo amore e
ai miei genitori, quale esempio di determinazione e costanza.

Acknowledgements

I would like to thank Paolo Vannucci and Angela Vincenti for their valuable advices and for their time: only under their direction it was possible to realise all the works presented in this thesis.

A sincere thanks goes also to my scientific supervisors at the Centre de Recherche Public Henri Tudor, Ahmed Makradi and Yao Koutsawa, for helping me with their support.

I am grateful to the National Research Fund (FNR) in Luxembourg, for supporting this work through Aides à la Formation Recherche Grant (PHD-09-139).

A very special thanks goes to all my friends, the old and the new ones, for all the support that they gave me during these last three years: Francesca, Antonella, Vita, Vanessa, Marco, Marco, Luca, Paolo, Daniele and Marco. They are not only simple friends, they are really true friends. I wish to thank all my friends for their love. They make me feel a rich person.

Last but not least, I wish to thank my family: my wife Anita, my parents, my two sisters, my brother in law Angelo, my nephews Margherita, Michele and Luigi, my mother in law and my father in law, Bruna and Mario, and finally my sister in law Mariantonietta. They have always believed in me, encouraged me and given me a helping hand in difficult moments, and they shared with me the successes as well as the delusions, making me feel the love and esteem that they have for me.

Contents

Introduction

This thesis mainly deals with the development of a strategy for the optimal design of advanced engineering structures and, more precisely, the optimal design of *modular systems*.

Two questions immediately arise: what is a modular system? And why do we focus on the design of modular systems? Let us start by trying to give an answer to the first question: a modular system is a system composed by "elementary units" (the *modules*) where each module is characterised by the same vector of unknowns (the constitutive parameters or design variables of the module) that can get different values for each module. Hence, the modules composing the system share the same general vector of unknowns, but they can be defined by different values of these unknowns.

The researches made within this thesis essentially concern a special class of engineering modular systems: structures. Modular structures are widely used in engineering, especially in aeronautics, helicopter and automotive fields. Classical examples of modular systems are:

- laminates made of n elementary plies, where each ply represents the module characterised by different constitutive parameters like, for instance, the material of the layer, its thickness and the fibre orientation angle;
- the structural parts of an aircraft, namely the stiffened panels composing the fuselage or the wings, where each panel can be seen as a modular system where the elementary unit is the stiffener;
- the hybrid active/passive systems, generally composed of a plate whose vibrations are damped by bonding in some well-chosen regions some viscoelastic (passive damping) or piezoelectric (active/passive damping) patches where each patch represents the module;
- etc.

The optimisation of a modular system is, often, an hard task which can be mathematically formalised as a non-classical optimisation problem. When dealing with this kind of problems the goal is to optimise the system, on one hand in terms of the number of modules N and on the other hand in terms of the constitutive parameters of each

module. From a mathematical point of view, this means to look for a global optimum configuration of the system over a search space having a variable dimension N_{var}, where the total number of design variables N_{var} strictly depends on the number of modules N composing the system. In addition, the unknowns can be of different nature: continuous, discrete and so on.

Therefore, in order to deal with the optimal design of modular systems, we need to conceive a procedure that includes on one side the number of modules N among the design variables of the problem (this implicitly corresponds to solve an optimisation problem defined over a domain of variable dimension N_{var}, i.e. a variable number of unknowns have to be determined), while on the other side it has to be able to deal with design variables of different nature.

Considering all the previous aspects and taking into account the fact that, often, the optimisation problems of modular systems are highly non-linear and non-convex, we decided to develop a numerical strategy in the framework of metaheuristics, and more precisely, in the context of genetic algorithms (GAs).

Nevertheless, standard GAs are not able to deal with optimisation problems of modular structures when they are stated in the most general way, i.e. they are not able to face optimisation problems defined over a search space having a variable dimension. In order to overcome such an issue, in this thesis we try to go beyond the classical structure of the standard GA, by introducing the concept of *species* and also by developing new genetic operators allowing the reproduction among individuals of different species: such operators will allow the parallel evolution of species and individuals. Our choice was inspired by an extended interpretation of the Darwinian concept of the *evolution of the species*. These particular operators have been developed in the framework of the genetic code BIANCA (*Biologically Inspired ANalysis of Composite Assemblages*), originally developed by Vincenti *et al.* to solve design problems of composite laminated structures [1, 2].

As we will discuss in Chapter 1, in BIANCA, the concept of species is linked to the number of individual's chromosomes which is, on its turn, linked to the number of modules composing the system and, hence, to the overall number of design variables which uniquely defines the behaviour of the system.

In some sense, we have been guided in this choice by a double natural paradigm: the evolution of individuals *and* of species. This consideration has conducted us to a simultaneous two-level Darwinian strategy. For this reason, the first part of this thesis concerns the development of new genetic operators able to deal with optimisation problems of modular systems and to include the number of modules among the design variables of the problem. These operators introduce substantial changes into the reproduction phase which represents the heart of the numerical procedure of a GA. In other words, they modify the phases of crossover and mutation by extending them and, thus, allowing the reproduction between individuals belonging to different species.

In this way, the new genetic operators are actually problem-independent since they

are strictly related to the concept of species that transcends the physical nature of the problem at hand. Therefore, BIANCA becomes a GA that allows the *parallel evolution* of species and individuals.

The points of originality and innovation of this first part of the thesis are several and articulated at different levels. The first one is the proposed numerical strategy, which is fully "genetic" and completely problem-independent. Another new feature introduced in the code BIANCA is the generalisation to the multi-constraint case of a new constraint-handling technique called Automatic Dynamic Penalisation (ADP) strategy, firstly presented in [1], which belongs to the class of penalty-based strategies. The key-point of the ADP method is that it is a very general technique that automatically chooses and updates the penalty coefficients, without the intervention of the user.

In the second part of the thesis, the algorithm has been applied to the solution of some problems. The main topic of the thesis being the design of modular structures, we have considered the following problems: the design of laminates with the least number of layers satisfying some given requirements, the design of stiffened composite structures having the least weight, the design of hybrid elastomer/composite laminates for maximising damping and, finally, the design of composite plates with bonded elastomer patches, also in this case for the optimisation of damping. We have also applied our strategy to a different kind of problem which does not concern the design of modular systems, i.e. the problem of identifying the constitutive properties of piezoelectric devices.
The previous problems share a common point of innovation: in all the considered cases the problem is formulated in the most general way without any simplifying hypotheses, unlike what is normally done, especially for the design of composite structures.

Therefore, the present thesis is organised as follows:

- in Chapter 1, after a literature overview on the different types of metaheuristic (and in particular on the evolutionary strategies), and a recall of the mathematical foundations of GAs, we introduce the GA BIANCA, describing its classical features and the new ones that we have developed in the framework of the present thesis. In particular, we detail the new genetic operators that perform the crossover and mutation among individuals belonging to different species and we also describe the very general ADP constraint-handling technique implemented within BIANCA. We test the ADP strategy with some well-known benchmark problems taken from the literature. Then, we briefly describe the structure of the interface between BIANCA and external software which can be used when the value of the objective function and/or constraints cannot be computed analytically, but it has to be evaluated using numerical codes (for example finite element codes). Finally, we briefly discuss the architecture and the main features of the BIANCA Graphical User Interface (GUI) that has been created in order to develop a tool that can be easily handled and employed by the user which wants to use the code BIANCA;

- in Chapter 2 the problem of identifying the electromechanical properties of piezoelec-

tric devices is studied. We propose a method to predict the whole three-dimensional set of electromechanical properties of active plate structures. The elastic properties of the patches, along with their piezoelectric properties, have significant effect on the dynamic response of the global structure; the inverse problem of the identification of those properties is stated as a constrained minimisation problem of an error function expressing the difference between the measured eigenfrequencies and the corresponding numerical values. Hence, this strategy relies on the dynamic response of the structure in terms of undamped natural frequencies and makes use of BIANCA. The numerical simulation is carried on for a laminated plate with surface mounted piezoelectric patches, in order to validate the accuracy and the reliability of the proposed numerical tool. This problem does not belong to the class of optimisation problems of modular systems, thus the new genetic operators that perform the crossover and mutation between different species are no longer required since the overall number of design variables (i.e. the electromechanical properties of the piezoelectric material) is fixed *a priori*;

- in Chapter 3 the problem of designing laminates having the minimum number of layers for obtaining given elastic properties is addressed. In this study, the problem is treated and solved in a general case, since no simplifying hypotheses are made on the type of the stacking sequence. This is a non-linear programming problem, where a unique objective function includes all the requirements to be satisfied by the solutions. The optimal solutions are found in the framework of the polar-genetic approach, since the objective function is written in terms of the laminate polar parameters, while BIANCA is used as numerical tool. The design variables include the number of layers, the layers orientations and the layers thickness. Some examples concerning some prescribed elastic symmetries, like orthotropy, bending-extension uncoupling, quasi-homogeneity and so on, are carried out in order to show the effectiveness of the proposed approach;

- in Chapter 4 a problem concerning a least-weight wing-box section is studied. The case-study considered is the least weight design of a stiffened wing-box section for an aircraft structure. The method is based on the use of the polar formalism and on the GA BIANCA and it is organised as a two-level approach. At the first level of the procedure, the optimal structure is designed as it was composed by a single equivalent layer, while a laminate realising the optimal structure is found at the second level. The method is able to automatically find the optimal number of modules, no simplifying assumptions are used and it can be easily generalised to other problems;

- in Chapter 5 the problem of designing the damping capabilities of hybrid elastomer/composite laminates is studied. The goal of the procedure is to maximise the first N modal loss factors of the laminate subject to constraints on the stiffness

and on the weight of the plate. The problem is considered in the most general case: no simplifying hypotheses are made on the behaviour of the hybrid laminate, thus allowing us to consider as design variables the number of layers (both of the elastic and viscoelastic layers), their thickness and orientations as well as the position of the viscoelastic plies within the stacking sequence. The proposed approach relies on one hand, upon the dynamic response of the structure in terms of natural undamped frequencies and modal loss factors, and on the other hand on the use of BIANCA as optimisation tool. The method is applied to the design of a rectangular plate;

- in Chapter 6 the problem of designing the damping capabilities of laminated plates with bonded viscoelastic patches is studied. As in Chapter 4, also in this case we adopt a two-level procedure for the design of hybrid elastomer/composite modular structures. The goal of the procedure consists again in maximising the first N modal loss factors of the plate subject to constraints on its bending stiffness, on its weight along with geometric constraints on the position of the rubber patches bonded over the plate. The problem is considered in the most general case: no simplifying hypotheses are made on the behaviour of the structure, thus allowing us to consider as design variables the number of viscoelastic patches, their sizes, their positions over the plate, besides the laminate thickness and polar parameters. Once again the second-level phase concerns the design of the laminated plate that has to be designed in order to have the optimal elastic properties and thickness issued from the first-level design problem.

Each Chapter composing this document corresponds to a scientific paper published and/or submitted to an International Journal. The only exception is Chapter 4 that corresponds to two scientific publications. A complete list of these publications is provided at the end of the manuscript.

A last remark about the structure of each Chapter. The Chapters concerning the engineering applications, namely Chapters from 2 to 6, are characterised by a complete, but not exhaustive, literature overview on the problem at hand and all of them are ended with some conclusive remarks.
The general conclusions and some future perspectives concerning the numerical genetic strategy used in this thesis are provided at the end of this manuscript.

Funding

This thesis is funded by the Fonds National de la Recherche (FNR) du Luxembourg through Aides à la Formation Recherche Grant (PHD-09-139). The works have been developed at the Institut Jean Le Rond d'Alembert (team MISES) of the Université Paris VI, at the Centre de Recherche Public Henri Tudor (team AMS-MODSI) in Luxembourg and at Université de Versailles St. Quentin-en-Yvelines.

Chapter 1

On the use of genetic algorithms in engineering applications

1.1 Introduction

1.1.1 Literature overview

Many researchers and scientists in the field of mechanics and mathematics are used to live into a "mathematical" world governed by precise laws based on cause-effect relationships. For this reason, they are, very often, unable to adapt their vision and their way of conceiving the world to the one proposed by biologists wherein the "hazard" plays a crucial role and imposes itself as a "master" of the *natural evolution*.

The encounter between mechanics and biology is not a present fact, but goes back to some great scientists of the past, founders of the modern sciences, namely Galilei, Hooke and Maupertuis, see [3].

Among the wide class of studies that Galilei conducted in the fields of mechanics and mathematics, he was the first which tried to apply its results on the problem of maximal dimensions not only to the structures, but also to the trees and animals dimensions [4].

For its part, Hooke can be viewed as one of the founders of the modern biology [5], because he introduced in 1665, for the first time, the term "cell" to describe the repetitive texture of the cork, observed with a microscope built by himself.

Maupertuis [6] was the first that formulated and demonstrated the transmission of genetic traits by the father and mother together, and he was also the first that formulated exact predictions about the transmission of a peculiar trait, namely the polydactyly in a Berlin family, and the albinism observed in black populations in Senegal, see [7]. Moreover, he was the first that had the intuition about the mutation as the main cause of the species diversity.

Nevertheless, these three great scientists can be counted among the early initiators of mechanics (and generally they are known for this) and it is anecdotal and, in a certain sense,

emblematic to look at what they did in biology, showing themselves that the distance between the two sciences is very small.

The concept of *Natural Selection* was developed and introduced, independently, in the second half of the 19^{th} century by Darwin [8] and Wallace [9]. The famous naturalist Charles Darwin [8] defined Natural Selection or *Survival of the Fittest* as the

> "... preservation of favorable individual differences and variations, and the destruction of those that are injurious."

In nature, individuals have to adapt to their environment in order to survive within a process known as *natural evolution*, wherein those features that make an individual more suited to compete and survive are preserved when it reproduces, and those ones which make it weaker are removed. Such features are controlled, at the genotype level, by units called *genes* which form, on their turn, structures called *chromosomes*. Through subsequent generations not only the fittest individuals survive, but also their fittest genes which are passed to their descendants during the sexual recombination process. This is a very complex and articulated but effective process which includes the meiotic cell divisions, the *crossover* phase, the *mutation* phase and the *dominance* mechanism. However, it is worth noting that in nature the mutation mechanism is almost always a deadly event and, in any case, it happens "accidentally".

During the last forty years, an increasing interest in problem solving systems based on the principles of evolution and hereditary has been emerged. Such systems are characterised by a population of potential solutions, they use some selection processes based on the fitness of individuals and some particular *genetic* operators. Among these systems we can include Evolution Algorithms (EAs) [10, 11, 12], i.e. algorithms that imitate the principles of natural evolution for parameter optimisation problems, Fogel's Evolutionary Programming [13] which is an exploring search technique within a space of finite-state machines, Glover's Scatter Search techniques [14] that, starting from an initial population of reference points, create a new generation of offspring through weighted linear combinations. Besides these techniques, one of the most popular and well-known evolution-based strategies is the Holland's Genetic Algorithm (GA) [15, 16].

More recently, other types of evolution-based search techniques have been developed. In literature we can find, for example, Bacteriologic algorithms (BAs) [17] inspired by evolutionary ecology and, more particularly, bacteriologic adaptation; Gaussian adaptation [18] (normal or natural adaptation, abbreviated NA to avoid confusion with GA) algorithms which rely on a certain theorem valid for all regions of acceptability and all Gaussian distributions: the NAs efficiency is defined as information divided by the work needed to get the information [18]. Because the NA maximises the average fitness rather than the fitness of the individual, the landscape is smoothed such that valleys between peaks may disappear, therefore it has a certain "ambition" to avoid local peaks in the fitness landscape.

An useful and common term often used for all the evolution-based systems cited beforehand is *Evolution Programs* (EPs).

The idea of evolution programming is not new and many researchers have studied and dealt with this subject in the last forty years. Several EPs have been conceived and developed for many different problems. However, despite many different EPs can be formulated to deal with a given problem, and even though these EPs can differ for several features (e.g. representation of the single individual, operators for transforming the individuals, methods for creating the initial populations and so on), all EPs share a common principle: a population of individuals undergoes a certain number of transformations and, during this evolution, each individual "fights" to survive.

Besides EPs, several kinds of metaheuristics can be found in literature. For example, among the so-called *swarm intelligence* we have: the Ant Colony Optimisation (ACO) method [19] which uses many ants (or agents) to pass through the solution space and find locally productive areas; the Particle Swarm Optimisation (PSO) strategy [20] which employs a population (swarm) of candidate solutions (particles) moving in the search space, and the movement of the particles is influenced both by their own best-known position and swarm's global best-known position; the Intelligent Water Drops (IWD) algorithm [21] which is an optimisation algorithm inspired from natural water drops which change their environment to find the near optimal or optimal path to their destination (in this method the memory is the river's bed and what is modified by the water drops is the amount of soil on the river's bed).
Other Metaheuristic methods, falling within the class of stochastic optimisation methods, are Simulated Annealing (SA) [22] and Tabu Search (TS) [23] algorithms. The SA method is a global optimisation technique that goes through the search space by testing random mutations on an individual solution. A mutation that increases fitness is always accepted. A mutation that lowers fitness is accepted probabilistically based on the difference in fitness and a decreasing temperature parameter. The TS strategy is similar to the simulated annealing method. While simulated annealing generates only one mutated solution, tabu search generates many mutated solutions and moves to the solution with the lowest energy of those generated. In order to prevent cycling and encourage greater movement through the solution space, a tabu list is maintained of partial or complete solutions.

In this Chapter, we do not discuss the different features characterising each Metaheuristic, neither we do not talk about any philosophical and/or conceptual differences between the various Metaheuristics. Rather we will focus our attention on EPs and, particularly, on a special class of EPs: the Genetic Algorithms. There is a huge literature on GAs, we cite only the fundamental texts of Holland [15], Goldberg [16], Michalewicz [12], Renders [24] and the independent contribution of Rechenberg [25].
GAs are search techniques, based on a simulation of the Darwinian concept of survival of the fittest and upon genetics, which operate on a population of points defined within

the definition domain of the considered problem [16, 15]. The GAs belong to the class of Artificial Intelligences (AI).

In these last thirty years, GAs have gained increasing popularity and have been extensively applied in the field of structural optimisation.
As an example, concerning the topology optimisation of structures, we can find, amongst others, the works of Chapman *et al.* [26] which use a GA for continuum topology optimisation with domain refinement, Lin and Hajela [27, 28] and Ryoo and Hajela [29] that use a GA for large scale problems and truss topology optimisation problems, Kim and Weck [30] which developed a Variable Chromosome Length GA (VCL-GA) and applied this technique to structural topology optimisation problems, i.e. a short cantilever problem and a bridge problem.
In the field of composite materials, GAs have been successfully applied to a wide class of problems. Several authors have considered different laminate design problems (rather complete but not exhaustive reviews on the state of the art can be found in [31, 32, 33]). Here we cite only the works of Le Riche and Hatfka [34], Todoroki and Hatfka [35] and Liu *et al.* [36] on the design of composite plates in order to maximise the first buckling load using the lamination parameters, and also the works of Muc [37], Tabakov [38], Nagendra *et al* [39], Kaletta and Wolf [40], Lillico *et al* [41] and Bisagni and Lanzi [42] which have employed GAs to study the problem of designing the least-weight composite stiffened panels. Still in the field of the optimal design of composite structures, we note the work of Vannucci [43] who has considered the problem of designing the general elastic properties of a laminate. In that work, a general approach based on polar tensor invariants was proposed: no simplifying hypotheses nor special stacks or orientations were used, hence the method allows to find a general solution to a given problem. This approach was applied in other works and extended in [1] to the constrained optimisation of laminated plates and in [44] to the optimal design of laminates with given elastic moduli.
In addition, GAs have been quite successfully applied to a wide class of optimisation problems that do not belong to the field of mechanics, for instance wire routing, scheduling, adaptive control, game playing, cognitive modeling, traveling salesman problems, database query optimisation, optimal control problem and so on (see [45, 46, 47, 48, 49, 50]).
Nevertheless, in this section we do not claim to provide a complete and exhaustive state of the art about all possible engineering applications wherein GAs have been successfully applied. An adequate literature overview concerning some peculiar real-world engineering applications will be given at the beginning of the next Chapters of the present thesis, depending on the considered application.

In this Chapter we want to provide, on one side a brief overview on GAs, their fundamental operators and the mathematical foundations which underlie the formulation of the standard GA. On the other side, we describe the main features of the GA BIANCA (*BIological ANalysis of Composite Assemblages*), originally developed by Vincenti *et al.* [1, 2],

and particularly we detail the new features and the new genetic operators conceived and developed in the framework of this thesis in order to deal with a special class of optimisation problems: the design problems of engineering modular structures. When dealing with this kind of problems two main difficulties arise: one one side we have to determine the *optimal number* of modules composing the modular system, and on the other side, each module has to be optimised with respect to its *constitutive parameters*, namely any geometrical, material and other physical variables characterising the module.

To deal with this class of problems the standard GA needs of some modifications in terms of representation of informations restrained in the single individual, i.e. the structure of the genotype, along with the creation of some peculiar genetic operators able to optimise, simultaneously, the number and the characteristics of each module. The problem of modular structures will be described in details in Chapters 3, 4, 5 and 6. We remark that, in this Chapter we focus our attention on the presentation and description of the new genetic operators by analysing the effect that they have on the individuals restrained in the populations during their evolution along the generations.

Along with the previous aspects we introduce, in the second part of the Chapter, a brief overview on the handling constraints techniques, usually adopted in the framework of genetic-based optimisation strategies, that can be found in the literature. After introducing the most common methods, we explain in detail an original technique for handling constraints implemented within BIANCA, i.e. the *Automatic Dynamic Penalisation* (ADP) method, originally presented in [1] and extended and generalised in the present work. Some benchmark problems, taken from the literature, are considered to show the effectiveness of the proposed technique.

Moreover, since in the most part of the real-world engineering optimisation problems the objective and constraint functions cannot be evaluated in a closed analytical form, while it is often possible to have an estimation of such functions via a numerical process, e.g. via a Finite Element (FE) calculation, we decided to develop an interface between BIANCA and some well-known FE commercial codes. Finally, a detailed description of this interface along with a short presentation of the Graphical User Interface (GUI), that we have developed in order to use the code BIANCA more easily, end the Chapter.

1.1.2 Genetic Algorithms (GAs): a brief description

Genetic Algorithms were introduced and studied first by Holland and his co-workers and students, see [15, 16].

As said beforehand, GAs are search algorithms based on one side on the Darwinian concept of the Natural Selection and on the other side upon the mechanisms of genetics. In a certain sense, GAs make their own the concept of the Survival of the most adapted structures (Survival of the Fittest) to a given environment and they employ a pseudo-random exchange of informations in order to create an exploration algorithm that shows some characteristics of the Natural Selection.

Even though they start from a pseudo-random exchange of informations and, consequently, from a pseudo-random exploration, GAs are not purely random algorithms: they effectively and smartly handle the information obtained through the exploration in order to investigate upon the possible presence and position of new and more performing individuals towards which the evolution is naturally oriented.

As previously said, the GA is based on a pseudo-random exploration of the domain of the problem at hand, and starting from this kind of search it handles in an effective way the information in order to find the desired solution. Nevertheless, it can be noticed that a pseudo-random search does not implies a blind exploration or, in other words, an exploration without directions.

In his book, Michalewicz [12] describes in a concise and ironic way the idea that underlies the GAs:

> "The idea behind the genetic algorithms is to do what nature does. Let us take rabbits as an example: at any given time there is a population of rabbits. Some of them are faster and smarter than other rabbits. These faster, smarter rabbits are less likely to be eaten by foxes, and therefore more of them survive to do what rabbits do best: make more rabbits. Of course, some of the slower, dumber rabbits will survive just because they are lucky. This surviving populations of rabbits starts breeding. The breeding results in a good mixture of rabbit genetic material: some slow rabbits breed with fast rabbits, some fast with fast, some smart rabbit with dumb rabbits, and so on. And of the top of that, nature throws in a ' wild hare ' every once in a while by mutating some of the rabbit genetic material. The resulting baby rabbits will (on average) be faster and smarter than these in the original population because more faster, smarter parents survived the foxes. (It is a good thing that the foxes are undergoing similar process - otherwise the rabbits might become too fast and smart for the foxes to catch any of them)."

GAs employ a vocabulary taken from genetics. The *population* evolving along the generations is composed of *individuals* and each individual, on its turn, is composed of *chromosomes* which constitute the individual's *genotype*. Very often, in standard GAs, the individual shows a genotype made of a single-chromosome, i.e. a *haploid* individual. This fact might be a little misleading: in nature, each cell of a given organism, belonging to a particular species, presents a certain number of chromosomes (e.g., man has 46 chromosomes). Such chromosomes are organised according to *diploidy*: each chromosome has a double, but only the genetic information restrained in one of the two is used, according to the biological mechanism of *dominance*. For more details and information on *haploidy*, *diploidy*, *dominance* and other related issues, in connection with GAs, the reader is referred to [16, 51]. Every chromosome is made of *genes* arranged in linear succession: each gene controls the inheritance of a particular character and it is located in a precise position within the chromosome (such positions are called *loci*).

GAs employ an alphabet of cardinality k (usually, in standard GAs $k = 2$, i.e. they employ a *binary* alphabet) to code the information restrained in the individuals' genotype. Each genotype codes a particular *phenotype* (i.e. the physical expression of the individual's genotype whose meaning is defined externally by the user) and represents a potential solution to the considered optimisation problem. In organisms, the phenotype includes physical characteristics, such as eyes color, hair color and so on, whilst in the framework of GAs the phenotype represents the set of all possible values (real, discrete and so on) that the variables of the considered problem can assume.

The evolution of a population of individuals along the generations corresponds to a search through a space of potential solutions. Such a search requires a balance among two objectives: exploring the whole domain and exploiting the best solutions within this space [16]. It can be noticed that GAs belong to a class of *domain independent* search strategies which realise an effective balance between exploration and exploitation of the search space.
In the next subsection we will explain the behaviour of the standard GA as well as its main genetic operators.

1.1.3 The standard GA

The standard GA is composed by the union of 3 fundamental operators:

1. the *selection* operator;
2. the *crossover* operator;
3. the *mutation* operator.

Let us introduce, firstly, the selection operator. Such an operator acts according to a precise rule: if we consider a population of size N_{ind} (i.e. composed of N_{ind} individuals), using the value of the *fitness function* of each individual, the selection operator selects, with a higher probability, the individuals having a high value of the fitness function. It can be noticed that the N_{ind} individuals composing the population are randomly created in the initial generation (this is just one choice among the different methods of creating the initial population that can be found in the literature, see for example [12]).
The fitness function is a particular function which can be defined in different ways depending on the considered optimisation problem, being the fitness closely related to the objective function. The fitness plays the same role that the environment plays within the framework of the Natural Selection: the fitness function gives a numerical value at each individual-point of the design space, and consequently the most adapted individuals (i.e. points which are candidates to be potential optimal solutions) will be the points having higher values of the fitness function. After assigning a fitness value to each individual of the population, the selection operator determines which individuals will take part into

the real reproduction process, which will have, as a final result, the creation of the new generation of individuals. Even though the fitness function can be defined in different ways, generally such a function represents a "filter" which on one side can influence the GA convergence process and on the other side (depending on the definition employed for its expression) can "normalise" the optimisation process (for example the fitness can be defined in such a way that the worst individual has a fitness equal to 0 while the best one has a fitness equal to 1).

An easily way to realise a selection operator consists in using a purely random-process known as *roulette-wheel* selection. Let us consider, as an example, a population made of 4 individuals. The fitness values for each individual and the percentage of its fitness with respect to the global fitness of the population (i.e. the sum of each individual's fitness) are listed in Table 1.1.

ID of individual	Fitness	% of the fitness with respect to the total fitness
1	10	0.1 (10%)
2	10	0.1 (10%)
3	20	0.2 (20%)
4	60	0.6 (60%)
Total fitness	100	1.0 (100%)

Table 1.1: Fitness values and percentages for every individual of the population

The roulette-wheel selection operator is built as follows: at each individual corresponds a portion of the wheel equal to the percentage of its fitness with respect to the total fitness of the population. Generally speaking, if the population is composed of N_{ind} individuals we have N_{ind} values of the fitness $\{f_1, f_2, ..., f_{N_{ind}}\}$: so, the k^{th} individual will occupy a portion of the wheel proportional to the ratio:

$$r_k = \frac{f_k}{\sum_{i=1}^{N_{ind}} f_i} \ , \tag{1.1}$$

where f_k is the fitness of the k^{th} individual. The roulette-wheel for the example described above is shown in Fig. 1.1.

The selection operator simply works by turning the roulette-wheel. It seems obvious that, according to this schema (which is only one among the different ways to realise the selection operator), the individuals which have greater probability of reproduction (and hence to pass their traits to the next generation) are those which show higher values of the fitness function. Since we assume that, during the evolution process along the different generations, the size of the population is constant and equal to N_{ind}, to give rise to the

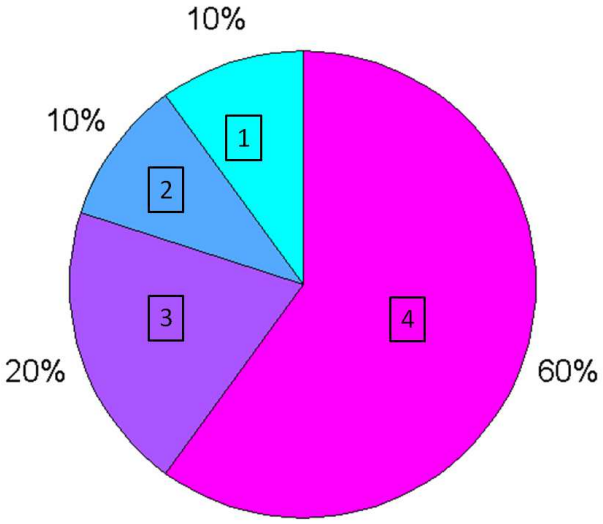

Figure 1.1: Roulette-wheel for the example listed in Table 1.1.

reproduction process we need to turn the wheel exactly N_{ind} times. At each turn of the wheel, an individual is extracted according to the portion that it occupies on the wheel and an exact copy of this individual is then realised.

The next phase of the process is the crossover phase, so let us describe the crossover operator. Such a operator achieves, concretely, the creation of new individuals. After the choice of the N_{ind} individuals for the reproduction process by the selection operator, the crossover phase takes place and it is articulated in two steps:

- the N_{ind} individuals are randomly coupled, forming in this way the couples of parents;
- for both individuals composing the generic couple, every single gene of each chromosome of the individual's genotype is randomly cut, with a probability p_{cross}, in one ore more locations (the same positions for each homologous gene of the couple genotype): at this point two new individuals are created by mixing and crossing the information restrained in the genes composing the chromosomes of the parents' genotype.

The effect of the crossover operator on two homologous genes of the parents' couple is depicted in Fig. 1.2. In this example we tacitly assume that the GA employs an alphabet of cardinality $k = 2$ to code the information. In this case, the position of the cut randomly occurs between the third and the fourth bit of the chain.

At the end of the crossover phase we obtain, by recombination of the $N_{ind}/2$ couples of parents, the N_{ind} individuals composing the new generation.

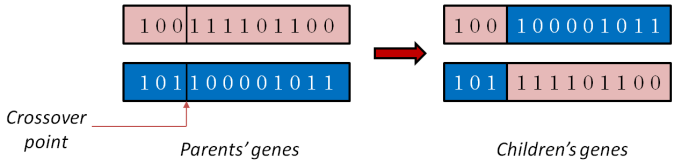

Figure 1.2: Effect of the crossover operator on two homologous genes of the parents' couple.

The third and last phase of the process is the mutation phase wherein the mutation operator acts on the structure of the individuals' genotype. Such a operator acts in a random way, with a probability p_{mut} (often this probability is very low), at the level of the genes of the new individuals generated after the crossover phase. The mutation operator works on the single bit of the chain, by switching it from 0 to 1 or vice-versa. The effect of the mutation operator is shown in Fig. 1.3. We can see that, in this case, the mutation randomly occurs on the fifth bit.

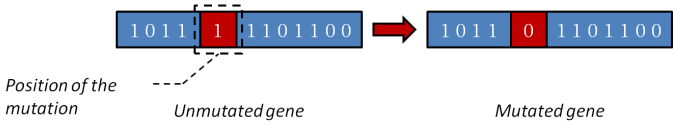

Figure 1.3: Effect of the mutation operator on the bits of the single gene.

The main aim of the mutation process consists in increasing *biodiversity* among the individuals composing the population. In addition, it can be noticed that such a process represents a random search process in the space of individuals' genes and plays the role of a *second-order adaptation mechanism* within the whole genetic search process, see [16]. It is worth noting that introducing and increasing biodiversity, through the mutation mechanism, within the population is a crucial point for what concerns the GA search process: in fact, through the biodiversity it is possible to avoid a premature convergence of the algorithm towards local minima and/or pseudo-optimal solutions, a phenomenon often called *genetic drift*.

Finally, we can assert, according to [12, 16], that a standard GA must have the following five features:

- a genetic representation for potential solutions to a given problem;
- a way to create an initial population of potential solutions;
- an evaluation (objective) function that plays the role of the environment (ranking solutions in terms of their fitness) along with a selection operator that chooses, according to a certain criterion, the individuals involved into the reproduction process;

- genetic operators that alter the composition of the individuals;
- values for various parameters employed by the GA (population size, crossover probability, mutation probability and so on).

1.1.4 The *schemata* within GAs

When dealing with genetic-based search processes, one could be interested to understand how the *similarities* or the *analogies* between the most performing chain of bits (and, hence, the information coded and restrained in those chains) could help the GA in exploring the definition domain of the considered problem and, simultaneously, leading the GA towards potential optimal solutions.
However, how do we assert that two chains (or strings) are similar? In other words, according to which criterion we can say that a given chain belongs to a particular "class" of chains which show some *invariants* concerning the *position* of particular bits within the chain itself?

Holland [15, 16] gave an answer to these questions, introducing the definition of *schema*. A schema is a "pattern of similarity" among two or more chains (belonging to different genes of different individuals) describing a set of sub-chains having some analogies between the elements (bits) located in well-defined positions. Generally speaking, two chains are similar, i.e. they belong to the same schema, if they have some elements (bits) in the same position within the chain.

To better describe the concept of schema, let us introduce the wildcard symbol $*$. We can easily describe the concept of schema using the ternary alphabet composed by the elements $\{0, 1, *\}$. The wildcard symbol $*$ is only a meta-symbol that can assume a value of either 0 or 1, and it is used to describe the potential schemata included into a chain of length l_c. As an example, the schema $*0111$ corresponds to the following two chains of bits: 00111 and 10111. Conversely, we can say that the strings 00111 and 10111 are similar because they share the same schema $*0111$.

In the following we assume that the individual's genotype has only one chromosome. Let us consider a binary alphabet and a string of bits of length l_c. Since every bit can assume the values $*$, 0 or 1, the number of *potential* schemata for a binary alphabet, included within a chain of length l_c, is $(2+1)^{l_c}$. Generally speaking, for an alphabet of cardinality k the number of potential schemata, restrained into a string of length l_c, is $(k+1)^{l_c}$. Nevertheless, this quantity represents the number of potential schemata associated to a chain of length l_c, but not the number of *effective* schemata.

Starting from these considerations a question arises: how many schemata does the GA handle in a population of N_{ind} individuals (i.e. N_{ind} chains) of length l_c? To understand how many schemata are handled by the GA for a population of N_{ind} chains of length l_c we must know the real structure of each string at each generation. Despite it is not possible

to know the details of each chain, we can only fix the upper and lower bounds to the number of effective schemata treated by the GA at each generation.

Holland [16] has demonstrated that the number of effective schemata, for an alphabet of cardinality k, associated to the single chain of length l_c, is k^{l_c}. Moreover, the population is composed of N_{ind} chains: thus, the number of effective schemata associated to a chain of length l_c, is, at most, $N_{ind} \times k^{l_c}$ at each generation. Finally, we can assert that the number of effective schemata, $n_{schemata}$, included within a string of length l_c, for a population of N_{ind} strings (handled by the GA at each generation) is in the following range:

$$n_{schemata} \in \left[k^{l_c} \ , \ N_{ind} \times k^{l_c}\right] \ . \tag{1.2}$$

After having clarified that issue, another question arises: what is the effect of each genetic operator on the number of effective schemata (included within a string of length l_c, for a population of N_{ind} strings) handled by the GA at each generation? We give an answer to this question in Section 1.2

1.2 Genetic Algorithms: mathematical foundations

Before describing in details the mathematical aspects that underlie GAs, it is appropriate to introduce some definitions which will give a more rigorous nature to our discussion. Without loss of generality, we assume to use a binary alphabet to describe the genotype of individuals. Such a alphabet is represented as:

$$\mathrm{V} = \{0, 1\} \ . \tag{1.3}$$

We assume that the population is composed of N_{ind} mono-chromosome individuals whose genotype is described by a single chain of bits. In addition all chains have the same length l_c. The population, at the generation t, can be expressed as:

$$\{A(t)\} = \{A_1(t), A_2(t), ..., A_{N_{ind}}(t)\} \ . \tag{1.4}$$

The elements (bits) of the chain are represented using lower case letters with a subscript identifying the position of the element within the chain. Each individual is described by a string of bits of length l_c as follows:

$$A_j = \{a_i\}_j \ , \ j = 1, ..., N_{ind} \ , \ i = 1, ..., l_c \ . \tag{1.5}$$

As an example, the chain of 4 bits $A = 0110$ can be written as $A = a_1a_2a_3a_4$, with $a_1 = a_4 = 0$ and $a_2 = a_3 = 1$.
To describe all the potential schemata restrained in the population, we introduce the ternary alphabet:

$$\mathrm{V}^+ = \{0, 1, *\} \ . \tag{1.6}$$

We remind that the number of potential schemata associated to a string of length l_c is $(k+1)^{l_c}$, where k is the cardinality of the considered alphabet. Since we use a binary alphabet, the number of potential schemata is 3^{l_c}. Moreover, we recall that the number of effective schemata (associated to a chain of length l_c) handled by the GA at each generation is expressed by Eq. (1.2). However, not all the schemata have the same meaning. The generic schema is indicated by the letter H. For example, the schema $H_1 = 0 * 110 * *$ hold more information than the schema $H_2 = 0 * * * * * *$. In order to univocally define a schema H, we need to introduce the following quantities:

- *order of the schema*: it represents the number of fixed bits within the chain and it is indicated by $o(H)$;
- *defining length of the schema*: it represents the distance between the first and the last position of the fixed elements within the chain and it is indicated by $\delta(H)$.

As an example, the schema $H_1 = 0 * 110 * *$ is of order $o(H_1) = 4$ and it has a defining length of $\delta(H) = 5 - 1 = 4$, while the schema $H_2 = 0 * * * * * *$ is of order $o(H_1) = 1$ and it has a defining length of $\delta(H) = 1 - 1 = 0$. It can be noticed that the length of the whole chain for both schemata is $l_c = 7$. Clearly, the above quantities can vary within the following ranges:

$$\begin{array}{l} o(H) \in [1, l_c] \quad , \\ \delta(H) \in [0, l_c - 1] \quad . \end{array} \tag{1.7}$$

In the next Subsections, we describe the effect produced by each genetic operator of the standard GA (i.e. selection, crossover and mutation operators) on the generic schema H.

1.2.1 Effect of the selection operator on *schemata*

Let us consider a generic schema H at the t^{th} generation. Let us suppose that, at this generation, we have $\widetilde{N}_{ind}$ individuals-chains possessing that schema within the whole population of size N_{ind}, with $\widetilde{N}_{ind} \leq N_{ind}$. In other words, we can express the number of chains having the schema H, at generation t, as:

$$\widetilde{N}_{ind} = \widetilde{N}_{ind}(H, t) \ . \tag{1.8}$$

As said beforehand, the selection operator, depending on the values of the fitness function, chooses a chain within the population and makes an exact copy of it in order to pass that chain to the next step of the process: the crossover phase. Mathematically speaking, the i^{th} chain is selected by the selection operator with a probability:

$$p_i = \frac{f_i}{\sum_{j=1}^{N_{ind}} f_j} \ , \tag{1.9}$$

where f_i is the fitness of the i^{th} chain, whilst $\sum_{j=1}^{N_{ind}} f_j$ is the fitness of the whole population. The fitness of the schema H can be defined as:

$$f(H) = \frac{\sum_{j=1}^{\widetilde{N}_{ind}} f_j}{\widetilde{N}_{ind}} \ . \tag{1.10}$$

Eq. (1.10) means that the fitness of the schema H corresponds to the average value of the fitness of the $\widetilde{N}_{ind}$ chains whereto the schema H is associated. The average value of the fitness of the whole population of chains can be expressed as:

$$\overline{f} = \frac{\sum_{j=1}^{N_{ind}} f_j}{N_{ind}} \ . \tag{1.11}$$

According to what we already said about the selection of the i^{th} chain, we expect that the schema H will be selected by the selection operator with a probability:

$$p(H) = \frac{f(H)}{\sum_{j=1}^{N_{ind}} f_j} \ . \tag{1.12}$$

At this point, in the next generation, i.e. the $t+1$ generation, the number of chains possessing the schema H, due to the action of the selection operator, will be equal to:

$$\widetilde{N}_{ind}\,(H, t+1) = \lceil \widetilde{N}_{ind}\,(H, t)\, p(H) N_{ind} \rceil \ . \tag{1.13}$$

where the $\lceil \ \rceil$ operator is the ceiling function (rounding to the next largest integer). Eq. (1.13) can be simplified. Indeed, considering Eq. (1.11) and (1.12) we can finally write:

$$\widetilde{N}_{ind}\,(H, t+1) = \lceil \widetilde{N}_{ind}\,(H, t)\, \frac{f(H)}{\overline{f}} \rceil \ . \tag{1.14}$$

The schema H is passed to the next generation with a rate proportional to the ratio between the fitness of the schema H itself (i.e. the average fitness of the chains possessing that schema), and the average fitness of the whole population. For this reason, the schemata belonging to a group of individuals-chains having an average value of the

fitness (evaluated with respect to this group of chains) greater than the average fitness of the population will be most probably transmitted to the new generation. On the contrary, those schemata with a fitness lower than the average fitness of the population will, probably, extinguish.

Without loss of generality, we can assume that the fitness of the schema H is proportional to the average fitness of the population as follows:

$$f(H) = \overline{f}\,(1 + C) \ , \tag{1.15}$$

where C is an arbitrary real constant. In such a case, Eq. (1.14) becomes:

$$\widetilde{N}_{ind}\,(H, t+1) = \lceil \widetilde{N}_{ind}\,(H, t)\,(1 + C) \rceil \ . \tag{1.16}$$

If we assume, now, that the quantity C remains unchanged through the generations, starting from the initial generation, i.e. $t = 0$, we can assert that, at the current generation t, the number of chains having the schema H is equal to:

$$\widetilde{N}_{ind}\,(H, t) = \lceil \widetilde{N}_{ind}\,(H, 0)\,(1 + C)^t \rceil \ . \tag{1.17}$$

From Eq. (1.17) we can see that the schema H is transmitted along the generations according to a geometric series relationship. This result has an interesting interpretation: the schemata which posses a fitness greater than the average fitness of the population will be passed exponentially to the next generation.

Finally, we remark that if the quantity C is not constant along the generations, the number of chains having the schema H, at the current generation t, can be expressed as:

$$\widetilde{N}_{ind}\,(H, t) = \lceil \widetilde{N}_{ind}\,(H, 0) \prod_{k=0}^{t} (1 + C_k) \rceil \ . \tag{1.18}$$

1.2.2 Effect of the crossover operator on *schemata*

Let us consider a chain A of length $l_c = 7$, which contains two (among the others) different schemata H_1 and H_2 as follows:

$A = 0111000$

$H_1 = *1****0$

$H_2 = ***10**$

the crossover randomly combines two different chains, A_i and A_j, by cutting them in a randomly-chosen position. For a string of length l_c, there are $l_c - 1$ possible points wherein the cut can take place. Concerning our example, we have 6 possible points wherein the

crossover operator can cut the chains. Let us suppose that the cut is done in position 3, i.e. between the third and the fourth bit of the chain A. The effect of the crossover on the schemata H_1 and H_2 is the following:

$$A = 011/1000$$

$$H_1 = *1*/***0$$

$$H_2 = ***/10**$$

as it can be noticed, the schema H_1 is destroyed, while the schema H_2 is retained. It is easy to understand that the schemata with a higher defining length $\delta(H)$ have a higher probability to be destroyed than the ones having a shorter defining length. Considering our example, the defining length of the schemata H_1 and H_2 are $\delta(H_1) = 5$ and $\delta(H_2) = 1$, respectively. The probability of disruption of the schema H_1 is $\delta(H_1)/(l_c - 1) = 5/6$, while the one of the schema H_2 is $\delta(H_2)/(l_c - 1) = 1/6$.

Generally speaking, if the crossover process takes place with a probability p_{cross}, the *disruption probability* of the generic schema H (i.e. the probability that the crossover will destroy that schema) can be defined as:

$$p_d(H) = p_{cross} \frac{\delta(H)}{l_c - 1} \ . \tag{1.19}$$

The probability of retain the schema H, after the action of the crossover operator, is defined as the complement to 1 of the disruption probability:

$$p_{sc}(H) = 1 - p_d(H) = 1 - p_{cross} \frac{\delta(H)}{l_c - 1} \ . \tag{1.20}$$

If we assume that, the selection and crossover processes are completely independent, we can deduce a lower bound for the number of individuals-chains possessing the schema H passed to the next generation:

$$\widetilde{N}_{ind}(H, t+1) \geq \lceil \widetilde{N}_{ind}(H, t) \frac{f(H)}{\overline{f}} \left[1 - p_{cross} \frac{\delta(H)}{l_c - 1} \right] \rceil \ . \tag{1.21}$$

From Eq. (1.21) we can conclude that, due to the effect of selection and crossover operators, the schemata which posses a fitness greater than the average fitness of the population and reduced defining length will be transmitted exponentially to the next generation.

1.2.3 Effect of the mutation operator on *schemata*

The mutation operator acts on the single bit of the chain by changing it with a probability p_{mut}. In order to transmit a schema H to the next generation, none of the fixed elements of the chain must be changed.

It can be noticed that the survival probability of the single bit is $1 - p_{mut}$. Since in a schema H we have $o(H)$ fixed elements, and since the mutation of the different fixed elements of the scheme are statistically independent events, the probability of retaining the schema H, after the action of the mutation operator, is:

$$p_{sm}(H) = (1 - p_{mut})^{o(H)} \quad . \tag{1.22}$$

From Eq. (1.22) we can conclude that the low-order schemata have a higher probability to be passed to the next generation, after the action of the mutation operator.

If we assume that, the selection, crossover and mutation processes are completely independent, we can deduce a lower bound for the number of individuals-chains possessing the schema H passed to the next generation:

$$\widetilde{N}_{ind}(H, t+1) \geq \lceil \widetilde{N}_{ind}(H, t) \frac{f(H)}{\overline{f}} \left[1 - p_{cross} \frac{\delta(H)}{l_c - 1} \right] (1 - p_{mut})^{o(H)} \rceil \ . \tag{1.23}$$

If the mutation probability p_{mut} is very low, i.e. $p_{mut} << 1$, Eq. (1.23) writes:

$$\widetilde{N}_{ind}(H, t+1) \geq \lceil \widetilde{N}_{ind}(H, t) \frac{f(H)}{\overline{f}} \left[1 - p_{cross} \frac{\delta(H)}{l_c - 1} - p_{mut} o(H) \right] \rceil \ . \tag{1.24}$$

1.2.4 The theorem of *schemata* and the Implicit Parallelism

After describing the effect of each genetic operator of the standard GA on the generic schema H, we can enunciate the well-known Holland's *theorem of schemata* [15, 16]. This theorem can be expressed as follows:

Theorem 1.2.1 (Holland's Theorem of Schemata) *The low-order schemata with short defining length and fitness greater than the average fitness of the population increase exponentially in successive generations.*

Eq. (1.23) or, equivalently, Eq. (1.24) are the natural result of this theorem.

As already discussed in the previous subsections, for a population composed of N_{ind} individuals-chains of length l_c the GA handles, at each generation, a number of effective schemata that varies between the bounds expressed by Eq. (1.2). As stated by the Holland's theorem of schemata, not all the chains are handled by the GA in the same way: as an example, the high-order schemata or the ones having long defining length show a high disruption probability due to the action of the mutation and crossover operators, respectively.

Nevertheless, Holland defined more precisely the lower bound of Eq. (1.2). Indeed, he demonstrated [15, 16] that the following assert subsists:

Theorem 1.2.2 (Holland's Implicit Parallelism) *The number of schemata usefully processed by the GA in a population of N_{ind} binary strings has a lower bound proportional to N_{ind}^3.*

Let us consider a population of size N_{ind} composed of chains of length l_c. We consider only the subset of chains associated to a particular schema H having a survival probability, after the crossover operation, greater than or equal to $\overline{p}_{sc}$. This fact lead us to evaluate the defining length of the generic schema H (and hence the length of the subset of chains possessing this schema) that satisfy the previous condition:

$$1 - p_{cross}\frac{\delta(H)}{l_c - 1} \geq \overline{p}_{sc} \Longrightarrow l_s \leq (l_c - 1)\lceil\frac{1 - \overline{p}_{sc}}{p_{cross}}\rceil \ , \tag{1.25}$$

where l_s is the *useful length* of the schemata (or the length of the subset of chains) which have a probability to be retained after the crossover not less than $\overline{p}_{sc}$.

In order to see how many sub-chains having an useful length l_s are contained within a chain of length $l_c > l_s$, let us consider the following example. Suppose we have a chain A of length $l_c = 10$ and a sub-string retaining the scheme H of useful length $l_s = 5$. In addition, we assume that only the last element of this sub-chain is fixed. As an example, the sub-chain H could be:

$$H = \%\%\%\%1,$$

where the percent sign % is a *jolly* symbol that can assume the values either 0, 1 or $*$. Since the last bit is fixed, one can notice that the number of schemata retained within the sub-string of useful length l_s is 2^{l_s-1}. For the above example, the number of possible schemata associated to the sub-chain H is $2^{5-1} = 16$. Consider, now, a string A of length $l_c = 10$, holding the sub-chain H, with the following structure:

$$A = \%\%\%\%1 * * * * *.$$

How many times the sub-chain H of useful length $l_s = 5$ is contained into the string A? To give an answer to this question, we can imagine to translate the sub-string H along the chain A as follows:

$A = \%\%\%\%1*****$, $A = *\%\%\%\%1****$, $A = **\%\%\%\%1***$, $A = ***\%\%\%\%1**$,
$A = ****\%\%\%\%1*$, $A = *****\%\%\%\%1$.

It can be noticed that the chain A retains the sub-chain H six times. Generally speaking, a string of length l_c retains a sub-string of useful length l_s, $(l_c - l_s + 1)$ times. In conclusion, we can assert that the number of possible schemata of a sub-chain of useful length l_s retained within a chain of length l_c is:

$$(l_c - l_s + 1)2^{l_s - 1} \ . \tag{1.26}$$

For a population made of N_{ind} chains of length l_c the number of schemata retained within a sub-chain of useful length l_s is at most:

$$N_{ind}(l_c - l_s + 1)2^{l_s - 1} \ . \tag{1.27}$$

Nevertheless, Eq. (1.27) still offers an overestimation of the number of schemata retained within a sub-chain of useful length l_s belonging to the population. Suppose, now, to consider a population of strings of length l_c having the following size:

$$N_{ind} = \lceil 2^{l_s/2} \rceil \ . \tag{1.28}$$

If we assume that the distribution of the number of schemata is a *binomial distribution*, we can easily see that half of these schemata will have an useful length greater than $\lceil l_s/2 \rceil$. So, we can conclude that, at each generation, the GA handles a number of schemata retained within a sub-chain having useful length l_s greater than or equal to:

$$n_{schemata} \geq \lceil \frac{(l_c - l_s + 1)}{2} N_{ind} 2^{l_s - 1} \rceil = \lceil \frac{(l_c - l_s + 1)}{4} N_{ind} 2^{l_s} \rceil \ . \tag{1.29}$$

Substituting Eq. (1.28) into Eq. (1.29) yields:

$$n_{schemata} \geq \lceil \frac{(l_c - l_s + 1)}{4} N_{ind}^3 \rceil \ . \tag{1.30}$$

Eq. (1.30) demonstrates the validity of the Holland's assertion (for more details see [16]). We can conclude that, despite GAs destroy the high-order long schemata due to the combined action of crossover and mutation operators, they can handle a huge number of schemata, starting from a relatively low number of chains.

As conclusive remark, it can be noticed that in 1993 Bertoni and Dorigo [52] showed that the lower-bound on the number of schemata of Eq. (1.30) evaluated by Holland has not general validity. Indeed, they demonstrated that the Holland's Implicit Parallelism is only a particular case of a more general rule found by the authors. Roughly speaking, Bertoni and Dorigo found that the number of schemata handled by the GA, for a population of $N_{ind} = 2^{\beta l_c}$ chains, is at least of order:

$$n_{schemata} \geq \lceil \frac{N_{ind}^{f(\beta)}}{\sqrt{\log_2(N_{ind})}} \rceil \ , \tag{1.31}$$

where $f(\beta)$ is a particular function defined as:

$$f(\beta) = \begin{cases} 1 + \dfrac{2}{\beta} & 0 < \beta < 1 \quad , \\ 1 + 2\dfrac{-\beta/2\log\beta/2 - (1-\beta/2)\log(1-\beta/2)}{\beta} & 1 < \beta < 4/3 \quad , \\ \dfrac{2\log_2 3}{\beta} & \beta > 4/3 \quad . \end{cases} \tag{1.32}$$

They showed that the Holland's Implicit Parallelism is a particular case that subsists when the following condition on the parameter β is satisfied: $\beta \geq 1$. For a deeper insight in the matter the reader is addressed to [52].

1.2.5 Advantages and drawbacks of GAs

Very often, in many different fields, GAs have proved to be more effective and robust than classical deterministic and/or gradient-based methods in the search of solutions for a given optimisation problem. To understand the reasons behind this fact, we have to analyse the main differences between classical methods and GAs:

- GAs employ a coding of the optimisation variables of the considered problem, instead of directly using them;
- GAs work on a population of points instead of a single point. For this reason GAs are well-suited when dealing with *non-convex* and/or *non-smooth* optimisation problems: the distribution of a population of points over the whole design space prevents the algorithm to converge towards a local minimum;
- GAs are "zero-order" methods, i.e. they only need of the evaluation of the objective function without any auxiliary information (e.g the calculation of the first derivatives of the function). This circumstance avoids the problem of the numerical calculation of the function derivatives and allows to deal with different types of variables (integer, discrete, scattered and so on) as well as a more wide class of functions (discontinuous, non-smooth, non-differentiable and so on);
- GAs uses probabilistic transition rules instead of deterministic ones. However, GAs are not completely blind in searching the solutions within the definition domain: they simultaneously explore several points belonging to different regions of the design space and, making simple evaluations of the objective function on such points, they are able to exploit these informations in order to drive the search of optimal solutions on some convenient sub-domains of the design space wherein the global optimum/optima is/are located.

Along with the previous advantages, as it happens in each numerical technique, GAs have the following drawbacks:

- repeated objective (and also fitness) function evaluation for complex problems is often the most prohibitive and limiting segment of GAs. Finding the optimal solution to complex high dimensional, multi-modal problems often requires very expensive fitness function evaluations. In real world problems such as structural optimisation problems, one single function evaluation may require from several hours to several days for a complete simulation. Typical optimisation methods cannot deal with such types of problem. In this case, it may be necessary to forgo an exact evaluation and use an approximated objective function that is computationally efficient. It is apparent that amalgamation of approximate models may be one of the most promising approaches to convincingly use GA to solve complex real life problems;
- GAs cannot effectively deal with problems wherein the only fitness measure is a single right/wrong measure (like decision problems), since there is no way to converge to the solution (no hill to climb). In such cases, a random search may find a solution as quickly as a GA;
- GAs require an adequate setting of the parameters which control the correct behaviour of the algorithm itself, namely the crossover and mutation probabilities, the size of the population, the choice of the selection operator and so on.

In the next Section we describe the main features of the GA BIANCA, originally presented in [1, 2], and particularly we introduce the new features and the new genetic operators conceived and developed in the framework of this thesis in order to deal with a special class of optimisation problems: the design problems of modular systems.

1.3 BIANCA: a genetic algorithm for engineering optimisation

As suggested by its name, the genetic code BIANCA (*Biologically Inspired ANalysis of Composite Assemblages*), was originally developed by Vincenti *et al.* in order to deal with design problems of composite laminated structures [1, 2]. BIANCA was based on the structure of the standard GA, see Fig. 1.4, and had some original features concerning the representation of the genotype for composite laminates and also a new strategy in the treatment of inequality constraints [1, 2]. The authors performed a large campaign of numerical tests using BIANCA which proved that this code is very effective and robust when dealing with design problems of composite laminates. Nevertheless, new laminates design problems led the authors to make some modifications to the GA BIANCA that renovate its structure in order to improve its performance and robustness [1].

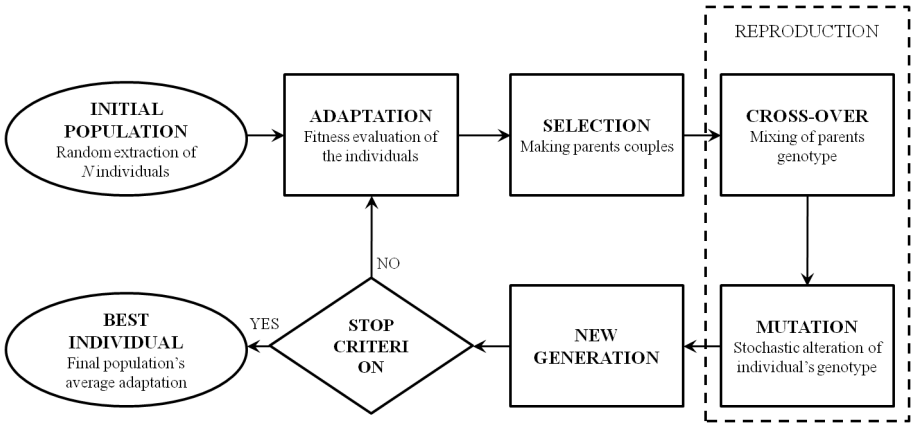

Figure 1.4: The architecture of the standard GA.

This first version of BIANCA (which is written in FORTRAN language) was based on a single population evolving along the generations and subject to the action of the genetic operators of crossover, mutation and elitism. Selection was based on the roulette-wheel method and the stop criterion was formulated as a maximum number of generations. In this form, the GA allowed the authors to treat unconstrained optimisation problems. Later on, due to the introduction of additional design criteria in the study of laminates elastic symmetries, the authors developed an original technique for handling constraints based on the combination between classical penalisation methods and the exploitation of the information retained within the population. Originally this strategy, whose authors called *Automatic Dynamic Penalisation* (ADP) technique [1], was conceived in order to handle both inequality and equality constraints as an equivalent single inequality constraint. A detailed description of the architecture of BIANCA in its first version can be found in [1, 2].

In engineering optimisation problems, the objects of the optimisation process can be often considered as *modular systems*. This is the case, for example, of composite laminated structures, which are an assembly of anisotropic layers: each ply can be considered as a module, and the whole structure is described in terms of number of constitutive modules as well as the properties (orientation angles, thickness and material) of each module. Other examples of modular structures are stiffened panels, often used in structural systems (e.g. in aeronautical applications): these structures are composed of plates stiffened by a set of longitudinal beams (stiffeners). Again, the global structure is characterised by the number of constitutive stiffeners along with the geometrical and material properties of each stiffener and the plate.

The optimisation of modular systems is the main topic of the present thesis. Nevertheless, as described below, when dealing with such problems some difficulties arise. In order to overcome these issues we searched for a solution inspired by a more rigorous and (at

the same time) deeper interpretation of the Darwinism and of the Natural Selection. To this purpose, we took advantage of the intrinsic capabilities of "algorithmic adaptation" of GAs: basically, a richer and well-structured encoding of the genetic information represents the necessary preamble for building an improved GA able to deal with optimisation problems concerning modular systems.

The optimisation of engineering modular systems/structures is a difficult task because it implies the optimisation of each constitutive module composing the system, as well as the optimisation of the number of constitutive modules. More precisely, all modules share a "common structure" in terms of the "constitutive parameters" characterising each module, such as geometrical dimensions, material properties and so on. However, and this is very important, the constitutive parameters of modules can assume different values for each module composing the system. Moreover, the number of constitutive modules is an integer value, i.e. a discrete variable, and the design space of such optimisation problems is therefore populated by points representing engineering systems/structures made of different numbers of modules. As a consequence, the number of constitutive parameters (variables of the optimisation problem) can be different for distinct points, thus the associated mathematical optimisation problem is defined over a design space of vectors of variable dimension.

According to the metaphor adopted by GAs, each point in the design space corresponds to an individual and its genetic structure is composed of chromosomes and genes [12, 16]. If the object of the optimisation problem is a modular system, each constitutive module can be represented by a chromosome, while a chromosome will be composed of genes corresponding to the constitutive parameters of the module. The most part of GAs perform the reproduction operations on a couple of individuals selected within the population according to a certain criterion. This way of working is surely correct in the context of the standard GA, but it may result to be not well-suited to deal with optimisation problems of modular systems. Moreover, another point of interest is that, in the most part of GAs, the concept of *Darwinian selection* is not properly employed. In fact, originally, the concept of natural selection is strictly linked to the concept of *species*: during a sufficiently long time interval, the selection, by operating on a certain number of individuals, can lead to the appearance of new species, better fitted to the new environmental conditions.

Then, to reproduce all the qualities of the Darwinian selection, one should conceive a GA wherein individuals and species evolve at the same time: in these terms the real natural selection is more closely synthetically reproduced in the context of the numerical algorithm. In this framework, the first step is the translation of the concept of species in the context of GAs. The fundamental consequence of this point is an adequate change of the structure of the individual's genotype. Chromosomes and genes must be organised in such a way that different species can be clearly identified. In agreement with the paradigm of Nature, within BIANCA the species is characterised by the number of

chromosomes of the individual's genome. So, individuals having a genotype composed of different number of chromosomes belong to different species. It appears clearly that a GA which performs the evolution of species and at the same time, but independently, the evolution of individuals, must be ruled by genetic operations able to cross species and individuals independently and simultaneously: to this purpose new genetic operators that allow the crossover and mutation among individuals belonging to different species have been developed.
The idea to develop a GA able to deal with a wide class of optimisation problems lead us to enrich and modify the original architecture of the code BIANCA in order to build a more general and adaptable numerical tool specially able to handle problems concerning modular systems.

Before describing the classical main features and the new ones that we have introduced in BIANCA, we briefly discuss the mathematical formulation of the non-linear programming problem (NLPP) which represents the main focus for which our code has been conceived.

1.3.1 The Non-Linear Programming Problem (NLPP)

Let us consider a constrained optimisation problem stated as follows:

$$\begin{aligned} &\min_{\mathbf{x}} \ \Phi(\mathbf{x}) \ , \\ &\text{subject to :} \\ &\begin{cases} g_i(\mathbf{x}) \leq 0 \quad i = 1, ..., r \ , \\ h_j(\mathbf{x}) = 0 \quad j = 1, ..., m \ , \\ \mathbf{x}_L \leq \mathbf{x} \leq \mathbf{x}_U \ , \end{cases} \end{aligned} \tag{1.33}$$

where vectors and matrix terms are marked in bold typeface. In this formulation $\mathbf{x}$ is the n-dimensional *vector of design variables*, while $\mathbf{x}_L$ and $\mathbf{x}_U$ are the n-dimensional vectors representing the lower and upper bounds of the design variables, i.e. the whole definition domain or search space. The full set of equality and inequality constraints along with the box constraints represents the *feasible domain* or *design space* Ω. Design variables can be of different type: continuous, regular discrete, scattered (i.e. discrete variables without a discretisation step) or "grouped", these last being a sort of "abstract" variables representing a group of different variables, such as, for example, in the case of the constitutive material of a structure, when the material is chosen within a database: once a particular material is associated to a part, the whole set of the properties of the material are determined, i.e. elastic moduli, mass density and so on.

The goal of the optimisation consists in minimising the objective function $\Phi(\mathbf{x})$ subject to a given number of constraints: $g_i(\mathbf{x})$ $(i = 1, ..., r)$ are the r functions of inequality constraints, while $h_j(\mathbf{x})$ $(j = 1, ..., m)$ are the m functions of equality constraints. For

any solution $\mathbf{x}$ in the feasible domain Ω, all equality constraints $h_j(\mathbf{x}) = 0$, are active at all points of Ω, and an inequality constraint that satisfies $g_i(\mathbf{x}) = 0$, is said an active constraint.

An optimisation problem can be characterised either by the type of constraints in the problem formulation or by the linearity or non-linearity of the objective and constraint functions. A problem where at least some of the objective and constraint functions are non-linear is called non-linear programming problem (NLPP). These NLPPs predominate in real-world engineering applications and constitute the primary focus of BIANCA.

1.3.2 The architecture of BIANCA

As said previously, the GA BIANCA is substantially constructed on the classical scheme of the standard GA, but it has however several original features. The classical features, already implemented in the previous version of the code (see [1] for more details) are:

- fitness evaluation: the choice of the fitness determines the kind of problem, i.e. if it is a minimisation or maximisation one, and the *selection pressure* that the user decides to introduce. The fitness is evaluated in such a way that the it can assume all the possible values in the range [0, 1], with the value 0 characterizing the least fitted individual and 1 the most fitted one. In BIANCA the fitness function is defined as:

$$\begin{aligned} f &= \left(1 - \frac{\Phi - \min\limits_{pop} \Phi}{\max\limits_{pop} \Phi - \min\limits_{pop} \Phi} \right)^C, \text{ minimisation} \\ f &= \left(1 - \frac{\max\limits_{pop} \Phi - \Phi}{\max\limits_{pop} \Phi - \min\limits_{pop} \Phi} \right)^C, \text{ maximisation} \end{aligned} \tag{1.34}$$

  where Φ is the objective function of the considered problem, while $C \geq 1$ is the exponent tuning the pressure's selection;

- selection: two known techniques of selection are included, i.e. roulette wheel and tournament;

- standard genetic operators: the main genetic operators are crossover and mutation, used with a certain probability on each gene of the individual's genotype, i.e. independently on each design variable;

- additional genetic operators: the *elitism* operator, used to preserve the best individual at each generation;

- handling constraints: the aforementioned ADP method is implemented;

- handling multiple populations: the need to simultaneously explore different regions of the design space, as well as the search of optima responding to distinct design criteria, led us to introduce the option of working with multiple populations in BIANCA. Moreover, a classical *ring-type migration* operator has been introduced in order to allow exchanges of informations between populations evolving through parallel generations;

- stop criterion: maximum number of generations reached or test of convergence, i.e. no improvements of the mean fitness of the population after a given number of cycles.

What mostly characterises BIANCA, is the representation of the information, which is particularly rich and detailed, though non redundant. Moreover, the information restrained in the population is treated in such a way to allow for a deep mixing of the individual genotype. In fact, as said above, the reproduction operators, i.e. crossover and mutation, act on every single gene of the individuals, so allowing for a true independent evolution of each design variable.
The reason underlying such a choice are substantially three: a) the crossover directly made at the chromosome level (we remind that, generally in the literature the most part of GAs work on individuals having a mono-chromosome genome) strongly limits the total number of "successful" combinations of the design variables satisfying the requirements expressed by the considered problem, b) the variables coded by the genes of the chromosome can be of different type and nature, thus they can code quantities having different physical meaning and, finally, c) the crossover directly made on each individual's gene can lead the GA to find more quickly and effectively an optimal solution for those problems wherein the objective and/or constraint functions depend, independently, upon a subset of the whole set of design variables.

In the version of BIANCA presented in this thesis, the structure of the individual and, consequently, the representation of the information, as well as the reproduction operators of crossover and mutation, have been modified in order to deal with evolution not only of the individuals, but of the species too; crossing individuals belonging to different species is now possible, thanks to new genetic operators that we have introduced in BIANCA. In particular, the new features introduced within BIANCA are:

- a new structure of the individual's genotype adapted and extended to represent the concept of *species*, described in Sec. 1.4;

- new genetic operators of crossover allowing the reproduction among individuals belonging to different species, detailed in Sec. 1.5;

- new mutation operators allowing the evolution of the different species restrained within the population, see Sec. 1.5;

- a generalisation of the ADP strategy, modified to handle inequality and equality constraints without evaluating an equivalent single constraint, see Sec. 1.6;
- a very general interface that makes BIANCA able to exchange input/output informations with mathematical models supported by external software (indeed, in several problems, the value of the objective function and/or constraints, cannot be computed analytically, but it has to be evaluated using special numerical codes, e.g. finite element (FE) codes), see Sec. 1.8;
- a Graphical User Interface (GUI), that we have developed in order to use the code BIANCA more easily, see Sec. 1.9.

1.4 Representation of individuals and species within BIANCA

In GAs, a crucial phase consists in the encoding step which translates the design variables from the *phenotypic* space to the *genotypic* one resulting, for example, in a binary, real or hexadecimal chromosome. The length of the chromosome, i.e. the number of genes, represents in the genotype space the amount of the information, restrained in the individual's genotype, coding a particular quantity in the corresponding phenotype space. In standard GAs, for individuals having a single-chromosome genotype, the chromosome length L_{chrom} can be expressed as:

$$L_{chrom} = \sum_{i=1}^{n_{var}} \lceil \ln \left(\frac{x_{iUB} - x_{iLB}}{\Delta x_i} \right) / \ln d_{EB} \rceil \ , \tag{1.35}$$

where n_{var} is the number of decision variables, x_i and Δx_i are the i^{th} decision (or design) variable and its resolution level, respectively, whilst d_{EB} is the dimensionality of the encoding base. x_{iLB} and x_{iUB} are the lower and upper bounds for the i^{th} decision variable.

Traditionally in GAs the chromosome length is fixed *a-priori* by the total number of variables along with their resolutions and cannot change during the whole genetic process. As described in other existing works on this subject (see for example [29, 30]) the traditional approach has, substantially, two drawbacks:

- the best achievable fitness is inherently limited by the chromosome length and hence by the total number of variables. Therefore, the genetic asymptote, which is typical of the genetic process, is a direct consequence of the constraints of the problem as well as the number of design variables and their level of resolution;
- we do not know *a priori* how many decision variables are required, and consequently how long the chromosome should be, for a given problem, in order to obtain a real global optimum.

In these last years, different research studies have been developed in the field of improved GAs which take into account for the variable chromosome length. Among them, Kim and Weck [30] developed a GA that can change the chromosome length using a "progressive refinement" technique. They assumed that significant fitness improvements can be obtained by gradually increasing the chromosome length. They achieved the increase in the chromosome length mainly in two way: either by increasing the resolution level of the existing design variables or by adding new design variables during the process. In every case these operations were realised by a particular mutation operator acting on the chromosome structure: the concept consists in seeding the design space of finer resolution with mutated best designs from the domain of coarser resolution. They applied their strategy to two structural topology optimisation problems: a short cantilever and a bridge problems. Despite Kim and Weck developed an effective GA technique in their context, they did not develop genetic operators which perform the classical reproduction phase, i.e. crossover and mutation operations, among individuals having different chromosome lengths. The variation of the number of variables is obtained through a mutation process which is linked to the concept "from coarse to fine" that is doubtless very effective when dealing with topology optimisation problems, but could appear not very effective for other types of problems.
Ryoo and Hajela [29] developed a GA for topology optimisation that also handles variable chromosome lengths. This GA allows only crossover between chromosomes of different lengths. Even though they implemented an inter-species crossover operator, they did not obtain an effective evolution of the species along the generations. In other words, the number of chromosomes with different length remains the same from the beginning until the end of the process, i.e. from the initial population until the final one.
Park *et al.* [53] developed an improved GA able to cross chromosomes with different lengths. Within their GA the individual is characterised by a single chromosome: at each generation the change in the length of the chromosome was realised by means of a special mutation operator acting directly on the number of genes composing the chromosome. Their strategy was applied to the weight minimization of laminated plates manufactured by the Resin Transfer Moulding (RTM) process, considering the technological requirements as constraints of the optimisation problem.

In the following subsections, we show the new structure of the individuals in BIANCA, which can also take into account for individuals belonging to different *species*.

1.4.1 The new structure of the individual's genotype

Unlike what is done in the most part of GAs presented in literature, that have a monochromosome algebraic structure, in BIANCA the information is organized in a genome composed of chromosomes which in turn are made of genes and, finally, each gene is a binary representation of a design variable. As an example, when the object of the optimisation problem is a modular system, each constitutive module is represented by a

chromosome, while each gene (composing a chromosome) codes a design variable related to the specific module.

In agreement with the paradigms of natural sciences, individuals characterised by different number of chromosomes belong to *different species*. BIANCA has been conceived for crossing also different species, and it is able to make in parallel (and without distinction) the optimisation of the species and individuals. In particular, the typical reproduction operators of crossover and mutation have been specially conceived for crossing species and individuals during the same iterations. Such operators are detailed in Sec. 1.5.

Considering what said above, from a practical point of view in BIANCA an individual is represented by an array of dimensions $n_{chrom} \times n_{gene}$. The number of rows, n_{chrom}, is the number of chromosomes, while the number of columns, n_{gene}, is the number of genes. Basically, each design variable is coded in the form of a gene, and its meaning is linked both to the position and to the value of the gene within the chromosome. In principle, there are no limits on the number of genes and chromosomes for an individual. A number N_{ind} of individuals compose a population, and in BIANCA it is possible to work, at the same time, with several populations whose number, N_{pop}, can be defined by the user.

In order to include the number of chromosomes (i.e. of modules, and hence of design variables) among the design variables, and then to allow the reproduction among individuals belonging to different species, some modifications of the individual genotype were necessary. The genotype of each individual in BIANCA is represented by a binary array, shown in Fig. 1.5. In this picture, the quantity $(g_{ij})^k$ represents the j^{th} gene of the i^{th} chromosome of the k^{th} individual. Letter e stands for empty location, i.e. there is no gene in this location while n^k is the k^{th} individual chromosomes number. Each individual can have a different number of chromosomes, i.e. it can belong to a different species.

$(g_{11})^k$	$(g_{12})^k$	...	$(g_{1m})^k$	n^k
$(g_{21})^k$	$(g_{22})^k$	...	$(g_{2m})^k$	
...	...	...	...	
...	...	...	...	
$(g_{n1})^k$	$(g_{n2})^k$	...	$(g_{nm})^k$	
e	e	e	e	

Figure 1.5: Structure of the individual's genotype with variable number of chromosome in BIANCA.

As an example, for a composite laminate, one can assume, as design variables, the number of layers, their orientation angles and thickness. The genotype of the individual-laminate is structured as shown in Fig. 1.6. In this case the number of layers of the k^{th} laminate is n^k while the orientation and the thickness of the i^{th} ply are δ_i and h_i, respectively. One can notice that the number of layers n^k is the number of chromosomes

of the k^{th} individual, while the orientation and thickness of the i^{th} layer correspond to the two genes of the i^{th} chromosome.

$(\delta_1)^k$	$(h_1)^k$	n^k
$(\delta_2)^k$	$(h_2)^k$	
...	...	
...	...	
$(\delta_n)^k$	$(h_n)^k$	
e	e	

Figure 1.6: Example of individual-laminate with variable number of layers in BIANCA.

1.4.2 Encoding/decoding of the optimisation variables

In BIANCA, the representation of the definition range of each design variable is realised using the *pointers*, which represent integer quantities. It exists a one-to-one relationship between variables and pointers. This relationship is immediate in the case of discrete or grouped variables, in fact if the domain of definition have a finite dimension N, it is possible to enumerate all admissible values $v_i, (i = 1, ..., N)$ and build a link between each value v_i and the corresponding index i, i.e. the pointer of that value. When the design space is unbounded, we need to restrict it, defining lower and upper bounds to the space of admissible values for v_i, i.e. v_{min} and v_{max}, respectively. In the case of continuous variables, the first step is the discretisation of the definition domain by choosing a given precision p, and then it is possible to apply the same representation (i.e. through pointers) as for the case of discrete and grouped variables, see Fig.1.7.
In BIANCA pointers constitute the phenotype that is the physical expression of the individual's genotype, more precisely the single pointer is coded by a gene, and all the genetic operators are directly applied on the genes representing the variables. Therefore, we have two encoding/decoding steps: firstly, a encoding/decoding step is necessary to translate the binary value of the gene into the corresponding value of the pointer, and vice-versa, then the second step take place to translate the value of the pointer into the corresponding value of the design variable. More details can be found in [1, 2].

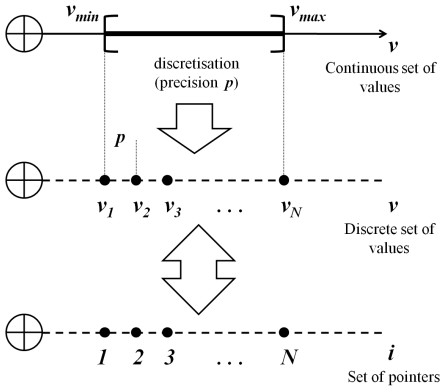

Figure 1.7: One-to-one relationship between continuous variables and *pointers* in BIANCA.

1.5 Evolution of individuals and species in BIANCA: new operators of crossover and mutation

In this Section, we present the new genetic operators introduced in BIANCA, for crossover and mutation on species. Some of these operators are inspired by the work of Park *et al* [53] and could be considered as a generalisation of those presented in [53]. These operators have, however, some original features because we intended to preserve, in this new version of the algorithm, a deep genetic recombination strategy, which proved to be effective in the previous version of the code.

In standard GAs, the classical reproduction phase takes place by means of crossover and mutation operators, which act on the genotype of the individuals.

In particular, in BIANCA crossover and mutation operate on a pair of homologous genes, with a given probability, p_{cross} and p_{mut} respectively, whose values are fixed by the user. Crossover and mutation are performed by means of Boolean operators, based on the computer-embedded binary representation of numbers. In this way, any decoding/encoding process, from binary to integer representation and vice-versa, is no longer needed and the genetic operations of crossover and mutation are much faster. The reader is addressed to [1] for more details on these aspects.

As previously said, with the introduction of the concept of reproduction between different species, new genetic operators are required in executing the reproduction phase. We remind that the number of design variables determines the number of chromosomes, i.e. the *biological species*. So, if the number of variables has to be included among the optimisation variables, and has to evolve during generations, a reproduction among the species has to be performed. In particular, the classical reproduction phase has been changed introducing new genetic operators called *Chromosome Shift operator*, *Chromosome Reorder*, *Chromosome Number Mutation* and *Chromosome Addition-Deletion*. A

brief description of these new operators and their use in the reproduction phase is given below.

1.5.1 The new crossover phase and the role of Chromosomes Shift and Reorder Operators

To explain the way whereby the reproduction phase takes place one can consider the following case. There are two *parents*, $P1$ and $P2$, with 3 and 5 chromosomes respectively, see Fig. 1.8 (a). In this example the maximum number of chromosomes is assumed equal to 6, while the minimum number can be chosen arbitrarily between 1 and 6: therefore in Fig. 1.8 (a), parent $P1$ shows 3 empty locations, while parent $P2$ only one. Moreover, there are two different variables for each individual, i.e. each chromosome has two different genes α and β. Before realizing the crossover on these two individuals, it can be noticed that there are different ways to pass the information restrained in the parents' genotype to the next generation, i.e. to their *children*. Here, at the next generation, two new individuals will be produced from this couple, one with 3 chromosomes and another one with 5 chromosomes. To improve the efficiency of the GA in terms of exploration and exploitation of the informations on the design space, the concept of *shift factor* is introduced. The shift factor (which is an integer number) is randomly sorted, with a given probability p_{shift}, in the range $\left[0, |n^{P1} - n^{P2}|\right]$, where $|n^{P1} - n^{P2}|$ is the absolute value of the difference of the parents' chromosomes number. Using the shift factor, various combinations of crossover are possible and the shift operator acts on the individual with the smaller number of chromosomes. In the example mentioned before, the minimum shift factor is 0 and the maximum is 2. For example, if the sorted value of the shift factor is 1, all the genes of $P1$, which has the smaller number of chromosomes, are shifted by a quantity equal to 1 up-to-down as shown in Fig. 1.8 (b).

After the shift operation, the crossover phase takes place. The crossover operator acts separately and independently on every single gene. The position of crossover is randomly chosen for each gene of both individuals. Naturally this operator involves all the chromosomes of the parent with the smaller number of them, i.e. in the case shown in Fig. 1.8 (c) all the genes of $P1$, while only the homologous genes of $P2$ undergo the action of crossover operator. At this point two new individuals are created, $C1$ and $C2$ that have 3 and 5 chromosomes respectively, see Fig. 1.8 (d). It can be noticed that the 1^{st} and 5^{th} chromosome of $P2$ have not undergone the crossover phase, so according to the notation of Fig. 1.8 (c) and (d) it is possible to write the following equalities, $(\alpha_1)^{P2} = (\alpha_1)^{C2}$,$(\alpha_5)^{P2} = (\alpha_5)^{C2}$ and $(\beta_1)^{P2} = (\beta_1)^{C2}$, $(\beta_5)^{P2} = (\beta_5)^{C2}$.
Before the mutation phase a readjustment of the chromosomes position is required. The *chromosome reorder* operator achieves this phase by a translation of all chromosomes down-to-up in the structure of the individual with the smaller number of them, see Fig. 1.8 (e).

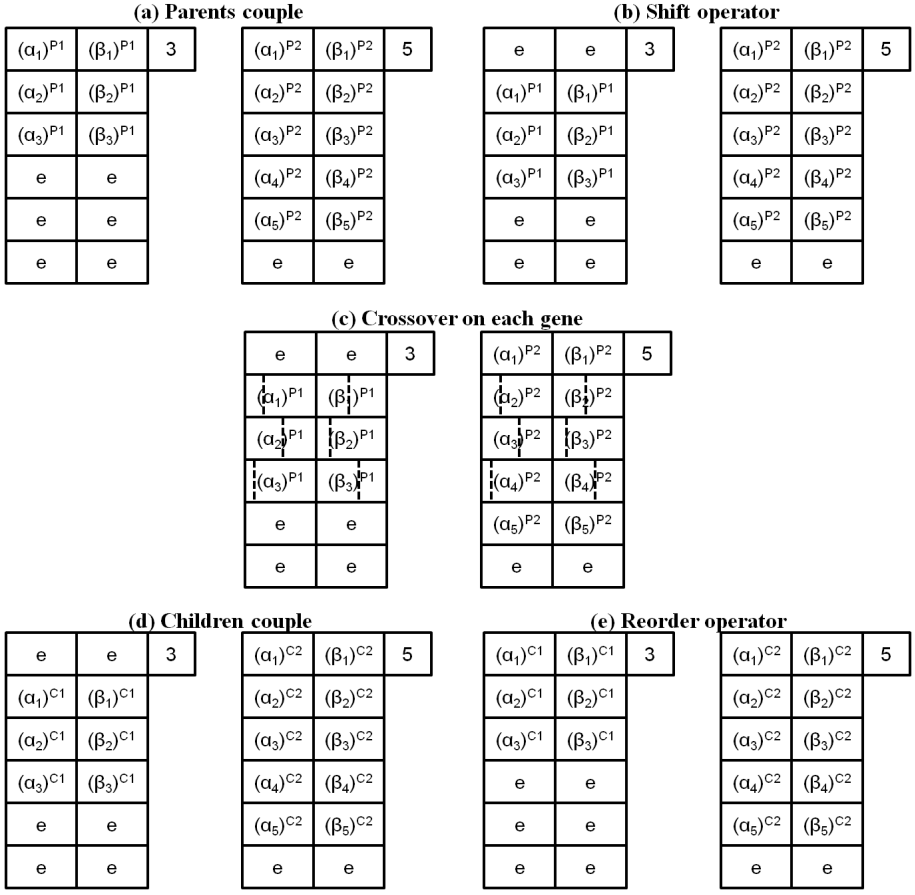

Figure 1.8: Crossover among species: (a) parents couple, (b) effect of the *shift* operator, (c) crossover on homologous genes, (d) children couple and (e) effect of the *chromosome reorder* operator.

1.5.2 The new mutation phase and the role of Chromosomes Number Mutation and Addition-Deletion Operators

Mutation is articulated in two phases: at a first stage, it acts on the number of chromosomes and then on the genes values.

During the first phase the chromosomes number is arbitrarily changed by one at time for each individual, with a given probability $(p_{mut})_{chrom}$, then the *chromosome addition-deletion* operator acts on the genotype of both individuals, by adding or deleting a chromosome. The location of chromosome addition-deletion is also randomly selected. Naturally, if the chromosomes number is equal to the maximum one, only deletion can occur. Similarly if the chromosomes number is equal to the minimum one, only addition can be applied. In the case shown in Fig. 1.9 (a) the number of chromosomes of $C1$ is decreased

by one and the chromosome deletion is randomly done at position 3, while the number of chromosomes of $C2$ is increased by one and a new one, $\left\{(\alpha_a)^{C2}, (\beta_a)^{C2}\right\}$, is randomly sorted and randomly added, in this example in correspondence of position 2.

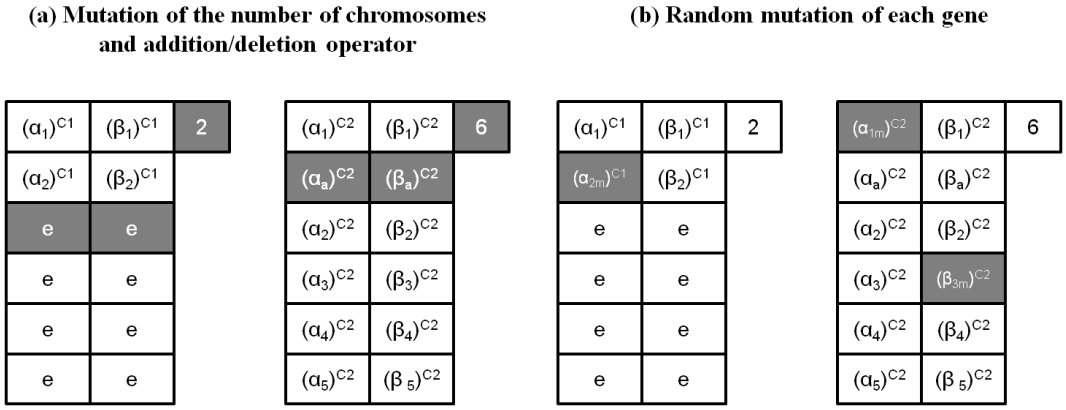

Figure 1.9: Mutation of species: (a) mutation of the number of chromosomes and effect of the *chromosome addition-deletion* operator, (b) effect of the mutation operator on every gene

During the second phase, the mutation of the genes value takes place, for instance one-bit change, with a probability p_{mut}, after a rearrangement of chromosomes position. In the example of Fig. 1.9 (b) the mutation occurs on the gene $(\alpha_2)^{C1}$ of the individual $C1$ and on the genes $(\alpha_1)^{C2}$ and $(\beta_3)^{C2}$ of the individual $C2$.

1.6 Handling constraints in BIANCA

1.6.1 Literature overview on constraints-handling techniques

Several authors put an effort in developing appropriate and effective strategies, in the framework of GAs, in order to deal with constrained optimisation problems. A certain number of surveys on constraint-handling techniques is available in the specialised literature, see for example [12, 54, 55, 56]. In this Section, we do not provide a complete and exhaustive survey on constraint-handling techniques that were developed in the last years to handle all types of constraints (linear, non-linear, equality and inequality) in the context of GAs. Rather, we focus our attention on penalty-based strategies for handling constraints.

The most common approach in the GA community to handle constraints (particularly, inequality constraints) consists in using penalties. Penalty functions were originally proposed by Courant in the 1940s [57] and later generalised by Carroll [58] and Fiacco and McCormick [59]. The idea that underlies such approaches consists in transforming

the constrained optimisation problem into an unconstrained one by adding some given values to the objective function, based on the amount of constraints violation (for each considered point within the design space).

In classical optimisation, two kinds of penalty functions are considered: exterior and interior. The exterior methods start by considering an infeasible solution and from there they move towards the feasible region. The interior methods set the penalty terms in such a way that their values are small at points located far from the constraint boundaries and go to infinity as the constraint boundaries are approached. Thus, if we start from a feasible point, the subsequent points generated will always belong to the feasible region since the constraint boundaries act as barriers during the optimisation process. Nevertheless, the requirement of starting from an initial feasible solution is precisely the main drawback of interior penalties. For this reason the method most commonly employed, in the framework of GAs, is the exterior penalty approach and therefore, we focus our discussion only on such a technique.

In the framework of the penalty-based approach the constrained NLPP of Eq. (1.33) is transformed into an unconstrained one, by defining a new modified objective function as follows:

$$\min_{\mathbf{x}} \ \Phi_p(\mathbf{x}) \ ,$$
$$\text{where :}$$
$$\Phi_p(\mathbf{x}) = \begin{cases} \Phi(\mathbf{x}) & \text{if } g_i(\mathbf{x}) \leq 0 \text{ and } h_j(\mathbf{x}) = 0 \ , \\ \Phi(\mathbf{x}) + \sum_{i=1}^{r} c_i G_i(\mathbf{x}) & \text{if } g_i(\mathbf{x}) > 0 \text{ and } h_j(\mathbf{x}) = 0 \ , \\ \Phi(\mathbf{x}) + \sum_{j=1}^{m} q_j H_j(\mathbf{x}) & \text{if } g_i(\mathbf{x}) \leq 0 \text{ and } h_j(\mathbf{x}) \neq 0 \ , \\ \Phi(\mathbf{x}) + \sum_{i=1}^{r} c_i G_i(\mathbf{x}) + \sum_{j=1}^{m} q_j H_j(\mathbf{x}) & \text{if } g_i(\mathbf{x}) > 0 \text{ and } h_j(\mathbf{x}) \neq 0 \ , \end{cases} \tag{1.36}$$
$$i = 1, ..., r \ , \ j = 1, ..., m \ ,$$

where Φ_p is the penalised (or expanded) objective function, while c_i and q_j are the penalty coefficients for inequality and equality constraints, respectively. The quantities $G_i(\mathbf{x})$ and $H_j(\mathbf{x})$ are defined as:

$$\begin{aligned} G_i(\mathbf{x}) &= \max[0, g_i(\mathbf{x})] \qquad i = 1, ..., r \ , \\ H_j(\mathbf{x}) &= \max[0, |h_j(\mathbf{x})| - \epsilon] \quad j = 1, ..., m \ . \end{aligned} \tag{1.37}$$

It can be noticed that in Eq.(1.36) and (1.37) equality constraints were transformed (as normally done in the literature) into inequality ones having the form:

$$|h_j(\mathbf{x})| - \epsilon \leq 0 \ , \tag{1.38}$$

which is numerically "acceptable" until the allowed tolerance ϵ assumes a sufficient small value that does not affect the quality of the solution of the problem. The advantage is that at this point all constraints are of the same nature (inequalities) and they can be treated by the same technique of constraint-handling.

As specified in [56], the penalty should be kept as low as possible, just above the limit below which infeasible solutions are optimal (this is called, the *minimum penalty rule* [60]). This is due to the fact that if the penalty is too high or too low, then the GA might have some difficulties in finding an appropriate feasible optimal solution [12, 60].

In fact, on one hand, if the penalty is too high and the optimum point is placed on the boundary of the feasible region, the GA is pushed inside the feasible region very quickly, and it is not able to move back towards the boundary between the feasible and infeasible regions, i.e. a large penalty discourages the exploration of the infeasible region since the beginning of the search process. As an example, if there are several disjointed feasible regions in the search space, the GA tends to move only to one of them, and, probably, it is not able to move towards a different feasible region unless they are very close to each other.

On the other hand, if the penalty is too low, a lot of the search time is spent in exploring the infeasible region because the penalty term is often negligible with respect to the objective function and the algorithm might converge to an optimum outside the feasible domain. These issues are very important in GAs, because in several problems the optimal solution lies close to or on the boundary between the feasible and the infeasible regions. The minimum penalty rule is conceptually simple, but it is not necessarily easy to implement. The main reason is that, in the most part of real-world engineering problems, we do not know *a priori* the exact location of the boundaries among feasible and infeasible regions (e.g. very often the constraints as well as the objective function are not given in algebraic form, but are the outcome of a numerical process).

Several researchers conducted different studies focused on the design of penalty functions: among them, the most well-known is the one conducted by Richardson *et al.* [61]. From this work the following guidelines were derived:

1. penalties which depend upon the distance of the current point-solution from the feasible region of the domain perform better than those which only depend on the number of violated constraints;

2. for a problem having few constraints, and few feasible solutions, penalties which are only functions of the number of violated constraints are not likely to produce any solutions;

3. good penalty functions can be built starting from two quantities: the *maximum completion cost* and the *expected completion cost*. The *completion cost* has to be intended as the distance of the considered point from the feasible region;

4. penalties should be close to the expected completion cost, but should not frequently fall below it. The more accurate the penalty, the better will be the solution found. When a penalty often underestimates the completion cost, then the search may fail to find a solution.

Following these guidelines, several researchers tried to derive good techniques to build penalty functions. In this Section we do not provide the mathematical details of each approach, rather, we briefly describe the different types of penalty-based strategies that can be found in the literature, along with the corresponding advantages and drawbacks.

The main and most common used penalty-based approaches are:

- *static penalties*. Under this category, we consider approaches wherein the penalty factors do not depend on the current generation and, therefore, they remain constant during the entire optimisation process. Several researchers have proposed different methods to define the expanded objective function using the static penalty approach, see for instance [61, 62, 63, 64]. In all cases the main drawback of those approaches consists in the fact that these strategies rely on some extra-parameters (namely one or more penalty factors) which are difficult to generalise and normally remain problem-dependent;

- *dynamic penalties*. Within this category, we consider penalty functions wherein the penalty factors depend upon the current generation (normally the extended objective function is defined in such a way that it increases over time, i.e. along the generations). Examples of dynamic penalties approaches can be found in [65, 66]. Some researchers argued that dynamic penalties work better than static penalties. Nevertheless, in practice it is difficult to built good dynamic penalty functions as it is difficult to produce good penalty factors for static functions. It seems that the problems associated to static penalty functions are also present in dynamic penalties strategies. All the techniques described in the works cited above depend on a certain number of extra-parameters: if a bad penalty factor is chosen, the GA may converge to either non-optimal feasible solutions (if the penalty is too high) or to infeasible solutions (if the penalty is too low);

- *adaptive penalties*. Such a strategy employs a penalty function which takes a feedback from the search process during the generations. Several researchers have tried to develop a penalty function that, taking some information from the population at the current generation (e.g. the amount of constraints violation, the number of violated constraints for each individual and so on), performs better than the previous methods, see [55, 67, 68, 69, 70, 71]. However, in all the previous works the expanded objective function depends upon a certain number of parameters that the user must set before starting the calculation (again, we have the same issues as in the case of static penalty approach);

- *death penalty.* The rejection of infeasible individuals is probably the easiest way to handle constraints and it is also computationally efficient, because when a point of the domain violates a constraint the GA assigns it a fitness equal to zero. Therefore, no further calculations are necessary to estimate the level of constraint violation of such a solution. Normally, the GA iterates recursively, generating a new point, until a feasible solution is found [72]. This might be a rather lengthy process in problems wherein is very difficult to approach the feasible region. Moreover, this method is limited to problems wherein the feasible region is convex and constitutes a reasonably large portion of the whole domain [56]. The main drawback of the death penalty strategy consists in a lack of exploitation and exploration of any information coming from the infeasible region that might be generated by the GA to guide the search. In fact, a common issue of such an approach is that if there are no feasible solutions in the initial population (which is normally randomly generated) then the evolutionary process will "stagnate" because all the individuals will have the same fitness (i.e., zero).

Within the framework of penalty-based approaches we can enumerate also other strategies like, for instance, *Segregated genetic algorithm*, *Annealing penalties* and *Co-evolutionary penalties*, see [56]. Nevertheless an adequate analysis of such methods falls outside the scopes of the present work (in fact, they represent particular numerical strategies originally developed to deal with particular kind of optimisation problems). For a deeper insight in the matter the reader is addressed to [56].
In the next subsection we introduce the Automatic Dynamic Penalisation (ADP) strategy for handling constraints that we have implemented within BIANCA.

1.6.2 The Automatic Dynamic Penalisation (ADP) strategy

The ADP strategy is an original method, firstly presented in [1], that we have developed and generalised in this work for automatically choosing and updating the penalty coefficients. The basic idea is that some infeasible individuals can be anyway important to drive the exploration towards interesting zones of the feasible domain, namely when the optimum point lies on its boundary, i.e. on an active constraint. For this reason, in the context of the ADP strategy, infeasible points are not automatically excluded from the population and are used to dynamically update the penalty coefficients in an automatic way, i.e. without the intervention of the user. This is especially important at the early stages of the search in order to widely explore the whole search space.

Concerning the penalty coefficients c_i and q_j of Eq.(1.36), in classical penalty-based methods, the user have to properly set their values in order to ensure that the search of solutions is forced within the feasible domain. Nevertheless, the choice of these coefficients is very difficult and it is common practice to estimate their values by trial and error. Moreover, it could be useful to adjust penalty pressure along the generations by tuning

these coefficients, but this is directly linked to a deep knowledge of the nature of the optimisation problem at hand.

The main concept that underlies the ADP strategy is that it is possible to exploit the information restrained in the whole population (also the infeasible part of it), at the current generation, to better guide the search through the whole search space. Generally, at the first generation the population is randomly generated. The individuals are more or less uniformly distributed over both feasible and infeasible regions of the definition domain and the corresponding values of objective and constraints functions can be used to estimate an appropriate level of penalisation, i.e. the values of the penalty coefficients c_i and q_j.

At each current generation, inside the population we can separate feasible and infeasible individuals, see Fig. 1.10, and we can also classify each one of the two groups in terms either of the values of the objective function or of the amount of constraint violation. Thus, the best individual of each group is the potential candidate to be solution of the optimisation problem on the feasible and infeasible sides of the domain, respectively. Then, we choose the following definition of the penalty coefficients:

$$\begin{aligned} c_i(t) &= \frac{|\Phi^F_{best} - \Phi^{NF}_{best}|}{(G_i)^{NF}_{best}} \quad i = 1, ..., r \ , \\ q_j(t) &= \frac{|\Phi^F_{best} - \Phi^F_{best}|}{(H_j)^{NF}_{best}} \quad j = 1, ..., m \ . \end{aligned} \tag{1.39}$$

In Eq.(1.39) the coefficients c_i and q_j are evaluated at the current generation t, while the superscripts F and NF stand for feasible and non-feasible, respectively. Φ^F_{best} and Φ^{NF}_{best} are the values of the objective function for the best individuals within the feasible and the infeasible side of the domain, respectively, whilst $(G_i)^{NF}_{best}$ and $(H_i)^{NF}_{best}$ represent the violated inequality and equality constraints for the best infeasible solution.

The main reason that underlies the definition of Eq.(1.39) is that some performing infeasible solutions (in terms of objective function values, i.e. infeasible minima) are retained within the population and act as "attraction points", improving in this way the search properties of the GA. In other words, the presence of such infeasible points within the population improves the exploration of the whole search domain, particularly around the boundaries between feasible and infeasible sides. In particular, it is worth noting that substituting Eq.(1.39) into Eq.(1.36), the value of the objective function for the best infeasible individual is forced to be equal to that of the best feasible individual. Such a situation is very convenient, mostly for what concerns the case of non-linear, non-convex optimisation problems wherein the global unconstrained minimum is located within the infeasible region and, potentially, the global constrained minimum lies on the boundary. In such conditions, the best individual of the infeasible side owns the same fitness as the best feasible individual, and thus the same probability to be selected in order to take part into the genetic operations of crossover and mutation. As a consequence, its genetic

patrimony is likely to be inherited by the following generation. Consequently, the GA can handle the information coming from the infeasible region in order to drive the search towards more convenient sub-domains (namely towards the boundaries between feasible and infeasible sides).

It appears clearly that the estimation of the penalty factors, according to Eq.(1.39), can be repeated at each generation, thus tuning the appropriate penalty pressure on the current population. The main advantages of such an approach are substantially two:

- this procedure is *automatic* and problem-independent because the GA can automatically calculate the values of the penalty coefficients without the intervention of the user by simply exploiting the values of the objective and constraint functions in the current population;
- the method is *dynamic* since the evaluation of the penalty level is updated at each generation, and this allows the values of the penalty coefficients to be the most suitable to the current distribution of feasible and infeasible individuals in the population, the expected effect being eventually to extinguish the infeasible group in the population or to limit infeasible individuals to regions close to the boundary between feasible and infeasible domains.

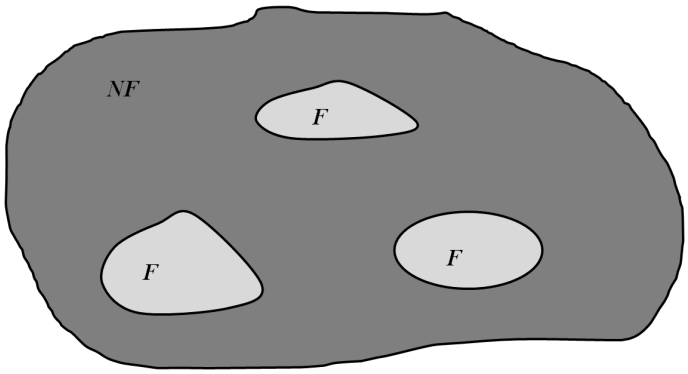

Figure 1.10: Feasible and infeasible regions of the definition domain

From a practical point of view, the ADP strategy is implemented within BIANCA according to the following logical steps:

- *Case 1*: feasible individuals (with respect to the k^{th} constraint function) within the current population
  1. the individuals of the whole population are firstly classified with respect to the violation or non-violation of the k^{th} constraint function;

2. the individuals which are infeasible with respect to the k^{th} constraint function, are then grouped and ranked with respect to their objective function values: the objective function of the best individual of such a sub-space is Φ_{best}^{NF}, while the k^{th} violated constrain function is $(G_k)_{best}^{NF}$ (or $(H_k)_{best}^{NF}$ in the case of equality constraints);
3. the individuals which are feasible with respect to the k^{th} constraint function, are then grouped and ranked with respect to their objective function values: the objective function of the best individual of such a group is Φ_{best}^{F};
4. the penalty coefficient c_k (or q_k) is then evaluated according to Eq.(1.39).

- *Case 2*: no feasible individuals (with respect to the k^{th} constraint function) within the current population

1. the individuals of the whole population are firstly classified with respect to the violation of the k^{th} constraint function;
2. the individuals are then sorted into two different groups: the individuals having smaller values of the k^{th} violated constraint are grouped in a sub-space of "virtually feasible" individuals (with respect to the k^{th} constraint function), while the rest are grouped in the sub-space of infeasible individuals. The number of individuals grouped in the "virtually feasible" region corresponds to 10% of the population size;
3. the remaining 90% individuals in the population, which are considered "effectively infeasible" with respect to the k^{th} constraint function are ranked in terms of their objective function values: the objective function of the best individual of such a sub-space is Φ_{best}^{NF}, while the k^{th} violated constraint function is $(G_k)_{best}^{NF}$ (or $(H_k)_{best}^{NF}$ in the case of equality constraints);
4. the individuals within the "virtually feasible" region (with respect to the k^{th} constraint function) are ranked with respect to their objective function values: the objective function of the best individual of such a group is Φ_{best}^{F};
5. the penalty coefficient c_k (or q_k) is then evaluated according to Eq.(1.39);

It is worth noting that, in the context of the ADP strategy, each constraint is treated separately and independently from each other.

To understand the way whereby the ADP strategy acts on the individuals within the population, and also to show its effectiveness, let us consider the following optimisation problem:

$$\min_{\mathbf{x}} \ \Phi(x_1, x_2) = -\mathrm{e}^{ka\sqrt{x_1^2+x_2^2}} \sin(ax_1)\cos(2bx_2) \ ,$$
$$\text{subject to :}$$
$$\begin{cases} g(x_1, x_2) = \mathrm{e}^{cx_1^2} - 1 - x_2 \leq 0 \ , \\ 0 \leq x_1 \leq 4\pi \ , \\ 0 \leq x_2 \leq 2\pi \ , \end{cases} \tag{1.40}$$

where $a = 1$, $b = 0.6$, $c = 0.012$ and $k = 0.2$ are constant parameters. A 3D plot of the objective function $\Phi(x_1, x_2)$ and of the constraint $g(x_1, x_2)$ is given in Fig. 1.11. It can be noticed that such a function is highly non-linear and non-convex with several local minima into the feasible region, while the global unconstrained minimum is placed on the infeasible side. However, the global constrained minimum lies on the boundary between the two regions and very close to the global unconstrained (infeasible) minimum.

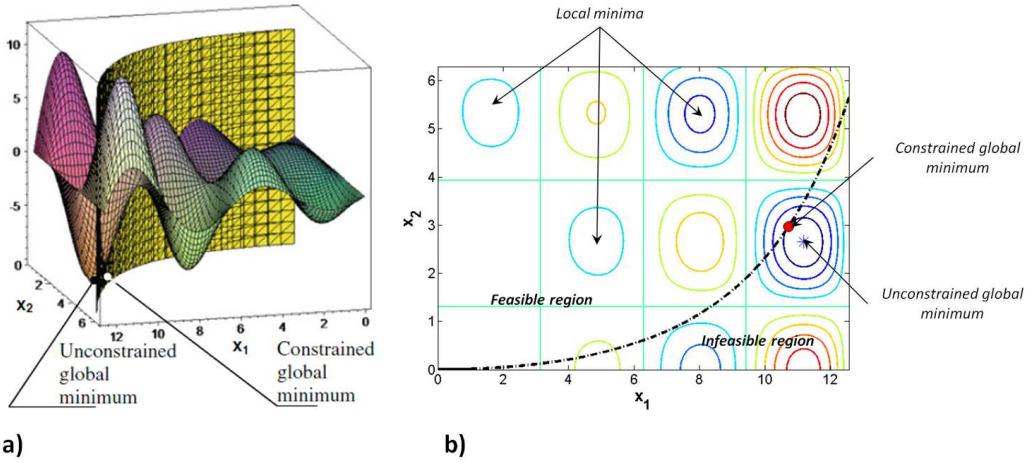

Figure 1.11: a) 3D plot and b) contour plot of the objective and constraint functions on the definition domain

To solve problem (1.40), we used the GA BIANCA with a population of $N_{ind} = 200$ individuals evolving along $N_{gen} = 100$ generations. In addition, the crossover and mutation probabilities are $p_{cross} = 0.85$ and $p_{mut} = 1/N_{ind}$, respectively. The selection is performed through the roulette-wheel operator, the elitism is active and the ADP method has been used for handling constraints.

The values of the constrained global minimum and of the constraint function found by BIANCA are $\Phi = -8.09933$ and $g = -0.00443$, respectively, whilst the optimal values of the design variables are $x_1 = 10.71119$ and $x_2 = 2.96646$. Fig. 1.12 shows the evolution of the distribution of the individuals over the definition domain along the generations. It can be noticed that at the initial generation the population is uniformly distributed over

the design space (Fig. 1.12 (a)). After 20 generations (Fig. 1.12 (b)) some individuals move towards the local feasible minimum, while the rest of the population moves towards the global constrained minimum. It can be noticed that after 20 generations we still have some infeasible individuals placed around the global unconstrained (infeasible) minimum that acts as an attractor for the solution search process. The GA uses such points (and the related genetic information) in order to drive the search to the regions placed near the boundary. After 50 generations (Fig. 1.12 (c)) all the individuals are very close to the true constrained minimum.

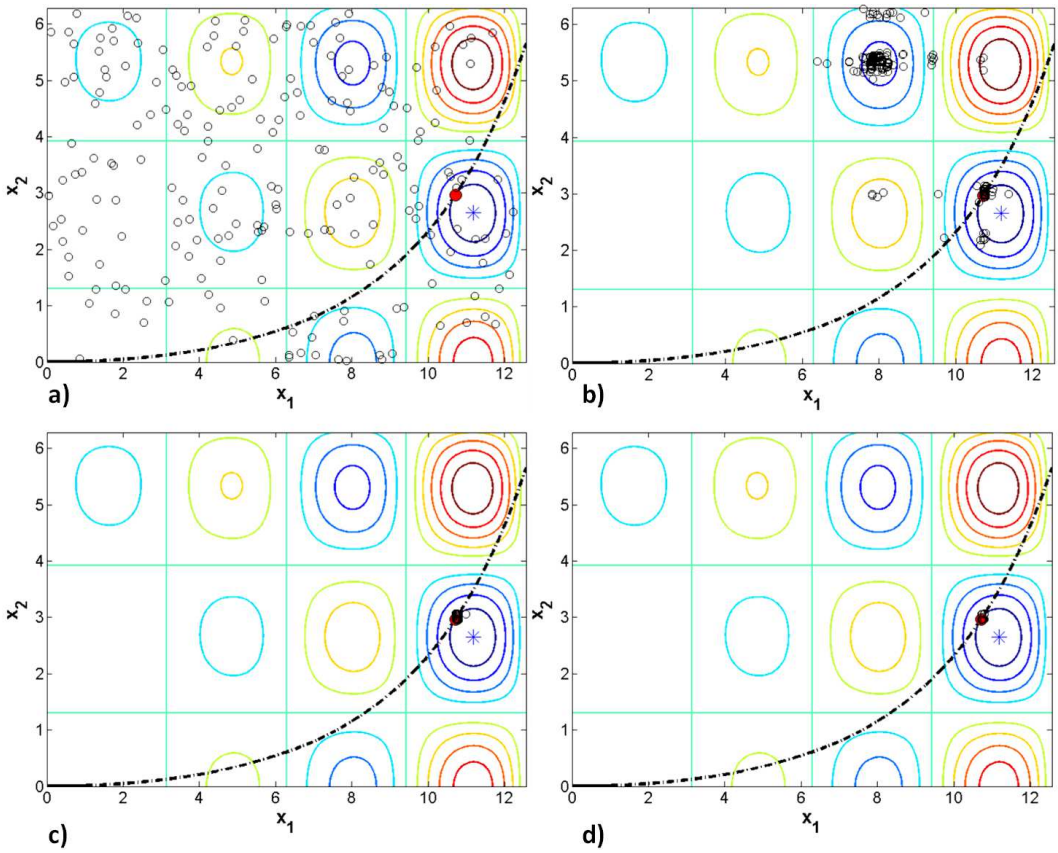

Figure 1.12: Distribution of the individuals over the search space along the generations for problem (1.40): a) initial generation, b) after 20 generations, c) after 50 generations, d) final generation

1.7 Some benchmark problems to test the ADP strategy

To have an idea of the effectiveness of the ADP strategy, we consider three benchmark problems belonging to the engineering world, which were extensively studied in the literature.

Such benchmark problems are: the welded beam problem, originally proposed by Rao [73], the pressure vessel problem, firstly studied by Kannan and Kramer [74], and the tension-compression spring problem taken from Arora [75] and Belugundu [76].

Concerning the genetic parameters employed in all the simulations, the population is composed of N_{ind} individuals evolving along a fixed maximum number of generation N_{gen}. For each considered benchmark we perform 30 runs of our GA, and, for each run, 80000 fitness evaluations are carried out. This implies that such a number of fitness evaluations can be obtained with various combinations of number of individuals and maximum number of generations, i.e. the parameters N_{ind} and N_{gen} must satisfy the following relationship:

$$N_{gen} \times N_{ind} = 80000 \ . \tag{1.41}$$

In addition, the crossover and mutation probabilities are $p_{cross} = 0.85$ and $p_{mut} = 1/N_{ind}$, respectively. The selection is performed by the roulette-wheel operator, the single-individual elitism is active and, of course, the ADP method is used for handling constraints. Moreover, since for such problems the genotype of the individual is composed by a single chromosome, the genetic operators that perform the crossover and mutation among individuals belonging to different species are no longer required.

For each test-case, we compare our results with the ones reported in the literature and obtained by other researchers by the use of several EA-based methods which employ different constraint-handling techniques.

1.7.1 The welded beam problem

The welded beam problem was originally studied by Rao [73]. In such a problem a welded beam is designed for minimum cost subject to constraints on shear stress (τ), bending stress in the beam (σ), buckling load on the bar (P_c), end deflection of the beam (δ), and side constraints. There are four design variables as shown in Fig. 1.13 : $x_1 = h$, $x_2 = l$, $x_3 = t$ and $x_4 = b$.

The problem can be stated as follows:

$$
\begin{aligned}
&\min_{\mathbf{x}} \ \Phi(\mathbf{x}) = 1.10471 x_1^2 x_2 + 0.04811 x_3 x_4 (14.0 + x_2) \ , \\
&\text{subject to :} \\
&\begin{cases}
g_1(\mathbf{x}) = \tau(\mathbf{x}) - \tau_{max} \leq 0 \ , \\
g_2(\mathbf{x}) = \sigma(\mathbf{x}) - \sigma_{max} \leq 0 \ , \\
g_3(\mathbf{x}) = x_1 - x_4 \leq 0 \ , \\
g_4(\mathbf{x}) = 0.10471 x_1^2 + 0.04811 x_3 x_4 (14.0 + x_2) - 5.0 \leq 0 \ , \\
g_5(\mathbf{x}) = 0.125 - x_1 \leq 0 \ , \\
g_6(\mathbf{x}) = \delta(\mathbf{x}) - \delta_{max} \leq 0 \ , \\
g_7(\mathbf{x}) = P - P_c(\mathbf{x}) \leq 0 \ , \\
0.1 \leq x_1 \leq 2.0 \ , \\
0.1 \leq x_2 \leq 10.0 \ , \\
0.1 \leq x_3 \leq 10.0 \ , \\
0.1 \leq x_4 \leq 2.0 \ ,
\end{cases}
\end{aligned}
\tag{1.42}
$$

where:

$$
\begin{aligned}
&\tau(\mathbf{x}) = \sqrt{\tau_1^2 + 2\tau_1\tau_2 \frac{x_2}{2R} + \tau_2^2} \ , \\
&\tau_1 = \frac{P}{\sqrt{2} x_1 x_2} \ , \ \tau_2 = \frac{MR}{J} \ , \ M = P(L + \frac{x_2}{2}) \ , \\
&R = \sqrt{\left(\frac{x_2}{2}\right)^2 + \left(\frac{x_1 + x_3}{2}\right)^2} \ , \\
&J = 2\left\{ \sqrt{2} x_1 x_2 \left[\frac{x_2^2}{12} + \left(\frac{x_1 + x_3}{2}\right)^2 \right] \right\} \ , \\
&\sigma(\mathbf{x}) = 6\frac{PL}{x_4 x_3^2} \ , \ \delta(\mathbf{x}) = \frac{4PL^3}{E x_4 x_3^3} \ , \\
&P_c(\mathbf{x}) = \frac{4.013 E \sqrt{x_3^2 x_4^6 / 36}}{L^2} \left(1 - \frac{x_3}{2L} \sqrt{\frac{E}{4G}} \right) \ .
\end{aligned}
\tag{1.43}
$$

The quantities P, L, δ_{max}, τ_{max}, σ_{max}, E and G are constant parameters and their numerical values, in the appropriate units [56], are: $P = 6000$, $L = 14$, $\delta_{max} = 0.25$, $\tau_{max} = 13600$, $\sigma_{max} = 30000$, $E = 30 \times 10^6$ and $G = 12 \times 10^6$.

The approaches employed to deal with such a problem are: geometric programming (Ragsdell and Phillips [77]), standard GA with static penalty function (Deb [78]), an

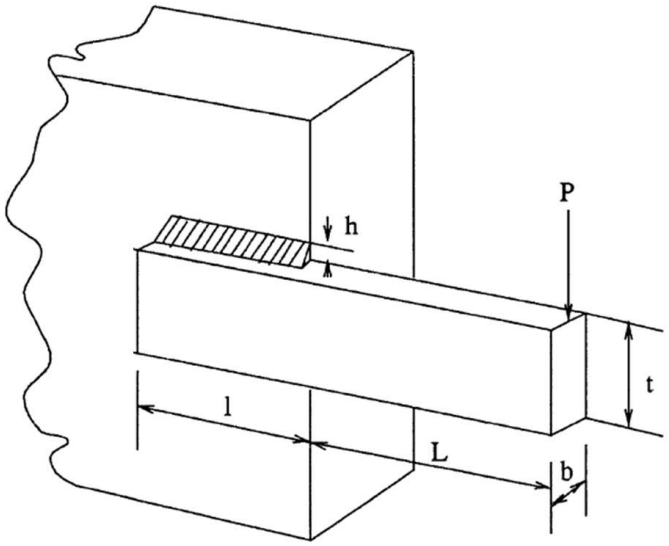

Figure 1.13: Rough sketch of the welded beam considered within the optimisation problem (1.42), taken from [56]

improved GA with a feasibility-based tournament selection scheme inspired by the multi-objective optimisation techniques (Coello and Montes [79]), a co-evolutionary particle-swarm strategy for constrained optimisation problems (He and Wang [80]), a hybrid particle-swarm optimisation with feasibility rules (He and Wang [81]) and a hybrid GA with flexible allowance technique (Zhao *et al.* [82]).

Concerning the GA BIANCA, in order to satisfy the condition on the maximum number of fitness evaluations of Eq.(1.41), we consider a population of $N_{ind} = 250$ individuals evolving along $N_{gen} = 320$ generations.
The best solution found by BIANCA as well as the best solutions obtained by the aforementioned approaches are listed in Table 1.2, while the statistical results for each considered strategy are detailed in Table 1.3. Fig. 1.14 shows the variation of the best solution along the generations. It can be noticed that the global minimum is found after 260 generations.

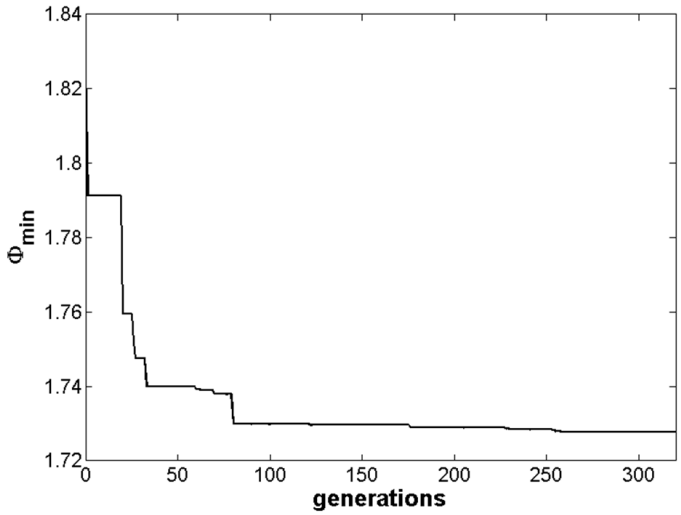

Figure 1.14: Best values of the objective function along the generations for the optimisation problem (1.42)

Design variables	BIANCA	Zhao *et al.* [82]	He and Wang [81]	He and Wang [80]	Coello and Montes [79]	Deb [78]	Ragsdell and Phillips [77]
x_1	0.205501	0.205730	0.205730	0.202369	0.205986	0.248900	0.245500
x_2	3.475070	3.470489	3.470489	3.544214	3.471328	6.173000	6.196000
x_3	9.037540	9.036624	9.036624	9.048210	9.020224	8.178900	8.273000
x_4	0.205751	0.205730	0.205730	0.205723	0.206480	0.253300	0.245500
Constraints							
$g_1(\mathbf{x})$	−0.021384	N.A.	N.A.	−12.839796	−0.074092	−5758.603777	−5743.826517
$g_2(\mathbf{x})$	−9.195431	N.A.	N.A.	−1.247467	−0.266227	−255.576901	−4.715097
$g_3(\mathbf{x})$	−0.000250	N.A.	N.A.	−0.001498	−0.000495	−0.004400	0
$g_4(\mathbf{x})$	−3.432263	N.A.	N.A.	−3.429347	−3.430043	−2.982866	−3.020289
$g_5(\mathbf{x})$	−0.080501	N.A.	N.A.	−0.079381	−0.080986	−0.123900	−0.120500
$g_6(\mathbf{x})$	−0.235546	N.A.	N.A.	−0.235536	−0.235514	−0.234160	−0.234208
$g_7(\mathbf{x})$	−2.269075	N.A.	N.A.	−11.681355	−58.666440	−4465.270928	−3604.275002
Objective							
$\Phi(\mathbf{x})$	1.725436	1.724852	1.724852	1.728024	1.728226	2.433116	2.385937

Table 1.2: Comparison between the best solutions found with different penalty-based approaches for the optimisation problem (1.42) (N.A. stands for "Not Available").

Method	Best	Mean	Worst	Standard deviation
BIANCA	1.725436	1.752201	1.793233	0.023001
Zhao *et al.* [82]	1.724852	1.724852	1.724852	5.8×10^{-16}
He and Wang [81]	1.724852	1.749040	1.814295	0.040000
He and Wang [80]	1.728024	1.748831	1.782143	0.012926
Coello and Montes [79]	1.728226	1.792654	1.993408	0.074713
Deb [78]	2.433116	N.A.	N.A.	N.A.
Ragsdell and Phillips [77]	2.385937	N.A.	N.A.	N.A.

Table 1.3: Statistical results found with different penalty-based approaches for the optimisation problem (1.42) (N.A. stands for "Not Available").

1.7.2 The pressure vessel problem

A cylindrical vessel is capped at both ends by hemispherical heads as shown in Fig. 1.15. The goal of this problems consists in minimising the total cost of the structure, including the cost of the material, forming and welding. The design variables are: the thickness of the shell $x_1 = T_s$, the thickness of the head $x_2 = T_h$, the inner radius $x_3 = R$ and the length of the cylindrical section of the vessel (not including the head) $x_4 = L$. Moreover, T_s and T_h are real discrete design variables discretised with a precision $\Delta x_1 = \Delta x_2 = 0.0625$ (which corresponds to the available thickness of rolled steel plates), while R and L are continuous.

Using the same notation adopted by Kannan and Kramer [74], the problem can be stated as follows:

$$
\begin{aligned}
&\min_{\mathbf{x}} \ \Phi(\mathbf{x}) = 0.6224 x_1 x_3 x_4 + 1.7781 x_2 x_3^2 + 3.1661 x_4 x_1^2 + 19.84 x_3 x_1^2 \ , \\
&\text{subject to :} \\
&\begin{cases}
g_1(\mathbf{x}) = -x_1 + 0.0193 x_3 \leq 0 \ , \\
g_2(\mathbf{x}) = -x_2 + 0.00954 x_3 \leq 0 \ , \\
g_3(\mathbf{x}) = -\pi x_3^2 x_4 - \dfrac{4}{3}\pi x_3^3 + 1296000.0 \leq 0 \ , \\
g_4(\mathbf{x}) = x_4 - 240.0 \leq 0 \ , \\
0.0625 \leq x_1 \leq 6.1875 \ , \ \text{with } \Delta x_1 = 0.0625 \ , \\
0.0625 \leq x_2 \leq 6.1875 \ , \ \text{with } \Delta x_2 = 0.0625 \ , \\
10.0 \leq x_3 \leq 200.0 \ , \\
10.0 \leq x_4 \leq 200.0 \ .
\end{cases}
\end{aligned}
\tag{1.44}
$$

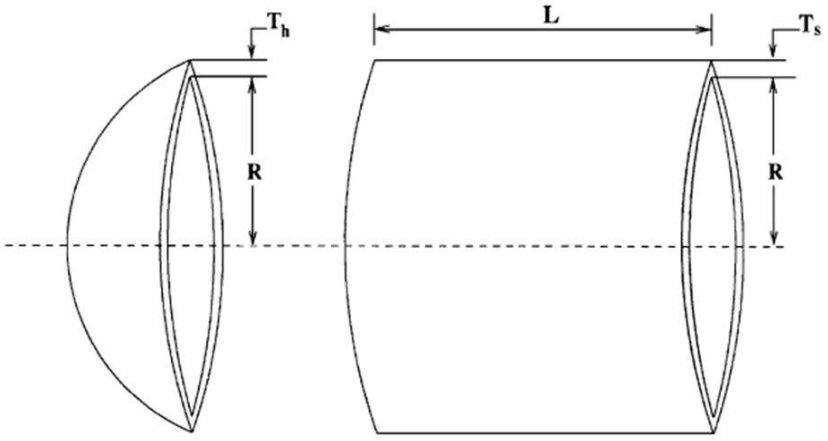

Figure 1.15: Rough sketch of the pressure vessel considered within the optimisation problem (1.44), taken from [56]

The approaches used in the literature to solve this problem are: an augmented Lagrangian multiplier approach (Kannan and Kramer [74]), a genetic adaptive search (Deb [83]), and, again, the aforementioned approaches of Coello and Montes [79], He and Wang [80, 81] and Zhao *et al.* [82].

In order to satisfy the condition on the maximum number of fitness evaluations of Eq.(1.41), the size of the population N_{ind} and the maximum number of generations N_{gen} in BIANCA are chosen equal to 400 and 200, respectively.
The best solution found by BIANCA as well as the best solutions obtained by the aforementioned approaches are listed in Table 1.4, while the statistical results for each considered strategy are detailed in Table 1.5. Fig. 1.16 shows the variation of the best solution along the generations. It can be noticed that the global minimum is found after only 20 generations.

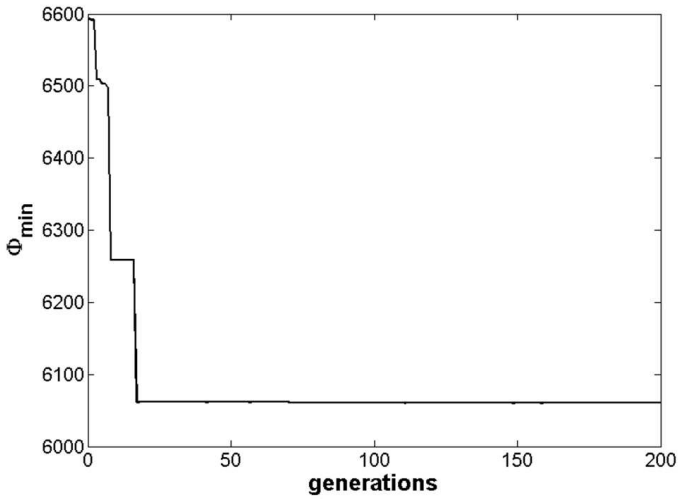

Figure 1.16: Best values of the objective function along the generations for the optimisation problem (1.44)

Design variables	BIANCA	Zhao *et al.* [82]	He and Wang [81]	He and Wang [80]	Coello and Montes [79]	Deb [83]	Kannan and Kramer [74]
x_1	0.812500	0.812500	0.812500	0.812500	0.812500	0.937500	1.125000
x_2	0.437500	0.437500	0.437500	0.437500	0.437500	0.500000	0.625000
x_3	42.096800	42.098456	42.098456	42.091266	42.097398	48.329000	58.291000
x_4	176.658000	176.636596	176.636596	176.746500	176.654050	112.679000	43.690000
Constraints							
$g_1(\mathbf{x})$	−0.000032	N.A.	N.A.	−0.000139	−0.000020	−0.004750	0.000016
$g_2(\mathbf{x})$	−0.035897	N.A.	N.A.	−0.035949	−0.035891	−0.038941	−0.068904
$g_3(\mathbf{x})$	−5.631534	N.A.	N.A.	−116.382700	−27.886075	−3652.876838	−21.220104
$g_4(\mathbf{x})$	−63.342000	N.A.	N.A.	−63.253500	−63.345953	−127.321000	−196.310000
Objective							
$\Phi(\mathbf{x})$	6059.9384	6059.7143	6059.7143	6061.0777	6059.9463	6410.3811	7198.0428

Table 1.4: Comparison between the best solutions found with different penalty-based approaches for the optimisation problem (1.44) (N.A. stands for "Not Available").

1.7.3 The tension-compression spring problem

The design problem of a tension-compression spring was firstly studied by Arora [75] and Belegundu [76]. The main goal is to minimise the weight of the tension-compression spring (as shown in Fig. 1.17) subject to constraints on the minimum deflection, the shear stress,

Method	Best	Mean	Worst	Standard deviation
BIANCA	6059.9384	6182.0022	6447.3251	122.3256
Zhao *et al.* [82]	6059.7143	6059.7143	6059.7143	2.8×10^{-12}
He and Wang [81]	6059.7143	6099.9323	6288.6770	86.2000
He and Wang [80]	6061.0777	6147.1332	6363.8041	86.4545
Coello and Montes [79]	6059.9463	6177.2533	6469.3220	130.9297
Deb [83]	6410.3811	N.A.	N.A.	N.A.
Kannan and Kramer [74]	7198.0428	N.A.	N.A.	N.A.

Table 1.5: Statistical results found with different penalty-based approaches for the optimisation problem (1.44) (N.A. stands for "Not Available").

the surge frequency and the outside diameter. The design variables are: the wire diameter $x_1 = d$, the mean coil diameter $x_2 = D$ and the number of active coils $x_3 = N_{coil}$.

Adopting the same notation of Arora [75], the problem can be stated as follows:

$$\begin{aligned}
&\min_{\mathbf{x}} \ \Phi(\mathbf{x}) = (x_3 + 2)\, x_2 x_1^2 \ , \\
&\text{subject to :} \\
&\begin{cases}
g_1(\mathbf{x}) = 1 - \dfrac{x_2^3 x_3}{71785.0 x_1^4} \leq 0 \ , \\
g_2(\mathbf{x}) = \dfrac{4x_2^2 - x_1 x_2}{12566.0(x_1^3 x_2 - x_1^4)} + \dfrac{1}{5108.0 x_1^2} - 1 \leq 0 \ , \\
g_3(\mathbf{x}) = 1 - \dfrac{140.45 x_1}{x_2^2 x_3} \leq 0 \ , \\
g_4(\mathbf{x}) = \dfrac{x_1 + x_2}{1.5} - 1 \leq 0 \ , \\
0.05 \leq x_1 \leq 2.0 \ , \\
0.25 \leq x_2 \leq 1.3 \ , \\
2.0 \leq x_3 \leq 15.0 \ ,
\end{cases}
\end{aligned} \tag{1.45}$$

We compare our results with the ones carried out through the following strategies taken from the literature: the numerical optimisation technique proposed by Belegundu [76], a numerical optimisation technique called "constraint correction at constant cost" (Arora [75]) and, again, the aforementioned approaches of Coello and Montes [79], He and Wang [80, 81] and Zhao *et al.* [82].

Concerning the GA BIANCA, in order to satisfy the condition on the maximum number of fitness evaluations of Eq.(1.41), we consider a population of $N_{ind} = 320$ individuals evolving along $N_{gen} = 250$ generations.

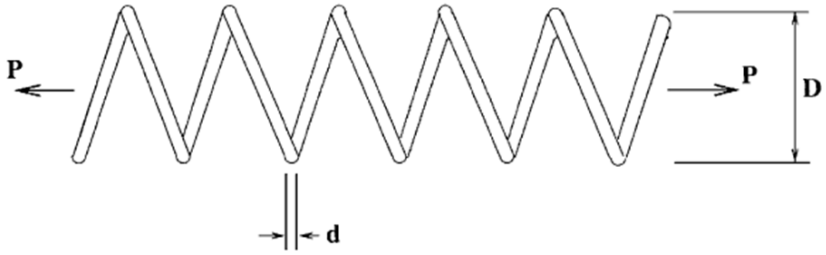

Figure 1.17: Rough sketch of tension-compression spring considered within the optimisation problem (1.45), taken from [80]

The best solution found by BIANCA as well as the best solutions obtained by the aforementioned approaches are listed in Table 1.6, while the statistical results for each considered strategy are detailed in Table 1.7. Fig. 1.18 shows the variation of the best solution along the generations. It can be noticed that the global minimum is found after only 50 generations.

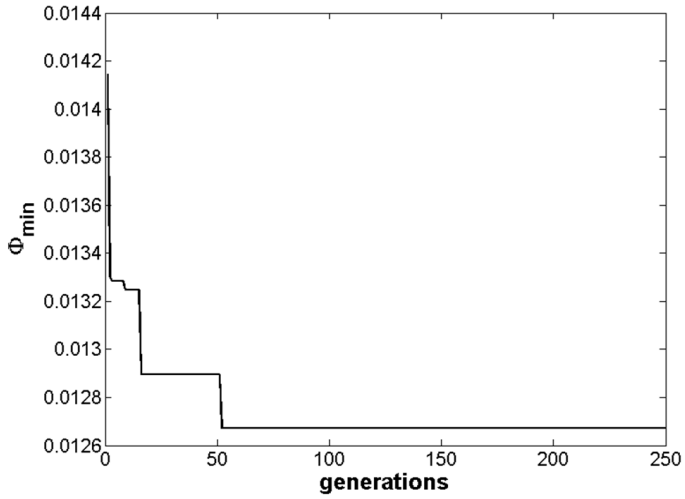

Figure 1.18: Best values of the objective function along the generations for the optimisation problem (1.45)

Design variables	BIANCA	Zhao *et al.* [82]	He and Wang [81]	He and Wang [80]	Coello and Montes [79]	Arora [75]	Belegundu [76]
x_1	0.051613	0.051689	0.051689	0.051728	0.051989	0.053396	0.050000
x_2	0.354839	0.356717	0.356717	0.357644	0.363965	0.399180	0.315900
x_3	11.404700	11.288966	11.288966	11.244543	10.890522	9.185400	14.250000
Constraints							
$g_1(\mathbf{x})$	-0.000256	N.A.	N.A.	-0.000845	-0.000013	0.000019	-0.000014
$g_2(\mathbf{x})$	-0.000112	N.A.	N.A.	-0.000013	-0.000021	-0.000018	-0.003782
$g_3(\mathbf{x})$	-4.048164	N.A.	N.A.	-4.051300	-4.061338	-4.123832	-3.938302
$g_4(\mathbf{x})$	-0.729032	N.A.	N.A.	-0.727090	-0.722698	-0.698283	-0.756067
Objective							
$\Phi(\mathbf{x})$	0.012671	0.012665	0.012665	0.012675	0.012681	0.012730	0.012833

Table 1.6: Comparison between the best solutions found with different penalty-based approaches for the optimisation problem (1.45) (N.A. stands for "Not Available").

Method	Best	Mean	Worst	Standard deviation
BIANCA	0.012671	0.012681	0.012913	5.123200×10^{-5}
Zhao *et al.* [82]	0.012665	0.012665	0.012665	3.200000×10^{-7}
He and Wang [81]	0.012665	0.012707	0.012719	1.608500×10^{-5}
He and Wang [80]	0.012675	0.012730	0.012924	5.198500×10^{-5}
Coello and Montes [79]	0.012681	0.012742	0.012973	5.900000×10^{-5}
Arora [75]	0.012730	N.A.	N.A.	N.A.
Belegundu [76]	0.012833	N.A.	N.A.	N.A.

Table 1.7: Statistical results found with different penalty-based approaches for the optimisation problem (1.45) (N.A. stands for "Not Available").

1.7.4 Discussion of results

Concerning the effectiveness and robustness of the GA BIANCA, we can see that for all the three considered benchmark problems, the quality of the results found using BIANCA is, practically, of the same order as that obtained via the hybrid strategies of He and Wang [81] and Zhao *et al.* [82]. Indeed, the relative errors (evaluated with respect to the solutions found by Zhao *et al.* [82]) are 0.0034% for the welded beam problem, 0.0004% for the pressure vessel problem and 0.0047% for the tension-compression string problem. In addition, one can notice that the average searching quality and the standard deviation of the results found by BIANCA in 30 independent runs are of the same order as the other methods (with the exception of the hybrid strategies).

Concerning the pressure vessel problem, it can be noticed that the strategy of Kannan and Kramer [74] produces a solution with a significantly lower value of L. This solution is, however, not feasible since the first constraint is slightly violated. The results produced by the other methods (including the ones found using BIANCA) indicate that it is more reasonable to variate the other design variables, allowing larger values of L because this leads to find feasible designs having a lower cost.

Concerning the tension-compression spring problem, it can be noticed that the solution found by Arora [75] has a lower value of the number of active coils N_{coil}. Indeed, such a solution is infeasible since the first constraint is slightly violated. We can see that the results produced by the other approaches (including the ones found using BIANCA) indicate that allowing greater values of the number of active coils N_{coil} leads the algorithm to find feasible designs showing a lower weight.

The hybrid GA with flexible allowance technique developed by Zhao *et al.* [82] is a hybrid GA with Levenberg-Marquardt mutation operator which creates new feasible individuals (offspring) by considering the auxiliary information coming from the evaluation of the constraints gradient. Such a strategy allows to obtain a numerically "exact" minimum for all the considered benchmarks. The authors assert that such solutions were found after only 20000 evaluations of the objective function (which corresponds to 1/4 of the number of evaluations carried out by the other considered methods).
Nevertheless, for such benchmark problems the objective and constraint functions are available in a closed algebraic form. Generally, this is not the case when dealing with optimisation of complex engineering systems (which require, for example, finite element calculations for the constraints and/or the objective function evaluation). In such cases, the results obtained via a hybrid GA, as the one proposed in [82], could be affected by the way wherein the derivatives of the constraints and objective function are evaluated (which represent a key-point for the Levenberg-Marquardt mutation operator). Moreover a more accurate analysis of the effectiveness and performances of such techniques (in terms of time spent to find a solution) could be made on the basis of the effective computing time rather than on the basis on the number of fitness evaluations, because the effective calculation cost includes also the evaluation of derivatives for the gradient-based operations of constraint repair.

Finally, we can assert that the main advantage of our approach relies on the fact that it remains a "purely" genetic approach: on one side, we do not need an estimation of auxiliary quantities, such as the derivatives of the constraint or objective functions, while on the other side, we practically have the same quality as the hybrid strategies in finding optimal solutions.

1.8 The interface of BIANCA with external software

In several problems, the value of the objective function and/or constraints, cannot be computed analytically, but it has to be evaluated using special numerical codes. Typically, this is the case of structural optimisation, where the most part of times the structural response is numerically assessed using finite-element (FE) codes. For these cases, a very general interface has been developed, which renders BIANCA able to exchange input/output informations with mathematical models supported by an external software.

Fig. 1.19 shows the structure of the data-exchange between BIANCA and a generic external software. For each individual, BIANCA performs the genetic operations, such as selection, crossover, mutation and so on, and then passes the design variables to the mathematical model built within the external environment. At this point, the external software evaluates the objective and the existing constraint functions values, and then passes them back to BIANCA. The data-exchange between BIANCA and the external software is simply done by means of two text files.

The first one is the text file written from BIANCA and passed to the external software, i.e. the *input file*, which contains the informations related to the current individual at the current generation, i.e. the number and the values of the design variables restrained in that individual's genotype. This *input file* contains also additional information such as the number of objective functions, inequality constraints and equality constraints.

The second one is the text file written from the external software and passed to BIANCA, i.e. the *output file*, wherein are written the values of the objective functions, equality and inequality constraints.

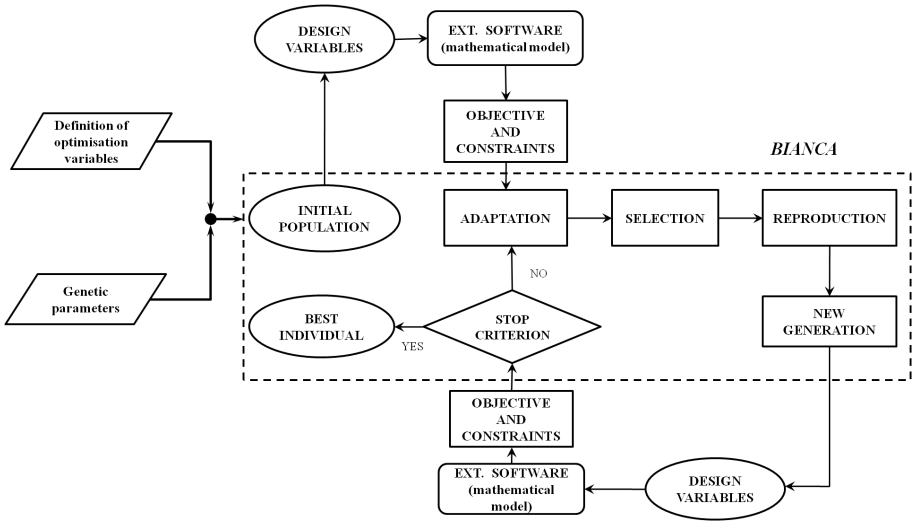

Figure 1.19: Structure of BIANCA interface with external software.

The writing operations of these files are made for each individual in the current gen-

eration, so the external software, during the whole optimisation process, is called from BIANCA $N_{ind} \times N_{gen}$ times, where N_{ind} is the number of individuals while N_{gen} is the number of generations. Up to now, some current and well known software packages have been interfaced with BIANCA in this way like, for instance, MATLAB, ABAQUS and ANSYS packages.

1.9 The Graphical User Interface (GUI) of BIANCA

In this Section we briefly describe the architecture and the main features of the BIANCA GUI. The main reason that underlies our choice of creating a GUI for the code BIANCA consists in developing a tool that can be easily handled and employed by the user which wants to use BIANCA as a numerical technique to perform the search of solutions for a given optimisation problem.

The BIANCA GUI has been realised in MATLAB environment [84]. The layout of the main window, that appears when the user launch the GUI, is depicted in Fig. 1.20.

As other standard GUI, the BIANCA GUI is organised in a certain number of sub-windows which the user can call by clicking on the appropriate buttons of the main window. In particular, after having chosen a name, e.g. *job-name*, for the current job session and after writing it in the text-box indicated by the number 1 in Fig. 1.20, in order to set correctly the various options of the code the user has to realise the following operations.

By clicking on the "Genetic parameters" button (number 2 in Fig. 1.20) it is possible to open the corresponding window, as shown in Fig. 1.21.

After having properly set the genetic parameters (like, for instance, number of population, population size, stop criterion, crossover and mutation probabilities and so on) for the current job session, to save such parameters we have to click on the "save" button. In this way the GUI creates an input file for BIANCA which contains all selected genetic parameters. Such a file has the same name of the current job session with the extension *.gen*, i.e. *job-name.gen*.

The second step consists in setting the optimisation parameters for the considered problem. To realise this operation, the user must click on the "Optimization parameters" button (number 3 in Fig. 1.20): in this case the corresponding window, depicted in Fig. 1.22, appears.

In this window the user can set the optimisation parameters concerning the considered optimisation problem. The user can choose: the problem type (minimisation or maximisation), the number of constraint functions, the nature and the number of design variables, the structure of the individual's genotype (number of chromosomes and genes), the working environment wherein the optimisation problem is implemented and, hence, if the interface between BIANCA and an external software has to be activate (e.g. this is the case wherein we want to optimise a model realised within a FE code). Again, by

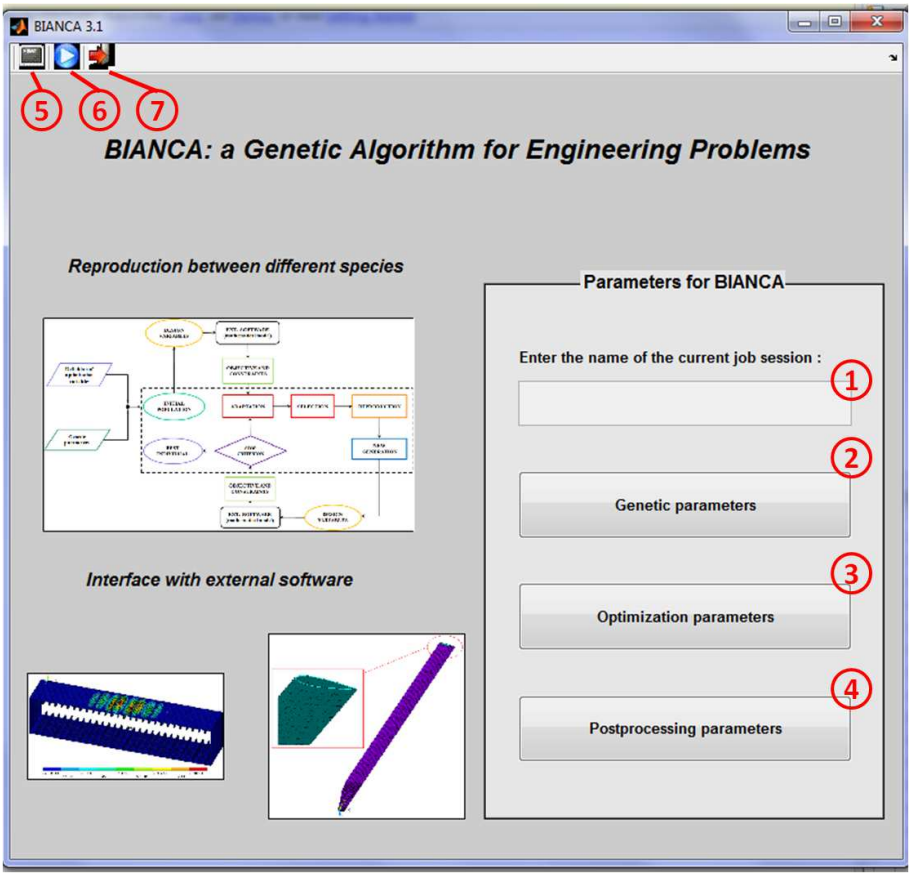

Figure 1.20: BIANCA GUI main window layout.

clicking on the "save" button a file having the same name of the current job session with the extension *.opt*, i.e. *job-name.opt*, is created.

Finally, by clicking on "Postoprocessing parameters" button (number 4 in Fig. 1.20) the window shown in Fig. 1.23 appears. In such window the user can set the options concerning the post-processing operations on the results, namely the plotting operations on the trend of the best solution along the generations as well as the trend of the average of the objective function along the generations. By clicking on the "save" button the file *postprocessing.inp*, containing such information, is then created.

Moreover, if the optimisation problem is written in FORTRAN environment, before running BIANCA by clicking on the "run" icon (number 6 in Fig. 1.20), we need to compile BIANCA by clicking on the "compile" icon (number 5 in Fig. 1.20). Finally, to quit the GUI we have to click on the "exit" icon indicated by number 7 in Fig. 1.20.

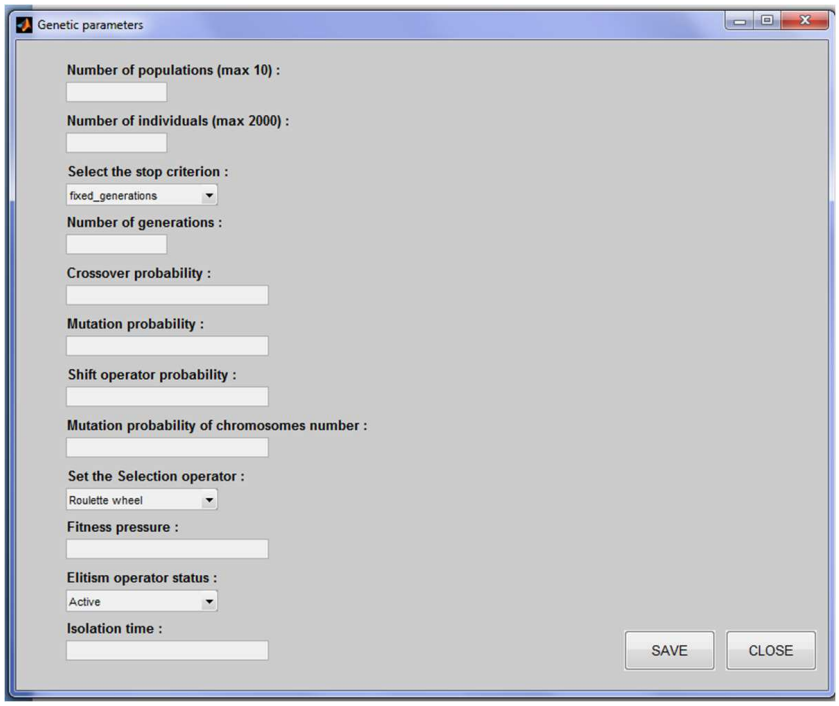

Figure 1.21: BIANCA GUI genetic parameters window layout.

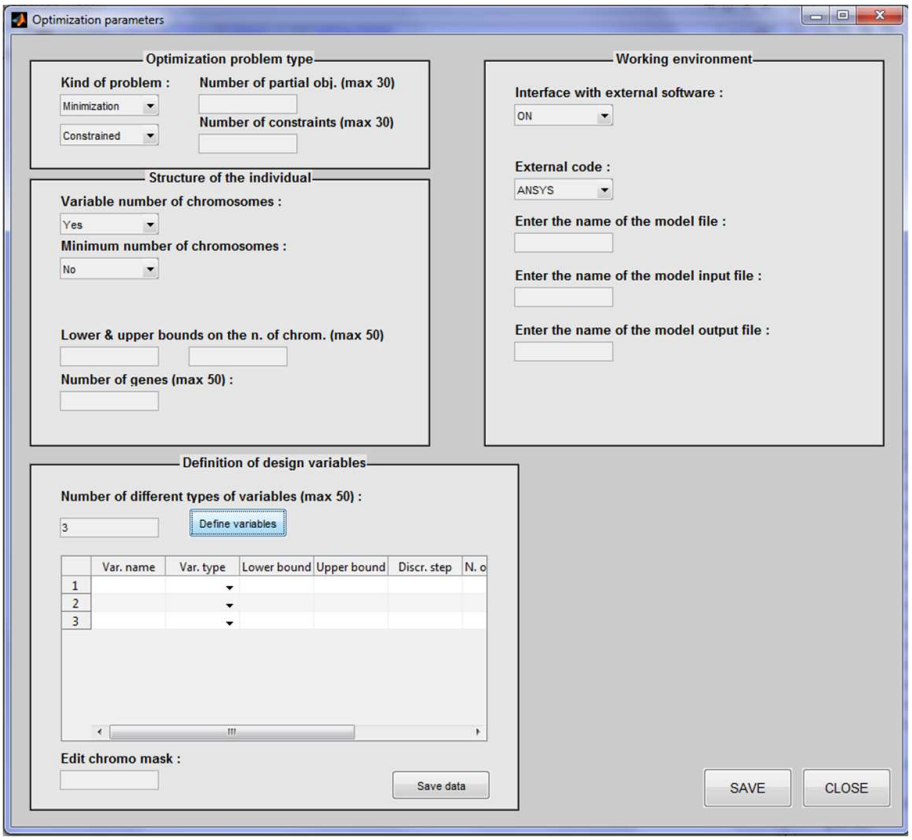

Figure 1.22: BIANCA GUI optimization parameters window layout.

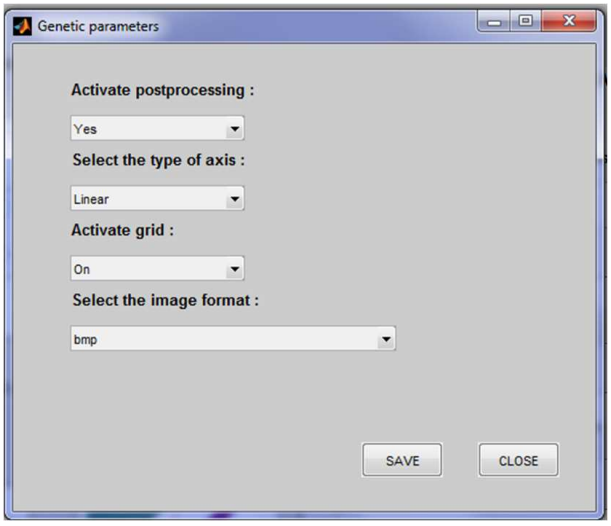

Figure 1.23: BIANCA GUI post-processing parameters window layout.

Chapter 2

Identification of constitutive properties of piezoelectric structures

2.1 Introduction

2.1.1 Literature overview

A great number of researches have been devoted to improve the characteristics of piezoelectric transducers. Piezocomposites have been developed to overcome many of the drawbacks of the standard monolithic piezoelectric wafer, in terms of flexibility and durability. The modelling of such smart structures equipped with piezoelectric transducers necessitates an accurate prediction of the electromechanical properties of the transducer itself.

The first attempts to model flat piezocomposites were carried out by using various homogenisation approaches, including the uniform field method (UFM) [85, 86], the self consistent approach [87], the asymptotic homogenisation method [88, 89] and finite element based techniques [90].

Moreover, piezocomposite transducers are composed of multi-layers of different materials including the active layer, the electrode layers, and the adhesive between different layers. The accurate modelling resides into the precise description of each layer in terms of geometry, dimensions and material properties which are usually not fully provided by the manufacturer. In such a case, an identification process based on numerical and experimental analyses can be used to obtain the overall electromechanical properties of such piezoelectric transducers. The study conducted in this Chapter aims to exploit the effective electromechanical properties of monolithic piezoelectric transducer attached to a thin composite plate-like structure. Such an approach can also be easily extended to piezocomposite structures.

Different numerical strategies, basically inverse problem procedures, have been developed for the identification of materials elastic moduli. A rather complete survey of such

approaches, concerning identification methods for the estimation of mechanical properties on different kind of laminated structures, can be found in [91]. Many techniques [92] use an optimisation procedure in order to minimise the difference between the measured eigenfrequencies and the corresponding ones obtained via a FE calculation. An improvement of these approaches has been proposed by Araújo *et al.* [93, 94]. The authors combined numerical analysis, using a finite element model, and experimental analysis, using experimental vibration data, in order to formulate the identification problem for a composite plate equipped with surface mounted piezoelectric transducers. In-plane properties have been obtained using a gradient-based optimisation algorithm, for which a sensitivity analysis with respect to the design variables is required. This analysis is delicate when dealing with optimisation of complex structures. Concerning the estimation of both elastic and piezoelectric properties of surface bonded sensors and actuators in active structures, other gradient-based methods, applied to a circular plate model, have been proposed by Banks *et al.* [95].

Other eigenfrequency-based approaches for the identification of elastic constants in laminated composite materials include methods based on response surfaces [96] and the use of model updating techniques [97]. Another class of inverse techniques is based on ultrasonic and wave propagation measurements along with optimisation techniques, in particular global optimisation strategies such as GAs [98, 99]. Artificial neural networks have also been applied to the identification problem of elastic properties of anisotropic laminated plates using surface displacement response in a wave propagation simulation [100]. A rather complete review on inverse problem procedures for the identification of elastic and piezoelectric properties of active structures can be found in [101].

The main focus of the study conducted in this Chapter concerns the definition of an identification technique based upon an optimisation procedure for the evaluation of the full 3D set of electromechanical properties of surface bonded sensors in active plates. Our strategy relies upon the dynamic response of the structure in terms of undamped natural frequencies and makes use of GAs as global optimisation techniques. The inverse problem of the identification of elastic and piezoelectric properties is stated as a constrained minimisation problem of an error function expressing the difference between the measured eigenfrequencies and the corresponding numerical values.

Starting from the strategy conceived by Araújo *et al.* [93, 94], which is a multi-step identification strategy, we consider the parameter estimation problem in the most general case, without simplifying hypotheses on the mechanical behaviour of the structure. To this purpose we built a 3D Finite Element (FE) model for the piezoelectric patches, in order to capture (with a good level of accuracy and reliability) the true mechanical response of the physical system.

The second innovative aspect of our approach (about the formulation of the inverse problem as a constrained minimisation problem) consists in the use of the full set of constraints that must be imposed to ensure the positive definiteness of the stiffness tensor of

the piezoelectric material of the transducers.

Concerning the optimisation tool, the new version of the GA BIANCA is employed in each phase of the optimisation procedure. On one side we want to test the effectiveness of the ADP strategy for handling constraints when dealing with the problem of identifying the electromechanical properties of piezoelectric structures, while on the other side we test the interface of BIANCA with external codes, especially when the objective as well as the constraint functions are not available in an algebraic form and are evaluated via a numerical process, e.g. a FE calculation, as the one shown in this Chapter.

The Chapter is organised as follows: firstly, the constitutive law for piezoelectric materials is briefly described in Sec. 2.2, then Sec. 2.3 details the aspects concerning the FE model adopted for the active plate along with the mathematical statement of the parameter estimation problem as an optimisation problem as well as the description of the adopted numerical strategy. The numerical results applied on an active plate with surface mounted piezoelectric patches are shown in Sec. 2.4, in order to validate the accuracy and the reliability of the proposed numerical tool and, finally, Sec. 2.5 ends the Chapter with some concluding remarks.
Starting from Sec. 2.3, this Chapter is substantially taken from the article [102].

2.2 Constitutive law for piezoelectric materials

2.2.1 Piezoelectric materials

The piezoelectric effect can be seen as a transfer of energy from electrical to mechanical energy and vice-versa. Such transfers can only occur if the material is composed of charged particles and can be polarised.

The necessary condition that a material must satisfy in order to show the piezoelectric behaviour is that its crystal structure must have no centre of symmetry, see [103]. In nature, 21 crystal structures out of 32 are non-centrosymmetric. A crystal having no center of symmetry possesses one or more crystallographically directional axes. All 21 non-centrosymmetric crystal classes, except 1, show piezoelectric effect along the directional axes. Out of the 20 piezoelectric classes, only 10 have one unique directional axis. Such crystals are called polar crystals because they show spontaneous polarization. The value of the spontaneous polarization depends on the temperature (this is called the *pyroelectric* effect). The pyroelectric crystals for which the magnitude and direction of the spontaneous polarization can be reversed by an external electric field are said to show the *ferroelectric* behaviour.

Most of the piezoelectric materials are crystalline solids. They can be single crystals (either naturally or artificially formed) or polycrystalline materials like ferroelectric ceramics which can be made piezoelectric and, in this case, they show, at a macroscopic scale, a single crystal symmetry obtained through the so-called process of poling (by sub-

jecting to a high electric field not far below the Curie temperature, see [103] for more details).
The piezoelectric effect can also appear in crystals composed of only one type of element (in this case, the polarization is due to a distortion in the electronic distribution). Certain polymers can also be made piezoelectric by stretching them under an electric field.

In the following we consider only the piezoelectric effect in the framework of the linear piezoelectric theory. Further additional aspects, like for instance, types of polarisation of piezoelectric materials (e.g. electric polarisation, ionic polarisation and so on), domain reorientation, hysteresis, doping effect and other kinds of non-linearity fall outside the scopes of the present thesis. For a deeper insight in the matter the reader is addressed to [103].

2.2.2 General constitutive equations

According to the first law of thermodynamics for a piezoelectric material, the variation of the stored internal energy dU_{int} depends upon three different contributions, i.e. the work of the external forces, the work of the electric field and the thermal energy brought to the system:

$$dU_{int} = \sigma_{ij} d\varepsilon_{ij} + \hat{E}_i dD_i + \Theta d\varsigma \ , \tag{2.1}$$

where σ_{ij} and ε_{ij} are the second-order tensors of stress and strain, respectively, while $\hat{E}_i$ and D_i are the vectors of the electric field and electric displacement, respectively. $\Theta = \Theta_0 + \theta$ is the temperature of the piezoelectric continuum (Θ_0 is the reference temperature, whilst $\theta \ll \Theta_0$ is a small perturbation around the reference value) and ς represents the entropy. In Eq. (2.1) the Einstein's summation convention on repeated indices is assumed and $i, j = 1, 2, 3$.

Let us now consider the constitutive equations taking ε_{ij}, $\hat{E}_i$ and θ as state variables:

$$\begin{aligned} d\sigma_{ij} &= \frac{\partial \sigma_{ij}}{\partial \varepsilon_{kl}} d\varepsilon_{kl} + \frac{\partial \sigma_{ij}}{\partial \hat{E}_m} d\hat{E}_m + \frac{\partial \sigma_{ij}}{\partial \theta} d\theta \quad , \\ dD_i &= \frac{\partial D_i}{\partial \varepsilon_{kl}} d\varepsilon_{kl} + \frac{\partial D_i}{\partial \hat{E}_m} d\hat{E}_m + \frac{\partial D_i}{\partial \theta} d\theta \quad , \\ d\varsigma &= \frac{\partial \varsigma}{\partial \varepsilon_{kl}} d\varepsilon_{kl} + \frac{\partial \varsigma}{\partial \hat{E}_m} d\hat{E}_m + \frac{\partial \varsigma}{\partial \theta} d\theta \quad . \end{aligned} \tag{2.2}$$

To completely describe the behaviour of the piezoelectric continuum, we have to consider the thermoelectric Gibbs state function G_{free} (or free energy) defined as follows:

$$G_{free} = U_{int} - \hat{E}_i D_i - \Theta \varsigma \ . \tag{2.3}$$

From Eq. (2.1) and (2.3) we get:

$$dG_{free} = \sigma_{ij} d\varepsilon_{ij} - D_i d\hat{E}_i - \varsigma d\theta \ , \tag{2.4}$$

and therefore,

$$\begin{aligned} \sigma_{ij} &= \frac{\partial G_{free}}{\partial \varepsilon_{ij}} \quad , \\ D_i &= -\frac{\partial G_{free}}{\partial \hat{E}_i} \quad , \\ \varsigma &= -\frac{\partial G_{free}}{\partial \theta} \quad . \end{aligned} \tag{2.5}$$

By deriving a second time the previous expressions we get:

$$\begin{aligned} \frac{\partial \sigma_{ij}}{\partial \hat{E}_m} &= -\frac{\partial D_m}{\partial \varepsilon_{ij}} \quad , \\ \frac{\partial \sigma_{ij}}{\partial \theta} &= -\frac{\partial \varsigma}{\partial \varepsilon_{ij}} \quad , \\ \frac{\partial D_i}{\partial \theta} &= \frac{\partial \varsigma}{\partial \hat{E}_i} \quad . \end{aligned} \tag{2.6}$$

In Eq. (2.2) and (2.6) each partial derivative has a peculiar physical meaning:

- $C_{ijkl}^{\hat{E},\theta} = \dfrac{\partial \sigma_{ij}}{\partial \varepsilon_{kl}}$ is the fourth-order elasticity (or stiffness) tensor at constant electric and temperature fields;
- $e_{ijm} = -\dfrac{\partial \sigma_{ij}}{\partial \hat{E}_m} = \dfrac{\partial D_m}{\partial \varepsilon_{ij}}$ is the third-order piezoelectric tensor (coupling between mechanical and electric behaviours);
- $\lambda_{ij} = -\dfrac{\partial \sigma_{ij}}{\partial \theta} = \dfrac{\partial \varsigma}{\partial \varepsilon_{ij}}$ is the second-order thermal stress tensor (coupling between mechanical and thermal behaviours);
- $\kappa_{im}^{\sigma,\theta} = \dfrac{\partial D_i}{\partial \hat{E}_m}$ is the second-order permittivity tensor at constant stress and temperature fields;
- $p_i = \dfrac{\partial D_i}{\partial \theta} = \dfrac{\partial \varsigma}{\partial \hat{E}_i}$ is the pyroelectricity vector (coupling between thermal and electric behaviours);
- $\alpha^{\sigma,\hat{E}} = \dfrac{\partial \varsigma}{\partial \theta}$ is the specific heat capacity at constant stress and electric field.

Considering the previous definitions, the free energy can be written as:

$$G_{free} = \frac{1}{2} C_{ijkl}^{\hat{E},\theta} \varepsilon_{ij} \varepsilon_{kl} - e_{kij} \hat{E}_k \varepsilon_{ij} - \frac{1}{2} \kappa_{ij}^{\sigma,\theta} \hat{E}_i \hat{E}_j - \frac{1}{2} \alpha^{\sigma,\hat{E}} \theta^2 - \lambda_{ij} \varepsilon_{ij} \theta - p_i E_i \theta \ . \tag{2.7}$$

From Eq. (2.7) and (2.5) we finally get the relationship expressing the linear thermopiezoelectric behaviour of the continuum:

$$\begin{aligned} \sigma_{ij} &= C_{ijkl}^{\hat{E},\theta} \varepsilon_{kl} - e_{kij} \hat{E}_k - \lambda_{ij} \theta \quad , \\ D_m &= e_{mij} \varepsilon_{ij} + \kappa_{mk}^{\sigma,\theta} \hat{E}_k + p_m \theta \quad , \\ \varsigma &= \lambda_{ij} \varepsilon_{ij} + p_k \hat{E}_k + \alpha^{\sigma,\hat{E}} \theta \quad . \end{aligned} \tag{2.8}$$

Eq. (2.8) can be expressed in a more compact form by adopting the matrix (or Voigt's) notation for tensors. Thus, neglecting the effect of the temperature (i.e. considering a temperature Θ equal to the reference temperature Θ_0) in Eq. (2.8) through such a notation the previous tensor components can be expressed as follows:

$$\begin{array}{llll} C_{ijkl}^{\hat{E}} = C_{pq}^{\hat{E}} & i,j,k,l = 1,2,3 & , & p,q = 1,...,6 \quad , \\ e_{ikl} = e_{iq} & i,k,l = 1,2,3 & , & q = 1,...,6 \quad , \\ \sigma_{ij} = \sigma_p & i,j = 1,2,3 & , & p = 1,...,6 \quad , \\ \varepsilon_{ij} = \varepsilon_p & i,j = 1,2,3 \ \text{ and } \ i = j & , & p = 1,...,6 \quad , \\ 2\varepsilon_{ij} = \varepsilon_p & i,j = 1,2,3 \ \text{ and } \ i \neq j & , & p = 1,...,6 \quad . \end{array} \tag{2.9}$$

According to the matrix notation the constitutive equations read (expressed with respect to the state variables ε_p and $\hat{E}_i$):

$$\begin{aligned} \{\sigma\} &= [C^{\hat{E}}]\{\varepsilon\} - [e]^{\mathrm{T}}\{\hat{E}\} \ , \\ \{D\} &= [e]\{\varepsilon\} + [\kappa^{\sigma}]\{\hat{E}\} \ , \end{aligned} \tag{2.10}$$

or, with a different choice of the state variables (e.g. σ_p and $\hat{E}_i$),

$$\begin{aligned} \{\varepsilon\} &= [S^{\hat{E}}]\{\sigma\} + [d]^{\mathrm{T}}\{\hat{E}\} \ , \\ \{D\} &= [d]\{\sigma\} + [\kappa^{\sigma}]\{\hat{E}\} \ . \end{aligned} \tag{2.11}$$

Eq. (2.10) and (2.11) represent the direct and inverse form of the constitutive equations for a piezoelectric material. In those equations $[C^{\hat{E}}]$ and $[S^{\hat{E}}]$ are the stiffness and compliance matrices (at constant electric field), respectively, while $[e]$ and $[d]$ are the direct (charge/strain) and converse (charge/stress) piezoelectric coefficient matrices, respectively. $[\kappa^{\sigma}]$ is the permittivity matrix at constant stress field, while $\{\varepsilon\}$, $\{\sigma\}$, $\{\hat{E}\}$ and $\{D\}$ are the strain, stress, electric field and electric displacement vectors, respectively.

Moreover, the following relationships between stiffness, compliance and piezoelectric matrices occurs:

$$\begin{aligned} [S^{\hat{E}}] &= [C^{\hat{E}}]^{-1} \ , \\ [e] &= [d][C^{\hat{E}}] \ . \end{aligned} \tag{2.12}$$

In the following, in order to express the behaviour of the piezoelectric material we consider the inverse form of the constitutive equations of the linear piezoelectricity, i.e. Eq. (2.11). In addition, due to crystal symmetries, the piezoelectric coupling matrices $[d]$ and $[e]$ may have only few non zero elements (see [104, 105]). In the material frame $R : \{O; x_1, x_2, x_3\}$ of the patches, if the constitutive material is orthotropic and assuming the x_3 axis as the direction of the polarization of the material, the matrices $[S^{\hat{E}}]$, $[d]$ and $[\kappa^{\sigma}]$ can be written as:

$$[S^{\hat{E}}] = \begin{bmatrix} \frac{1}{E_1} & -\frac{\nu_{12}}{E_1} & -\frac{\nu_{13}}{E_1} & 0 & 0 & 0 \\ -\frac{\nu_{12}}{E_1} & \frac{1}{E_2} & -\frac{\nu_{23}}{E_2} & 0 & 0 & 0 \\ -\frac{\nu_{13}}{E_1} & -\frac{\nu_{23}}{E_2} & \frac{1}{E_3} & 0 & 0 & 0 \\ 0 & 0 & 0 & \frac{1}{G_{23}} & 0 & 0 \\ 0 & 0 & 0 & 0 & \frac{1}{G_{13}} & 0 \\ 0 & 0 & 0 & 0 & 0 & \frac{1}{G_{12}} \end{bmatrix},$$

$$[d] = \begin{bmatrix} 0 & 0 & 0 & 0 & d_{15} & 0 \\ 0 & 0 & 0 & d_{24} & 0 & 0 \\ d_{31} & d_{32} & d_{33} & 0 & 0 & 0 \end{bmatrix}, \tag{2.13}$$

$$[\kappa^{\sigma}] = \begin{bmatrix} \kappa_{11} & 0 & 0 \\ 0 & \kappa_{22} & 0 \\ 0 & 0 & \kappa_{33} \end{bmatrix}.$$

Since the main goal of this work is to identify the electromechanical properties of the piezoelectric patches of an active plate-like structure, an estimation of the parameters of the tensors of Eq. (2.13) will be performed. These parameters represent the design variables of the optimisation problem. In Sec. 2.3 further details about the design variables and the mathematical statement of the optimisation problem are presented.

2.3 Identification of electromechanical properties of active plates

2.3.1 Problem description

The optimisation strategy presented in this Chapter allows to find a solution for the material parameters identification problem and it is applied to the active plate structure depicted in Fig. 2.1. In particular we are concerned in identifying the electromechanical properties of the piezoelectric patches, the elastic moduli of the composite plate being completely known. The composite plate is made of highly anisotropic unidirectional carbon-epoxy plies (T300/5280), with 12 layers having the following stacking sequence: $[0°/90°/45°/-45°/0°/90°]_S$. For both the composite base plate and the piezoelectric patches, a linear elastic behaviour is assumed as constitutive material law. The material properties for the elementary ply of the composite plate are listed in Table 2.1 and are taken from [106].

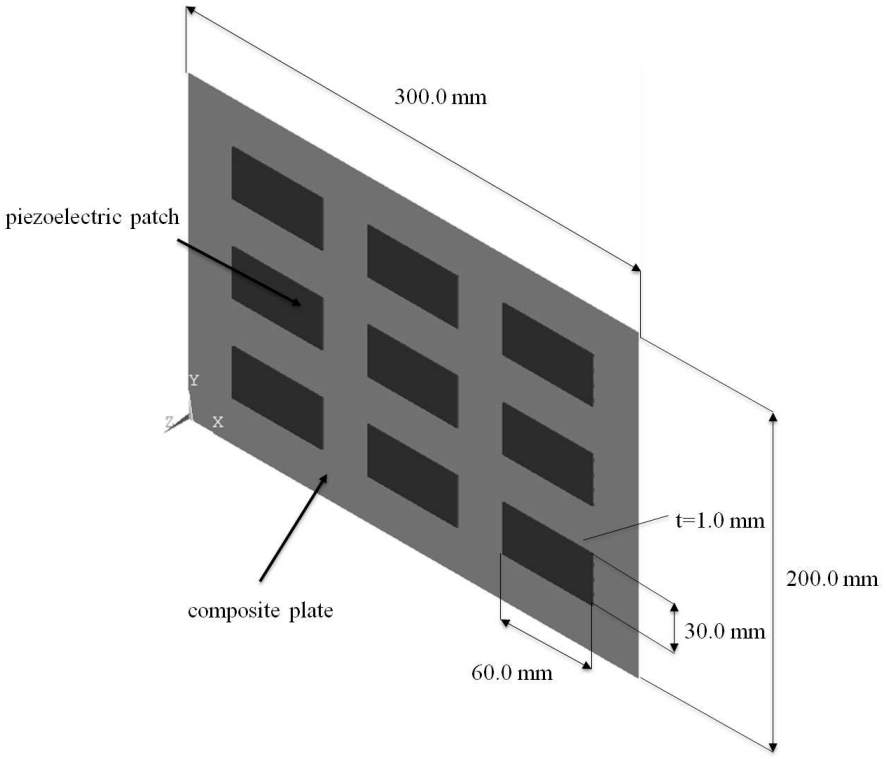

Figure 2.1: Geometry of the active plate.

As shown in Fig. 2.1, the active plate has 9 equally spaced electroded piezoelectric patches bonded to one of the exterior surfaces of the laminate. The constitutive law for

Young's modulus E_1 [GPa]	132.40
Young's modulus E_2 [GPa]	10.70
Young's modulus E_3 [GPa]	10.70
Shear modulus G_{12} [GPa]	5.65
Shear modulus G_{23} [GPa]	3.38
Shear modulus G_{13} [GPa]	5.65
Poisson's ratio ν_{12}	0.24
Poisson's ratio ν_{23}	0.49
Poisson's ratio ν_{13}	0.24
Density ρ [kg/m^3]	1580
Ply thickness t_{ply} [mm]	0.133

Table 2.1: Material properties for unidirectional carbon/epoxy ply T300/5208

the material of the patches is described by Eq. (2.11) and (2.13).

2.3.2 Mathematical statement of the problem and solving strategy

Mathematical statement of the parameter estimation problem

In this section, the problem of the estimation of the electromechanical properties of an active plate structure is stated as a constrained minimisation problem. The inverse problem considered here belongs to the class of the *minimum distance* problems. Our strategy consists in finding, through a genetic process, the physical parameters that, entering into a FE model, minimise the distance between the *real* model and the *numerical* one. This distance depends upon the measured and evaluated eigenfrequencies (and this choice is just one among others). For such problems, the existence of a solution is not guaranteed *a priori*. Moreover, it is rare that any parameter set can exactly match given data. On the contrary, the parameter set matching a given *observed state* might not be unique.

In particular, the goal of our strategy is to identify the electromechanical properties of the piezoelectric patches (in terms of the components of stiffness, piezoelectric and dielectric tensors) through the measurement of a set of N undamped natural frequencies of the reference structure, which represents the system response or the *observed state*. Indeed, the parameter estimation technique consists in minimising the difference between the response of the physical system and the finite element numerical model which simulates the system response as function of the elastic and piezoelectric coefficients. The set of coefficients minimising, i.e. putting to zero, this difference is assumed to be the set of the actual physical parameters to be identified. The reference values of the undamped natural frequencies can be measured experimentally or can be obtained numerically (via

a FE calculation on a reference structure).

In the general 3D case, the design variables of the optimisation process are the technical constants of elasticity, i.e. $E_1,\ E_2,\ E_3,\ \nu_{12},\ \nu_{23},\ \nu_{13},\ G_{12},\ G_{23},\ G_{13}$, and the charge coefficients of the piezoelectric patches, i.e. $d_{31},\ d_{32},\ d_{33},\ d_{24},\ d_{15}$. We do not need to estimate the dielectric coefficients at constant stress κ_{ij}^{σ}, because these values are, normally, provided by manufacturers and can be easily obtained through capacitance measurements, so they do not take part into the optimisation process as parameters to be identified. The vector of design variables can be written as:

$$\mathbf{x} = \{E_1,\ E_2,\ E_3,\ \nu_{12},\ \nu_{23},\ \nu_{13},\ G_{12},\ G_{23},\ G_{13},\ d_{31},\ d_{32},\ d_{33},\ d_{24},\ d_{15}\}\ . \tag{2.14}$$

Concerning the expression of the objective function, we consider an error estimator of least-square type:

$$\Phi\left(\mathbf{x}\right) = \sum_{i=1}^{N} \left(\frac{\overline{\lambda}_i - \lambda_i(\mathbf{x})}{\overline{\lambda}_i} \right)^2 \ , \tag{2.15}$$

where $\overline{\lambda}_i$ and $\lambda_i(\mathbf{x})$ are the eigenfrequencies of the reference structure and of the FE model, respectively, whilst N is the total number of natural frequencies used in the analyses.

At this point a fundamental question arises: how can we choose the number N of measured state variables (or data points) in order to have a good estimation of the system parameters? Unfortunately, no proved theoretical rules exist in the literature, see [107, 108], to define the number of data points N for a given number of design variables n that have to be identified. Generally, the inverse problem is stated as a non-linear least-square problem and it can be viewed as an *over-determined system of equations* [107, 108]. Since more observation points exist than parameters (N is usually much greater than n) there are more equations than unknowns. If an optimal point exists, it may be not unique, thus implying the existence of many combinations of parameters that result to be equivalent optimal solutions for the non-linear least-square problem.

According to the aforementioned considerations, we considered a number of natural frequencies N (the observed state) greater than the number of the parameters to be identified. In particular, the number of eigenfrequencies N is chosen in such a way that the numerical model shows a certain level of redundancy, i.e. the number of considered natural frequencies is at least twice the number of the design variables.

Along with the previous remarks, we have to consider the existence constraints that must be imposed on the technical constants of elasticity of the piezoelectric patches, in order to ensure the positive definiteness of the stiffness tensor $\mathbf{C}^{\hat{E}} = (\mathbf{S}^{\hat{E}})^{-1}$, see [109]. In particular, for an orthotropic material, they can be expressed as:

$$
\begin{aligned}
&\mathbf{g}\left(\mathbf{x}\right) \leq \mathbf{0} \ , \\
&\text{with :} \\
&\begin{cases}
\mathrm{g}_1\left(\mathbf{x}\right) = -E_1 \ , \\
\mathrm{g}_2\left(\mathbf{x}\right) = -E_2 \ , \\
\mathrm{g}_3\left(\mathbf{x}\right) = -E_3 \ , \\
\mathrm{g}_4\left(\mathbf{x}\right) = E_2 - E_1 \ , \\
\mathrm{g}_5\left(\mathbf{x}\right) = E_3 - E_1 \ , \\
\mathrm{g}_6\left(\mathbf{x}\right) = \mid \nu_{12} \mid - \sqrt{\dfrac{E_1}{E_2}} \ , \\
\mathrm{g}_7\left(\mathbf{x}\right) = \mid \nu_{23} \mid - \sqrt{\dfrac{E_2}{E_3}} \ , \\
\mathrm{g}_8\left(\mathbf{x}\right) = \mid \nu_{13} \mid - \sqrt{\dfrac{E_1}{E_3}} \ , \\
\mathrm{g}_9\left(\mathbf{x}\right) = -G_{12} \ , \\
\mathrm{g}_{10}\left(\mathbf{x}\right) = -G_{23} \ , \\
\mathrm{g}_{11}\left(\mathbf{x}\right) = -G_{13} \ , \\
\mathrm{g}_{12}\left(\mathbf{x}\right) = 2\nu_{12}\nu_{23}\nu_{13}\dfrac{E_3}{E_1} + \nu_{12}^2\dfrac{E_2}{E_1} + \nu_{23}^2\dfrac{E_3}{E_2} + \nu_{13}^2\dfrac{E_3}{E_1} - 1 \ , \\
\mathrm{g}_{13}\left(\mathbf{x}\right) = \nu_{12} + \nu_{23} + \nu_{13}\dfrac{E_3}{E_1} - \dfrac{3}{2} \ .
\end{cases}
\end{aligned}
\tag{2.16}
$$

Several works, that can be found in literature, make use only of some of the previous constraints. In particular, in these studies, only the g_1, g_4, g_6, g_9, g_{10} and g_{11} constraints are considered. Nevertheless, they are not sufficient in order to ensure the positive definiteness of the tensor $\mathbf{C}^{\hat{E}}$. To this purpose, in this work we adopt, for the first time, the full set of constraints that have to be imposed to ensure the existence of the tensor $\mathbf{C}^{\hat{E}}$ (even if higher-order 2D theories are employed to model the piezoelectric patches) in agreement with the formulation reported in [109]. To our knowledge, this is the first time that the whole set of constraints of Eq. (2.16) is used in such kind of problems.

It can be noticed that, in Eq. (2.16), constraints g_4 and g_5 do not represent thermodynamic existence conditions, but they are anyway imposed in order to ensure that the Young's moduli E_2 and E_3 have to be less than or equal to the Young's modulus E_1 measured along the main orthotropy axis of the material.

Finally, the problem of the identification of the electromechanical properties of the

patches for the active plate can be stated as a classical constrained Non-Linear Programming Problem (NLPP) as follows:

$$\begin{cases} \min\limits_{\mathbf{x}} \ \Phi(\mathbf{x}) \ , \\ \text{subject to :} \\ \mathbf{g}(\mathbf{x}) \leq \mathbf{0} \ . \end{cases} \tag{2.17}$$

Numerical strategy

To search a solution for the parameter identification problem of Eq. (2.17) we use the code BIANCA interfaced with the FE code ANSYS: for every individual at each generation, the evaluation of the objective and constraint functions is performed via a FE calculation. In addition, since the number of decision variables (i.e. the parameters to be identified) is fixed *a priori* the new genetic operators that perform the crossover and mutation among different species are no longer required.

The structure of the individual's genotype is depicted in Fig. 2.2, whilst Table 2.2 shows the design domain for the optimisation problem of Eq. (2.17).

E_1	E_2	E_3	ν_{12}	ν_{23}	ν_{13}	G_{12}	G_{23}	G_{13}	d_{31}	d_{32}	d_{33}	d_{24}	d_{15}

Figure 2.2: Structure of the individual's genotype for the optimisation problem (2.17).

The behaviour of the active plate in terms of natural frequencies is, substantially, a purely mechanical phenomenon: in fact the elastic properties of the piezoelectric material have a stronger effect on the response of the structure, when compared to the one of the piezoelectric coefficients. Thus, due to the different order of magnitude of the sensitivities of the eigenfrequencies to the different types of design variables, in agreement with the strategy conceived by Araújo *et al.* [93, 94], we divided the optimisation process into two phases (we recall that the elastic properties of the composite plate are known *a priori*):

- in the first phase, only the elastic properties of the sensors are identified, imposing the closed-circuit condition (in order to obtain the elastic constants at constant electric field);
- in the second phase we impose the open circuit condition on the piezoelectric sensors in order to estimate the value of the piezoelectric charge coefficients of the material.

In this way, the inverse problem of the identification of material parameters is solved separately in two different subspaces: in other words, we try to find a solution for the problem of minimum distance (between target values of the eigenfrequencies and the

Design variable	Type	Lower bound	Upper Bound
E_1 [GPa]	continuous	1.0	100.0
E_2 [GPa]	continuous	1.0	100.0
E_3 [GPa]	continuous	1.0	100.0
ν_{12}	continuous	-1.0	0.5
ν_{23}	continuous	-1.0	0.5
ν_{13}	continuous	-1.0	0.5
G_{12} [GPa]	continuous	1.0	50.0
G_{23} [GPa]	continuous	1.0	50.0
G_{13} [GPa]	continuous	1.0	50.0
d_{31} [10^{-12}m/V]	continuous	-500.0	-100.0
d_{32} [10^{-12}m/V]	continuous	-500.0	-100.0
d_{33} [10^{-12}m/V]	continuous	100.0	800.0
d_{24} [10^{-12}m/V]	continuous	100.0	800.0
d_{15} [10^{-12}m/V]	continuous	100.0	800.0

Table 2.2: Design variables and their bounds for the optimisation problem (2.17)

numerical ones) by solving the problem firstly in the space of elastic parameters (which have the strongest effect on the values of natural frequencies) and then, using the elastic parameters found in the first step, in the subspace of piezoelectric parameters (whose effect on the dynamic response of the structure is negligible when compared to the previous one).

To prove the convergence of this approach we could restart the whole process by inserting in the first phase, for the piezoelectric charge coefficients, the values issued from the second phase. Then we could evaluate the new set of elastic constants of the piezoelectric material and we could use them in the second phase and so on, until to reach the convergence between two consecutive values of the design variables. We have always checked that only one step, i.e. solving the optimisation problem only one time in closed and open circuit conditions, is sufficient to obtain good values of the electromechanical properties of the patches.

2.3.3 Finite element model of the active plate

The FE model of the active plate is realised in ANSYS environment. The structure is modelled with a combination of shell and solid elements. In particular, the laminate is modelled using SHELL281 elements with 8 nodes and 6 degrees of freedom (DOFs) per node with 3 integration points along the thickness of each ply. The piezoelectric patches are modelled using SOLID226 elements which are solid elements with 20 nodes used for

coupled-field analyses with a variable number of DOFs per node that depends upon the kind of analysis that has to be performed: for a coupled-field analysis with piezoelectric materials this solid element has 4 DOFs per node, i.e. the three displacements and the electric potential.

The choice of using solid elements to model the piezoelectric patches is strictly related to the main goal of our optimisation strategy: since we have to estimate the electromechanical properties of the patches in the most general case, i.e. in the 3D case, we need to build a mathematical model able to describe (with a good level of accuracy and reliability) the mechanical response of the physical system. To this purpose the FE model of the active plate has to be able to catch those phenomena which normally, even with higher-order 2D theories, are not well described, e.g. the effect of the out-of-plane Poisson's ratios, the effect of the shear response through-the-thickness and so on.

As said previously, we conduct a free-vibration analysis in order to evaluate the first N eigenfrequencies of the FE model of the active plate. It is worth noting that when electroded surfaces exist in a given patch, equipotential conditions must be imposed. Moreover, in order to minimise the errors linked to the modelling of boundary conditions, a completely free-edge plate is considered and the extraction of the non-rigid modes from the FE analysis is carried-out.

As conclusive remark, it can be noticed that the compatibility of the displacement field between the patches (modelled with solid elements) and the plate (modelled with shell elements) is realised by means of constraint equations on each corresponding node belonging to contiguous solid and shell elements. In particular, we specified rigid constraints between the nodes of the middle surface of the plate structure and the corresponding ones of the bottom surface of the patches (only for what concerns the displacement DOFs). Rigid constraints equations are specified according to the classical scheme implemented within the ANSYS code: the master nodes are those belonging to the middle plane of the composite plate, whilst the slave nodes are those located on the bottom surface of every patch. Through these constraint equations, the displacement of the nodes belonging to the top surface of the plate (in the region wherein the patch is bonded) is equal to that of the nodes belonging to the bottom surface of the patch.

2.4 Numerical results

With the purpose of validating our optimisation strategy, in this section we present a simulated case study. The geometry of the active plate and the material properties of the elementary layer of the base laminate are those discussed in Sec. 2.3. In order to find a solution to the optimisation problem of Eq. (2.17) we need to define the reference values of the eigenfrequencies $\overline{\lambda}_i$ in Eq. (2.15). Moreover, these values must be estimated for both the phases of the whole procedure, i.e. for both closed and open circuit conditions.

Concerning the piezoelectric patches we use as target material (and hence as reference

solution) the PZT-5H piezoelectric alloy [106], which is a transversely-isotropic material and whose properties are listed in Table 2.3. For both phases of the optimisation procedure we perform a free-vibration analysis and we evaluate the first $N = 30$ eigenfrequencies. Moreover, after a preliminary mesh sensitivity study, the dimensions of the shell elements are chosen equal to 2.5×2.5 mm^2, while the dimensions of solid elements are $2.5 \times 2.5 \times 1.0$ mm^3 (we have previously checked that a single element in the thickness of the patch is sufficient to capture the correct mechanical response of the patch). Finally, the number of DOFs of the whole model is 148876. We remark that, as said in Sec. 2.3, the design variables are only the technical constants of elasticity and the piezoelectric charge coefficients: for both open and closed-circuit conditions we assume that the values of the permittivity coefficients are those of the reference material shown in Table 2.3.

Elastic coeff.		Charge coeff.		Permittivity coeff.		Density	
E_1 [GPa]	62.0	d_{31} [10^{-12}m/V]	-240.0	ϵ_{11} [10^{-9}F/m]	15.0	ρ [kg/m^3]	7730
E_2 [GPa]	62.0	d_{32} [10^{-12}m/V]	-240.0	ϵ_{22} [10^{-9}F/m]	15.0		
E_3 [GPa]	57.0	d_{33} [10^{-12}m/V]	500.0	ϵ_{33} [10^{-9}F/m]	13.0		
G_{12} [GPa]	23.3	d_{24} [10^{-12}m/V]	730.0				
G_{23} [GPa]	23.0	d_{15} [10^{-12}m/V]	730.0				
G_{13} [GPa]	23.0						
ν_{12}	0.33						
ν_{23}	0.44						
ν_{13}	0.44						

Table 2.3: Electromechanical properties for the reference material PZT-5H

2.4.1 Phase I: closed-circuit conditions

The main goal of this phase is the estimation of the elastic material properties of the piezoelectric sensors at constant electric field. Concerning the genetic parameters for this first calculation, we use $N_{pop} = 2$ different populations with $N_{ind} = 50$ individuals for each population evolving along 100 generations. The exchange of information among the populations is performed through a ring-type operator every 20 generations, with a probability which is automatically evaluated by the GA itself. The crossover and mutation probability are $p_{cross} = 0.85$ and $p_{mut} = 1/N_{ind}$, respectively.

The choice of using multiple populations of small size, i.e. with a small number of individuals, is motivated by the fact that we want to find the global minimum with a good level of accuracy without increasing too much the time of calculations. Indeed, the exchange of informations between the best individuals of different populations (through the use of the ring-type operator), and hence the possibility of crossing them, allow the GA to explore the feasible design domain and to handle the genetic information in the best way. More details about the use of multiple populations can be found in [110, 1].

Table 2.4 shows the values of the technical constants estimated in this phase compared to the target values, along with the values of the natural frequencies of free vibration and the residuals r_i obtained after the identification. Residuals are defined as:

$$r_i = \frac{\overline{\lambda}_i - \lambda_i}{\overline{\lambda}_i} \times 100 \ , \tag{2.18}$$

where λ_i and $\overline{\lambda}_i$ are the eigenfrequencies produced by the FE model after identification and the corresponding reference values, respectively. In this simulated test case, for both phases of the optimisation procedure, $\overline{\lambda}_i$ are evaluated using in the FE model the properties of the reference material listed in Table 2.3. The definition of the residuals of Eq. (2.18) is also used in the second phase of the optimisation procedure.

Fig. 2.3 shows the variation of the best solution along the generations and that of the average of the objective function on the whole population vs. the number of generations. It can be noticed that the second population reaches the optimal solution after only 15 generations.

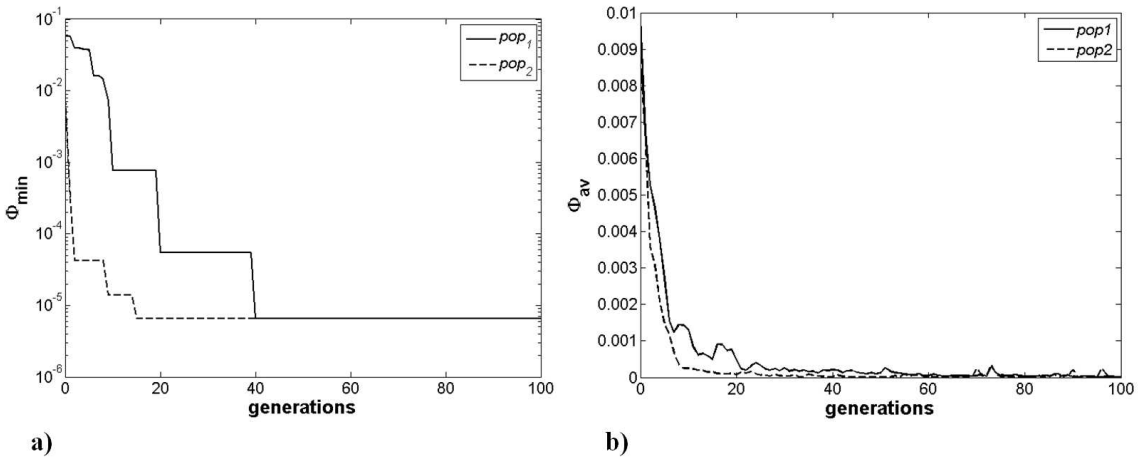

Figure 2.3: (a) Best and (b) Average values of the objective function along generations for the active plate FE model, closed-circuit conditions.

2.4.2 Phase II: open circuit conditions

In this second phase of the optimisation process, open circuit conditions are imposed on the electroded piezoelectric patches in order to identify the piezoelectric charge/stress coefficients. Thus, the design variables of this phase are the components of the matrix $[d]$. Concerning the stiffness properties of the patches, they are defined using the values of the technical constant of elasticity issued from the first phase. Moreover, also in this phase

Material properties		
	Goal	Identified
E_1 [GPa]	62.0	61.5
E_2 [GPa]	62.0	61.5
E_3 [GPa]	57.0	51.0
ν_{12}	0.33	0.33
ν_{23}	0.44	0.43
ν_{13}	0.44	0.43
G_{12} [GPa]	23.3	23.12
G_{23} [GPa]	23.0	23.0
G_{13} [GPa]	23.0	23.0
Eigenfrequencies		
Mode n.	$\overline{\lambda}_i$ [Hz]	r_i [%]
1	98.54	0.01
2	127.76	0.06
3	238.96	0.02
4	245.67	0.03
5	315.55	0.02
6	356.06	0.05
7	468.77	0.02
8	498.06	0.01
9	683.44	0.03
10	734.69	0.10
11	744.79	0.02
12	771.95	0.03
13	802.68	0.07
14	932.58	0.02
15	1031.77	0.04
16	1165.48	0.08
17	1223.70	0.04
18	1273.27	0.03
19	1371.70	0.07
20	1371.86	0.05
21	1468.10	0.03
22	1505.67	0.05
23	1532.24	0.04
24	1689.08	0.07
25	1708.42	0.04
26	1763.72	0.05
27	1918.89	0.04
28	1996.46	0.03
29	2070.39	0.04
30	2172.20	0.04

Table 2.4: Identified properties, simulated eigenfrequencies and residuals obtained after identification, closed-circuit conditions

the reference values of the natural frequencies $\overline{\lambda}_i$ are evaluated using in the FE model (with open circuit conditions) the properties of the target material listed in Table 2.3.

Concerning the genetic parameters, they are strictly those used in the previous phase. Table 2.5 shows the values of the piezoelectric charge coefficients estimated in this phase compared to the target values, along with the values of the eigenfrequencies and the residuals r_i obtained after the identification. Fig. 2.4 shows the variation of the best solution along the generations and that of the average of the objective function on the whole population vs. the number of generations. It can be noticed that the second population reaches the optimal solution after only 20 generations.

We remark that the use of the stacking sequence discussed in Sec. 2.3 for the composite base plate along with its geometrical dimensions avoids the problem of having double modes.

The results of the simulated test case show that, for both the phases of the optimisation process, the error function is drastically minimised. From Tables 2.4 and 2.5, it can be noticed that we have a good agreement among the target properties and the identified ones. Moreover, our GA leads us to reach, with a high precision, the values of the reference natural frequencies of the active plate for both closed and open circuit conditions (the highest residual on the eigenfrequencies in the whole process is about 0.1%). This means that the proposed approach is very effective in finding a real global minimum when dealing with such optimisation problems.

Nevertheless, looking at the results presented in Tables 2.4 and 2.5, we can conclude that the identification of E_3 and d_{33} is not very good, because these quantities are estimated with a relative error of about 10%. This is due to the fact that, despite 3D elements are employed to model the piezoelectric transducers, the effect of E_3 and d_{33} on the dynamical response of the plate, in terms of natural frequencies, is negligible: in fact, the thickness-to-length ratio of such a patch is low, i.e. the patch itself is a thin plate.

2.4.3 Effect of the noise on the identified properties

The presence of noise on the target data (in the present problem, the measured eigenfrequencies of the plate) in inverse problems can cause difficulties for the identification process. The existence of a solution is not guaranteed, particularly if the observed data contains errors or if the mathematical model, used to describe the physical system, is grossly incorrect. Parameter identification is an inherently noisy process. There are several unavoidable sources of error, including observation error, model structure error and forward solution error. For a deeper insight in the matter the reader is addressed to [107].

Though parameter identification problems are subject to several source of noise, any optimisation problem that depends upon numerical approximations can also be prone to the presence of noise. Optimisation in presence of noise is a well known topic that has already been treated by several authors, see for example [111, 112, 113].

Material properties		
	Goal	Identified
d_{31} [10^{-12}m/V]	-240.0	-250.0
d_{32} [10^{-12}m/V]	-240.0	-250.0
d_{33} [10^{-12}m/V]	500.0	550.0
d_{24} [10^{-12}m/V]	730.0	750.0
d_{15} [10^{-12}m/V]	730.0	750.0
Eigenfrequencies		
Mode n.	$\overline{\lambda}_i$ [Hz]	r_i [%]
1	98.63	0.01
2	128.93	0.04
3	239.97	0.01
4	247.28	0.01
5	316.61	0.01
6	359.07	0.03
7	471.02	0.02
8	500.20	0.01
9	687.66	0.01
10	748.10	0.02
11	751.98	0.06
12	776.09	0.01
13	815.18	0.04
14	935.12	0.01
15	1046.41	0.02
16	1182.78	0.05
17	1227.95	0.03
18	1284.39	0.02
19	1393.57	0.02
20	1395.16	0.03
21	1475.51	0.02
22	1523.47	0.03
23	1538.22	0.03
24	1703.98	0.05
25	1717.81	0.03
26	1778.60	0.04
27	1939.95	0.02
28	2014.98	0.02
29	2090.25	0.02
30	2186.37	0.03

Table 2.5: Identified properties, simulated eigenfrequencies and residuals obtained after identification,open circuit conditions

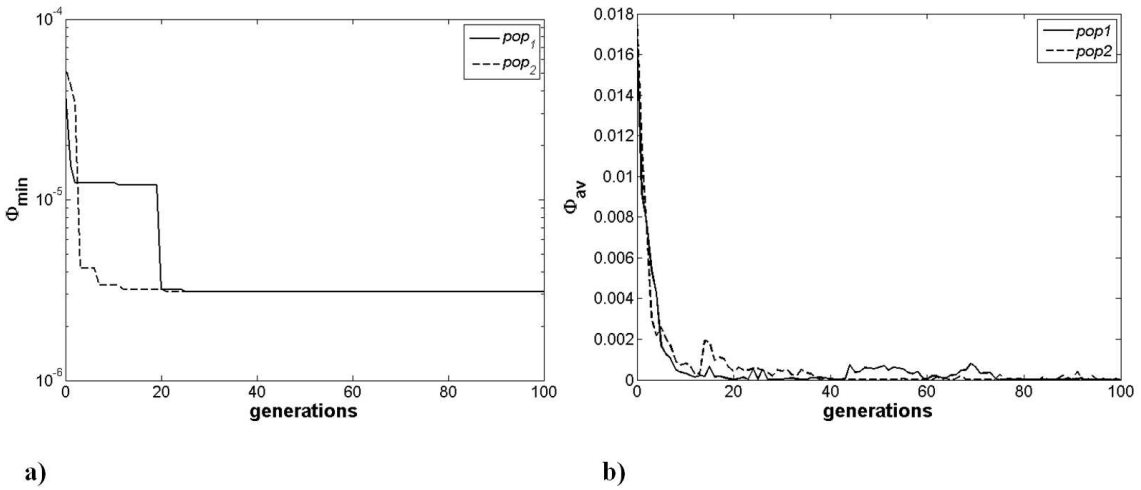

Figure 2.4: (a) Best and (b) Average values of the objective function along generations for the active plate FE model, open circuit conditions.

Noise might strongly affect identification when the optimisation problem is solved by the use of a gradient-based algorithm. On the contrary, even if the performances of GAs can be affected by numerical noise, the absence of gradient approximations reduces the effect of noise on the evolutionary strategies. Spurious local minima or discontinuities caused by noise will not preclude the use of the metaheuristics. Noise, however, can affect the decisions made during exploration of the search space, thus affecting the outcomes of the algorithm. Evolutionary algorithms have been hailed as effective in the presence of numerical noise [113, 98].

Even if we use an evolutionary strategy, namely a GA-based approach, in order to solve the identification problem of Eq. (1.33), it is interesting to evaluate the effect of noise on the performances of the optimisation process: therefore we artificially introduce statistical errors within the observed data, and we study the effect on the values of the identified electromechanical parameters found at the end of the optimisation process.

The influence of the noise on the reference values of the eigenfrequencies $\overline{\lambda}_i$ (both for closed and open circuit conditions) is considered through the following steps:

- firstly, a subset of m eigenfrequencies is extracted from the whole set of $N = 30$ reference eigenfrequencies considered in the previous analyses. The number m as well as the involved natural frequencies composing this subset are randomly chosen. The number m of frequencies of the subset can randomly vary between 8 and 16;

- secondly, the eigenfrequencies composing this subset are perturbed with a given level of noise. We consider 3 different cases: in the first case each one of the m natural frequencies is disturbed with a noise that can vary randomly between 0.1%

and 1.0% of the corresponding unperturbed reference value, in the second case the noise on each frequency can vary between 0.1% and 2.0%, and finally in the last one the noise level can vary between 0.1% and 5.0%.

Concerning the genetic parameters, they are strictly those used in the previous calculations. Fig. 2.5 shows the variation of the best solution along the generations (both for closed and open circuit conditions) in presence of noise for each of the three considered noise levels within the response data, whilst the effect of the noise on the identified electromechanical properties is detailed in Table 2.6. From Fig. 2.5, we can see that if the noise level is smaller than 2%, the GA converges toward the global feasible minimum after about 15 generations. Moreover, concerning the first two cases, the objective function for the best individual is still within acceptable values, the estimated electromechanical properties being within reasonable relative errors.

We can conclude that if the noise level on the natural frequencies is smaller than 2%, the GA leads to obtain a good estimation of the electromechanical properties of the patches, the maximum relative error on the identified parameters being always on the values of E_3 and d_{33} (about 10%). Nevertheless, if the noise level is greater than 2% the electromechanical properties are not well estimated, particularly the in-plane elastic constants, i.e. ν_{12} and G_{12}, whose relative errors become greater than 54% and 21%, respectively.

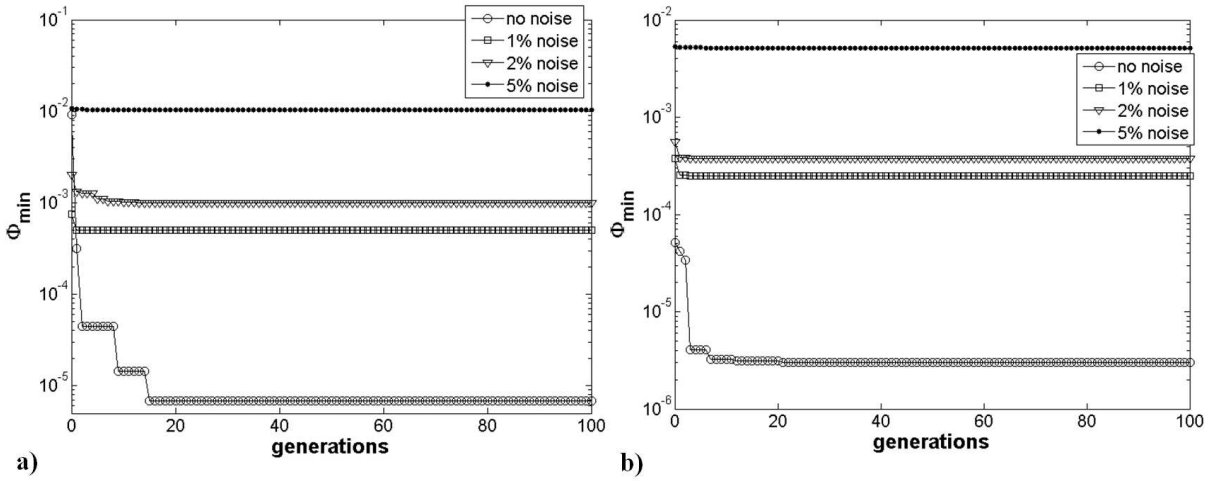

Figure 2.5: Best values of the objective function along generations in presence of noise for the active plate FE model, (a) closed-circuit conditions and (b) open circuit conditions.

	Reference value	1% noise (% error)	2% noise (% error)	5% noise (% error)
E_1 [GPa]	62.0	62.5 (0.81)	62.7 (1.13)	65.0 (4.83)
E_2 [GPa]	62.0	62.5 (0.81)	62.7 (1.13)	65.0 (4.83)
E_3 [GPa]	57.0	51.0 (−10.53)	51.5 (−9.65)	60.0 (5.26)
G_{12} [GPa]	23.3	24.03 (3.13)	24.11 (3.48)	28.26 (21.29)
G_{23} [GPa]	23.0	23.0 (0.0)	23.3 (1.3)	23.5 (2.17)
G_{13} [GPa]	23.0	23.0 (0.0)	23.3 (1.3)	23.5 (2.17)
ν_{12}	0.33	0.30 (−9.09)	0.30 (−9.09)	0.15 (−54.55)
ν_{23}	0.44	0.43 (−2.27)	0.43 (−2.27)	0.42 (−4.55)
ν_{13}	0.44	0.43 (−2.27)	0.43 (−2.27)	0.42 (−4.55)
d_{31} [10^{-12}m/V]	−240.0	−255.0 (6.25)	−256.0 (6.67)	−283.0 (17.92)
d_{32} [10^{-12}m/V]	−240.0	−255.0 (6.25)	−256.0 (6.67)	−283.0 (17.92)
d_{33} [10^{-12}m/V]	500.0	551.0 (10.2)	551.0 (10.2)	542.0 (8.4)
d_{24} [10^{-12}m/V]	730.0	750.0 (2.74)	751.0 (2.88)	785.0 (7.53)
d_{15} [10^{-12}m/V]	730.0	750.0 (2.74)	751.0 (2.88)	785.0 (7.53)

Table 2.6: Effect of noise on the identified electromechanical properties

2.5 Concluding remarks

In this Chapter, an investigation to identify the overall electromechanical properties of piezoelectric transducers in the full three dimensional case has been conducted. The problem of the estimation of the electromechanical properties of an active plate is stated as a constrained minimisation problem: the objective function is built as an error estimator of the least squares type and it is based on the dynamic response of the structure in terms of its eigenfrequencies. The GA BIANCA is employed to solve the minimum problem so formulated. The numerical strategy is articulated into two phases: the first part concerns the identification of the elastic properties of the transducer under short circuit condition of the electrodes, while the second one is done under open circuit condition in order to

increase the effect of the electric field on the dynamic responses of the structure.

The GA BIANCA leads us to reach, with a high precision, the values of the reference natural frequencies of the active plate for both closed and open circuit conditions: this means that the proposed strategy results very effective when dealing with such kind of problems. Moreover, we have a good agreement among the target properties and the identified ones.

The key points of this research are, on one hand the estimation of the whole 3D set of electromechanical properties of the piezoelectric transducers and, on the other side, concerning the formulation of the inverse problem as a constrained minimisation problem, the use of the full set of constraints that must be imposed to ensure the positive definiteness of the stiffness tensor of the material of the patches.

This approach is not limited to monolithic piezoelectric transducers but can be easily applied to the identification of the electromechanical properties of piezocomposite transducers, even in the case of active structures with complex geometry.

Chapter 3

Optimal design of elastic properties of laminates

3.1 Introduction

The design of elastic properties is very important in many applications, e.g. for aircraft and space structures. Unlike classical materials, composite laminates can be designed to obtain certain properties: this design process is known in the literature as *tailoring*. Some classical examples of elastic properties that can be tailored are bending-extension uncoupling, in-plane and/or bending orthotropy, isotropy and so on. Tailoring can be mainly done by a correct design of the stacking sequence of the laminate. The problem of tailoring a composite plate to realise a given elastic or hygral-thermal-elastic behaviour has attracted the attention of several researchers. A wide though not complete state of the art, at least for what concerns the design with respect to stiffness, can be found in two recent papers by Ghiasi *et al.* [32, 33]. The design of laminates considered as an optimisation problem is rather cumbersome and difficult to be solved due to the high non-linearity and non-convexity of the objective function; these circumstances are brought by the fact that the laminate properties depend upon a combination of powers of circular functions of the layers orientations, these last being normally the natural design variables. As a consequence, designers generally limit the search of solutions to a restricted class of laminates, usually to symmetric stacking sequences to ensure bending-extension uncoupling, or balanced sequences to have in-plane orthotropy and so on. In other words, difficulty has almost always suggested to the designers to avoid dealing with the real, complete design problem and to simplify it using some simple but limiting rules.

The problem of designing laminates elastic properties as a global optimisation problem has received a general formulation, especially concerning the design of elastic symmetries, with the works of Vannucci, Vincenti and Verchery [43, 114, 115]. They have shown that it is possible to built, through the so-called "polar method", a unique objective function

which takes into account several design criteria, e.g. elastic properties, such as uncoupling, orthotropy and many others, and given hygral-thermal responses in extension and/or in bending. The general problem is therefore reduced to a classical Non-Linear Programming Problem (NLPP) and its solutions are the minima of a non-linear, non-convex function in the design space of the layers orientations. In these studies many optimal solutions were found for several different problems.
In all the aforementioned research studies the number of plies was always fixed *a priori*, the design process focusing only on the importance of the geometry of the stacking sequence, i.e. the only design variables were the layers orientation angles.

As a natural continuation of [43, 114, 115, 116] the focus of this Chapter consists in a new formulation of the problem of designing the laminate elastic symmetries that can be attained with the *minimum number of plies*. To this purpose the number and orientations of plies, as well as the thickness of each layer, are taken into account as design variables. More precisely, this Chapter tries to give an answer to a question which is usually left apart by designers, but which is a classical and fundamental question in any mathematical problem, i.e. the question about the existence of a solution. In the case of laminates design, this question should be: which is the minimum number of layers that guarantees the existence of at least one solution to a given problem of tailoring the elastic properties of a laminate?

To our best knowledge, only in one case the minimal number of layers to obtain some prescribed properties is known exactly thanks to a theoretical result. This is the case of in-plane isotropy, solved by Werren and Norris [117]: at least three unidirectional plies are needed to obtain a laminate that will be isotropic in extension, although membrane-bending coupled. Nevertheless, if we consider an additional or a different requirement, like for instance uncoupling or bending isotropy, the result is unknown. Finding the minimum number of layers for which a given optimum laminate design problem can be solved is actually a very difficult task. In fact, the minimum number of layers varies with the type of elastic requirements to be obtained: the results are strictly problem-dependent and unfortunately in all the cases, the optimal solutions are unknown and there is no analytical model describing their evolution with the number of layers. Therefore, a numerical investigation seems to be an appropriate approach.

It is worth noting that the optimal design of a laminate in terms of number and properties (orientation, material and thickness) of its layers is a *combinatorial optimisation problem*, which is arduous to solve for small numbers of layers. In fact, the fewer the number of plies, the smaller becomes the design space, and the number of available solutions decreases. However, solutions with minimum number of plies are important when the problem of minimum weight of laminates is addressed.

The main focus of this Chapter is to formulate the problem in the form of a search for the minima of a positive semi-definite form, including the number of layers n among the variables. The function takes into account the variable n as a penalty term, in order to

strongly drive the search of optimal solutions towards laminates with the lowest number of layers.

The GA BIANCA is still used for the solution search. In addition, to obtain an effective formulation, the polar formalism has been employed. Such a formalism is based upon an algebraic formulation making use of tensor invariants for representing plane tensors (see [114, 118]) and it has been successfully employed in the resolution of several design problems concerning laminates [43, 115, 116].

In particular, concerning the GA BIANCA, in this Chapter we test the effective of the new genetic operators of crossover and mutation between individuals belonging to different species when dealing with the problem of tailoring multilayer plates, which attain given elastic symmetries with the minimum number of plies. Indeed, as we will explain in detail in Sec. 3.4, since the number of layers n is included among the design variables, the related optimisation problem is formulated over a definition domain composed of vectors having different lengths.

The Chapter is organised as follows: in Sec. 3.2 the polar formalism is introduced. In Sec. 3.3 the general equations of the Classical Laminated Plate Theory (CLPT) are recalled, while in Sec. 3.4 the design problem of laminates elastic symmetries with minimum number of plies is stated in the framework of the polar method and formulated as an optimisation problem. Finally several numerical examples are given in Sec. 3.5 in order to show the effectiveness of the proposed approach and then some general considerations end the Chapter.
Starting from Sec. 3.4, this Chapter is substantially taken from the article [119].

3.2 Polar representation of the plane anisotropy

The polar formalism is a mathematical technique introduced in 1979 by Verchery [114]. Through this method, it is possible to express any plane tensor (of any order) by means of its *polar invariants*. Such a technique has already been employed in several design problems concerning laminates, see for example [43, 115, 120]. A complete survey on the polar method and on the applications of such a technique to tensors of various order can be found in [3]. In this section, we briefly recall some fundamental expressions of the polar representation, which we need in order to formulate the optimisation problem of designing the elastic symmetries of laminates having the minimum number of plies.

Usually, the Cartesian formulation is the most used method to express tensors of any order. However, the main drawback of such a representation is that the tensor components are frame-dependent. Starting from such an issue, the main idea that underlies the polar formalism consists in expressing the tensor components through other parameters which are frame-independent, i.e. which are *tensor invariants*. Clearly, the tensor invariants can be chosen in different ways. The quantities introduced by Verchery are directly linked to the elastic symmetries of the tensor and to the strain energy decomposition.

Before the Verchery's polar formalism, different empirical-nature algebraic techniques were proposed by others researchers in order to represent plane tensors, see for instance the works of Tsai and Pagano [121], Wu [122] and Hahn [123]. The work of Verchery completes and deepens the results of the previous studies, but, and this is very important, it employs a more rigorous approach that it is classical in physics and mathematics: the polar formalism is a mathematical technique based upon a complex-variable transformation (this is also the main reason that explains why the polar formalism can be used only in the case of bi-dimensional tensors). Such an approach finds its starting point in the works of Michell [124], Kolosov [125], Muskhelishvili [126] and the well-known treatise of Green and Zerna [127].
However, a detailed description of the mathematical aspects of the polar formalism falls outside the scope of the present Thesis. For a deeper insight in the matter the reader is addressed to [3].

3.2.1 Polar representation of second-order tensors

Let us consider a second-order plane symmetric tensor $\mathbf{L}$. The polar representation of such a tensor, in its material frame $\{O; x_1, x_2\}$, is:

$$\begin{array}{rcrl} L_{11} & = & T & +R\cos 2\Phi \quad , \\ L_{12} & = & & R\sin 2\Phi \quad , \\ L_{22} & = & T & -R\cos 2\Phi \quad , \end{array} \tag{3.1}$$

where L_{ij} $(i,j=1,2)$ are the Cartesian components of the tensor $\mathbf{L}$, while T, R and Φ are its polar components. T and R are the *polar moduli* and represent tensor invariants, whilst Φ is the *polar angle* which depends on the choice of the frame. The converse of Eq. (3.1) is:

$$\begin{array}{rcrrl} 2T & = & L_{11} & +L_{22} & \quad , \\ 2R\mathrm{e}^{2\mathrm{i}\Phi} & = & L_{11} & -L_{22} \quad +2\mathrm{i}L_{12} & \quad , \end{array} \tag{3.2}$$

Representation (3.1) can be applied to any plane second-order tensor. Let us consider the plane stress tensor expressed (in the framework of the well-known Mohr's circle representation) in terms of principal stresses σ_I and σ_{II} (with $\sigma_I > \sigma_{II}$) and the corresponding principal directions in the form:

$$\begin{array}{rcrl} 2T & = & \sigma_I & +\sigma_{II} \quad , \\ 2R\mathrm{e}^{2\mathrm{i}\Phi} & = & \sigma_I & -\sigma_{II} \quad . \end{array} \tag{3.3}$$

As stated by Eq. (3.3), T and R represent the spherical and the deviatoric parts of the plane stress tensor $\boldsymbol{\sigma}$, respectively. The polar angle Φ corresponds to the direction of the principal stress σ_I.

Eq. (3.1) can also be applied to the plane strain tensor $\boldsymbol{\varepsilon}$, whose polar components are indicated using the lower-case characters t, r and ϕ.

3.2.2 Polar representation of fourth-order tensors

Let us consider, now, a fourth-order plane elasticity-like tensor $\mathbf{L}$, i.e. possessing the major and minor symmetries o, the indexes. In such a case, the polar formalism states that the Cartesian components of the tensor $\mathbf{L}$ can be expressed through 4 polar moduli, i.e. T_0, T_1, R_0 and R_1, and 2 polar angles, Φ_0 and Φ_1 (see [3, 118] for more details). The relationship between the Cartesian components L_{ijkl} $(i,j,k,l=1,2)$ in the material frame $\{O;x_1,x_2\}$ and the polar parameters is:

$$\begin{array}{rcrrrrr}
L_{1111} &=& T_0 & +2T_1 & +R_0\cos 4\Phi_0 & +4R_1\cos 2\Phi_1 & , \\
L_{1122} &=& -T_0 & +2T_1 & -R_0\cos 4\Phi_0 & & , \\
L_{1112} &=& & & R_0\sin 4\Phi_0 & +2R_1\sin 2\Phi_1 & , \\
L_{2222} &=& T_0 & +2T_1 & +R_0\cos 4\Phi_0 & -4R_1\cos 2\Phi_1 & , \\
L_{2212} &=& & & -R_0\sin 4\Phi_0 & +2R_1\sin 2\Phi_1 & , \\
L_{1212} &=& T_0 & & -R_0\cos 4\Phi_0 & & .
\end{array} \tag{3.4}$$

The converse of Eq. (3.4) is:

$$\begin{array}{rcrrrrrr}
8T_0 &=& L_{1111} & & -2L_{1122} & +4L_{1212} & & +L_{2222} & , \\
8T_1 &=& L_{1111} & & +2L_{1122} & & & +L_{2222} & , \\
8R_0\mathrm{e}^{4\mathrm{i}\Phi_0} &=& L_{1111} & +4\mathrm{i}L_{1112} & -2L_{1122} & -4L_{1212} & -4\mathrm{i}L_{2212} & +L_{2222} & , \\
8R_1\mathrm{e}^{2\mathrm{i}\Phi_1} &=& L_{1111} & +2\mathrm{i}L_{1112} & & & +2\mathrm{i}L_{2212} & -L_{2222} & .
\end{array} \tag{3.5}$$

A rotation of the frame by an angle δ causes the following changes in the expression of the tensor components (which are expressed now in the rotated frame $\{O;x,y\}$):

$$\begin{array}{rcrrrrr}
L_{xxxx} &=& T_0 & +2T_1 & +R_0\cos 4(\Phi_0-\delta) & +4R_1\cos 2(\Phi_1-\delta) & , \\
L_{xxyy} &=& -T_0 & +2T_1 & -R_0\cos 4(\Phi_0-\delta) & & , \\
L_{xxxy} &=& & & R_0\sin 4(\Phi_0-\delta) & +2R_1\sin 2(\Phi_1-\delta) & , \\
L_{yyyy} &=& T_0 & +2T_1 & +R_0\cos 4(\Phi_0-\delta) & -4R_1\cos 2(\Phi_1-\delta) & , \\
L_{yyxy} &=& & & -R_0\sin 4(\Phi_0-\delta) & +2R_1\sin 2(\Phi_1-\delta) & , \\
L_{xyxy} &=& T_0 & & -R_0\cos 4(\Phi_0-\delta) & & .
\end{array} \tag{3.6}$$

Eq. (3.6) shows that a rotation of the frame influence only the polar angles by changing them from Φ_0 and Φ_1 into $\Phi_0-\delta$ and $\Phi_1-\delta$, respectively. In addition, from Eq. (3.6) it is apparent that T_0 and T_1 are the polar moduli of the isotropic part of the tensor, while R_0 and R_1 are the polar moduli of the tensor anisotropic part. T_0, T_1, R_0 and R_1 as well as the angular difference $\Phi_0-\Phi_1$ are the tensor invariants. These features represent two advantages of the polar formalism, especially when such a technique is employed to describe the plane anisotropy of composite laminated structures, as the ones discussed in this Chapter.

Along with the previous aspect, another advantage of the polar formalism concerns the expression of the elastic symmetries of a tensor. Indeed, such conditions are expressed in

a simple way when using polar invariants and a summary of elastic symmetry conditions for a fourth-order elasticity-like tensor is given in Table 3.1. Here, we recall that square symmetry corresponds, in the context of plane elasticity, to the cubic syngony, i.e. such a symmetry is characterised by a periodicity of $\pi/2$ of the elastic moduli, while R_0-orthotropy is a special case of plane orthotropy, see [128, 129]. From Table 3.1, we can

Elastic symmetry	Polar condition
Orthotropy	$\Phi_0 - \Phi_1 = K\frac{\pi}{4}$, with $K = 0, 1$
R_0-orthotropy	$R_0 = 0$
Square symmetry	$R_1 = 0$
Isotropy	$R_0 = R_1 = 0$

Table 3.1: Conditions for elastic symmetries in terms of polar invariants

notice that a fourth-order elasticity-like tensor can have (for a given set of polar moduli T_0, T_1, R_0 and R_1) two different types (or shapes) of ordinary orthotropy, depending on the value of the parameter K: this is a very important aspect, especially when dealing with the problem of designing the elastic properties of a given structure, because the shape of orthotropy normally has opposite effects on the final result for a given optimum problem, see [130] for more details.
It is worth noting that the mathematical formalisation of the ordinary orthotropy differs from the one of the special symmetries, i.e. the square symmetry and the R_0-orthotropy, these last being linked to the conditions on the quadratic invariants of the tensor, namely R_1 and R_0, respectively, whilst the ordinary orthotropy arises from a condition on the cubic invariant of the tensor, i.e. the angular difference $\Phi_0 - \Phi_1$ (see [3] for more details).

The norm of the fourth-order tensor can be evaluated using the tensor norm proposed by Kandil and Verchery [131]:

$$\|\mathbf{L}\| = \sqrt{T_0^2 + 2T_1^2 + R_0^2 + 4R_1^2}\ . \tag{3.7}$$

Eq. (3.4) and (3.5) can be applied to the layer reduced stiffness tensor $\mathbf{Q}$ as well as to the compliance tensor $\mathbf{S} = \mathbf{Q}^{-1}$. Let us consider the reduced stiffness tensor of the ply. In the framework of the Voigt's representation of stress and strain tensors (matrix notation), the relationships between the Cartesian components Q_{ij}, $(i, j = 1, 2, 6)$ and the polar components of such a tensor T_0, T_1, R_0, R_1, Φ_0 and Φ_1 are:

$$\begin{array}{rcrcrcrl} Q_{11} &=& T_0 &+2T_1 &+R_0\cos 4\Phi_0 &+4R_1\cos 2\Phi_1 &, \\ Q_{12} &=& -T_0 &+2T_1 &-R_0\cos 4\Phi_0 & &, \\ Q_{16} &=& & &R_0\sin 4\Phi_0 &+2R_1\sin 2\Phi_1 &, \\ Q_{22} &=& T_0 &+2T_1 &+R_0\cos 4\Phi_0 &-4R_1\cos 2\Phi_1 &, \\ Q_{26} &=& & &-R_0\sin 4\Phi_0 &+2R_1\sin 2\Phi_1 &, \\ Q_{66} &=& T_0 & &-R_0\cos 4\Phi_0 & &. \end{array} \tag{3.8}$$

In an analogous way, the relationship between the Cartesian components of the compliance tensor S_{ij}, $(i,j=1,2,6)$ and the corresponding polar parameters t_0, t_1, r_0, r_1, ϕ_0 and ϕ_1 are:

$$\begin{array}{rcrcrcrl} S_{11} &=& t_0 &+2t_1 &+r_0\cos 4\phi_0 &+4r_1\cos 2\phi_1 &, \\ S_{12} &=& -t_0 &+2t_1 &-r_0\cos 4\phi_0 & &, \\ S_{16} &=& & &2r_0\sin 4\phi_0 &+4r_1\sin 2\phi_1 &, \\ S_{22} &=& t_0 &+2t_1 &+r_0\cos 4\phi_0 &-4r_1\cos 2\phi_1 &, \\ S_{26} &=& & &-2r_0\sin 4\phi_0 &+4r_1\sin 2\phi_1 &, \\ S_{66} &=& 4t_0 & &-4r_0\cos 4\phi_0 & &. \end{array} \tag{3.9}$$

Finally, we can express the polar components of the compliance tensor $\mathbf{S}$ in terms of those of the reduced stiffness tensor $\mathbf{Q}$ as follows:

$$\begin{array}{rcll} t_0 &=& 2\dfrac{T_0T_1-R_1^2}{\Delta} &, \\ t_1 &=& \dfrac{T_0^2-R_0^2}{2\Delta} &, \\ r_0\mathrm{e}^{4\mathrm{i}\phi_0} &=& 2\dfrac{R_1^2\mathrm{e}^{4\mathrm{i}\Phi_1}-T_1R_0\mathrm{e}^{4\mathrm{i}\Phi_0}}{\Delta} &, \\ r_1\mathrm{e}^{2\mathrm{i}\phi_1} &=& -R_1\mathrm{e}^{2\mathrm{i}\Phi_1}\dfrac{T_0-R_0\mathrm{e}^{4\mathrm{i}(\Phi_0-\Phi_1)}}{\Delta} &, \end{array} \tag{3.10}$$

where Δ is the determinant of the reduced stiffness tensor $\mathbf{Q}$ having the following expression:

$$\Delta = 8T_1\left(T_0^2-R_0^2\right)-16R_1^2\left[T_0-R_0\cos 4(\Phi_0-\Phi_1)\right] . \tag{3.11}$$

3.2.3 Thermodynamic existence conditions

Let us consider a layer made of linear anisotropic elastic material subject to a plane stress field having components T, R and Φ and submitted to a strain field of components t, r and ϕ. The elastic energy density of such a layer is:

$$W = \frac{1}{2}\boldsymbol{\sigma}\cdot\boldsymbol{\varepsilon} = Tt + Rr\cos 2(\Phi-\phi) . \tag{3.12}$$

Eq. (3.13) can be written in terms of polar components of the reduced stiffness tensor $\mathbf{Q}$ and of the strain tensor as follows:

$$W = 2T_0 r^2 + 4T_1 t^2 + 2R_0 r^2 \cos 4(\Phi_0 - \phi) + 8R_1 tr \cos 2(\Phi_1 - \phi) \ . \tag{3.13}$$

Eq. (3.13) lets us understand the different roles played by each polar parameter in the decomposition of the elastic energy density. In particular it is possible to show that the spherical part, W_S, and the deviatoric part, W_D, of W can be written as:

$$\begin{aligned} W_S &= 4T_1 t^2 + 4R_1 tr \cos 2(\Phi_1 - \phi) \quad , \\ W_D &= 2T_0 r^2 + 2R_0 r^2 \cos 4(\Phi_0 - \phi) + 4R_1 tr \cos 2(\Phi_1 - \phi) \quad . \end{aligned} \tag{3.14}$$

From Eq. (3.14) we can deduce a result that it is classical in plane elasticity: for an anisotropic material it is not possible to decompose the elastic energy W in spherical and deviatoric parts. In addition, from Eq. (3.14) we can see that the spherical part W_S depends directly upon the isotropic polar modulus T_1, while the deviatoric part W_D depends directly on the polar moduli T_0 and R_0 as well as the polar angle Φ_0. The polar parameters R_1 and Φ_1 are responsible of the coupling between the two parts. Therefore, it seems clear that we can decompose the elastic energy into two distinct parts at least when the material satisfies the condition (in terms of elastic symmetry) of square-symmetry, i.e. when $R_1 = 0$.

Through the positive definiteness of W, we can deduce the existence conditions which ensure the positive definiteness of the reduced stiffness tensor of the ply $\mathbf{Q}$, expressed in terms of its polar parameters. The result is that it must be:

$$\begin{cases} T_0 - R_0 > 0 \ , \\ T_1 \left(T_0^2 - R_0^2\right) - 2R_1^2 \left[T_0 - R_0 \cos 4(\Phi_0 - \Phi_1)\right] > 0 \ . \end{cases} \tag{3.15}$$

For a deeper insight in the matter on all the previous aspects the reader is addressed to [3].

3.3 The polar formalism for the mechanics of laminates

3.3.1 The Classical Laminated Plate Theory (CLPT)

A multilayer plate is a thin structure composed of a stack of elementary plies, as shown in Fig. 3.1. Each layer is characterised by its position k within the stack, its orientation angle δ_k with respect the global reference frame of the plate, its thickness t_k and its elastic properties, expressed through the reduced stiffness tensor of the ply $\mathbf{Q}(\delta_k)$.

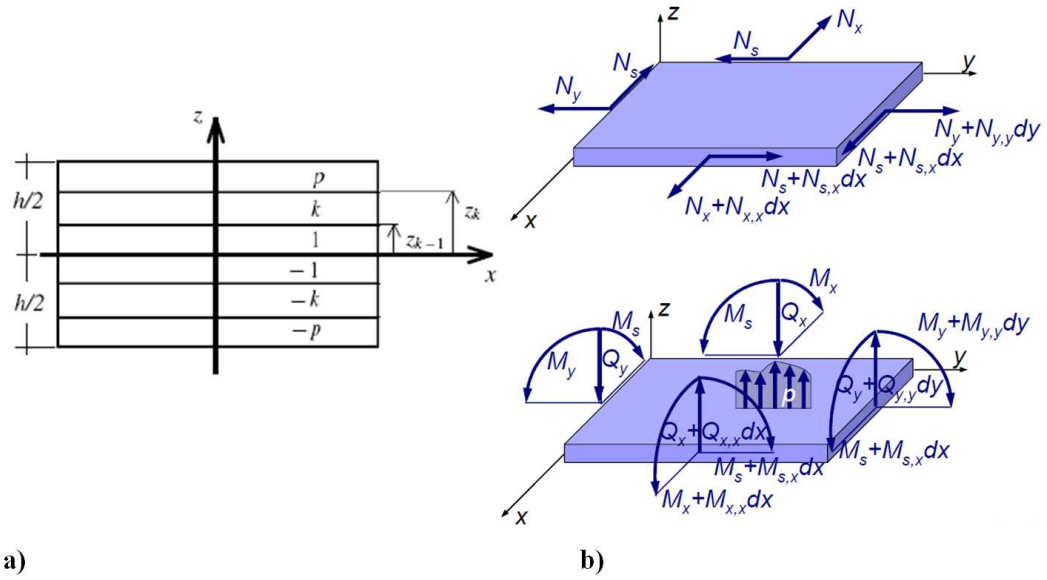

Figure 3.1: (a) Sketch of the laminate layers and interfaces and (b) internal actions per unit length.

The mechanical response of a composite laminated plate can be described in the framework of the Classical Laminated Plate Theory (CLPT), see for instance [109]. The fundamental hypotheses that underlies such a theory include small displacements and strains as well as the Kirchhoff assumptions on the kinematics of the plate. Thus, the general equations describing the behaviour of a composite laminate are:

$$\left\{ \begin{array}{c} \mathbf{N} \\ \mathbf{M} \end{array} \right\} = \left[\begin{array}{cc} \mathbf{A} & \mathbf{B} \\ \mathbf{B} & \mathbf{D} \end{array} \right] \left\{ \begin{array}{c} \boldsymbol{\varepsilon} \\ \boldsymbol{\chi} \end{array} \right\} , \tag{3.16}$$

where:

$$\mathbf{N} = \left\{ \begin{array}{c} N_x \\ N_y \\ N_s \end{array} \right\}, \quad \mathbf{M} = \left\{ \begin{array}{c} M_x \\ M_y \\ M_s \end{array} \right\}, \quad \boldsymbol{\varepsilon} = \left\{ \begin{array}{c} \varepsilon_x \\ \varepsilon_y \\ \varepsilon_s \end{array} \right\}, \quad \boldsymbol{\chi} = \left\{ \begin{array}{c} \chi_x \\ \chi_y \\ \chi_s \end{array} \right\}. \tag{3.17}$$

In Eq. (3.16) all the quantities are expressed in the laminate global frame, i.e. $R = \{O; x, y, z\}$, see Fig. 3.1 (b). $\mathbf{N}$ and $\mathbf{M}$ are the in-plane forces and bending moment tensors, whilst $\boldsymbol{\varepsilon}$ and $\boldsymbol{\chi}$ are the in-plane strain and the curvature tensors of the plate middle plane, respectively. $\mathbf{A}$ and $\mathbf{D}$ are the extension and bending stiffness tensors, respectively, while $\mathbf{B}$ is the membrane-bending coupling tensor. If $\mathbf{B}$ is not null, as an effect of the application of in-plane forces, the laminate will stretch and bend. In addition, tensors $\mathbf{A}$, $\mathbf{B}$ and $\mathbf{D}$ depend on the layer mechanical and geometrical properties, namely

on the orientation of the layers. For a laminate with n plies the expression of $\mathbf{A}$, $\mathbf{B}$ and $\mathbf{D}$ are:

$$\begin{aligned} \mathbf{A} &= \sum_{k=-p}^{p} \mathbf{Q}_k(\delta_k)(z_k - z_{k-1}) \quad , \\ \mathbf{B} &= \frac{1}{2}\sum_{k=-p}^{p} \mathbf{Q}_k(\delta_k)\left(z_k^2 - z_{k-1}^2\right) \quad , \\ \mathbf{D} &= \frac{1}{3}\sum_{k=-p}^{p} \mathbf{Q}_k(\delta_k)\left(z_k^3 - z_{k-1}^3\right) \quad . \end{aligned} \tag{3.18}$$

In Eq. (3.18) $\mathbf{Q}_k(\delta_k)$ is the k^{th} ply reduced stiffness tensor oriented at the angle δ_k with respect to the global reference of the laminate, while p is linked to the number of plies n as follows:

$$n = \begin{cases} 2p & \text{if even} \ , \\ 2p+1 & \text{if odd} \ . \end{cases} \tag{3.19}$$

In Eq. (3.18) z_k and z_{k-1} are the z coordinates of the top and bottom surfaces of the k^{th} layer. Fig. 3.1 (a) shows the definition of z_k used here.

The converse relationship of Eq. (3.16) is:

$$\begin{Bmatrix} \boldsymbol{\varepsilon} \\ \boldsymbol{\chi} \end{Bmatrix} = \begin{bmatrix} \mathbf{a} & \mathbf{b} \\ \mathbf{b}^{\mathrm{T}} & \mathbf{d} \end{bmatrix} \begin{Bmatrix} \mathbf{N} \\ \mathbf{M} \end{Bmatrix} \ , \tag{3.20}$$

where:

$$\begin{aligned} \mathbf{a} &= (\mathbf{A} - \mathbf{B}\mathbf{D}^{-1}\mathbf{B})^{-1}, \\ \mathbf{b} &= -\mathbf{a}\mathbf{B}\mathbf{D}^{-1}, \\ \mathbf{d} &= (\mathbf{D} - \mathbf{B}\mathbf{A}^{-1}\mathbf{B})^{-1}. \end{aligned} \tag{3.21}$$

In Eq. (3.20) $\mathbf{a}$, $\mathbf{b}$ and $\mathbf{d}$ are the in-plane, coupling and bending compliance tensors, respectively. To remark that, generally speaking, tensor $\mathbf{b}$ has not the major symmetries: $b_{ijkl} \neq b_{klij}$, hence its component cannot be represented by Eq. (3.4).

Finally, in order to compare the extension and the bending mechanical behaviours of the laminate we can consider the homogenised stiffness tensors $\mathbf{A}^*$, $\mathbf{B}^*$, $\mathbf{D}^*$ along with the homogeneity tensor $\mathbf{C}$, defined as follows:

$$\begin{aligned}
\mathbf{A}^* &= \frac{1}{h_{tot}}\mathbf{A} \quad , \\
\mathbf{B}^* &= \frac{2}{h_{tot}^2}\mathbf{B} \quad , \\
\mathbf{D}^* &= \frac{12}{h_{tot}^3}\mathbf{D} \quad , \\
\mathbf{C} &= \mathbf{A}^* - \mathbf{D}^* \quad .
\end{aligned} \tag{3.22}$$

where h_{tot} is the laminate total thickness. Tensors $\mathbf{A}^*$, $\mathbf{B}^*$, $\mathbf{D}^*$ and $\mathbf{C}$ have all the same units, those of a stress. A laminate is said to be *quasi-homogeneous* whenever $\mathbf{B}^* = \mathbf{O}$ and $\mathbf{C} = \mathbf{O}$. In such a case the laminate behaves just like an homogeneous plate (though, generally speaking, anisotropic): it is uncoupled and its behaviours in bending and in extension are perfectly identical, for each direction [132].

3.3.2 Polar expression of the laminate tensors

The polar representation (3.4) can be applied to a generic plane tensor. Namely, it can be applied also to the stiffness tensors of the laminate $\mathbf{A}$, $\mathbf{B}$ and $\mathbf{D}$ as well as to their homogenised counterpart $\mathbf{A}^*$, $\mathbf{B}^*$, $\mathbf{D}^*$.

It is possible to deduce the polar components of the laminate stiffness tensors $\mathbf{A}$, $\mathbf{B}$ and $\mathbf{D}$ as functions of the polar components of the plies reduced stiffness tensors $\mathbf{Q}$, using Eq. (3.18):

$$\begin{aligned}
T_0^A, T_0^B, T_0^D &= \frac{1}{m}\sum_{k=-p}^{p} T_{0k}\left(z_k^m - z_{k-1}^m\right) \quad , \\
T_1^A, T_1^B, T_1^D &= \frac{1}{m}\sum_{k=-p}^{p} T_{1k}\left(z_k^m - z_{k-1}^m\right) \quad , \\
R_0^A \mathrm{e}^{4\mathrm{i}\Phi_0^A}, R_0^B \mathrm{e}^{4\mathrm{i}\Phi_0^B}, R_0^D \mathrm{e}^{4\mathrm{i}\Phi_0^D} &= \frac{1}{m}\sum_{k=-p}^{p} R_{0k}\mathrm{e}^{4\mathrm{i}(\Phi_{0k}+\delta_k)}\left(z_k^m - z_{k-1}^m\right) \quad , \\
R_1^A \mathrm{e}^{2\mathrm{i}\Phi_1^A}, R_1^B \mathrm{e}^{2\mathrm{i}\Phi_1^B}, R_1^D \mathrm{e}^{2\mathrm{i}\Phi_1^D} &= \frac{1}{m}\sum_{k=-p}^{p} R_{1k}\mathrm{e}^{2\mathrm{i}(\Phi_{1k}+\delta_k)}\left(z_k^m - z_{k-1}^m\right) \quad ,
\end{aligned} \tag{3.23}$$

where the superscripts A, B and D indicate the polar components of $\mathbf{A}$, $\mathbf{B}$ and $\mathbf{D}$, respectively. In Eq. (3.23), $m = 1, 2, 3$ for the extension, coupling and bending stiffness tensor, respectively.

In a similar way, also the homogeneity tensor $\mathbf{C}$ admits a polar representation and its polar components can be expressed as functions of the polar parameters of tensors $\mathbf{A}^*$ and $\mathbf{D}^*$ as follows:

$$\begin{aligned} T_0^C &= T_0^{A^*} - T_0^{D^*} \quad , \\ T_1^C &= T_1^{A^*} - T_1^{D^*} \quad , \\ R_0^C \mathrm{e}^{4\mathrm{i}\Phi_0^C} &= R_0^{A^*} \mathrm{e}^{4\mathrm{i}\Phi_0^A} - R_0^{D^*} \mathrm{e}^{4\mathrm{i}\Phi_0^D} \quad , \\ R_1^C \mathrm{e}^{2\mathrm{i}\Phi_1^C} &= R_1^{A^*} \mathrm{e}^{2\mathrm{i}\Phi_1^A} - R_1^{D^*} \mathrm{e}^{2\mathrm{i}\Phi_1^D} \quad , \end{aligned} \tag{3.24}$$

where $T_0^{A^*}$, $T_1^{A^*}$, $R_0^{A^*}$, $R_1^{A^*}$, Φ_0^A, Φ_1^A and $T_0^{D^*}$, $T_1^{D^*}$, $R_0^{D^*}$, $R_1^{D^*}$, Φ_0^D, Φ_1^D are the polar parameters of the homogenised extension and bending stiffness tensors, respectively, whose expression can be easily obtained by combining Eq. (3.22) and Eq. (3.23). To remark that the polar angles of the homogenised tensors coincide with the ones of their non-homogenised counterparts.

It is interesting to consider the case of a laminate with identical layers, i.e. a laminate whose plies are made of the same material and have the same thickness but not the same orientation. In such a case the polar parameters of tensors $\mathbf{A}$, $\mathbf{B}$ and $\mathbf{D}$ are:

$$\begin{aligned} T_0^A &= h_{tot} T_0 \quad , \\ T_1^A &= h_{tot} T_1 \quad , \\ R_0^A \mathrm{e}^{4\mathrm{i}\Phi_0^A} &= \frac{h_{tot}}{n} R_0 \mathrm{e}^{4\mathrm{i}\Phi_0} \sum_{k=-p}^{p} \mathrm{e}^{4\mathrm{i}\delta_k} \quad , \\ R_1^A \mathrm{e}^{2\mathrm{i}\Phi_1^A} &= \frac{h_{tot}}{n} R_1 \mathrm{e}^{2\mathrm{i}\Phi_1} \sum_{k=-p}^{p} \mathrm{e}^{2\mathrm{i}\delta_k} \quad , \end{aligned} \tag{3.25}$$

$$\begin{aligned} T_0^B &= \frac{1}{2} \left(\frac{h_{tot}}{n} \right)^2 T_0 \sum_{k=-p}^{p} b_k \quad , \\ T_1^B &= \frac{1}{2} \left(\frac{h_{tot}}{n} \right)^2 T_1 \sum_{k=-p}^{p} b_k \quad , \\ R_0^B \mathrm{e}^{4\mathrm{i}\Phi_0^B} &= \frac{1}{2} \left(\frac{h_{tot}}{n} \right)^2 R_0 \mathrm{e}^{4\mathrm{i}\Phi_0} \sum_{k=-p}^{p} b_k \mathrm{e}^{4\mathrm{i}\delta_k} \quad , \\ R_1^B \mathrm{e}^{2\mathrm{i}\Phi_1^B} &= \frac{1}{2} \left(\frac{h_{tot}}{n} \right)^2 R_1 \mathrm{e}^{2\mathrm{i}\Phi_1} \sum_{k=-p}^{p} b_k \mathrm{e}^{2\mathrm{i}\delta_k} \quad , \end{aligned} \tag{3.26}$$

$$\begin{aligned}
T_0^D &= \frac{1}{12}\left(\frac{h_{tot}}{n}\right)^3 T_0 \sum_{k=-p}^{p} d_k \quad , \\
T_1^D &= \frac{1}{12}\left(\frac{h_{tot}}{n}\right)^3 T_1 \sum_{k=-p}^{p} d_k \quad , \\
R_0^D \mathrm{e}^{4\mathrm{i}\Phi_0^D} &= \frac{1}{12}\left(\frac{h_{tot}}{n}\right)^3 R_0 \mathrm{e}^{4\mathrm{i}\Phi_0} \sum_{k=-p}^{p} d_k \mathrm{e}^{4\mathrm{i}\delta_k} \quad , \\
R_1^D \mathrm{e}^{2\mathrm{i}\Phi_1^D} &= \frac{1}{12}\left(\frac{h_{tot}}{n}\right)^3 R_1 \mathrm{e}^{2\mathrm{i}\Phi_1} \sum_{k=-p}^{p} d_k \mathrm{e}^{2\mathrm{i}\delta_k} \quad ,
\end{aligned} \tag{3.27}$$

where:

$$b_k = \begin{cases} 2k & \text{if} \quad n = 2p+1 \quad , \\ 2k - \dfrac{k}{|k|} \ , \ b_0 = 0 & \text{if} \quad n = 2p \quad , \end{cases} \tag{3.28}$$

and

$$d_k = \begin{cases} 12k^2 + 1 & \text{if} \quad n = 2p+1 \quad , \\ 12k^2 - 12|k| + 4 \ , \ d_0 = 0 & \text{if} \quad n = 2p \quad . \end{cases} \tag{3.29}$$

To remark that the following properties subsist for the coefficients b_k and d_k:

$$\begin{aligned}
\sum_{k=-p}^{p} b_k &= 0 \quad , \\
\sum_{k=-p}^{p} d_k &= n^3 \quad .
\end{aligned} \tag{3.30}$$

Considering the definition of tensors $\mathbf{A}^*$, $\mathbf{B}^*$, $\mathbf{D}^*$ and $\mathbf{C}$ of Eq. (3.22) and also the properties (3.30) we can easily deduce the expression of the polar parameters of the homogenised stiffness tensors for a laminate with identical plies:

$$\begin{aligned}
T_0^{A^*} &= T_0 \quad , \\
T_1^{A^*} &= T_1 \quad , \\
R_0^{A^*} \mathrm{e}^{4\mathrm{i}\Phi_0^{A^*}} &= \frac{1}{n} R_0 \mathrm{e}^{4\mathrm{i}\Phi_0} \sum_{k=-p}^{p} \mathrm{e}^{4\mathrm{i}\delta_k} \quad , \\
R_1^{A^*} \mathrm{e}^{2\mathrm{i}\Phi_1^{A^*}} &= \frac{1}{n} R_1 \mathrm{e}^{2\mathrm{i}\Phi_1} \sum_{k=-p}^{p} \mathrm{e}^{2\mathrm{i}\delta_k} \quad ,
\end{aligned} \tag{3.31}$$

$$
\begin{aligned}
T_0^{B^*} &= 0 \quad , \\
T_1^{B^*} &= 0 \quad , \\
R_0^{B^*}\mathrm{e}^{4\mathrm{i}\Phi_0^{B^*}} &= \frac{1}{n^2}R_0\mathrm{e}^{4\mathrm{i}\Phi_0}\sum_{k=-p}^{p} b_k\mathrm{e}^{4\mathrm{i}\delta_k} \quad , \\
R_1^{B^*}\mathrm{e}^{2\mathrm{i}\Phi_1^{B^*}} &= \frac{1}{n^2}R_1\mathrm{e}^{2\mathrm{i}\Phi_1}\sum_{k=-p}^{p} b_k\mathrm{e}^{2\mathrm{i}\delta_k} \quad ,
\end{aligned}
\tag{3.32}
$$

$$
\begin{aligned}
T_0^{D^*} &= T_0 \quad , \\
T_1^{D^*} &= T_1 \quad , \\
R_0^{D^*}\mathrm{e}^{4\mathrm{i}\Phi_0^{D^*}} &= \frac{1}{n^3}R_0\mathrm{e}^{4\mathrm{i}\Phi_0}\sum_{k=-p}^{p} d_k\mathrm{e}^{4\mathrm{i}\delta_k} \quad , \\
R_1^{D^*}\mathrm{e}^{2\mathrm{i}\Phi_1^{D^*}} &= \frac{1}{n^3}R_1\mathrm{e}^{2\mathrm{i}\Phi_1}\sum_{k=-p}^{p} d_k\mathrm{e}^{2\mathrm{i}\delta_k} \quad ,
\end{aligned}
\tag{3.33}
$$

$$
\begin{aligned}
T_0^{C} &= 0 \quad , \\
T_1^{C} &= 0 \quad , \\
R_0^{C}\mathrm{e}^{4\mathrm{i}\Phi_0^{C}} &= \frac{1}{n}R_0\mathrm{e}^{4\mathrm{i}\Phi_0}\left(\sum_{k=-p}^{p}\mathrm{e}^{4\mathrm{i}\delta_k} - \frac{1}{n^2}\sum_{k=-p}^{p} d_k\mathrm{e}^{4\mathrm{i}\delta_k}\right) \quad , \\
R_1^{C}\mathrm{e}^{2\mathrm{i}\Phi_1^{C}} &= \frac{1}{n}R_1\mathrm{e}^{2\mathrm{i}\Phi_1}\left(\sum_{k=-p}^{p}\mathrm{e}^{2\mathrm{i}\delta_k} - \frac{1}{n^2}\sum_{k=-p}^{p} d_k\mathrm{e}^{2\mathrm{i}\delta_k}\right) \quad .
\end{aligned}
\tag{3.34}
$$

From Eq. (3.32) and (3.34) we can notice that for a laminate with identical layers the isotropic part of tensors $\mathbf{B}^*$ and $\mathbf{C}$ is identically zero, while from Eq. (3.31) and (3.33) we can see that the isotropic parts of tensors $\mathbf{A}^*$ and $\mathbf{D}^*$ are equal and coincide to that of the elementary layer. In other words, the "average behaviour" (i.e. the isotropic part) of the laminate thought as an equivalent single layer is the same as that of the elementary layer. In addition, it is worth noting that, for a laminate with identical plies, the design of the elastic symmetries is always reduced to the design of the anisotropic part of tensors $\mathbf{A}^*$, $\mathbf{B}^*$ and $\mathbf{D}^*$, since the isotropic one is strictly related to that of the elementary lamina and, hence, is known whenever we fix the material of the ply: this aspect is very important especially when the design problem of laminated structures is conceived within the framework of a *two-level procedure*, as we will discuss in Chapters 4 and 6, because the number of material design variables (i.e. those characterising the laminate behaviour) involved into the optimisation process is reduced since the isotropic moduli are known *a priori* (indeed, we need to determine 12 polar parameters instead of 18).

From Eq. (3.23), it can be noticed that the elastic symmetries of the laminate in terms of extension, coupling and stiffness behaviour depend on the stacking sequence, i.e. on the layer materials, orientation, thickness and of course on the number of plies. When dealing with laminate design, a designer has to satisfy several conditions at the same time, including not only common objectives, like buckling load or strength, but also general properties of the elastic response of the laminate, such as uncoupling, extension orthotropy, bending orthotropy and so on. It is not easy to take into account all these aspects, and normally designers use some short-cuts, to get automatically some properties such as uncoupling or extension orthotropy. Vannucci and Vincenti have shown in previous studies (see [43, 115, 116]) that it is possible, in the framework of the polar method, to formulate in a completely general way all the problems of optimal design of laminates, including the requirements on elastic symmetries; therefore, a general approach to the design of laminates is possible. The reader is addressed to the previously cited works for a deeper insight in the matter. In Section 3.4 we present an important modification to this approach that also includes the number of layers among the design variables.

3.3.3 Existence and geometric bounds on laminate polar parameters

The existence constraints of Eq. (3.15) can be applied also to the laminate polar parameters, more precisely to the polar parameters of tensors $\mathbf{A}^*$ and $\mathbf{D}^*$ which have to satisfy, independently, the requirement of positive definiteness, as any other elastic tensor. Such conditions bound an *elastic domain* containing the admissible values of the elastic parameters. Therefore, $\mathbf{A}^*$ and $\mathbf{D}^*$ can be considered as the elastic tensors of two fictitious materials whereby one can imagine to build an equivalent single-layer plate with thickness h_{tot}, having the same extension and bending elastic responses of the laminate in all directions. The case of $\mathbf{B}^*$ is different, because it is not positive-definite, actually it is simply not definite. In addition, the idea of a fictitious material for the coupled response has not a precise and direct mechanical meaning, thus for these reasons, the case of the coupling tensor will not be considered in the following.

Vannucci [133] has shown that when a laminate is tailored by bonding together identical layers of a given material, the aforementioned elastic domain is impossible to be entirely covered, because some more restrictive bounds are given by the combinations of the trigonometric functions appearing in (3.23). Such more restrictive bounds are called *geometric bounds* because they arise from the combination of the layer orientations and position in the stack. In particular, for an uncoupled, fully-orthotropic laminate, the independent bounds are:

$$\begin{cases} T_1^{A^*}\left[T_0^{A^*} + (-1)^{K^{A^*}} R_0^{A^*}\right] - 2R_1^{A^*2} > 0 \ , \\ R_0 - R_0^{A^*} > 0 \ , \\ (-1)^{\left(K^{A^*}-K\right)} \dfrac{R_0^{A^*}}{R_0} + 1 - 2\left(\dfrac{R_1^{A^*}}{R_1}\right)^2 > 0 \ , \\ R_0^{A^*} > 0 \ , \\ R_1^{A^*} > 0 \ . \end{cases} \tag{3.35}$$

Eq. (3.35) is written for the polar parameters of the in-plane homogenised stiffness tensor $\mathbf{A}^*$, but it can be applied to the polar parameters of the tensor $\mathbf{D}^*$, too. In Eq. (3.35) the first constraint is an elastic constraint, while the last four conditions are geometrical constraints. The previous bounds can be written using the well-known *lamination parameters*, introduced by Tsai and Hahn [134], and a wide discussion about the geometric bounds is given in [135].

Moreover, Vannucci showed that the geometric domain is always smaller than the elastic domain, and more precisely he proved that the geometric domain is always entirely contained within the elastic domain. Mechanically, this means that laminates constitute a sort of *smaller elastic class*, in the sense that they never can cover the whole elastic parameters range that can be covered by a single elementary layer.

Finally, the complete set of constraints that we have to consider, in the case of uncoupled, fully-orthotropic laminates is:

$$\begin{cases} R_0 - R_0^{A^*} > 0 \ , \\ (-1)^{\left(K^{A^*}-K\right)} \dfrac{R_0^{A^*}}{R_0} + 1 - 2\left(\dfrac{R_1^{A^*}}{R_1}\right)^2 > 0 \ , \\ R_0^{A^*} > 0 \ , \\ R_1^{A^*} > 0 \ . \end{cases} \tag{3.36}$$

3.4 Design of elastic properties of laminates with minimum number of plies

The problem of designing the elastic properties of laminates with the minimal number of plies, discussed in this Section, belongs to the class of design problems concerning modular systems. In fact, the laminate can be seen as a modular structure whose constitutive modules are the layers that, in the most general case, can be different from each other: they can have different thickness, orientation angle and can be made of different material. More precisely, in the following, we formulate the optimisation problem assuming that

the layers are made of the same material: in such a case the only variables characterising the generic module-layer are the thickness and the orientation.

3.4.1 Mathematical statement of the problem and numerical strategy

In order to formulate the design of laminate elastic properties as an optimisation problem, the key point is the construction of the objective function. For a laminate with n plies the design variables can be: the number of layers n, the vector of layers orientations $\boldsymbol{\delta}$, the vector of layers thickness $\mathbf{h}$. In order to formulate a laminate design problem in the most general way, the objective function $f = f(n, \boldsymbol{\delta}, \mathbf{h})$ should include all the design requirements, and, in particular, those on the elastic symmetries.

Vannucci [43] has shown that the problem of designing the laminate elastic symmetries can be reduced to the search of the minima of a positive semi-definite function in the space of the laminate polar parameters. In the aforementioned work and in some subsequent others, like [115, 116], the number, the thickness and the material of the layers were fixed and the orientations were assumed as the only optimisation variables. The optimisation problem was defined as:

$$\min_{\boldsymbol{\delta}} \left[f(\boldsymbol{\delta}) \right]. \tag{3.37}$$

Since the objective function $f(\boldsymbol{\delta})$ is positive semi-definite, its minima are also the zeros of the function. For more details on the definition of this objective function for different combinations of elastic symmetries, see [43, 115, 116].

As previously specified, the objective of this Chapter consists in designing a laminate having assigned symmetries with the minimum number of layers. In such a case, the number of the plies and, eventually, the thickness of each layer must belong to the set of design variables, thus a modification of the objective function is necessary. The new unconstrained optimisation problem is:

$$\begin{cases} \min\limits_{n,\boldsymbol{\delta},\mathbf{h}} \left[F(n, \boldsymbol{\delta}, \mathbf{h}) \right] \ , \quad \text{with :} \\ F(n, \boldsymbol{\delta}, \mathbf{h}) = f(n, \boldsymbol{\delta}, \mathbf{h})\, n^s \ . \end{cases} \tag{3.38}$$

It can be noticed that the new objective function $F(n, \boldsymbol{\delta}, \mathbf{h})$ is still a positive semi-definite function in the polar parameters space, whose zeros are still solutions of our problem and are also zeros of the function. It is worth noting that the function $F(n, \boldsymbol{\delta}, \mathbf{h})$ (as well as the function $f(n, \boldsymbol{\delta}, \mathbf{h})$) is a dimensionless, homogenised, convex function of the polar parameters of the tensors $\mathbf{A}$, $\mathbf{B}$ and $\mathbf{D}$, while it is a highly non-linear, non-convex function of the design variables, i.e. number of layers n, orientations $\boldsymbol{\delta}$ and thickness $\mathbf{h}$. The influence of the number of layers n is introduced as a penalty term, where s is an exponent whose value can be chosen in a certain range. The large number of numerical

tests that we conducted, show that the best results are obtained when s belongs to the interval [1 ; 4].

Eq. (3.38) formalises a classical unconstrained NLPP for which several numerical solving techniques are available. It can be noticed that, being $f(n, \boldsymbol{\delta}, \mathbf{h})$ a non-convex function having several non-global minima, a suitable and robust solving algorithm must be employed to perform the search process. To this purpose, for all the calculations presented in this Chapter we have employed the GA BIANCA.

In addition, concerning the GA BIANCA, in this Chapter we test the effectiveness of the new genetic operators of crossover and mutation between individuals belonging to different species. Indeed, since the number of layers n is included among the design variables, the related optimisation problem is then defined over a space composed of vectors (i.e. vectors of decision variables) having different lengths. Mathematically speaking, such a problem corresponds on one side to determine the optimal dimension of the domain (i.e. the number of layers n) and on the other side to determine the optimal values of the constitutive parameters of the layers (orientations and thickness) which satisfy, with a good level of accuracy, the requirements imposed by the optimisation problem.

The structure of the individual's genotype for such a problem is the one depicted in Fig. 1.6 in Chapter 1. As shown in that picture, the genotype of the generic k^{th} individual for the optimisation problem (3.38) has n chromosomes. Chromosomes from 2 to n are composed of 2 genes representing the design variables for each constitutive ply: orientation angle and thickness. An exception is chromosome 2 that has 3 genes: the third additional gene codes the number of modules, i.e. for our problem the number of layers n for the k^{th} individual. Hence, individuals with a different value of n belong to different species.

As a concluding remark of this section, it can be noticed that the proposed approach is general, i.e. no simplifying assumptions are introduced such as, for example, the restriction to a given set of stacks like symmetric, balanced, cross-ply or angle-ply stacking sequences.

3.5 Studied cases

To demonstrate the effectiveness of the polar formulation and that of our code BIANCA in order to obtain composite laminates with variable number of plies and with certain elastic properties, several calculations have been carried out and a great number of solutions that satisfy different combinations of design objectives are found. Among all the possible design cases, the following ones are discussed in this Section:

1. uncoupling, total orthotropy with $K = 0$ and axis coincidence, i.e. in-plane and bending orthotropy with the same axes;

2. uncoupling, total orthotropy with $K = 1$ and axis coincidence, i.e. in-plane and bending orthotropy, with the same axes;

3. uncoupling and total isotropy, i.e. in-plane and bending isotropy;

4. uncoupling and quasi-homogeneity, i.e. identical behaviour for the homogenized in-plane and bending stiffness tensors.

We remind that uncoupling is intended to be the bending-extension uncoupling determined by the fact that the stiffness tensor $\mathbf{B}$ is null.

3.5.1 Sample problems

Here we specify the expression of the objective function $F(n, \boldsymbol{\delta}, \mathbf{h})$ for each one of the four cases cited beforehand. In all the cases the value of the power s in Eq. (3.38) is assumed equal to 2.

The objective function for each case is defined in such a way that the solutions, i.e. the minima, are also the zeros of the function. Since each case corresponds to a given combination of elastic symmetries, the global objective function is constructed as a sum of partial objective functions, and each partial objective function is normalised, in such a way that its value varies in $[0, 1]$.

Cases n.1 and n.2

In order to obtain elastic uncoupling, i.e. $\mathbf{B} = \mathbf{0}$, the norm of the coupling tensor $\mathbf{B}$ must be zero. To obtain orthotropy the difference between polar angles Φ_0 and Φ_1 must be a multiple of $\frac{\pi}{4}$, both for membrane and bending stiffness tensors. The last required elastic property, considered here, is the coincidence of the orthotropy axes, i.e. angle Φ_1 has to be the same for $\mathbf{A}$ and $\mathbf{D}$. The expression of the global objective function including all these conditions is:

$$F(n, \boldsymbol{\delta}, \mathbf{h}) = \left[\left(\frac{\|\mathbf{B}^*\|}{\|\mathbf{Q}\|} \right)^2 + \left(\frac{\Phi_0^{A^*} - \Phi_1^{A^*} - K^{A^*} \frac{\pi}{4}}{\frac{\pi}{4}} \right)^2 + \right. \\ \left. + \left(\frac{\Phi_0^{D^*} - \Phi_1^{D^*} - K^{D^*} \frac{\pi}{4}}{\frac{\pi}{4}} \right)^2 + \left(\frac{\Phi_1^{A^*} - \Phi_1^{D^*}}{\frac{\pi}{4}} \right)^2 \right] n^2 \,. \tag{3.39}$$

In Eq. (3.39), $\|\mathbf{B}^*\|$ is the norm of the homogenised coupling tensor, while the normalisation factor $\|\mathbf{Q}\|$ is the one of the layer stiffness tensor. Both norms are calculated

according to Eq. (3.7). All the other polar parameters are referred to their respective homogenised tensors, i.e. $\mathbf{A}^*$ and $\mathbf{D}^*$. The constants K^{A^*} and K^{D^*} can assume the values 0 or 1, depending upon the different kind of orthotropy (case 1: $K^{A^*} = K^{D^*} = 0$; case 2: $K^{A^*} = K^{D^*} = 1$). The normalisation factor of the orthotropy and of the coincidence of the orthotropy axes requirements is assumed equal to $\frac{\pi}{4}$.

Case n.3

In this case, along with the elastic uncoupling the total isotropy requirement has been formalised. The partial objective function for uncoupling is expressed as in cases 1 and 2, see Eq. (3.39). In order to attain the isotropy requirement for in-plane and bending stiffness, the anisotropic part of tensors $\mathbf{A}^*$ and $\mathbf{D}^*$ must be zero. Therefore, the global objective function has the following form:

$$F\left(n, \boldsymbol{\delta}, \mathbf{h}\right) = \left[\left(\frac{\|\mathbf{B}^*\|}{\|\mathbf{Q}\|}\right)^2 + \left(\frac{R_0^{A^*2} + 4R_1^{A^*2}}{R_0^{Q^2} + 4R_1^{Q^2}}\right) + \left(\frac{R_0^{D^*2} + 4R_1^{D^*2}}{R_0^{Q^2} + 4R_1^{Q^2}}\right)\right] n^2 \ . \tag{3.40}$$

In Eq. (3.40), $R_0^{A^*}$, $R_1^{A^*}$ and $R_0^{D^*}$, $R_1^{D^*}$ are referred to the laminate homogenised in-plane and bending stiffness tensors, respectively. The polar moduli R_0^Q and R_1^Q are referred to the layer reduced stiffness tensor and they are employed for the normalisation sake.

Case n.4

In this last case, the requirements are uncoupling and homogeneity, i.e. the laminate has the same behaviour in extension and bending. To realise the objective of homogeneity, the polar parameters T_0, T_1, R_0, R_1, Φ_0, Φ_1 must assume the same value for both the tensors $\mathbf{A}^*$ and $\mathbf{D}^*$, thus the homogeneity tensor is equal to zero, $\mathbf{C} = \mathbf{0}$. The objective function is:

$$F\left(n, \boldsymbol{\delta}, \mathbf{h}\right) = \left[\left(\frac{\|\mathbf{B}^*\|}{\|\mathbf{Q}\|}\right)^2 + \left(\frac{\|\mathbf{C}\|}{\|\mathbf{Q}\|}\right)^2\right] n^2 \ , \tag{3.41}$$

where $\|\mathbf{C}\|$ is the norm of the homogeneity tensor.

3.5.2 Numerical results

Since the laminate elastic behaviour depends upon the elastic properties of the elementary ply, the results must refer to a given material. For all the cases, a highly anisotropic unidirectional carbon/epoxy ply (T300/5208) [134] has been chosen. Its properties are shown in Table 3.2.

Technical moduli		**Polar parameters**	
Young's modulus E_1 [MPa]	181000	T_0 [MPa]	26880
Young's modulus E_2 [MPa]	10300	T_1 [MPa]	24744
Shear modulus G_{12} [MPa]	7170	R_0 [MPa]	19710
Poisson's ratio ν_{12}	0.28	R_1 [MPa]	21433
Density ρ [kg/m^3]	1580	Φ_0 [deg]	0
Ply thickness t_{ply} [mm]	0.125	Φ_1 [deg]	0

Table 3.2: Technical moduli and polar parameters for unidirectional plies of carbon-epoxy T300/5208

For each case two kinds of simulations have been performed. In the first one, the thickness of the elementary ply is assumed equal to 0.125 mm, thus the design variables are only the number and the orientations of the layers. In the second one, also the thickness is included among the design variables of the optimisation. We have considered also this possibility in order to evaluate the influence of such a variable on the determination of the minimum number of layers that we need to obtain some specified elastic properties. Practically, this corresponds to increase the number of design variables for the same kind of problem, and should result in a better quality of the results, with respect to the corresponding cases of fixed thickness, and perhaps in a lower final minimum number of layers. Actually, the results shown below indicate that this is the case. Of course, in doing this we do not consider the practical and technical (e.g. manufacturing) aspects of such a choice, because here we are merely concerned with the theoretical solution of the mathematical problem of finding the laminate having the minimum number of layers to satisfy some elastic requirements. We assume only that the layers have the same elastic properties but different thickness, which implies the assumption that the volume fraction and arrangement of the fibres are constant for all the plies.

For each simulation, the number of plies n varies in the range $[4\ ;\ 16]$, while the orientation of each layer $\delta_k\ \ (k = 1, .., n)$ can assume any value in $[-90^\circ\ ;\ 90^\circ]$ discretised by a step of 1°. For the simulations wherein also the layer thickness is a design variable, the thickness $h_k\ \ (k = 1, .., n)$ varies in a continuous way in the range $[0.1\ ;\ 0.2]$ mm.

Concerning the genetic parameters, the population size is $N_{ind} = 500$ and the maximum number of generations is $N_{gen} = 500$. The crossover and mutation probabilities are $p_{cross} = 0.85$ and $p_{mut} = 1/N_{ind}$, while the shift operator and chromosomes number mutation probabilities are $p_{shift} = 0.5$ and $(p_{mut})_{chrom} = (n_{chrommax} - n_{chrommin})/N_{ind}$, where $n_{chrommin}$ and $n_{chrommax}$ correspond to the lower and upper bound defined for the number of layers n. Selection is performed by the roulette-wheel operator and the elitism is active.

Tables 3.3 and 3.4 show examples of stacking sequences for laminates responding to design criteria from cases n. 1 to 4, in the case of fixed and variable layer thickness,

respectively. The residual in the last column is the value of the global objective function $F(n, \boldsymbol{\delta}, \mathbf{h})$ for the solution indicated aside (we recall that exact solutions correspond to zeros of the objective function). As in each numerical technique, the real solution is found within a small numerical tolerance that represents the residual. For a discussion on the importance of the numerical residual in such a kind of problems, see [43, 2].

Tables from 3.5 to 3.12 show the polar parameters values for all the stacking sequences found in both cases of constant and variable ply thickness. It is possible to see that all the laminates are extension-bending uncoupled although the stacking sequences are not symmetric. Actually, some of these sequences are anti-symmetric (a condition that guarantees bending orthotropy, but not always bending-extension uncoupling, see [136]). For instance, the sequence of case n. 1, with plies of constant thickness, can be reduced to the sequence [2/-7/11/-11/7/-2], which is anti-symmetric, simply by a rotation of -7°. Actually, such an angle corresponds to the value of the polar angle Φ_1, see Table 3.5, and in this case, having imposed $K = 0$, also of Φ_0. In fact, for a given elastic tensor $\mathbf{L}$, in the case of orthotropy with $K = 0$, the direction determined by the angle Φ_1 corresponds to the main orthotropy axis, i.e. to the direction of the highest value of the component L_{xxxx}, as it can be easily seen from Eq. (3.6), see also [118]. An analogous result is valid also for case n. 2, always when the plies have a constant thickness, as well as for cases n.1 and n.4, when the plies have variable thickness. Nevertheless, the condition of antisymmetrical stacks is a sufficient condition to obtain bending orthotropy that is valid only for laminates with identical layers, while, normally, this condition cannot be applied for laminates having plies with variable thickness.

In our calculations, we do not fix the orthotropy direction, because the properties that we are looking for are intrinsic, i.e. frame independent. The use of the polar formalism allows, in fact, not only for fixing the frame, for instance imposing a given value of the polar angle Φ_1 simply adding a term of the type $\left(\Phi_1 - \overline{\Phi}_1\right)^2$ to the definition of f, but also (as in the considered cases) to make completely abstraction from the frame, whenever intrinsic properties are sought for independently from any frame. Of course, a post-processing operation of frame rotation, as the one described above, can always been done, if one wishes to have the final result in a particular frame.

Figs. from 3.2 to 3.9 show the directional plots of some of the elastic properties for the laminates solution for cases from n. 1 to 4. For the sake of clarity and shortness, not all the elastic properties have been plotted, but those presented here are sufficient to show that the prescribed elastic properties have really been obtained.

For the sake of brevity, a detailed discussion of the results is presented only for the laminates obtained as solution of cases 2 and 3, but similar considerations can be done also for the other cases.

One can consider first the requirement expressed by the case n.2. In Tables 3.7 and 3.8, it is possible to notice that the laminate solution, in both cases of constant and variable ply thickness, respects the design criteria:

Objective	Stacking sequence (angles [°])	n. of plies	Residual
Case n. 1	$[9/0/18/-4/14/5]$	6	3.5873×10^{-6}
Case n. 2	$[-16/-65/-67/-8/-10/-59]$	6	1.7547×10^{-2}
Case n. 3	$[0/-50/61/42/-87/-90/-49/-10/-12/36/26/-47/83]$	13	1.6117×10^{-2}
Case n. 4	$[64/71/74/65/66/63/70]$	7	1.7547×10^{-2}

Table 3.3: Best stacking sequences for the design problems 1 to 4, fixed layer thickness

Objective	Stacking sequence (angles [°] and thickness [mm])	n. of plies	Residual
Case n. 1	$[-9/-6/-4/-11/-9/-6]$ $[0.118/0.126/0.140/0.126/0.103/0.152]$	6	3.2976×10^{-7}
Case n. 2	$[-24/-73/-18/-67]$ $[0.100/0.200/0.200/0.100]$	4	7.3315×10^{-3}
Case n. 3	$[-19/-74/45/20/75/-17/-53/-83/2/51]$ $[0.113/0.168/0.200/0.137/0.149/0.190/0.199/0.113/0.106/0.116]$	10	2.0476×10^{-3}
Case n. 4	$[-15/-2/-12/-10/-21/-6]$ $[0.156/0.188/0.158/0.151/0.111/0.182]$	6	2.9945×10^{-5}

Table 3.4: Best stacking sequences for the design problems 1 to 4, variable layer thickness

1. in-plane orthotropy with $K^A = 1$:
   - plies with identical thickness, $\Phi_0^A - \Phi_1^A = 7.50° - (-37.50°) = 45.00°$;
   - plies with non-identical thickness, $\Phi_0^A - \Phi_1^A = -0.50° - (-45.50°) = 45.00°$;
2. bending orthotropy with $K^D = 1$:
   - plies with identical thickness, $\Phi_0^D - \Phi_1^D = 7.50° - (-37.50°) = 45.00°$;
   - plies with non-identical thickness, $\Phi_0^D - \Phi_1^D = -0.50° - (-45.50°) = 45.00°$;
3. elastic uncoupling expressed by polar condition $\|\mathbf{B}^*\| = 0$. The norm of tensor $\mathbf{B}^*$ is really negligible compared to the one of tensor $\mathbf{A}^*$ or $\mathbf{D}^*$:
   - plies with identical thickness, $\dfrac{\|\mathbf{B}^*\|}{\|\mathbf{A}^*\|} = 0.0270$;
   - plies with non-identical thickness, $\dfrac{\|\mathbf{B}^*\|}{\|\mathbf{A}^*\|} = 0.0260$;
4. coincidence of orthotropy axes, polar condition $\Phi_1^A = \Phi_1^D$:
   - plies with identical thickness, $\Phi_1^A = \Phi_1^D = -37.50°$;
   - plies with non-identical thickness, $\Phi_1^A = \Phi_1^D = -45.50°$.

For the case n. 2 it is worth noting that, concerning the laminate with identical layers thickness, the solution which satisfies all the requirements with the minimum number of plies is only made by 6 layers, see Table 3.3. When the ply thickness becomes a design variable the solution found has many improvements as shown in Table 3.4. First, the minimum layers number to obtain a solution is decreased from 6 to 4, then, this solution has a lower value of the residual, i.e. the laminate satisfies the requirements in a more satisfactory way. Figs. 3.4 and 3.5 show the polar diagrams of the elastic properties of the laminates solution of this case.

Let us turn the attention to the case n. 3. In Table 3.9 and 3.10 one can notice that the laminate solution of the problem n.3, in both cases of constant and variable ply thickness, respects the design criteria:

1. in-plane isotropy, expressed by the polar condition that the anisotropic part of the tensor $\mathbf{A}^*$ must be zero, i.e. $R_0^{A^*2} + 4R_1^{A^*2} = 0$. The ratio between the tensor anisotropic and isotropic part is very close to zero, i.e. the anisotropic components are negligible compared to the isotropic ones:
   - plies with identical thickness, $\sqrt{\dfrac{R_0^{A^*2} + 4R_1^{A^*2}}{T_0^{A^*2} + 2T_1^{A^*2}}} = 0.0023$;
   - plies with non-identical thickness, $\sqrt{\dfrac{R_0^{A^*2} + 4R_1^{A^*2}}{T_0^{A^*2} + 2T_1^{A^*2}}} = 0.0017$;
2. bending isotropy, expressed by the polar condition that the anisotropic part of the tensor $\mathbf{D}^*$ must be zero, i.e. $R_0^{D^*2} + 4R_1^{D^*2} = 0$. The ratio between the tensor anisotropic and isotropic part is very close to zero, i.e. the anisotropic components are negligible compared to the isotropic ones:
   - plies with identical thickness, $\sqrt{\dfrac{R_0^{D^*2} + 4R_1^{D^*2}}{T_0^{D^*2} + 2T_1^{D^*2}}} = 0.0040$;
   - plies with non-identical thickness, $\sqrt{\dfrac{R_0^{A^*2} + 4R_1^{A^*2}}{T_0^{D^*2} + 2T_1^{D^*2}}} = 0.0007$;
3. elastic uncoupling expressed by polar condition $\|\mathbf{B}^*\| = 0$. The norm of tensor $\mathbf{B}^*$ is negligible compared to the one of tensor $\mathbf{A}^*$ or $\mathbf{D}^*$:
   - plies with identical thickness, $\dfrac{\|\mathbf{B}^*\|}{\|\mathbf{A}^*\|} = 0.0130$;
   - plies with non-identical thickness, $\dfrac{\|\mathbf{B}^*\|}{\|\mathbf{A}^*\|} = 0.0060$;

In such a case, concerning the laminate with identical layers thickness, the solution which satisfies all the requirements with the minimum number of plies is made by 13 layers, see Table 3.3. When the ply thickness becomes a design variable, the best solution is really improved, as shown in Table 3.4. As in the previous case, the minimum layers number to obtain a solution is decreased from 13 to 10 and the value of the residual is lower, i.e. the laminate satisfies the requirements more accurately. Figs. 3.6 and 3.7 show the polar diagrams of the elastic properties of the laminates solution of this case.

3.6 Concluding remarks

The problem of determining which is the lowest number of layers ensuring some given elastic properties of a laminate has been addressed in this Chapter. The approach proposed to deal with such a problem consists in reducing it to a classical unconstrained NLPP by searching the minima of a semi-definite positive function over the space of the design variables. Such a method is totally general, i.e. no simplifying assumptions are required.

The formulation of the problem is based on the polar representation of plane tensors while, as numerical strategy to perform the solutions search for the considered cases, we have employed the new version of the GA BIANCA. In particular, we have tested and proved the effectiveness of the new genetic operators for crossover and mutation among different species when dealing with the problem of designing the elastic properties of composite laminates having the minimum number of layers.

The numerical results presented in this Chapter, which are completely new and non-classical examples, show the effectiveness of the proposed approach.

Elastic properties	Tensor $\mathbf{A}^*$	Tensor $\mathbf{B}^*$	Tensor $\mathbf{D}^*$
T_0 [MPa]	26880.4311	0	26880.4311
T_1 [MPa]	24743.8933	0	24743.8933
R_0 [MPa]	17033.4619	19.5909	18772.4089
R_1 [MPa]	20683.2749	2.83	21173.5205
Φ_0 [°]	7	–	7
Φ_1 [°]	7	–	7

Table 3.5: Polar parameters for the laminate case n.1, constant ply thickness

Elastic properties	Tensor $\mathbf{A}^*$	Tensor $\mathbf{B}^*$	Tensor $\mathbf{D}^*$
T_0 [MPa]	26880.4311	0	26880.4311
T_1 [MPa]	24743.8933	0	24743.8933
R_0 [MPa]	19437.9543	2.5019	19583.8459
R_1 [MPa]	21358.8283	0.90806	21398.6655
Φ_0 [°]	-7.32	–	-7.32
Φ_1 [°]	-7.32	–	-7.32

Table 3.6: Polar parameters for the laminate case n.1, variable ply thickness

Elastic properties	Tensor $\mathbf{A}^*$	Tensor $\mathbf{B}^*$	Tensor $\mathbf{D}^*$
T_0 [MPa]	26880.4311	0	26880.4311
T_1 [MPa]	24743.8933	0	24743.8933
R_0 [MPa]	4873.3071	1407.9761	1122.9394
R_1 [MPa]	13002.5339	113.5579	14626.7514
Φ_0 [°]	7.5	–	7.5
Φ_1 [°]	-37.5	–	-37.5

Table 3.7: Polar parameters for the laminate case n.2, constant ply thickness

Elastic properties	Tensor $\mathbf{A}^*$	Tensor $\mathbf{B}^*$	Tensor $\mathbf{D}^*$
T_0 [MPa]	26880.4311	0	26880.4311
T_1 [MPa]	24743.8933	0	24743.8933
R_0 [MPa]	4035.9329	1345.8389	1029.8979
R_1 [MPa]	13420.7539	158.8238	14673.2203
Φ_0 [°]	-0.5	–	-0.5
Φ_1 [°]	-45.5	–	-45.5

Table 3.8: Polar parameters for the laminate case n.2, variable ply thickness

Elastic properties	Tensor $\mathbf{A}^*$	Tensor $\mathbf{B}^*$	Tensor $\mathbf{D}^*$
T_0 [MPa]	26880.4311	0	26880.4311
T_1 [MPa]	24743.8933	0	24743.8933
R_0 [MPa]	101.0911	536.0837	120.9914
R_1 [MPa]	9.3146	90.7468	63.6677
Φ_0 [°]	–	–	–
Φ_1 [°]	–	–	–

Table 3.9: Polar parameters for the laminate case n.3, constant ply thickness

Elastic properties	Tensor $\mathbf{A}^*$	Tensor $\mathbf{B}^*$	Tensor $\mathbf{D}^*$
T_0 [MPa]	26880.4311	0	26880.4311
T_1 [MPa]	24743.8933	0	24743.8933
R_0 [MPa]	45.4948	253.7272	30.4769
R_1 [MPa]	29.3042	46.5314	6.8212
Φ_0 [°]	–	–	–
Φ_1 [°]	–	–	–

Table 3.10: Polar parameters for the laminate case n.3, variable ply thickness

Elastic properties	Tensor $\mathbf{A}^*$	Tensor $\mathbf{B}^*$	Tensor $\mathbf{D}^*$
T_0 [MPa]	26880.4311	0	26880.4311
T_1 [MPa]	24743.8933	0	24743.8933
R_0 [MPa]	18929.7208	6.4786	18921.6397
R_1 [MPa]	21219.3737	0.8899	21217.4539
Φ_0 [°]	−22.15	–	−22.14
Φ_1 [°]	67.85	–	67.85

Table 3.11: Polar parameters for the laminate case n.4, constant ply thickness

Elastic properties	Tensor $\mathbf{A}^*$	Tensor $\mathbf{B}^*$	Tensor $\mathbf{D}^*$
T_0 [MPa]	26880.4311	0	26880.4311
T_1 [MPa]	24743.8933	0	24743.8933
R_0 [MPa]	18090.7546	44.438	18088.1731
R_1 [MPa]	20982.3915	19.2386	20983.6104
Φ_0 [°]	−10.05	–	−10.05
Φ_1 [°]	−10.08	–	−10.08

Table 3.12: Polar parameters for the laminate case n.4, variable ply thickness

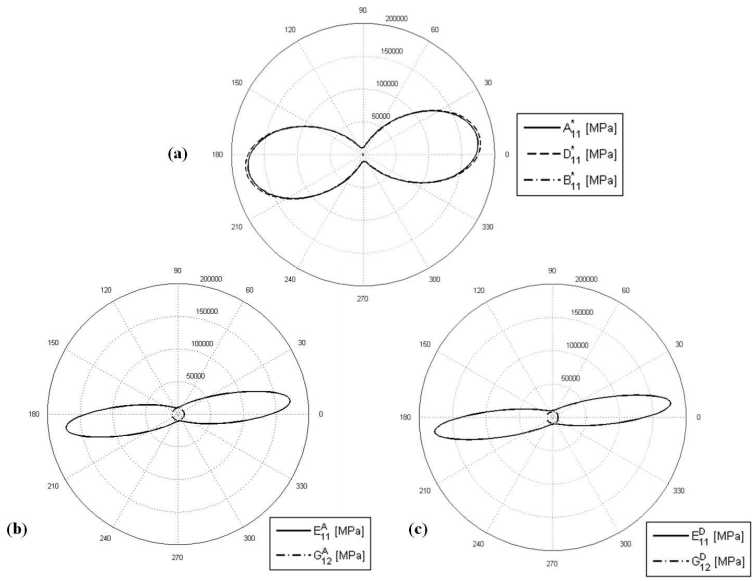

Figure 3.2: Polar variations for laminate n.1, identical ply thickness. (a) Stiffness components, (b) membrane Young's modulus E_{11} and shear modulus G_{12} and (c) bending Young's modulus E_{11} and shear modulus G_{12}.

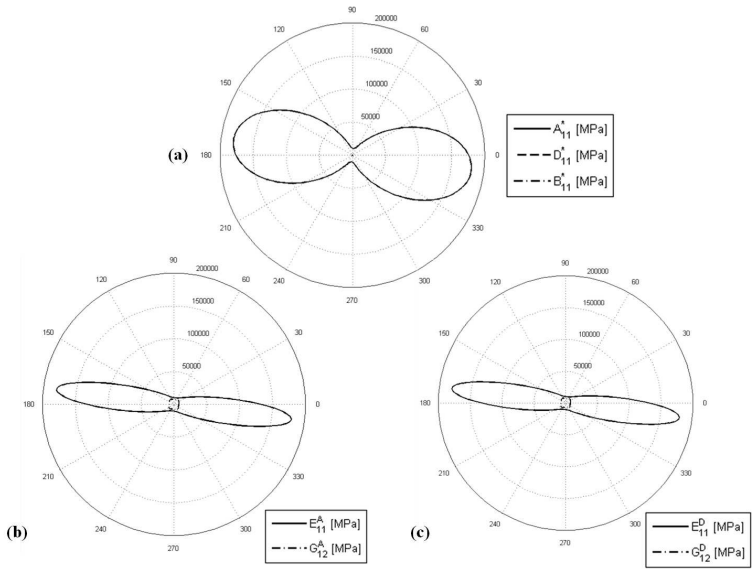

Figure 3.3: Polar variations for laminate n.1, non-identical ply thickness. (a) Stiffness components, (b) membrane Young's modulus E_{11} and shear modulus G_{12} and (c) bending Young's modulus E_{11} and shear modulus G_{12}.

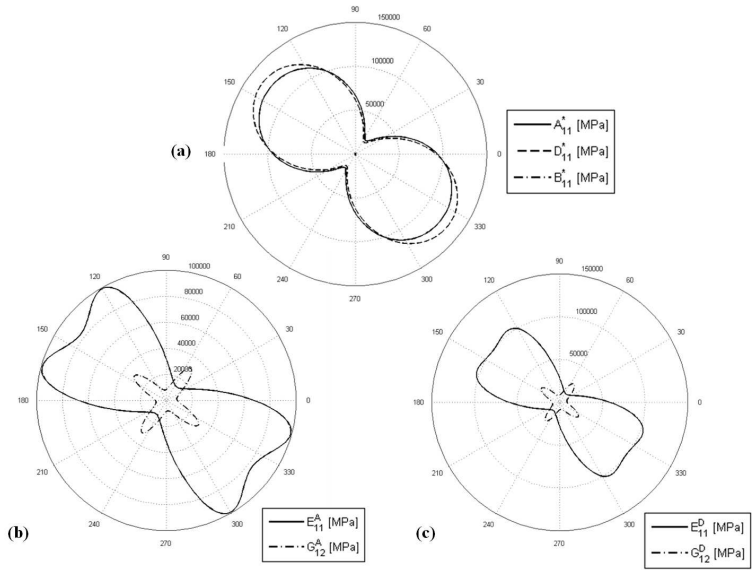

Figure 3.4: Polar variations for laminate n.2, identical ply thickness. (a) Stiffness components, (b) membrane Young's modulus E_{11} and shear modulus G_{12} and (c) bending Young's modulus E_{11} and shear modulus G_{12}.

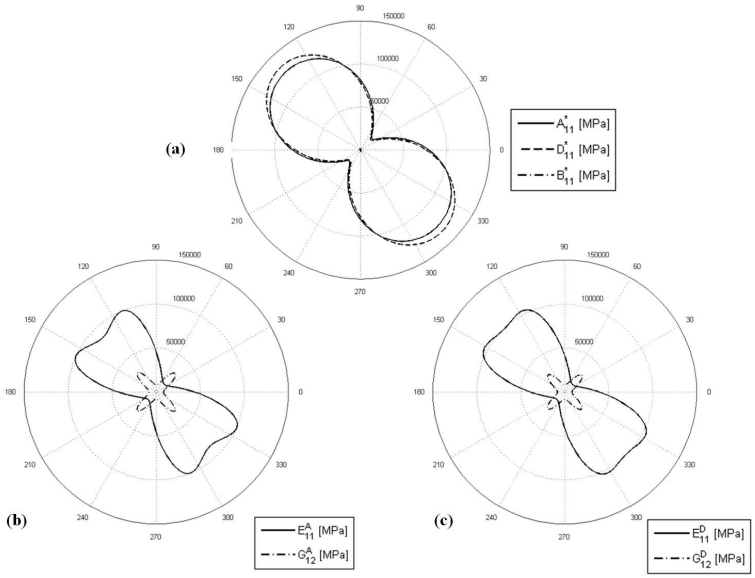

Figure 3.5: Polar variations for laminate n.2, non-identical ply thickness. (a) Stiffness components, (b) membrane Young's modulus E_{11} and shear modulus G_{12} and (c) bending Young's modulus E_{11} and shear modulus G_{12}.

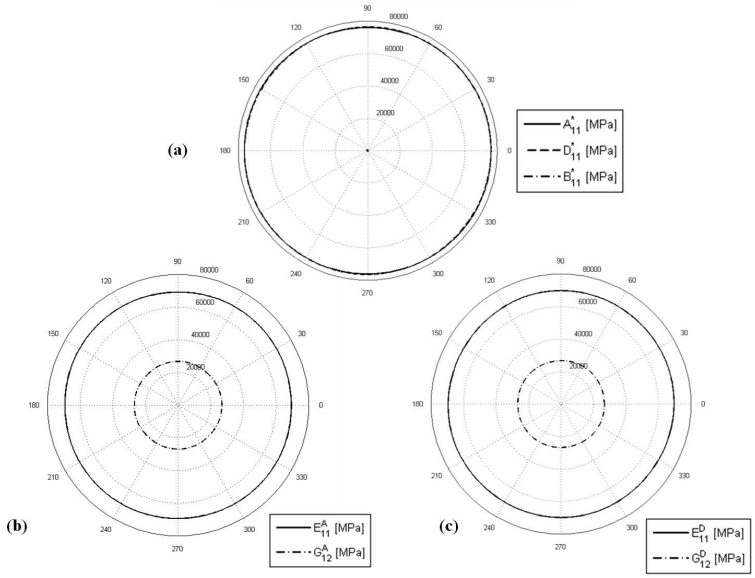

Figure 3.6: Polar variations for laminate n.3, identical ply thickness. (a) Stiffness components, (b) membrane Young's modulus E_{11} and shear modulus G_{12} and (c) bending Young's modulus E_{11} and shear modulus G_{12}.

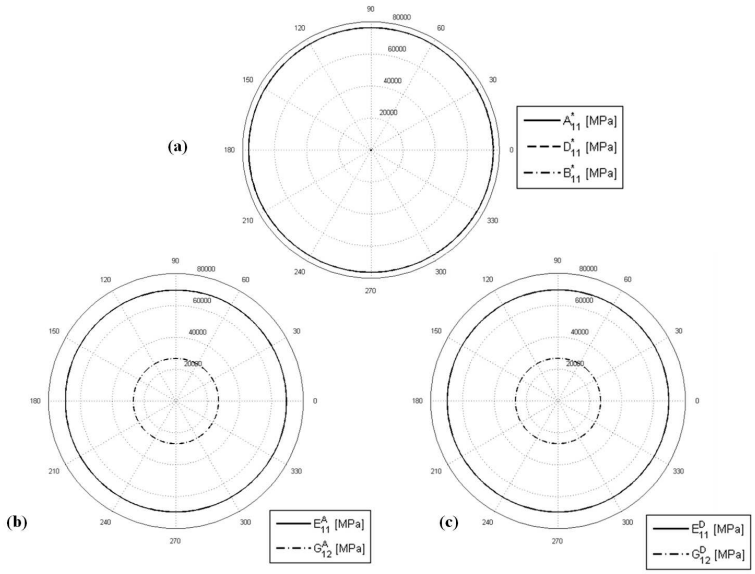

Figure 3.7: Polar variations for laminate n.3, non-identical ply thickness. (a) Stiffness components, (b) membrane Young's modulus E_{11} and shear modulus G_{12} and (c) bending Young's modulus E_{11} and shear modulus G_{12}.

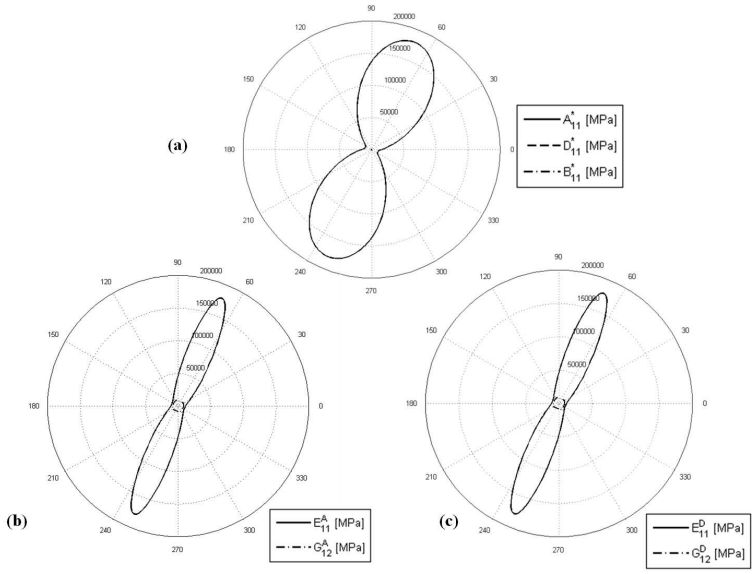

Figure 3.8: Polar variations for laminate n.4, identical ply thickness. (a) Stiffness components, (b) membrane Young's modulus E_{11} and shear modulus G_{12} and (c) bending Young's modulus E_{11} and shear modulus G_{12}.

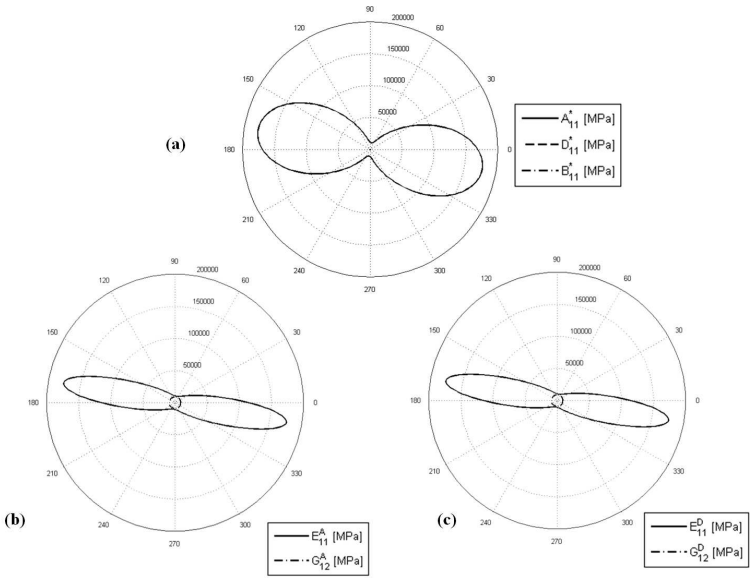

Figure 3.9: Polar variations for laminate n.4, non-identical ply thickness. (a) Stiffness components, (b) membrane Young's modulus E_{11} and shear modulus G_{12} and (c) bending Young's modulus E_{11} and shear modulus G_{12}.

Chapter 4

Optimal design of modular systems: application to stiffened composite structures

4.1 Introduction

The design of modular systems is a difficult task whenever the number of modules is unknown. The difficulty increases even more when the modules can have different dimensions. Similar problems arise in several engineering domains. Modular systems (or structures) are widely used in engineering field: classical examples are modular structures employed in the aeronautical field (such as, for example, stiffened panels for wing and fuselage, covering panels of the aircraft tail, modular components of the landing gear structure, modular systems for the flaps and slats actuators and so on), in the helicopter field (stiffened and sandwich-like panels employed for the blades, modular structure of the rotor hub) and also in the automotive field (the car engine itself can be viewed as a modular system, other examples are the repetitive units of the car chassis, the modular components of the brake system and so on).

In this Chapter we consider the most general case of modular systems whose constitutive modules are "structurally identical" (i.e. they are characterised by the same physical parameters) but, at the same time, they can be "quantitatively different" (namely, the physical parameters describing each module can assume different values). As an illustrative example of our approach to the design of modular systems, we consider here a case which can be viewed as paradigmatic: the design of a least weight wing-box girder, with an unknown number of stiffeners, that has to be realized by composite laminates.

Stiffened panels are widely used in many structural applications, mostly because they allow for a substantial weight saving. Of course, this point is of paramount importance especially in aircraft design, where an important reduction of the structural weight can be

achieved if composite laminates are used in place of aluminum alloys. A drawback of such a choice is that the optimal design of the structure is much more cumbersome than that of a classical metallic structure. In fact, though the use of laminated structures is not a recent achievement in structural mechanics, up to now no general rules and methods exist for their optimal design, and engineers always use some simplifying assumptions or rules.

These assumptions are used on one side to obtain a short-cut to a possible solution, i.e. to eliminate from the true problem some particularly difficult points or properties to be obtained. On the other side, some of such rules are considered to prevent the final structure from some undesired phenomena, though this is never clearly and rigorously stated and proved. Unfortunately, the most part of times the use of such simple rules leads only to a *sub-optimal solution*, i.e. to a solution which is not a real global optimal one. Two examples are the use of symmetric stacking sequences, a sufficient but not necessary condition for bending-extension uncoupling, and the use of balanced stacks to obtain orthotropic laminates in extension. When symmetric stacking sequences are used, the design is done using half of the layers, which means also half of the design variables. Once half of the stack has been designed, the other half is simply added, symmetrically with respect to the mid-plane, in order to obtain uncoupling. Of course, it is very difficult to obtain the lightest structure using a similar strategy.

The use of balanced stacks, on the other side, leads systematically to mechanically false solutions: whenever such a rule is used, bending orthotropy, a rather difficult property to be obtained [136], is simply understated, assumed, but not really obtained, as in [137] or [138], sometimes ignored, like in [139] (about this topic, see [116] for more details). In aircraft structural design, some other rules are imposed to the design of laminated panels, see for instance [138]; none of them are mechanically well justified. Certainly, an appropriate mathematical formulation of the design process could take into account the mechanical and technological problems that such drastic, empirical rules want to prevent.

Several studies have been conducted on the optimisation of composite stiffened panels subject to buckling and/or strength constraints. A minimum-weight design was performed by Butler and Williams [140] using VICONOPT, a program for buckling and strength analyses based on the direct solutions of the governing equations assuming a sinusoidal law for the deformed shape of the structure. Another minimum-weight design approach, with a constraint on the buckling load, was proposed by Wiggenraad *et al* [141] using the code PANOPT which is based on Riks' derivation for finite-strip analyses. Damage tolerance and soft-skin concepts were introduced to take into account the technological limits on ply thickness and geometry. Nevertheless, the presence of integers or discrete variables, such as the number and the orientation of the layers, number of the stiffeners and so on, makes the use of methaeuristics, in particular genetic algorithms (GAs), more profitable in the optimisation of composite structures [37, 38]. Nagendra *et al* [39] studied the weight-optimisation problem of composite stiffened shells and they found a solution through an improved GA and a finite-strip element method implemented in PASCO, a

program used for the evaluation of the buckling load and strain constraints. Kaletta and Wolf [40] used a parallel computing GA to solve the minimum weight design problem of a stiffened composite plate panel, considering constraints on buckling load and maximum strength. They applied this technique using directly a finite element (FE) analysis to evaluate objective and constraint functions. Lillico *et al* [41] studied the problem of the optimal design of the stiffened panel made of aluminium alloy, with constraints on buckling load and post-buckling maximum strength, and solve them through the code VICONOPT. More recently, Bisagni and Lanzi [42] developed a global approximation strategy in order to find a minimum-weight design for low curvature composite stiffened panel considering, at the same time, the constraints on the buckling load, pre-buckling stiffness and post-buckling collapse load. They developed a neural network system, trained by means of FE analyses, which reproduced the structural response of the whole panel. They used this model, coupled with a standard GA, in order to find the optimal configuration.

The research presented in this Chapter has been motivated by the following purpose: to show that an appropriate optimisation procedure can lead to a substantial weight saving in the design of modular composite structures. The case that we have considered is that of a wing-box stiffened girder made of composite laminates. The objective of the optimal problem is to design the lightest structure, submitted to a constraint on the buckling load, which is a classical problem in aircraft structural engineering. The same procedure, however, can be applied to other problems and also other requirements (in the form of additional constraints to the optimisation problem) can be taken into account.

The design procedure that we propose is inspired by a radical point of view: to design a modular composite laminated structure by a mathematically rigorous numerical optimisation procedure that will not use any simplifying assumption. Only avoiding the use of *a priori* assumptions one can hope to obtain the true global optimum for a given problem: this is a key-point in our approach. The design process that we propose is, on one side, completely free, i.e. not submitted to restrictions, and on the other side completely automatic: the operator does not need to take any preliminary decision, for instance on the number of the layers or of the stiffeners, because the method will do that for him, in the best way. In fact, the approach presented in this Chapter can automatically optimise also the number of design variables during the iterations.

Actually our hope is twofold: first, to show that, if old design rules and *a priori* assumptions are abandoned in the design of structural laminates, interesting solutions can be obtained, especially in weight saving. Then, that modern numerical methods allow such an approach and make it possible to substitute old simplifying and limiting assumptions with more rigorous requirements that can be included into the numerical procedure.

Concerning the optimisation code BIANCA, the aims of the work presented in this Chapter are substantially two: on one side we test the effectiveness of the genetic operators allowing the crossover and mutation between different species when dealing with the

problem of the least-weight design of composite modular structures, while on the other side we test the effectiveness of the ADP handling-constraint strategy as well as that of the interface with external software.

The Chapter is organised as follows: the mechanical problem considered in the study is introduced in Sec. 4.2 and the optimisation strategy is explained in Sec. 4.3. The mathematical formulation of the minimum weight design problem is detailed in Sec. 4.4 and the problem of determining a suitable laminate is formulated in Sec. 4.5. A concise description of the FE model of the wing-box structure is given in Sec. 4.6, while in Sec. 4.7 we show the numerical results of the whole optimisation procedure. Finally, Sec. 4.8 ends the Chapter with some concluding remarks and perspectives.
This Chapter is substantially taken from the publications [142, 143].

4.2 Description of the problem: application to the design of an aircraft wing

The optimisation procedure is applied to a classical long-range aircraft wing-box stiffened panel. Fig. 4.1 shows the conceptual steps which lead to the construction of the approximate model of the wing-box section. In particular, we have considered the wing-box section located at the 60% of the wing span, whose typical dimensions are shown in Fig. 4.1. These values represent specific dimensions for a long-range aircraft with a design range of about 9300 km, 350 passengers, two engines, cruising altitude between $\sim 7600 \div 10700$ m and Mach number of about 0.82. For more details see [144].

The structure has a width w of 2610 mm, height h_b of 720 mm and a length L of 700 mm. The wing-box section represents a portion of the wing between two consecutive ribs. We consider the wing-box simply-supported on these ribs. Fig. 4.1 shows also the loads acting on the structure in normal flight conditions: in such a case, only the upper panel can undergo buckling phenomena. The whole wing-box is made of composite laminates composed of highly anisotropic unidirectional carbon-epoxy layers T300/5280 [134]. The material properties of the elementary layer are shown in Table 3.2. Both upper and lower panels have Z-shaped stiffeners with equal flanges. The core and the flanges of each stiffener have the same thickness.

As previously said, no simplifying assumptions are used for the panel: indeed each stiffener can be different from any other, in terms of geometrical and mechanical behaviour, but for evident mechanical reasons we impose that each plate composing the structure is orthotropic both in bending and in extension, and with the orthotropy axes aligned with the axes of the wing-box. Indeed, about the geometry of the structure, we only assume that, for constructive reasons, the wing-box section is symmetric with respect to the global $x - y$ plane, as shown in Fig. 4.1.

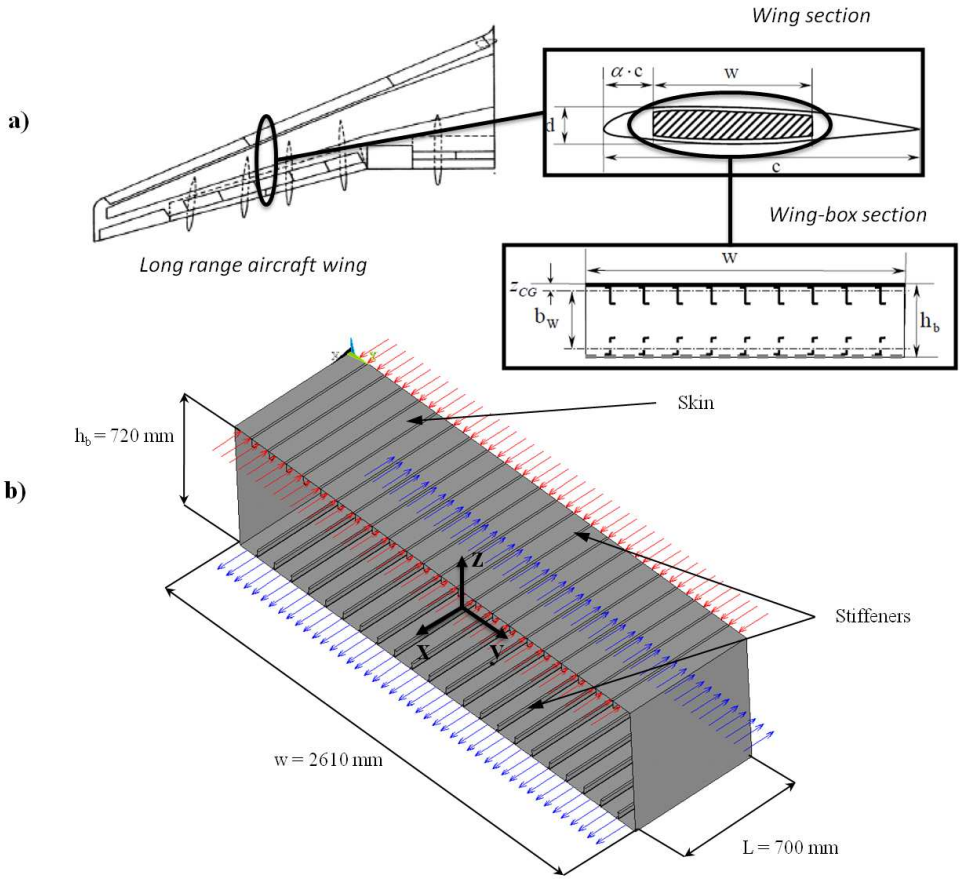

Figure 4.1: (a) Conceptual phases which lead to the construction of the wing-box model (b) Structure of the wing-box stiffened panel and applied loads.

4.3 The two-level optimisation strategy

The optimal design of a stiffened wing-box section made of composite laminates is an hard task, if no simplifying assumptions are used. Actually, such a problem, like many other similar problems in structural engineering, has some peculiarities and the optimisation strategy must take into account all of them:

- the structure is a mechanical system composed by modules. Actually, there are two types of modules in this system: the modules of the first type are the stiffeners. All the stiffeners are modules because they have the same function and geometry, but not necessarily the same dimensions and mechanical properties. In fact, in the most general case each stiffener can be different from another one, because it can have different dimensions, number and orientation of the plies and hence different mechanical properties. The modules of the second type are the layers: all the layers,

composing each part of the structure, are identical, but each member of the structure (stiffeners, skins) can be composed by a different number of layers that normally are differently oriented;

- the design process must be able to completely determine the *optimal configuration of each module* and their *optimal number*: this point is of a particular importance whenever the objective is the least weight, because dimensions and number of modules greatly affect the final weight of the structure;

- the design process must be able to take into account all the *mechanical prescriptions imposed to the structure*, without using simplifying assumptions: namely, it must be possible to take into account general properties concerning the elastic symmetries, like orthotropy for both bending and extension behaviour, uncoupling and so on; this can be done effectively by a proper choice of the anisotropy representation;

- the design procedure must be able to *handle the direction of anisotropy*, namely the orientation of the orthotropy axes, without imposing particular stacking sequences and/or orientation angles that automatically fix the anisotropy direction in a particular direction, like cross-ply, angle-ply or balanced quasi-isotropic sequences;

- all the *constraints imposed to the problem*, of either mechanical or technological nature (inequality and/or equality constraints), must be effectively handled by the procedure;

- the numerical tool used for the solution of the optimisation problem must be able to simultaneously handle design variables of different nature: *continuous*, *discrete* or *grouped* variables, these last being a sort of pointers that, when chosen in a list, imply the automatic choice of a set of variables;

- the numerical strategy used to solve the optimisation problem must be able to effectively handle *highly non-convex problems*.

Another point is very important when the design concerns composite laminated structures: there is not a bijective correspondence between the elastic properties of the laminate and the stacking sequence, see for instance [145]: the same mechanical behaviour in bending, coupling or extension can be obtained by several different laminates, all composed of the same identical plies but not necessarily by the same number of plies or with the same orientations.

All the above points have suggested us the optimisation strategy to be used to deal with structural problems like the one considered in this Chapter (the same strategy is also adopted for a different application shown in Chapter 6). In particular, they have inspired us in the choice of the general organisation of the procedure, of the mathematical formulation, of the mechanical parameters and of the numerical algorithm.

Concerning the general organisation of the procedure, we adopted a *two-level strategy*: the problem of finding the lightest stiffened wing-box, composed of identical layers of a chosen material, is split into two different but linked optimisation problems:

- **First level**: at this stage, *we consider each part of the structure, skins and stiffeners, as composed of a single equivalent homogeneous layer*; the problem of finding the least-weight structure with imposed constraints is formulated and solved. The output of this step is, hence, the geometry of the structure, i.e. the number of stiffeners as well as the stiffeners and skins dimensions in terms of number of constitutive layers, mechanical properties (i.e. the components of the stiffness tensors of the skin and of each stiffener). Thus, this is the step where the true optimal design of the structure is done, in terms of its overall properties.

- **Second level**: during this phase, *we look for one stacking sequence giving the optimal overall properties found during the first step*, and this is done for all the laminates composing the structure, i.e. for each laminate of skin and stiffeners. At this stage, the design variables are the layers orientations and we can add some requirements concerning different aspects. For instance, more constraints on the elastic behaviour can be added for different reasons, or the orientations of the layers can be restricted to a set of possible values and so on. This is possible because the fact that several laminates share the same overall elastic behaviour allows us a large panel of possibilities in terms of suitable laminates, and this panel rapidly increases with the number of plies.

It is worth noting that such a strategy has already been used in other works, with various approaches to the first and second level, see for example [120, 145, 146].

Concerning the mathematical formulation, this will be detailed, for both the first and second step, in the next Section.

4.4 Mathematical formulation of the first-level problem

The overall characteristics of the optimal structure are to be designed during this phase. For the problem at hand, this means that in this phase we have to determine the optimal values of the following parameters:

- the number of stiffeners;

- the thickness, and hence the number of layers, of the skin and of each stiffener;

- the geometrical dimensions of each stiffener;

- the mechanical properties of the skin and of each stiffener.

It is worth noting the peculiarity of this structural optimisation problem: unlike classical optimisation problems of structural engineering, where the only design variables are the geometrical dimensions of the structure, in this case we need also determine the optimal number of modules and their mechanical characteristics, besides their dimensions. We recall, in fact, that in the most general situation, the stiffeners share the same form but can have different dimensions and mechanical properties.

We can immediately see that during this stage of the optimisation procedure, the design of the thickness of the different parts of the structure must be done using discrete variables, with a step equal to the thickness of the material layer used for the fabrication of the structure. Of course, this responds to a technological need and, moreover, this will give us also another important result: the number of layers to be used during the second-level design.

We recall that the objective of the procedure consists in minimising the weight of the wing-box section: this must be done satisfying on one side the constraint on the buckling load, and on the other side the geometric bounds for the elastic moduli. Such aspects are described in detail in the following subsections.

4.4.1 Geometrical design variables

Before specifying the mathematical formulation, we introduce the design variables; these are of two types: *geometrical* and *mechanical*. Concerning the geometrical design variables, they are shown in Fig. 4.2 and are:

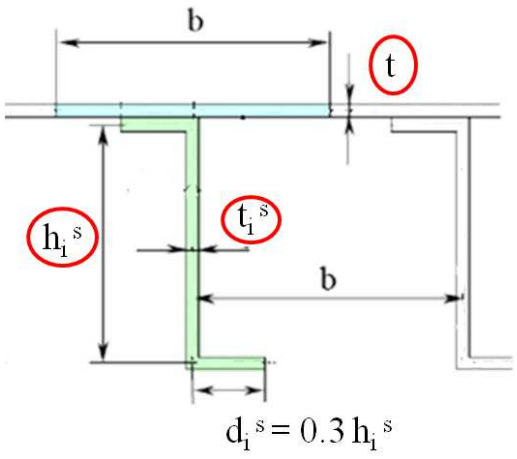

Figure 4.2: Geometrical design variables of the wing-box stiffened panel.

- the number of stiffeners N;

- the thickness of each stiffener t_i^S, $i = 1, ..., N$;
- the height of each stiffener h_i^S $(i = 1, ..., N)$;
- the thickness of the skin t.

All these variables are discrete valued: the ranges of their variation, along with their steps, are shown in Table 4.1. As previously said, the step of the thickness is equal to the thickness of the carbon-epoxy T300/5208 layers, the material chosen for the structure, see Table 3.2.

Design variable	**Type**	**Lower bound**	**Upper Bound**	**Step**
N	discrete	18	23	1
t_i^S [mm]	discrete	2.0	5.0	0.125
h_i^S [mm]	discrete	40.0	90.0	0.5
$(R_{0K}^{A^*})_i^S$ [MPa]	continuous	-19710	19710	–
$(R_1^{A^*})_i^S$ [MPa]	continuous	0.0	21433	–
t [mm]	discrete	2.0	5.0	0.125
$(R_{0K}^{A^*})$ [MPa]	continuous	-19710	19710	–
$(R_1^{A^*})$ [MPa]	continuous	0.0	21433	–

Table 4.1: Design variables for the first optimisation problem.

For technological reasons, the width of the flange of each stiffener, d_i^S $(i = 1, ..., N)$, is not a design variable and depends on the height of the stiffener as shown in Fig. 4.2. The stiffeners are automatically equispaced, with a step b which depends on the number of stiffeners through the following relation:

$$b = \frac{w}{N+1} \ , \tag{4.1}$$

where w is the width of the whole wing-box section.

An important point to be remarked: the dimension of the design space, i.e. the number of the design variables, depends on the number of modules, the stiffeners, and must be optimally determined by the procedure. The determination of the optimal number of the second type of modules, i.e. the layers, is implicitly done by determining the optimal value of the thicknesses.

4.4.2 Mechanical design variables

Concerning the mechanical variables, we adopt the *polar formalism*, already introduced in Sec. 3.3 of Chapter 3, to represent the homogenised stiffness tensors $\mathbf{A}^*$, $\mathbf{B}^*$, $\mathbf{D}^*$ which describe the mechanical behaviour of the laminate in the framework of the CLPT. As previously said, the polar formalism gives a representation of any planar tensor by means of a complete set of independent invariants. These invariants are called *polar parameters* and a great advantage in the design of anisotropic structures is that they are directly linked to the different symmetries of the tensor [114, 118].

The structural problem considered in this Chapter mainly concerns, through the constraint on the buckling load, the bending behaviour of the different laminates that compose the structure. Nevertheless, we have also imposed a condition on the extension behaviour of the laminates: each laminate is required to be *quasi-homogeneous*. Quasi-homogeneity is a property first introduced by Kandil and Verchery [131]: a laminate is quasi-homogeneous when its extension and bending behaviours are uncoupled and identical in each direction [132]. In this way, only the extension tensor $\mathbf{A}$ has to be designed, the bending one, $\mathbf{D}$, is automatically obtained. So, the choice of using quasi-homogeneous sequences, a mechanical assumption, has two direct mathematical consequences on the optimisation problem: (a) it reduces to only six the elastic parameters to be designed for the laminate (instead of the 18 polar parameters that we need to completely describe the behaviour of a laminate, see also Eq. (3.23) of Chapter 3), and (b) transforms the problem from the design of the bending tensor to that of the extension tensor, much easier to be done.

Another mathematical consequence, important for a correct definition of the constraints to be imposed to the optimum problem, as specified below, is the fact that with quasi-homogeneity the interdependency of the elastic parameters of extension and bending is complete. Finally, it must be noticed that this choice does not diminish the generality of the approach under a mechanical point of view, because for the bending behaviour, the fundamental one for this kind of problems, no restrictions are given and all the situations are still possible.

Along with the condition of quasi-homogeneity we assume that each laminate composing the structure is orthotropic, thus mathematically such conditions can be expressed as:

$$\begin{aligned} \mathbf{B}^* &= \mathbf{O} && \textit{uncoupling condition}, \\ \mathbf{A}^* &= \mathbf{D}^* && \textit{homogeneity condition}, \\ \Phi_0^{A^*} - \Phi_1^{A^*} &= K^{A^*}\frac{\pi}{4} && \textit{orthotropy condition}. \end{aligned} \tag{4.2}$$

If the first two conditions of Eq. (4.2) are satisfied, the laminate is said to be quasi-homogeneous. As already discussed in Sec. 3.3, the invariant K^{A^*} determines the type of ordinary orthotropy, see [118], and it can assume only the values 0 or 1. Vannucci [130], has shown the importance of this material invariant parameter in some problems of optimal

design; namely, if a solution is optimal for $K = 0$, it is normally anti-optimal for $K = 1$ and inversely, in some cases, the change of K can lead to a loss of uniqueness of the solution of an optimisation problem. To be remarked that the second and third of Eq. (4.2) give also bending orthotropy.

A simple result of the polar formalism is that, for the general case of laminates with identical layers, the isotropic moduli $T_0^{A^*}$ and $T_1^{A^*}$ are equal to those of the elementary layer, T_0 and T_1 respectively, see [132]. $T_0^{A^*}$ and $T_1^{A^*}$ are hence fixed by the choice of the material of the layers, so they are no more design variables: the polar formalism allows for easily eliminating some redundant mechanical variables from a design problem of a laminate composed of identical layers.

From the third condition of Eq. (4.2), we get:

$$\begin{aligned} \cos 4\Phi_0^{A^*} &= (-1)^{K^{A^*}} \cos 4\Phi_1^{A^*}, \\ \sin 4\Phi_0^{A^*} &= (-1)^{K^{A^*}} \sin 4\Phi_1^{A^*}, \end{aligned} \tag{4.3}$$

relations that can be used in Eq. (3.4), valid for any fourth-order elasticity-like tensor, so for tensor $\mathbf{A}^*$ too. Therefore, introducing the quantity $R_{0K}^{A^*} = (-1)^{K^{A^*}} R_0^{A^*}$ (see also [44]) thanks to the quasi-homogeneity condition, we reduced to only 3 the number of mechanical design variables for each laminate: the polar parameters $R_{0K}^{A^*}$, $R_1^{A^*}$, concerning the anisotropic part, and the polar angle $\Phi_1^{A^*}$, that represents the direction of the orthotropy axis. A theoretical remark: $R_{0K}^{A^*}$ is still a tensor invariant, because it is a combination of two distinct tensor invariants, K^{A^*} and $R_0^{A^*}$.

Another important point is constituted by the *feasibility conditions*: during the first step, an anisotropic equivalent layer is designed and, as for any other elastic material, some bounds are to be imposed to the search, in order to obtain elastic parameters that satisfy physical existence conditions. Nevertheless, this is not sufficient because the fictitious homogeneous anisotropic material designed during the first step, is not really fabricated. In fact, the optimal mechanical properties obtained as results of the first-level problem are realised in practice using composite laminates, that in general are different for the skin and for the stiffeners. So, in the second level problem, a laminate having the overall elastic properties optimised in the first step is looked for, and this is done for the skin and for each stiffener.

As said in Sec. 3.3, Vannucci [133] has shown that laminates constitute a sort of *restricted elastic class*: the elastic bounds valid for a homogeneous anisotropic material can never be attained by a laminate composed by the same material. This happens because the stacking sequence imposes some links among the different elastic moduli of the extension and/or the bending tensor, links that shrink the existence domain of the elastic moduli of the tensor. Such links are of geometrical nature, because they depends on the geometry of the stack, i.e. upon the orientation angle and the position of each layer in the stacking sequence. Since the fictitious material focus of the first-level design will be (in the second-level problem) realised by a laminate, in order to obtain a feasible

laminate, the geometric constraints of Eq. (3.36) (already introduced in Sec. 3.3) on the feasibility of the laminate are to be imposed directly to the first-level problem, otherwise one could get an optimum elastic tensor that cannot be obtained using a laminate of the same material.

To this purpose, it is worth noting also the importance of the quasi-homogeneity requirement: the bounds for the elastic moduli of the extension and bending tensors taken together are not known, and it should be impossible to specify them correctly in the first step problem. The assumption of quasi-homogeneity allows for considering in the first phase a fictitious material that has the same properties for bending and extension, for which the same geometric bounds are valid for both the tensors and hence are mathematically correct.

Thus, we must introduce in this phase the geometric bounds for the design of the laminate, that will be done during the next second-level problem. Such bounds can be written independently for tensors $\mathbf{A}^*$ or $\mathbf{D}^*$, and are of course the same for the case of quasi-homogeneous laminates.

Here, we recall the expression of such bounds using the polar formalism that in the case of an orthotropic tensor $\mathbf{A}^*$ can be expressed as follows (the quantities without the superscript A^* refer to the elementary layer):

$$\begin{cases} -R_0 \leq R_{0K}^{A^*} \leq R_0 \ , \\ 0 \leq R_1^{A^*} \leq R_1 \ , \\ 2\left(\dfrac{R_1^{A^*}}{R_1}\right)^2 - 1 - \dfrac{R_{0K}^{A^*}}{R_0} \leq 0 \ . \end{cases} \tag{4.4}$$

These constraints are to be considered for the optimal design of every laminate composing either the skin or the stiffeners of the wing-box section.

4.4.3 Mathematical statement of the problem

As said previously, the goal of the global structural optimisation is to find a minimum-weight wing-box configuration respecting the buckling and geometric constraints. To state the optimisation problem in a standard form, we first reorder the design variables according to the following scheme (the superscript S stands for stiffeners, the quantities without this superscript are referred to the skin):

- the vector $\mathbf{x}$ collects the following design variables, concerning the overall structure and the skin:

$$\mathbf{x} = \begin{Bmatrix} x_1 = N \\ x_2 = t \\ x_3 = R_{0K}^{A^*} \\ x_4 = R_1^{A^*} \end{Bmatrix} \ , \tag{4.5}$$

- each one of the vectors $\mathbf{y}^i$ collects the design variables of the i^{th} stiffener, $i = 1, ..., N$:

$$\mathbf{y}^i = \left\{ \begin{array}{c} y_1 = h_i^S \\ y_2 = t_i^S \\ y_3 = (R_{0K}^{A^*})_i^S \\ y_4 = (R_1^{A^*})_i^S \end{array} \right\} . \tag{4.6}$$

Then, we introduce the following functions:

- the objective function W, expressing the overall weight of the structure:

$$W = W\left(\mathbf{x}, \mathbf{y}^i\right) , \tag{4.7}$$

- the function that expresses the constraint on the critical buckling load:

$$f\left(\mathbf{x}, \mathbf{y}^i\right) = p_{ref} - p_{cr}\left(\mathbf{x}, \mathbf{y}^i\right) , \tag{4.8}$$

- the functions expressing the five geometric constraints (4.4) on the polar parameters of the skin:

$$g_1\left(x_3\right) = -x_3 - R_0 , \tag{4.9}$$

$$g_2\left(x_3\right) = x_3 - R_0 , \tag{4.10}$$

$$g_3\left(x_4\right) = -x_4 , \tag{4.11}$$

$$g_4\left(x_4\right) = x_4 - R_1 , \tag{4.12}$$

$$g_5\left(x_3, x_4\right) = 2\left(\frac{x_4}{R_1}\right)^2 - 1 - \frac{x_3}{R_0} , \tag{4.13}$$

- the functions expressing the five geometric constraints (4.4) on the polar parameters of the i^{th} stiffener, with $i = 1, ..., N$:

$$h_1^i\left(y_3^i\right) = -y_3^i - R_0 , \tag{4.14}$$

$$h_2^i\left(y_3^i\right) = y_3^i - R_0 , \tag{4.15}$$

$$h_3^i\left(y_4^i\right) = -y_4^i , \tag{4.16}$$

$$h_4^i\left(y_4^i\right) = y_4^i - R_1 , \tag{4.17}$$

$$h_5^i\left(y_3^i, y_4^i\right) = 2\left(\frac{y_4^i}{R_1}\right)^2 - 1 - \frac{y_3^i}{R_0} . \tag{4.18}$$

In (4.8), p_{ref} is a reference value for the critical buckling load of the structure, p_{cr}. Finally, the problem can be stated in the standard form:

$$\begin{cases} \min\ W\left(\mathbf{x}, \mathbf{y}^1, ..., \mathbf{y}^N\right)\ , \\ \text{s.t.} \\ f\left(\mathbf{x}, \mathbf{y}^i, ..., \mathbf{y}^N\right) \leq 0\ , \\ g_j(\mathbf{x}) \leq 0\ , \qquad\qquad j = 1, ..., 5\ , \\ h_l^i(\mathbf{y}^i) \leq 0\ , \qquad\qquad i = 1, ..., N, \quad l = 1, ..., 5\ . \end{cases} \tag{4.19}$$

Problem (4.19) is non-linear, in terms of both geometrical and mechanical variables. Its non-linearity is given not only by the objective function and the geometrical constraints like those in (4.13) and (4.18), but, in a stronger way, by the constraint on the value of the buckling load, $p_{cr} \geq p_{ref}$. The value of the buckling load can be computed analytically if it has a theoretical expression, which happens for some particularly simple structures, like beams or plates of simple form. Unfortunately, no analytical solution is known for the buckling load of a structure as complicate as the one considered in this research, see Fig. 4.1. Hence, for the solution of problem (4.19) we need a tool for the numerical evaluation of p_{cr}. To this purpose, the structure, a *continuum*, is *discretized in finite elements* and the computation of p_{cr} is done using the well known technique of the finite elements method.

From a mathematical point of view, the transformation of a continuum, i.e. of a body having infinite degrees of freedom, into a discrete structure, that has a finite number of degrees of freedom, transforms the search of the buckling load into a classical algebraic problem: p_{cr} is the smallest eigenvalue λ of

$$[[K] - \lambda]\,\{u\} = \{0\}\ . \tag{4.20}$$

$[K]$ is the stiffness matrix of the discretised structure, it is symmetric, positive definite and its dimension is equal to the number of the degrees of freedom of the structure, while $\{u\}$ is the vector of the state variables of the problem which, in the classical formulation of the finite element method, are physically the displacements, i.e. the degrees of freedom of the discrete structure. In our case, as we will specify in Sec. 4.6, the discretisation of the structure leads to a model having some hundreds of thousands of degrees of freedom. The solution of the Laplace's equation for a matrix having a so great dimension is clearly a non-linear problem whose solution can only be obtained numerically.

In addition, we impose that the fictitious material designed in this first step must be orthotropic, with the orthotropy axes aligned with the axes of the structure, and uncoupled. Thus, we fix the orthotropy direction, for both the skin and the stiffener laminates, simply posing:

$$\Phi_1^{A^*} = (\Phi_1^{A^*})_i^S = 0,\ \forall i = 1, ..., N, \tag{4.21}$$

which means that the principal orthotropy axis of each laminate composing the structure is aligned with the global x axis of the whole wing-box section, see Fig. 4.1. In this way, we eliminate from the problem a mechanical design variable for each laminate.

Finally, the dimension of the design space, i.e. the number of design variables, and the number of constraint equations depend on the number N of stiffeners. In particular the total number of design variables is $4N + 4$ (there are in fact 4 variables for each stiffener, 3 variables for the skin and the number of stiffeners, N), while the total number of constraint equations is $5N + 6$: the buckling constraint, 5 constraints for the skin and finally 5 constraints for each stiffener, see the second, third and fourth of Eq. (4.19), respectively. Nevertheless, though the number of constraints is variable, each constraint added by the addition of a module depends only on the unknowns concerning that module, not on the other ones too, see again the fourth of Eq. (4.19).

Concerning the GA BIANCA, in the case of the first-level problem we need the use of the new genetic operators of crossover and mutation between individuals belonging to different species. In fact, since the number of stiffeners N is included among the design variables, the related optimisation problem is defined over a space having variable dimension (the dimension of such a space is $4N + 4$). Mathematically speaking, such a problem corresponds on one side to determine the optimal dimension of the domain (i.e. the number of stiffeners N) and on the other side to determine the optimal values of the constitutive parameters of the stiffeners which satisfy the requirements imposed by the optimisation problem. In addition, we use the code BIANCA interfaced with the FE code ANSYS, because for each individual at each generation, the evaluation of the constraint function on the buckling load needs a numerical evaluation, as said above.

Fig. 4.3 shows the genotype of the generic r^{th} individual for the optimisation problem of the wing-box structure. This individual has N_r+1 chromosomes. The first chromosome is composed by 3 genes representing the design variables for the skin, i.e. thickness and polar parameters. Chromosomes from 2 to $N_r + 1$ contain 4 genes which are the design variables for each stiffener: thickness, height and the two anisotropy polar parameters. An exception is chromosome 2 that has 5 genes: the fifth additional gene codes the number of modules, i.e. for our problem the number of stiffeners (we remind the use of the superscript S for all quantities related to the stiffeners).

4.5 Mathematical formulation of the second-level problem

The second problem of the optimisation procedure concerns the design of the laminates. Of course, this second problem depends upon the results of the first one, because the laminates to be designed must have the optimal elastic properties and thickness obtained as results of the first-level design problem.

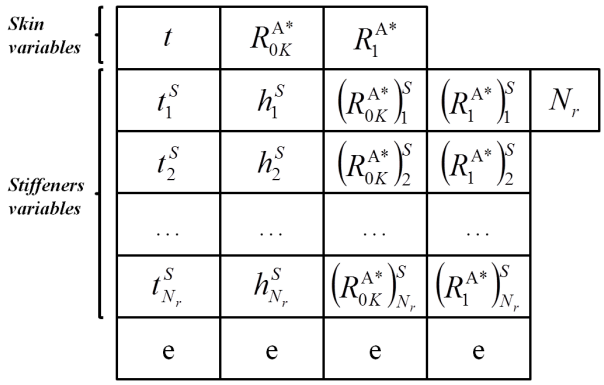

Figure 4.3: Structure of the individual genotype for the first-level optimisation problem.

It is to be highlighted that in our approach, that wants to be completely general, hence not using special stacking sequences nor orientations, also general elastic properties are concerned by the design problem, in particular quasi-homogeneity and orthotropy.

As already done in Chapter 3, also in this case we use the approach introduced by Vannucci [43] to deal with the problem of designing the general elastic properties of a laminate, later extended Vannucci [146] and by Julien [44] to the optimal design of laminates with given piezoelectric or elastic properties. By this approach, the design of a laminate conceived to have some given properties is reduced to an unconstrained minimisation problem. Mathematically, the technique is very simple: in the space of the polar parameters, a target tensor is fixed in some way. Then, the distance from this target is minimised, this leading to the evaluation of the optimal design variables. For the problem that we consider in this second step of the procedure, the target is fixed by the optimal values of the polar parameters of the laminate, issued from the first-level problem.

The key-point of this phase is hence the construction of the distance function, objective of the minimisation problem. This function drives the search for a quasi-homogeneous, orthotropic laminate, having the optimal elastic polar moduli issued from the first step. The design variables of this second level problem are the layer orientations δ_j, see Eq. (3.23), and the optimisation process has to be repeated for the laminates of each stiffener and of the skin.

To construct the distance function in this case, we recall that we need to find a stacking sequence which satisfies the conditions of Eq. (4.2), and that has the optimal polar parameters found in the first step, $\widehat{K}^{A^*}$, $\widehat{R}_0^{A^*}$ and $\widehat{R}_1^{A^*}$. The relation among the polar parameters $\widehat{R}_0^{A^*}$ and $\widehat{K}^{A^*}$, and the polar quantity $\widehat{R}_{0K}^{A^*}$ is of course

$$\widehat{R}_0^{A^*} = |\widehat{R}_{0K}^{A^*}| \ , \ \widehat{K}^{A^*} = \begin{cases} 0 & \text{if} \quad \widehat{R}_{0K}^{A^*} > 0 \ , \\ 1 & \text{if} \quad \widehat{R}_{0K}^{A^*} < 0 \ . \end{cases} \tag{4.22}$$

In addition, we need to orient the orthotropy axes, imposing:

$$\Phi_1^{A^*} = \widehat{\Phi}_1^{A^*} \ . \tag{4.23}$$

In our case $\widehat{\Phi}_1^{A^*} = 0$, which means that the principal orthotropy axis of each laminate has to be aligned with the x axis of the whole structure. Unlike in other more common approaches, where the orthotropy and its direction are normally imposed choosing particular sequences that automatically place the orthotropy axes in a direction, normally aligned with the axes of the laminate, with the polar formalism orthotropy and its direction are imposed by simple independent conditions, and any direction different from the axes of the laminate can be easily imposed, simply choosing an angle $\widehat{\Phi}_1^{A^*}$ different from zero (see also Sec. 3.5).

We remind that from the first-level problem we know also the thickness of the skin and of the stiffener laminates. Being each laminate thickness a multiple of that of the elementary ply, the number of the laminate plies is also known.

Considering all these points, the tensor distance, objective function of the second-level problem, can be stated, for each laminate of the skin and of the stiffeners, as:

$$\begin{aligned}
&\min_{\boldsymbol{\delta}} \ F(\boldsymbol{\delta}) = \sum_{j=1}^{6} f_j(\boldsymbol{\delta}) \ \text{with :} \\
&f_1(\boldsymbol{\delta}) = \left(\frac{\|\mathbf{B}^*\|}{\|\mathbf{Q}\|} \right)^2 , \ f_2(\boldsymbol{\delta}) = \left(\frac{\|\mathbf{C}\|}{\|\mathbf{Q}\|} \right)^2 , \\
&f_3(\boldsymbol{\delta}) = \left(\frac{\Phi_0^{A^*} - \Phi_1^{A^*} - \widehat{K}^{A^*} \dfrac{\pi}{4}}{\dfrac{\pi}{4}} \right)^2 , \ f_4(\boldsymbol{\delta}) = \left(\frac{R_0^{A^*} - \widehat{R}_0^{A^*}}{\widehat{R}_0^{A^*}} \right)^2 , \\
&f_5(\boldsymbol{\delta}) = \left(\frac{R_1^{A^*} - \widehat{R}_1^{A^*}}{\widehat{R}_1^{A^*}} \right)^2 , \ f_6(\boldsymbol{\delta}) = \left(\frac{\Phi_1^{A^*} - \widehat{\Phi}_1^{A^*}}{\dfrac{\pi}{4}} \right)^2 .
\end{aligned} \tag{4.24}$$

In (4.24), $\boldsymbol{\delta}$ is the vector of layer orientations, while $f_j(\boldsymbol{\delta})$ is the j^{th} partial term of the objective function, $j = 1, ..., 6$. The terms $f_1(\boldsymbol{\delta})$ and $f_2(\boldsymbol{\delta})$ are related to the quasi-homogeneity conditions, while the third one, $f_3(\boldsymbol{\delta})$, is linked to the orthotropy condition, see Eq. (4.2). The function $f_3(\boldsymbol{\delta})$ takes also into account the prescribed value $\widehat{K}^{A^*}$ of parameter K^{A^*} issued from the first optimisation phase. The terms $f_4(\boldsymbol{\delta})$ and $f_5(\boldsymbol{\delta})$ correspond to the prescribed optimal values $\widehat{R}_0^{A^*}$ and $\widehat{R}_1^{A^*}$ of the polar moduli $R_0^{A^*}$ and $R_1^{A^*}$. The term $f_6(\boldsymbol{\delta})$ corresponds to the imposed direction of orthotropy of the laminate: $\Phi_1^{A^*} = \widehat{\Phi}_1^{A^*} = 0$. Finally, $\|\mathbf{B}^*\|$ is the norm of the homogenised coupling tensor and $\|\mathbf{C}\|$ is the norm of the homogeneity tensor.

The function defined in Eq. (4.24) is actually the square of a dimensionless tensor distance. In fact, we have normalised all the terms, which allows for all the terms to

have a similar weight in the function. The tensor norms have been transformed into dimensionless quantities dividing them by the normalisation factor $\|\mathbf{Q}\|$, that is the norm of the layer reduced stiffness tensor. All the norms have been computed using Eq. (3.7). The normalisation factor of the orthotropy requirement is assumed equal to $\frac{\pi}{4}$, while for the anisotropy parameters of tensor $\mathbf{A}^*$, it is equal to the corresponding target polar parameter.

We recall that, the quadratic form of Eq. (4.24) is a non-dimensional, positive semi-definite function of the polar parameters of the laminate. It depends on all the mechanical and geometrical properties of the laminate, i.e. stacking sequence, ply orientations, material and thickness of the plies. In addition, the objective function of Eq. (4.24) is non-convex in the space of layer orientations, since the polar parameters of the laminate depend upon circular functions of the orientations, see Eq. (3.23).

A true advantage of formulation (4.24) is that the global minima of the function are zero valued. This is important for the numerical search strategy, because the knowledge of the value of the global minima is useful on one side to stop the numerical search, and on the other side to ensure that the solution so found is really a global minimum.

Finally, we remark that, unlike the first-level problem, this second problem is an unconstrained problem with a known number of design variables, but the objective is still a highly non-convex function; a simple glance at Eq. (3.23) is sufficient to realise this. For what concerns the nature of the design variables, the operator is free to chose continuous, discrete equally stepped variables or variables whose possible values belong to a defined set; actually, such a choice is mostly a practical, technological choice.

The code BIANCA has also been used in the search for the laminates, i.e. for the second step of the procedure. The structure of the genotype of the individual-laminate is shown in Fig. 4.4. The genotype is made of n chromosomes, which correspond to the number of layers, determined in the first step, and each chromosome is composed, on its turn, by a single gene which represents the ply orientation.

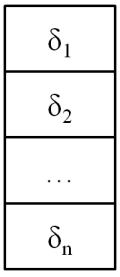

Figure 4.4: Structure of the individual genotype for the second-level optimisation problem.

4.6 Finite element model of the structure

The finite-element analysis is used for evaluating the objective and constraint functions for each individual at each iteration of the first-level problem. The need to analyse, within the same generation, different geometrical configurations, each one corresponding to an individual, requires the creation of an ad-hoc input file for the FE code, that has to be interfaced with BIANCA. Since the number of modules is included among the decision variables, the FE model must be conceived in order to take into account for variable geometry and mesh. Indeed, for each individual at the current generation, depending on the number of chromosomes and, hence, on the number of stiffeners the FE code has to be able to vary in a correct way the number of elements wherein the structure is discretised, thus a correct parametrisation of the model has to be done.

The geometry, mesh, loads and boundary conditions of the wing-box FE model are shown in Fig. 4.5. The structure is modeled using ANSYS SHELL99 elements with 8 nodes having 6 degrees of freedom per node. These shell elements have 3 integration points along the thickness. The mechanical properties of the material are defined specifying the Cartesian components of tensors $\mathbf{A}^*$, $\mathbf{B}^*$ and $\mathbf{D}^*$ that are functions of the mechanical unknowns, the polar parameters.

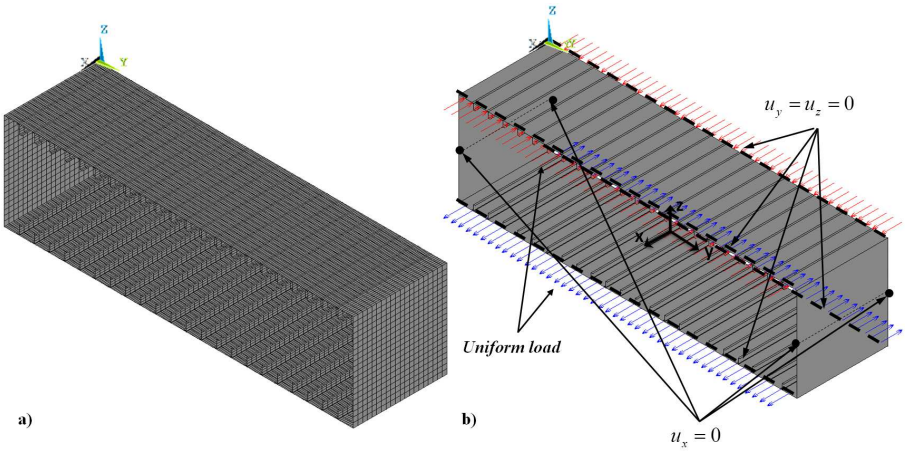

Figure 4.5: (a) Mesh and (b) loads and boundary conditions for the wing-box FE model.

The wing box is considered simply supported at its terminal sections on two wing ribs. The upper panel is loaded with a uniform compression unit force per unit length and the lower one with a uniform tensile unit force per unit length. Under such kind of loads, which are representative of the loads that the structural elements of the wing-box undergo in normal flight conditions, only the upper panel and the corresponding stiffeners can undergo compression instability phenomena. Both upper and lower panels have N Z-shaped stiffeners.

After a preliminary mesh sensitivity study, the average dimensions of the shell elements have been chosen equal to 14×14 mm^2. The number of shell elements in the whole wing-box structure can vary from 14080 to 17680, depending on the number of stiffeners N, whilst the number of degrees of freedom of the whole model can vary from 270744 to 340164. For each individual, a linear buckling analysis is performed for assessing the first buckling load of the structure.

In order to fix a correct reference value of the first buckling load, i.e. of the quantity p_{ref} appearing in the formulation of the first level problem, see Eq. (4.19), a preliminary buckling analysis on a reference wing-box section model has been performed for the type of wing-box section considered here and represented in Fig. 4.5. The reference wing-box, which represents a standard structure, is made by Al-7075-T6 alloy with Young's modulus $E = 72395$ MPa, Poisson's ratio $\nu = 0.33$, yield stress $\sigma_y = 475$ MPa and density $\rho = 2760$ kg/m^3. Concerning the geometrical properties, the whole wing box has the global dimensions shown in Fig. 4.1, while the upper and lower panels are made by 20 identical stiffeners having the following dimensions: $t^S = 2.96$ mm and $h^S = 62.33$ mm for the stiffeners thickness and height respectively, and $t = 4.93$ mm for the skin thickness. The reference values p_{ref} of the first buckling load and W_{ref} of the wing-box weight are the outcomes of this preliminary simulation: $p_{ref} = 1928$ N/mm and $W_{ref} = 1222.62$ N.

This structure is also compared in the following Section with the solutions found for the considered examples. Actually, our goal is to compare the optimal solutions that we find with a case that carries the same buckling load and that can be considered as a usual, typical situation, briefly a standard wing-box section for a standard aircraft structure. Of course, other comparisons could be done, nevertheless it is really significant to compare what can be done as an optimum with what is usually done as a standard: that was our goal.

4.7 Studied cases and results

For our optimisation problem we have considered three different examples. The design variables, their nature and bounds for the optimisation problem at hand are detailed in Table 4.1.

- **Example 1**: the stiffeners are identical, i.e. they have the same value of thickness t^S, height h^S and polar parameters, i.e $(R_{0K}^{A^*})^S$ and $(R_1^{A^*})^S$. Therefore, in this case, we have 8 design variables: the number of stiffeners N, the geometrical and polar parameters for the stiffeners, i.e. t^S, h^S, $(R_{0K}^{A^*})^S$, $(R_1^{A^*})^S$ and the geometrical and polar parameters for the skin, i.e. t, $R_{0K}^{A^*}$, $R_1^{A^*}$. In addition, for this first case, the total number of constraints is 11: 1 constraint on the buckling load, 5 geometric constraints for the skin and 5 for the stiffener polar parameters. However, 8 constraints on 11 are box-constraints, so they are not treated by the ADP method,

but simply used to specify the variation range of the anisotropy design variables $R_{0K}^{A^*}$ and $R_1^{A^*}$.

- **Example 2**: the problem of the minimum weight for the wing-box stiffened panel is now formulated in the most general case, i.e. with non-identical stiffeners. The total number of design variables depends on the number of stiffeners N, as explained in Sec. 4.4, and can vary between 76 and 96. Moreover, also the number of constraint equations is variable with the number of stiffeners: the minimum number of constraints is 96 and the maximum 121, respectively 19 and 24 without the box-constraints.

- **Example 3**: we still consider the problem of the minimum weight for the wing-box stiffened panel with non-identical stiffeners. Nevertheless in this last case, for obvious mechanical reasons, we assume that the whole wing-box section has a symmetric distribution of the geometrical and polar parameters for the stiffeners with respect to the $x - z$ plane of the global reference system, see Fig. 4.5. With this assumption the total number of design variables and constraints is considerably reduced and can vary between 40 and 52 for the design variables, and between 51 and 66 for the constraints, respectively 10 and 13 without the box-constraints.

The three different cases are detailed hereafter separately, for both the first and the second step. We precise that in all the three cases, the design is guided by the buckling constraint, regardless if it appears as a global or local phenomenon, which means that the best solution should belong to the boundary between the feasible and infeasible domain. This is a precise choice for the mechanical design of the structure, though other situations can be considered, for instance admitting the possibility of a post-buckling design.

Concerning the second-level problem, in all the three examples, the design variables are the layers orientations, which can vary between $-90°$ and $90°$ with a step of $1°$. In all the cases, the population size has been set to $N_{ind} = 500$ and the maximum number of generations to $N_{gen} = 500$. The crossover and mutation probability are $p_{cross} = 0.85$ and $p_{mut} = 1/N_{ind}$, respectively. Selection is performed by the roulette-wheel operator and the elitism is active. Moreover, always concerning the second-level problem, as in each numerical technique, the quality of solutions found by BIANCA can be estimated on the basis of a numerical tolerance, that is the residual. For a discussion on the importance of the numerical residual in problems of this type, see [116]. It is worth noting that, being $F(\boldsymbol{\delta})$ a non-dimensional function, the residual of the solution is a non-dimensional quantity too. It is worth to recall that the second-level problem must be solved for the skin and for each stiffener separately, when they are not identical.

4.7.1 Case 1: identical stiffeners

In this first case, since the stiffeners are identical, the genetic operators that perform the crossover between different species are no longer required: the genotype of each individual is composed by only one chromosome with 8 genes: the first gene represents the number of stiffeners N, the genes from 2 to 4 represent the skin design variables, i.e. t, $R_{0K}^{A^*}$ and $R_1^{A^*}$, while the last 4 genes represent the stiffeners design variables, i.e. t^S, h^S, $(R_{0K}^{A^*})^S$ and $(R_1^{A^*})^S$.

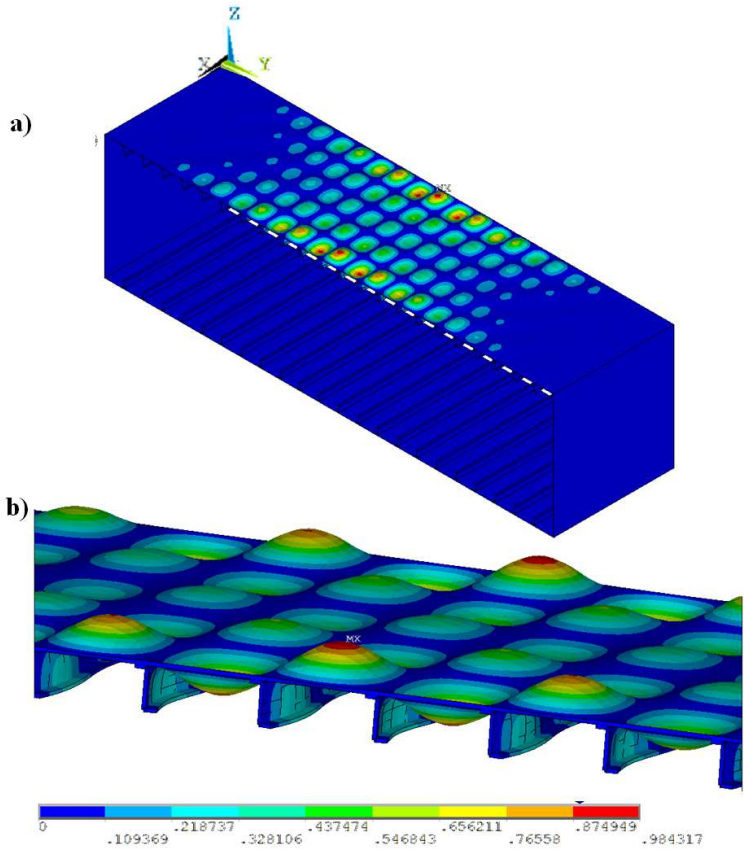

Figure 4.6: Example 1: deformed shape of the a) whole wing-box section and b) upper-panel stiffeners.

Concerning the genetic parameters that regulate the iterations of the GA BIANCA, the population size is set to $N_{ind} = 50$ and the maximum number of generations is assumed equal to $N_{gen} = 80$. The crossover and mutation probability are $p_{cross} = 0.85$ and $p_{mut} = 1/N_{ind}$, respectively. Selection is performed by the roulette-wheel method, the elitism is active and the ADP method is used for handling constraints.

The best solution found by BIANCA is shown in Table 4.2. The optimal number of stiffeners for the weight minimization is 22. The buckling load and the wing-box weight

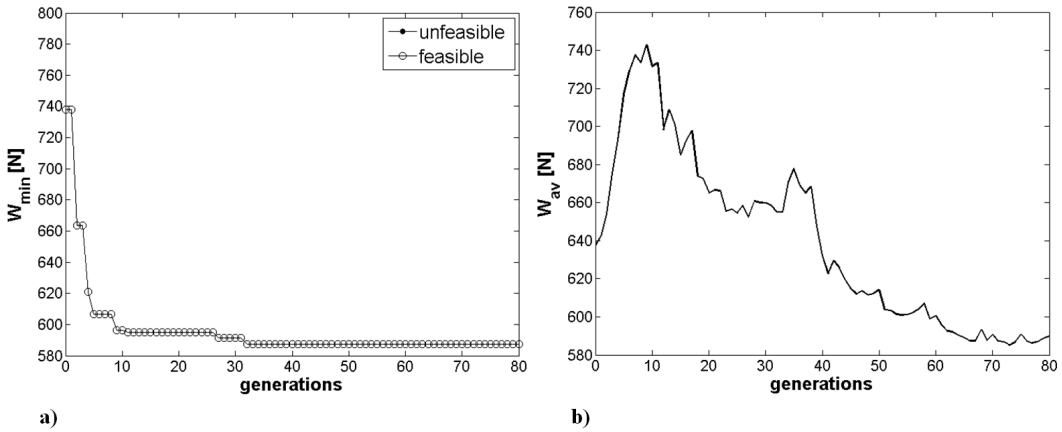

Figure 4.7: Example 1: (a) best and (b) average values of the objective function along generations.

are $p_{cr} = 1943$ N/mm and $W = 587.28$ N, respectively. Fig. 4.6 shows the deformed shape of the structure when the applied load is equal to p_{cr}: we can see that, during the buckling phenomenon, the wing-box section is characterised by a local skin buckling around the stiffeners.

Considering that the value of the ply thickness is 0.125 mm, we can notice that the laminate of each stiffener is made of 29 plies and has the orthotropy with $\widehat{K}^{A^*} = 1$, because the value of the polar quantity $(R_{0K}^{A^*})^S$ is negative. Instead, the skin laminate is made of 32 layers and has $\widehat{K}^{A^*} = 0$, because $R_{0K}^{A^*}$ is positive.

The global constrained minimum has been found after 32 generations, see Fig. 4.7 a). This solution gives a reduction of the weight of the whole structure of about 52%, when compared to the reference solution, and the solution found is practically on the boundary of the feasible domain, $p_{cr} \simeq p_{ref}$. From Fig. 4.7 b), it can also be noticed that the variation of the average value of the weight over the whole population along generations firstly increases (for about 9 iterations) and then decreases. This trend is due to the presence of a large amount of infeasible individuals within the population in the initial generations: infeasible points represent solutions which are lighter than the feasible ones but that violate the constraint on the buckling load, thus these individuals are penalised by the ADP strategy and this results in an increase of the average of the objective function. However, though these individuals belong to the infeasible region, they are preserved within the population because they can be useful for driving the search for the optimum point towards regions close to the boundary of the feasible domain, see Section 1.6.

Table 4.3 shows the best stacking sequences found using BIANCA for the second level problem. The residual in the last column is the value of the global objective function $F(\boldsymbol{\delta})$ for the solution indicated aside (we remind that exact solutions correspond to the zeroes

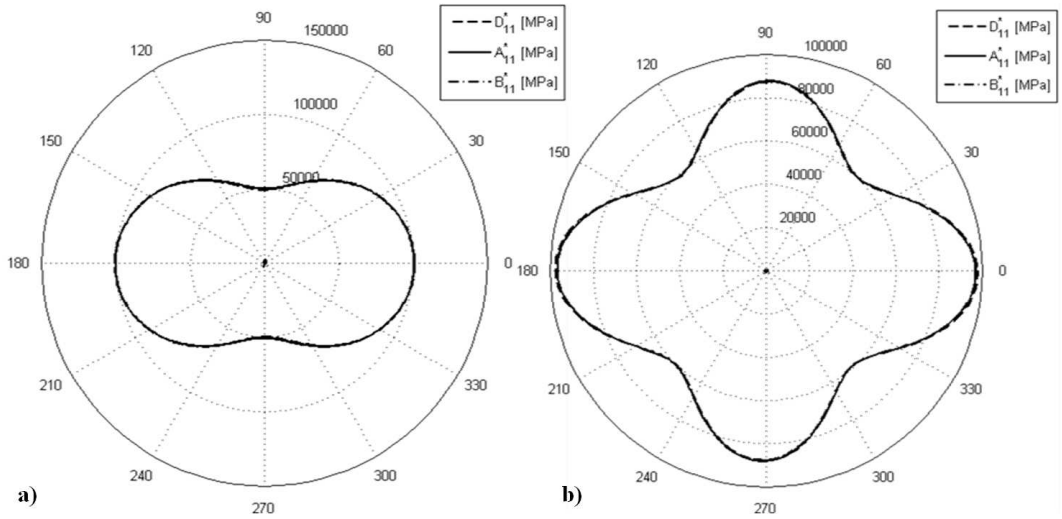

Figure 4.8: Example 1: first component of the homogenised stiffness tensors of the laminate for a) stiffeners and b) skin.

of the objective function). Fig. 4.8 shows the first component of the homogenised stiffness tensors of the laminate, i.e. $\mathbf{A}^*$, $\mathbf{B}^*$ and $\mathbf{D}^*$, for stiffeners and skin: the solid line refers to the extension tensor, the dashed one to the bending tensor, while the dash-dotted one is linked to the coupling stiffness tensor. We can see that both laminates are uncoupled (the dash-dotted curve is reduced to a small black point in the center of the plot, because B^*_{11} is practically null), homogeneous (the solid and dashed curves are practically coincident) and orthotropic (there are two orthogonal axes of symmetry in the plane). Moreover, the main orthotropy axis is aligned with the x axis of the structure, in fact it is oriented at 0°. Similar considerations can be done for the other components of these tensors, not shown in Fig. 4.8 for the sake of brevity.

Fig. 4.9 shows the variation of the best solution during iterations, for stiffener and skin laminates, respectively. The best solution is found after 340 generations for the stiffener laminate, while for the laminate of the skin it is found after 250 generations.

4.7.2 Case 2: non-identical stiffeners

Since the number of stiffeners is variable and they are not identical, a crossover between species is required and the optimal value of N is an outcome of the optimal search: the most adapted species automatically issues as a natural result of the Darwinian selection. The genotype of an individual for this case has been detailed in Sec. 4.4 and shown in Fig. 4.3.

Concerning the genetic parameters, the population size is $N_{ind} = 70$ and the maximum number of generations is $N_{gen} = 80$. The crossover and mutation probability are still

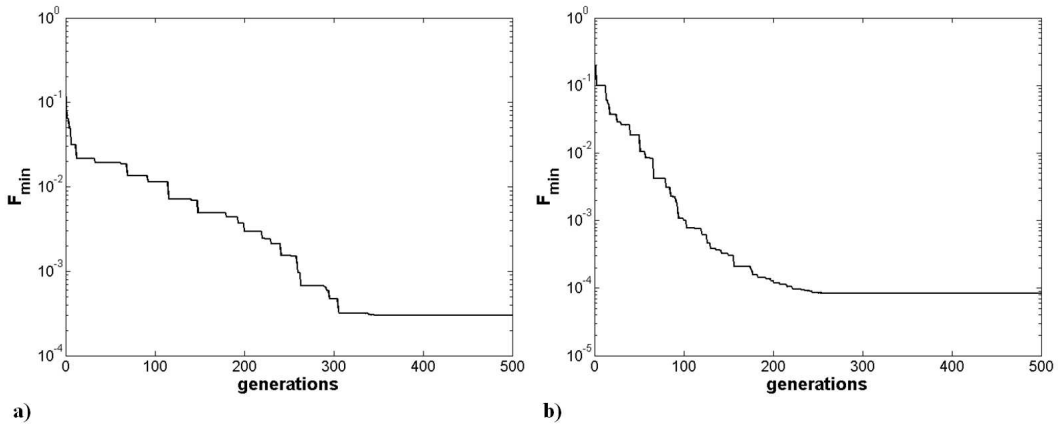

Figure 4.9: Example 1: best values of the objective function during iterations for a) stiffeners and b) skin laminates.

Design variable	**Value**
N	22
t^S [mm]	3.625
h^S [mm]	40.0
$(R_{0K}^{A^*})^S$ [MPa]	−984.36
$(R_1^{A^*})^S$ [MPa]	6425.22
t [mm]	4.0
$R_{0K}^{A^*}$ [MPa]	16399.8
$R_1^{A^*}$ [MPa]	1293.26

Table 4.2: Example 1: best values of the design variables.

$p_{cross} = 0.85$ and $p_{mut} = 1/N_{ind}$, while the shift operator and chromosomes number mutation probability are $p_{shift} = 0.5$ and $(p_{mut})_{chrom} = (n_{chrommax} - n_{chrommin})/N_{ind}$. Once again, selection is performed by the roulette-wheel method, the elitism is active and the ADP method has been used for handling constraints.

The best solution found by BIANCA is shown in Table 4.4. The optimal number of stiffeners for the weight minimisation is 23. The buckling load and the wing-box weight are $p_{cr} = 1931$ N/mm and $W = 620.19$ N respectively. Fig. 4.10 shows the deformed shape of the structure when the applied load is equal to p_{cr}. From Table 4.4, it can be noticed that the orthotropy type can be different for the stiffener laminates: despite every laminate is quasi-homogeneous and orthotropic, there are some orthotropic laminates

Stiffeners		
N. of plies	Stacking sequence (°)	Residual
29	$[-8/28/26/-45/-58/-3/55/-31/76/34/-39/-87/-7/6/30/$ $-12/-21/-51/18/-55/49/-8/18/12/57/44/-27/-79/-18]$	2.9×10^{-4}
Skin		
N. of plies	Stacking sequence (°)	Residual
32	$[-81/7/-3/-12/82/86/-87/20/-6/76/-7/85/-6/90/-7/87/$ $10/-82/-4/-7/-82/18/-11/-84/-83/7/70/85/1/-12/1/89]$	8.4×10^{-5}

Table 4.3: Example 1: best stacking sequences for the optimal solution.

with $(K^{A^*})^S = 1$ and others with $(K^{A^*})^S = 0$. The global constrained minimum has been found after 57 generations, see Fig. 4.11 a). This solution gives a reduction of the weight of the whole structure of about 49%, when compared to the reference solution and it is very close to the boundary of the feasible domain, $p_{cr} \simeq p_{ref}$.

Fig. 4.12 a) shows the evolution of species restrained in the whole population from the initial until the final generation. Since the individuals are randomly sorted in the first generation, also the species are uniformly distributed over the population, i.e. the number of individuals belonging to different species is equiprobable. We can notice that all the species can be found in the initial generations, whilst some of them *extinguish* during the generations and cannot be found within the final population: only solutions with 20 to 23 stiffeners can be found within the population in the last generation. In addition, thanks to the genetic operators detailed in Sec. 1.5, the number of individuals belonging to the fittest species is increased when compared to the initial population. Fig 4.12 b) shows the variation of the optimal number of stiffeners along the generations: it can be seen that for the first 15 generations the best species is the one showing 22 stiffeners, while from the 16^{th} iteration until the end of the optimisation process the best number of stiffeners is 23.

Another point deserves attention; comparing the plots in Fig. 4.11 a) and 4.12 b), one can notice something that systematically happens: convergence, towards the best value, of the number of modules (here, the number of stiffeners) and of the objective function are independent. They never occur at the same time, and the optimisation of the number of modules happens always before that of the objective function. In other words, the strategy used in BIANCA for evolving at the same time species and individuals, normally let attain first the best species, and then continues to evolve individuals within the best species towards the best individual.

Concerning the second problem for this case, since the stiffeners are not identical, we have solved the second level problem for each laminate of the stiffeners and for the

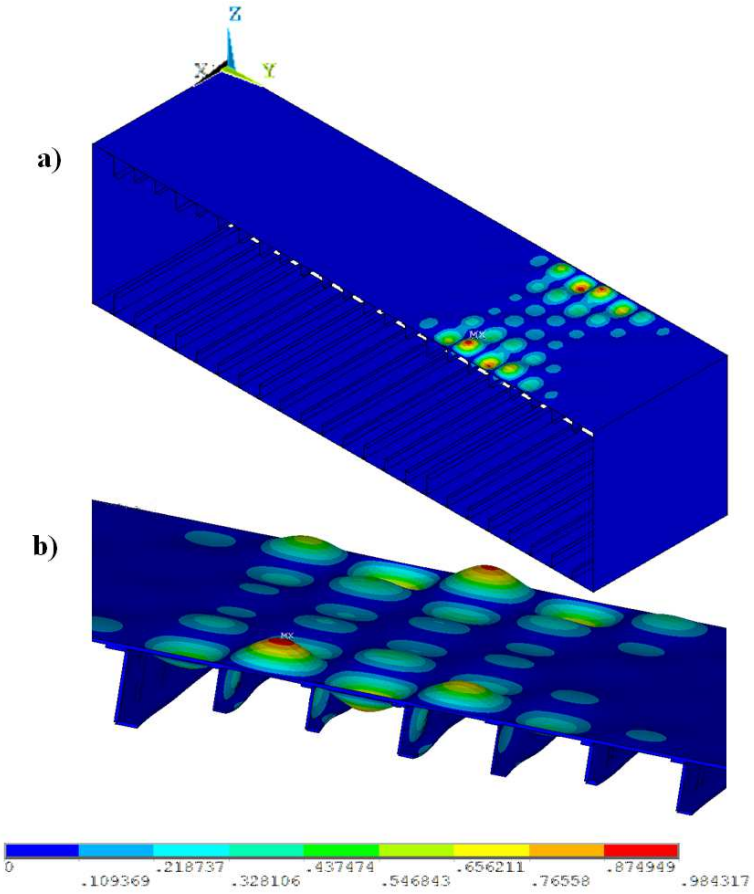

Figure 4.10: Example 2: deformed shape of the a) whole wing-box section and b) upper-panel stiffeners.

skin. Table 4.5 shows the best stacking sequences found by BIANCA. The number of plies for each laminate, indicated in column 3, is computed considering that the value of the thickness of the elementary layer is 0.125 mm. For the sake of brevity, we do not show the polar diagrams and the variation of the best solution for the stiffener and skin laminates. Nevertheless, they are quite similar to those obtained for the wing-box section of the previous example and the same considerations can be done for this second case too.

4.7.3 Case 3: non-identical stiffeners, symmetric distribution

In this last case, we consider a wing-box section with symmetric distribution of the geometrical and polar parameters for the stiffeners with respect to the $x - z$ plane of the global reference system, see Fig. 4.5. The genotype of an individual and the genetic parameters are precisely the same of the previous case.

Stiffeners				
ID	t^S [mm]	h^S [mm]	$(R_{0K}^{A^*})^S$ [MPa]	$(R_1^{A^*})^S$ [MPa]
01	2.75	86.5	−7052.03	11899.10
02	4.75	55.5	−9565.0	1970.67
03	2.625	55.0	−1129.82	14037.45
04	2.125	73.5	18888.6	14574.8
05	3.625	46.0	−5404.69	2750.73
06	4.625	49.0	5701.86	13261.0
07	2.125	58.0	5924.73	11249.3
08	2.0	65.0	−8450.64	8847.51
09	4.0	48.0	14876.8	4495.6
10	4.0	43.0	−1578.69	739.0
11	3.0	43.5	1801.56	7574.78
12	3.75	41.5	8042.03	4290.32
13	3.0	59.0	−1095.8	11495.6
14	4.25	52.0	17811.3	1149.56
15	4.375	54.0	10865.1	2832.84
16	4.0	84.0	12536.7	13178.9
17	2.125	48.5	3993.16	10633.4
18	3.125	48.5	12276.6	14349.0
19	3.0	56.0	12610.9	11536.7
20	2.125	56.5	−6333.33	7615.84
21	4.375	43.0	15322.6	8950.15
22	3.375	56.0	17551.3	5994.13
23	3.625	41.0	13242.4	7020.53
Skin				
	t [mm]		$R_{0K}^{A^*}$ [MPa]	$R_1^{A^*}$ [MPa]
	4.0		12945.3	882.70

Table 4.4: Example 2: best values of the design variables.

		Stiffeners	
ID	N. of plies	Stacking sequence (°)	Residual
01	22	[28/ − 29/ − 30/28/25/ − 29/ − 29/28/ − 26/42/ − 26/ 26/24/27/ − 29/ − 26/ − 27/25/30/ − 31/ − 22/29]	1.5×10^{-3}
02	38	[40/ − 36/ − 72/ − 38/59/ − 45/24/42/85/ − 20/12/56/43/13/ − 41/ − 35/ − 41/45/ − 61/ −39/56/39/ − 65/7/51/ − 70/ − 50/45/ − 28/ − 20/ − 24/45/ − 32/45/41/ − 74/32/ − 31]	3.3×10^{-4}
03	21	[20/20/ − 17/ − 35/ − 16/38/ − 23/ − 24/ − 10/17/ 29/22/19/ − 23/26/ − 27/24/ − 42/ − 18/ − 18/30]	1.9×10^{-3}
04	17	[0/ − 7/0/86/5/2/2/89/2/0/ − 24/1/0/2/ − 87/6/ − 3]	2.1×10^{-3}
05	29	[37/ − 57/ − 3/40/58/ − 44/ − 11/ − 87/50/ − 22/ − 65/ − 38/ − 41/23/ −33/ − 70/18/29/63/41/42/2/61/ − 14/ − 50/87/ − 19/29/ − 48]	2.9×10^{-4}
06	37	[6/8/1/61/ − 45/5/ − 24/22/ − 50/6/ − 7/8/7/51/ − 21/ − 34/12/ − 21/ −11/6/33/ − 6/16/78/5/7/ − 6/ − 51/25/ − 4/6/18/ − 42/54/ − 12/ − 20/9]	2.4×10^{-5}
07	17	[5/38/ − 27/ − 56/ − 9/7/60/16/ − 8/7/ − 29/27/9/ − 40/81/ − 8/6]	1.5×10^{-3}
08	16	[−25/ − 47/28/45/ − 16/23/35/1/ − 42/48/ − 41/ − 36/0/ − 33/45/24]	5.6×10^{-4}
09	32	[6/ − 1/3/6/77/ − 74/ − 85/ − 21/71/ − 17/ − 86/ − 1/90/ − 1/67/ − 85/ 83/1/1/3/3/1/3/ − 66/ − 6/23/8/ − 77/ − 11/ − 12/85/83]	1.4×10^{-4}
10	32	[−37/79/36/ − 77/ − 1/ − 43/46/52/ − 35/ − 13/90/30/ − 31/ − 45/ − 3/36/ 69/ − 76/87/89/ − 28/ − 57/51/21/ − 34/35/14/17/9/ − 73/ − 37/71]	1.3×10^{-3}
11	24	[7/65/15/ − 66/ − 10/ − 9/ − 49/ − 45/ − 22/50/13/5/ 70/ − 22/49/17/19/89/6/ − 33/ − 5/ − 5/ − 45/43]	6.8×10^{-4}
12	30	[2/ − 89/81/ − 15/ − 83/ − 50/ − 19/29/6/34/10/4/ − 10/19/75/ −10/86/3/90/ − 69/ − 39/3/ − 32/87/84/51/0/ − 33/4/21]	5.0×10^{-4}
13	24	[34/ − 45/5/5/ − 30/40/28/3/ − 29/ − 9/ − 25/25/ 9/ − 21/ − 24/ − 56/29/20/55/48/4/ − 39/ − 5/ − 15]	1.0×10^{-3}
14	34	[85/ − 4/ − 75/4/ − 2/84/ − 2/83/88/ − 16/6/2/ − 83/0/87/4/3/ 84/ − 7/84/ − 85/ − 74/86/ − 9/15/ − 86/10/1/ − 6/88/ − 3/ − 89/88/5]	1.9×10^{-4}
15	35	[4/ − 79/82/37/ − 2/ − 10/ − 38/ − 70/76/90/10/ − 9/2/ − 2/18/ − 77/ − 5/ 90/ − 3/78/81/ − 21/ − 87/28/9/ − 66/ − 13/45/8/ − 14/82/ − 71/78/ − 2/ − 2]	1.6×10^{-4}
16	32	[12/11/ − 7/5/ − 85/ − 9/ − 14/ − 66/50/ − 5/ − 5/ − 16/2/87/4/3/ 3/ − 8/ − 6/19/17/ − 15/17/ − 9/17/14/ − 67/ − 9/67/ − 12/4/ − 6]	2.8×10^{-4}
17	17	[−19/20/ − 29/20/ − 71/ − 4/35/62/ − 7/ − 8/3/7/ − 45/ − 35/7/70/12]	9.2×10^{-4}
18	25	[13/0/4/ − 23/ − 31/82/18/22/ − 1/2/ − 3/ − 3/ −30/2/3/14/ − 7/18/3/70/ − 77/ − 2/ − 14/ − 6/12]	4.4×10^{-4}
19	24	[2/ − 79/ − 17/27/ − 5/ − 2/ − 5/ − 4/68/ − 5/24/ − 2/ −83/ − 1/4/ − 69/ − 9/8/ − 18/ − 10/25/81/ − 11/7]	3.7×10^{-5}
20	17	[31/46/ − 14/ − 61/ − 38/ − 22/ − 17/25/ − 50/30/47/6/62/28/ − 29/3/ − 44]	7.4×10^{-4}
21	35	[89/ − 10/9/5/5/ − 6/ − 75/58/ − 4/ − 3/ − 3/ − 2/73/ − 74/ − 2/ − 86/ − 2/ −3/ − 1/ − 3/22/22/ − 5/ − 11/ − 6/ − 86/ − 82/ − 6/71/ − 9/16/4/ − 82/5/ − 10]	2.2×10^{-4}
22	27	[−5/7/ − 83/5/10/ − 15/ − 85/75/90/ − 4/ − 4/83/0/ 3/3/3/2/ − 85/ − 85/ − 85/ − 6/1/3/83/7/ − 8/89]	9.3×10^{-4}
23	29	[89/0/12/ − 25/62/10/ − 6/ − 10/ − 1/ − 74/ − 3/ − 1/ − 82/73/ − 86/ 22/ − 1/26/ − 2/86/10/ − 23/ − 8/ − 10/ − 18/ − 81/13/ − 89/9]	3.3×10^{-4}
		Skin	
	N. of plies	Stacking sequence (°)	Residual
	32	[3/ − 79/9/ − 12/85/47/78/ − 5/ − 8/ − 78/81/ − 73/85/ − 37/ − 86/ − 4/ −2/ − 90/6/6/ − 90/5/ − 5/25/86/40/ − 8/ − 5/ − 69/90/ − 10/88]	9.6×10^{-5}

Table 4.5: Example 2: best stacking sequences for the optimal solution.

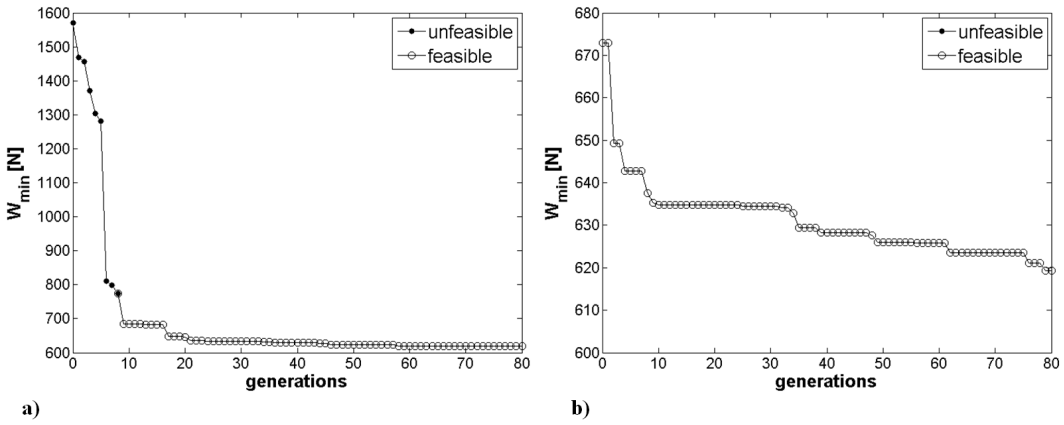

Figure 4.11: Best values of the objective function along generations; a) Example 2, b) Example 3.

The best solution found by BIANCA is shown in Table 4.6. The optimal number of stiffeners for the weight minimisation is 22, but in Table 4.6 only one half of the stiffeners, 11 on a whole of 22, is detailed, the other half being symmetrically placed with respect to the $x - z$ plane. The buckling load and the wing-box weight are $p_{cr} = 1933$ N/mm and $W = 619.26$ N, respectively. Fig. 4.13 shows the deformed shape of the structure when the applied load is equal to p_{cr}. Despite this solution has a symmetric distribution of the geometrical and polar parameters of the stiffeners, the buckling shape is not symmetric. This happens because the structure is not perfectly geometrically symmetric, because the Z-shaped stiffeners are not symmetrically disposed, for practical reasons; consequently the buckling deformed shape is not symmetric too.

As in the previous case, the stiffeners do not all belong to the same orthotropy type, some of them having $(K^{A^*})^S = 1$ while others $(K^{A^*})^S = 0$. The global constrained minimum has been found after 78 generations, see Fig. 4.11 b). This solution gives a reduction of the weight of the whole structure of about 49%, when compared to the reference solution, and the solution is still very close to the boundary of the feasible domain, $p_{cr} \simeq p_{ref}$.

Table 4.7 shows the best stacking sequences found by BIANCA when the second step is solved for this example. Furthermore, in Table 4.7, only one half of the stiffeners is detailed. The remarks done for the case of Example 2 can be rephrased *verbatim* also for this case.

4.7.4 Verification of the optimal stacking sequences

For the sake of completeness, we have verified the best solution of each one of the three examples above by a finite element analysis, though this is not strictly necessary. The FE

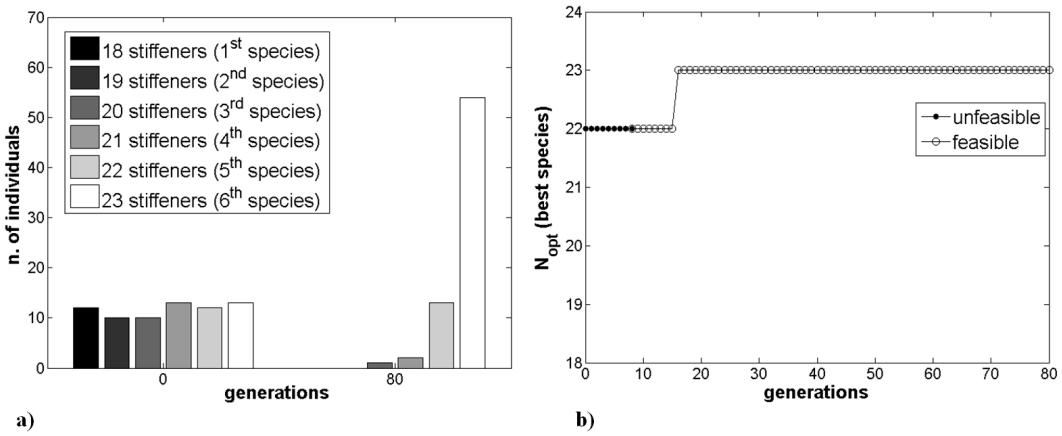

Figure 4.12: Evolution of species, Example 2; a) Number of individuals belonging to the same species in initial and final populations, b) Best number of stiffeners vs. generations.

model is exactly the same as in the first optimisation phase, namely for what concerns boundary and loading conditions. For both the cases of the wing-box section with identical and non-identical stiffeners, the quality of the solution of the second-level problem is evaluated. This is done in the following way: the buckling load and the deformed shape of the FE model created directly with the stacking sequences of the laminates, are compared to those obtained with the FE model used in the first optimisation phase, where the mechanical characteristics were entered through the Cartesian components of tensor $\mathbf{A}^*$. So, entering directly the stacking sequences we can assess the effect of the small imperfections of the final stacks with respect to the optimal solution found in the first-level problem, imperfections that give rise to the residuals shown in Tables 4.3, 4.5 and 4.7.

For the case of Example 1, the deformed shape is identical to that of Fig. 4.6, while the value of the buckling load now is $p_{crver} = 1949$ N/mm, which is slightly greater than $p_{cr} = 1943$ N/mm found at the end of the first optimisation step.

Furthermore, for the case of Example 2 the deformed shape practically does not change with respect to that presented in Fig. 4.10, and the buckling load is now $p_{crver} = 2124$ N/mm, about 10% greater than $p_{cr} = 1931$ N/mm, found at the end of the first step problem.

Finally, in the case of Example 3, the buckling load is now $p_{crver} = 2115$ N/mm, which is 9.4 % greater than $p_{cr} = 1933$ N/mm, the value found at the end of the first optimisation step; also in this case, the deformed shape does not change with respect to that shown in Fig. 4.13.

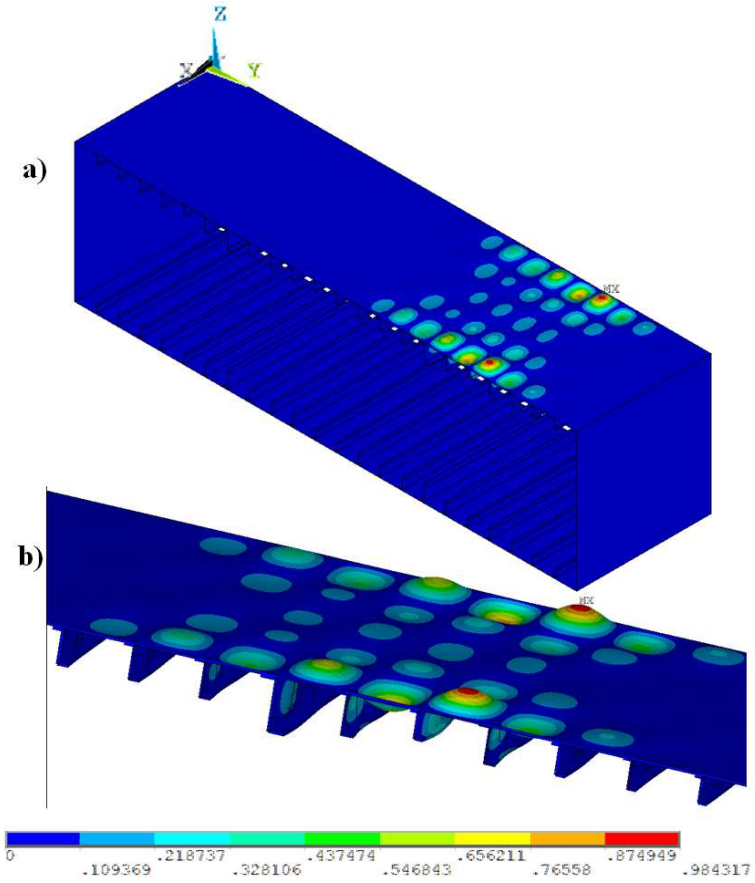

Figure 4.13: Example 3: deformed shape of the a) whole wing-box section and b) upper-panel stiffeners.

4.7.5 Some remarks on the type of laminate stacking sequence

In this section we want to highlight the importance of the use of non-standard stacking sequences for composite laminated panels. To this purpose, we consider again the Example 1, comparing the results already obtained with the ones that can be found using standard stacking sequences often employed in the aeronautical field, i.e. symmetric sequences with only the values $0°$, $\pm 45°$ and $90°$ for the ply orientations. The aim is to obtain the outcomes of the first optimisation step for Example 1, shown in Table 4.2. It can be noticed that, for symmetric stacking sequences the coupling stiffness tensor of the laminate is null, so the first term in Eq. (4.24) is identically zero. Concerning the genetic parameters, they are strictly those already used in the previous calculations.

To obtain a standard sequence solution to the second-level problem with a sufficiently small residual, we have found that 30 layers are necessary for the stiffeners and 40 for the skin. Table 4.8 shows the best stacking sequences found by BIANCA when using

Stiffeners				
ID	t^S [mm]	h^S [mm]	$(R_{0K}^{A^*})^S$ [MPa]	$(R_1^{A^*})^S$ [MPa]
01	4.0	40.0	−10642.20	5850.44
02	2.375	45.0	−5999.02	9648.09
03	4.875	46.5	−3101.66	4844.57
04	2.0	57.0	650.049	14266.9
05	4.25	42.0	16102.6	8211.14
06	2.5	63.0	−1578.69	11557.2
07	4.125	82.5	17477.0	4741.94
08	2.625	55.5	−14545.20	6656.71
09	3.25	52.5	−2990.22	13363.6
10	4.75	53.5	−2581.62	6343.11
11	4.625	43.5	15619.7	11228.7
Skin				
	t [mm]		$R_{0K}^{A^*}$ [MPa]	$R_1^{A^*}$ [MPa]
	4.0		9527.86	205.279

Table 4.6: Example 3: best values of the design variables.

symmetric stacking sequences with standard orientations. What is apparent is that we need now a higher number of layers than the solution shown in Table 4.3. This means that the solution found using symmetric stacking sequences with standard orientations is not a global minimum. Indeed, in this case, the weight of the whole wing-box section is 710.23 N, with an increase of about 20% of the weight of the structure when compared to the non-standard stacking sequence solution shown in Table 4.3, whose weight is 587.28 N.

Fig. 4.14 is the equivalent of Fig. 4.8 for the present case of symmetric sequences; the remarks previously done for the Example 1 can be rephrased *verbatim*, with the only difference that now coupling is exactly null.

Fig. 4.15 shows the variation of the best solution during the iterations, for stiffeners and skin laminates. In particular, we can notice that the best solution is found after 40 generations for the stiffener laminate, while for the laminate of the skin it is found after 150 generations.

To remark that the solutions so found are not balanced, as often used to obtain in-plane orthotropy, but not bending orthotropy. Nevertheless, they are orthotropic, and not only in extension, but also in bending. The assumption of balanced stacks will obviously lead to a further increase of the final weight of the structure. Therefore, the use of unconventional stacking sequences, as done in this work, is really more convenient for the reduction of the weight, as proved by the results shown above.

		Stiffeners	
ID	N. of plies	Stacking sequence (°)	Residual
01	32	[31/ − 39/35/ − 54/ − 38/ − 12/ − 30/41/20/ − 56/ − 26/55/55/38/37/31/ −30/ − 38/39/ − 9/ − 44/ − 43/ − 44/ − 50/19/8/23/35/50/ − 45/54/ − 23]	3.1×10^{-4}
02	19	[28/ − 33/ − 40/42/ − 23/0/ − 20/26/33/17/ 34/ − 32/ − 39/72/ − 52/8/6/ − 26/36]	1.4×10^{-3}
03	39	[−3/ − 37/39/50/88/29/48/ − 59/9/ − 60/ − 38/3/ − 15/ 25/ − 29/ − 26/ − 7/33/ − 27/ − 36/ − 71/34/57/ − 55/34/81/ 53/50/12/8/8/ − 61/ − 17/76/ − 26/ − 35/ − 1/ − 55/38]	2.7×10^{-4}
04	16	[30/ − 22/ − 28/ − 27/23/5/ − 10/27/ − 14/27/ − 52/ − 13/14/32/ − 22/7]	2.8×10^{-3}
05	34	[10/ − 12/ − 1/6/ − 82/2/ − 11/77/90/ − 86/ − 88/ − 88/ − 3/1/6/ − 19/10/ 46/5/6/ − 65/3/ − 6/1/2/ − 3/ − 16/90/89/ − 18/ − 10/9/87/13]	1.1×10^{-3}
06	20	[−7/26/17/ − 42/69/ − 38/22/ − 19/10/ − 6/ −33/3/36/ − 40/28/1/46/ − 33/17/ − 29]	8.1×10^{-4}
07	33	[5/1/85/ − 4/ − 4/90/ − 86/ − 18/ − 77/8/82/6/ − 3/85/1/7/0/ 81/1/2/79/ − 3/ − 69/ − 87/0/0/ − 90/ − 21/4/2/ − 88/83/5]	2.3×10^{-4}
08	21	[35/33/ − 38/ − 37/35/ − 36/35/ − 38/ − 38/51/ 10/ − 42/34/35/34/34/ − 38/ − 38/ − 36/ − 36/34]	5.4×10^{-3}
09	26	[−39/34/17/ − 21/34/ − 7/ − 23/ − 14/ − 21/24/1/33/39/ 10/ − 46/ − 35/ − 26/26/ − 27/15/27/34/ − 34/ − 24/ − 10/23]	8.9×10^{-4}
10	38	[13/39/ − 57/1/ − 19/ − 55/77/24/10/ − 43/ − 25/55/48/ −78/ − 15/ − 15/ − 23/35/ − 42/33/8/28/ − 55/ − 12/ − 29/ − 80/ 18/61/ − 16/7/37/21/ − 55/64/ − 31/47/ − 4/ − 35]	4.3×10^{-4}
11	37	[16/ − 16/7/ − 1/ − 7/ − 18/85/9/ − 4/ − 81/3/88/ −88/2/0/9/9/ − 4/ − 24/1/ − 8/ − 2/41/ − 2/ −2/ − 2/9/73/ − 4/ − 72/ − 4/83/ − 4/ − 3/ − 89/ − 5/9]	5.9×10^{-4}
		Skin	
	N. of plies	Stacking sequence (°)	Residual
	32	[80/ − 9/85/ − 1/ − 63/19/7/14/ − 34/54/ − 59/85/89/ − 83/87/ − 13/ 78/ − 4/ − 90/4/6/71/ − 11/16/ − 70/36/ − 15/ − 70/ − 26/79/13/ − 90]	3.9×10^{-5}

Table 4.7: Example 3: best stacking sequences for the optimal solution.

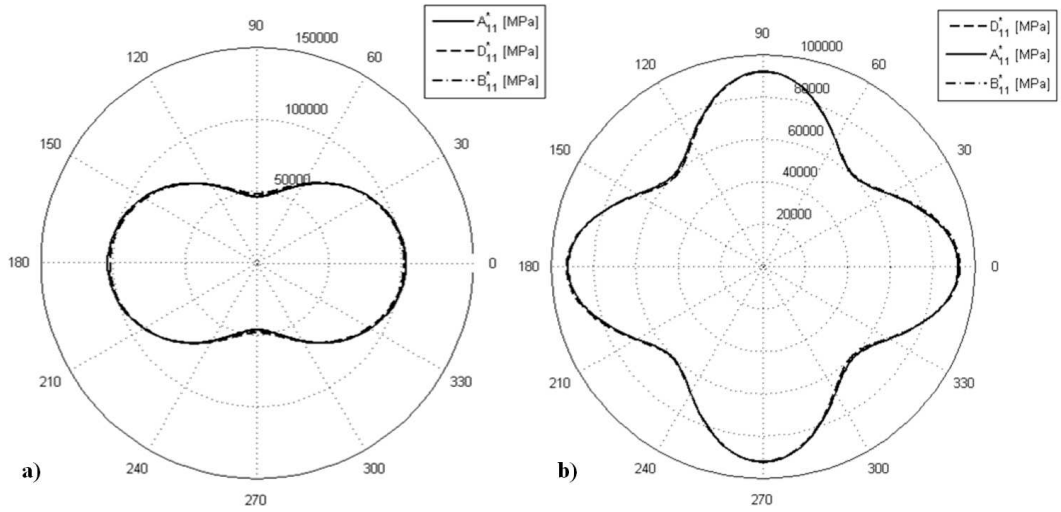

Figure 4.14: Example 1 with symmetric stacking sequence and standard orientations: first component of the homogenised stiffness tensors of the laminate for a) stiffeners and b) skin.

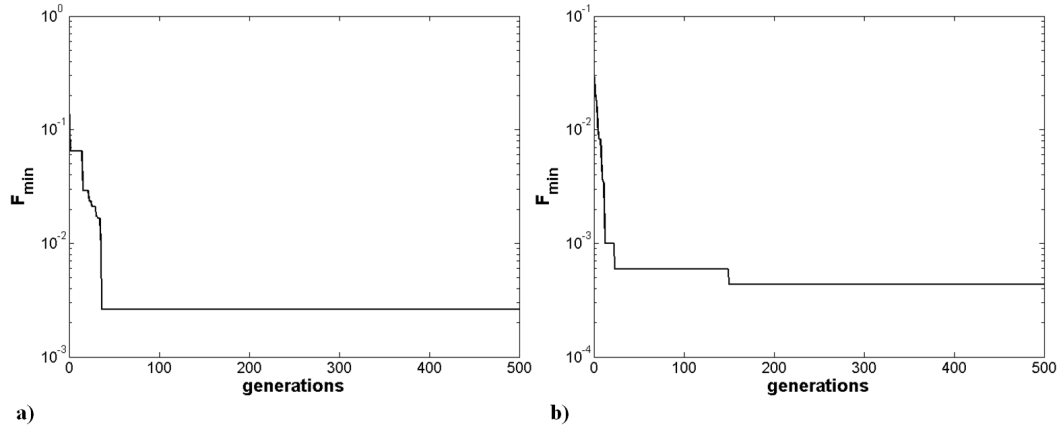

Figure 4.15: Example 1 with symmetric stacking sequence and standard orientations: best values of the objective function during iterations for a) stiffeners and b) skin laminates.

4.8 Concluding remarks

The optimisation procedure presented in this work is characterised by several points that make it an innovative, effective, general method for the design of composite stiffened panels. Our motivation was to create a general procedure for the optimisation of modular systems, with the number of modules that belongs to the set of the design variables and without using special assumptions to get some results. The numerical method is, however, a fundamental part of the procedure, because it is thanks to an appropriate numerical tool

Stiffeners		
N. of layers	Stacking sequence	Residual
30	$[-45/45/0_3/90/45/-45/45/0/-45/0/-45/0/45/]_s$	6.6×10^{-4}
Skin		
N. of layers	Stacking sequence	Residual
40	$[0/90/0/90/0/90_2/0/45/-45/90/0/90/0/90_2/0_2/90/0]_s$	9.6×10^{-5}

Table 4.8: Example 1: best symmetric stacking sequences with standard orientations.

that the simultaneous optimisation of the number of modules and of their characteristics is possible. We briefly recall the features of the procedure:

- no simplifying assumptions nor standard rules are used to design the composite structure; this allows for looking for a *true global minimum*, hard to be obtained otherwise;
- the procedure is composed by two distinct but linked non-linear minimisation problems: the first one is a constrained problem that uses a *free material approach* to the design of the geometric and material properties of the anisotropic structure, considered as composed by a single-layer fictitious anisotropic material; the second step is an unconstrained problem formulated to design a laminate able to realise the overall optimal mechanical properties designed in the first step; the link between the two problems is twofold: the second step makes use of the mechanical parameters found in the first step for determining a laminate and in the first step the geometrical constraints for the search of a suitable laminate are directly used in the formulation of the minimum problem, in order to have mechanical parameters that can really be obtained with a laminate in the second step;
- quasi-homogeneous sequences are used; this allows for writing exact geometric bounds, valid for both the extension and bending behaviour and for reducing the number of mechanical design variables in the first step;
- bending orthotropy is really obtained, its type specified and the orthotropy direction directly managed, without using special sequences or orientations;
- the number of the modules, i.e. the number of layers and of stiffeners, is directly optimised by the procedure, and this is entirely done by a genetic approach able to select not only individuals, but also species; in practice, the algorithm determines automatically the optimal number of design variables;

- the mechanical characteristics are represented by the polar formalism, that gives several advantages, namely to explicit elastic symmetries, elastic and geometric bounds, and to eliminate from the procedure redundant mechanical properties;
- the numerical computations are carried on by a special GA, the code BIANCA, able to cross simultaneously species and individuals, to handle continuous and discrete valued variables during the same iterations and to effectively handle the constraints imposed to the problem;
- for the solution of the first-level problem, the code BIANCA has been interfaced with a FE code, in order to numerically compute some mechanical quantities, namely the buckling load;
- the mathematical formulation of the second step problem allows for taking into account for all the possible combinations of elastic requirements and properties; it is stated as an unconstrained minimum problem of a positive semi-definite function, whose absolute minimum is equal to 0, which renders possible to know if a true global minimum has been attained.

The results presented in this Chapter show that when standard rules for the stacks of laminates are abandoned and the design of the optimal number of the modules composing the structure is included into the design procedure, significant savings of the weight of the structure can be obtained: up to 50%, when compared with a classical solution using an aluminium alloy, and up to 20% when compared with standard aeronautical stacking sequences.

Nevertheless, it is worth noting a fundamental point, already introduced in section 4.5: the correspondence between an elastic tensor and a laminate is not bijective. This is extremely important, because it renders the two-level approach feasible and effective. In fact, at the first level we can consider the structure as it was formed by a fictitious single layer, while the second level concerns the other properties to be designed, just because the mechanical parameters are not uniquely determined by the stacking sequence. For instance, in our case this allows us to use quasi-homogeneous laminates: at the first level this assumption let us consider only one elastic tensor to be designed, at the second level this property has to be obtained, but this would be, generally speaking, impossible to be done if only one sequence should give the elastic tensor found at the first level. On the contrary, because several laminates share the same elastic behaviour obtained at the first step, we can look for one of them which is also quasi-homogeneous.

Of course, in the same way, we could add at the second step other requirements to select, among the possible laminates, one having some other additional properties, for instance on the laminar strength or something else. Nevertheless, there is not any guarantee of finding a laminate satisfying all the requirements: mathematical conditions

ensuring that a given optimal design problem for a laminate has at least one solution are in general unknown. Anyway, the condition for not having an overdetermined problem is

$$n - 1 \geq n_r, \tag{4.25}$$

where n is the number of layers and n_r the number of requirements imposed to the search of the layer. Actually, one layer must be subtracted because the requirements have to be frame independent, and eventual conditions on the direction of the anisotropy are not to be considered; in our case, this is the condition given by $f_6(\delta)$ in Eq. (4.24). For the problem considered here, we have 7 requirements: 3 for getting $\widehat{K}^{A^*}$, $\widehat{R}_0^{A^*}$ and $\widehat{R}_1^{A^*}$, 2 for imposing that $\mathbf{D}^*$-$\mathbf{A}^* = \mathbf{O}$ and 2 for having $\mathbf{B} = \mathbf{O}$, see [132]. Hence, we can hope to obtain a solution if, for the skin and for each one of the stiffeners, we obtain a number of layers not less than 8. For this reason, but also for technological reasons, we have put, for the ply thickness, a lower bound of 2 mm, that gives a minimum of 16 layers of T300/5208 carbon-epoxy, see Table 4.1.

The proposed approach appears to be very flexible and applicable to various problems of structural engineering. Moreover, the procedure has a high level of versatility: more constraints could be easily added to the optimisation problem, e.g. constraints on the strength, yielding or de-lamination of the laminates which compose the structure, without reducing the power and the robustness of the proposed approach. This is a substantial part of the future developments that we intend to study.

Some final remarks: the structural problem considered here, namely the one concerning the first level of the procedure, is actually one of the oldest structural optimum problems. In fact, the first to study a problem of this type was Lagrange in 1770 [147]. He considered the case of a column subjected to a tip compressive load; the objective was to design the lightest column able to withstand a given load without buckling, which is just the problem that we have considered at the first level. He gave an erroneous result, subsequently corrected by Clausen in 1851 [148]. All along the last century, several other authors considered the same or a closely similar problem. The dual of the problem originally considered by Lagrange has also been treated: to maximize the buckling load for a column composed by a fixed amount of matter and charged by a compressive force at its top. A rather complete bibliography on this topic can be found in the classical book from Banichuk [149].

The problem that we have considered in this Chapter, however, is slightly different from the classical ones considered since Lagrange. In fact, the constraint on the minimum buckling load is not the only one, see Eq. (4.19). The geometrical constraints, namely those in the third of Eq. (4.4), are particularly important. They change, of course, the problem and its dual too. To our best knowledge, it is the first time that a similar problem has been formulated in the form given in this Chapter, and the formulation of its dual is still an open problem.

There are at least two other reasons that render the problem considered here different from those, more classical, cited beforehand. In fact, normally the authors consider the

case of the optimal shape of the structure, and look for a function defining the best form to be given to it. In our problem, the shape is known and the dimensions are to be determined along with the number of the modules, the stiffeners. In some sense, the number of modules changes the shape, but the changes are not continuous, because the number of modules is an integer.

The second reason, is the fact that our structure is anisotropic, while normally isotropic structures are considered. Hence, in our problem we need at the same time to optimise geometrical and mechanical quantities (in our case, we have chosen the polar invariants to represent the physical properties of the structure). Hence, we deal with a problem which is at the same time mechanical and geometrical, for its design variables.

The anisotropic nature of the problem, which in particular enters directly, though not explicitly, in the definition of the buckling constraint, is important also for another reason. In fact, we have already said that the first-level problem is non linear; this is easy to be understood, simply considering the objective function and the geometrical constraints. About the buckling constraint, we have already recalled that it is impossible to be explicitly written: the buckling load can be computed only by a numerical approach. Nevertheless, it depends upon the stiffness of the structure, which in turns depends on the mechanical and geometrical variables. It is well known, for instance, that stiffness is a non-convex function of the orientation of the anisotropy. So, it is likely that the buckling load is a non-convex function of the design variables.

Finally, concerning the second-level problem, it is always strongly non-convex. To our best knowledge, its dual is not known. More generally, in laminate design duality is an unexplored domain: no dual methods are known in this field. In the reference book on laminated composite design and optimisation [150], the word duality is never employed.

In addition, the solution is almost never unique, nor isolate. This is still an open mathematical problem in laminates design. Actually, no rules are known up to day to state if a problem like (4.24) has a solution and if it is unique or not. Such problems are, in fact, constituted by a sum of optimisation sub-problems that are not independent and that are, in some cases, compatible. In other words, if the number of layers, i.e. of unknowns, is sufficiently large, a problem of this type will have at least one solution. In this case, all the sub-objectives that compose the objective function are compatible. On the contrary, if the number of unknowns is not sufficiently large, the sub-objectives become incompatible and the global problem becomes a multi-objective one without any mechanical meaning nor interest.

The minimum number of unknowns, i.e. the minimum number of layers, to ensure the existence of the solution to a given problem of the type (4.24) is not known; of course, it depends upon the type of sub-objectives composing the global objective function. An attempt to give a numerical answer to such kind of questions have already been discussed in Chapter 3. In that Chapter the general problem is stated in a slightly different manner from (4.24), including the number of layers among the design variables. The

result is a laminate with the least number of layers satisfying the imposed requirements. Nevertheless, this is just a numerical approach, and a general rigorous theoretical study of the conditions for a laminate design problem like that in (4.24) have a solution, is still lacking.

What we have observed in all the cases that we have solved, is that when the solution exists, it is not unique nor isolate. Actually, there exist some functional relations among the solutions, that allows to change solutions changing with continuity some of the design variables. Unfortunately, it is possible, in general, to express analytically such relations only in very elementary cases [3], while in some other cases, very simple too, a graphical representation of the locus of all the solutions has been found numerically [136].

All these aspects have also influenced the choice of the numerical procedure used for solving the problem described in this Chapter.

Chapter 5

Optimal design of hybrid elastomer/composite laminates

5.1 Introduction

Even though polymer-based materials exhibit internal damping, the amount of damping often appears to be not sufficient for some applications involving noise and vibration phenomena. In order to improve the damping characteristics of composite materials, the most common solution consists in bonding an elastomer patch (a rubber-like material) combined with a stiffer layer (which constrains the elastomer patch) in particular locations of the structure.

Several works have been carried out on the study of damping properties of hybrid plates, shells and beams. Rather complete, but not exhaustive reviews on this subject can be found in [151, 152, 153, 154, 155]. As it can be noticed from the large amount of papers published on this subject in the last years, an improvement of the damping properties of composite materials can be obtained either by changing the laminate lay-up [156], or by introducing layers of material with pronounced damping properties, e.g. a high damping rubber material [157]. In addition, such viscoelastic plies can be constrained on their outer surfaces by stiffer layers [158], thus increasing the damping capacity of the structure: in fact, the constrained layer introduce shear deformation in the rubber material and thereby a significant amount of the damping in the structure. Through this solution, which is often called Constrained-Layer Damping (CLD) treatment, an effective passive control of the vibratory levels of the structure is performed, but, at the same time, the resulting structure shows an increase of the weight and costs.

Several numerical studies have been conducted on the effect of adding viscoelastic layers to vibrating beams and plates. In [159, 160, 161] simulations based on the finite element method (FEM) are carried out. In particular, in the work of Zhang *et al.* [162] the dynamical response of a hybrid beam with integral viscoelastic layers is studied, taking

into account the frequency dependence of the rubber material and the contribution of energy dissipation due to fibre-reinforced composite plies. The dynamical response of the structure is evaluated using the Iterative Modal Strain Energy (IMSE) method. Moreover, the effect of the thickness and position of the viscoelastic layers on the modal loss factors of the structure is analysed. Ganapathi *et al.* [163] predicted the system loss factors of sandwich and laminated composite beams by using geometrical non-linear dynamic analysis. Cho *et al.* [164] presented a damping analysis of laminated plates with fully and partially covered damping layers based on layerwise displacement theory. Kristensen *et al.* [165] studied the influence of the position of the partially constrained viscoelastic layer over a composite beam along with the effect of the thickness of the stiff layer on the loss factors of the structure. Concerning the behaviour of the rubber layer, they used the Kelvin-Voigt model and carried out the numerical simulations for both semi-analytical and FEM models of the structure.

Considering the large number of parameters involved in viscoelastically damped systems, it is desirable to carry out multi-parameter optimisation analyses, with specified geometrical and physical constraints in order to arrive at a dynamically optimum configuration. A possible solution consists in inserting a certain number of damping layers within the stack of the laminate during the design of the structure [166, 167]. Nevertheless, such solution needs the determination of the more relevant positions and thickness of the viscoelastic layers in order to maximise the modal loss factors without degrading the mechanical properties and increasing too much the weight of the structure. Lunden [168] conducted optimisation studies to find an optimal configuration of unconstrained distributed damping on beams and frames by minimising resonant vibrations subject to constraints on weight or cost of the additive damping along with a constraint on the loss factor of the available material. Lall *et al.* [169] carried out an optimal design study on a sandwich plate with constrained viscoelastic core. The objective function was built on the basis of the system's displacement response and also on the loss factors of the structure considering the densities and thickness of each layer as design variables. Linear relationship between material density and Young's modulus of Krokosky [170] were employed in addition to the temperature-frequency principle [171] in order to simplify the problem. Chen *et al.* [172] studied the problem of the optimal placement of CLD treatment to reduce the vibratory levels in plate-like structures. The main goal was to maximise the damping ratios of the structure subject to constraints on resonant frequencies shift and CLD thickness, considering as design variables the position as well as the thickness of the CLD patch. In [173] optimisation studies were performed in order to determine the optimum parameters of a four-element model used to represent the viscoelastic characteristics of the core for the sandwich plate: the material properties of the core, i.e. the parameters describing the shear modulus and the material loss factor as function of the time were kept as design variables. Recently, Le Maoût *et al.* [174] carried out an optimisation study of a hybrid sandwich plate: the objective was to maximise the modal loss factors of the

plate, in a given frequency range, with constraints on the weight and on the stiffness of the structure. They used as optimisation variables the orientation and the thickness of elastic plies and the thickness of viscoelastic layers. An optimal solution was found for different number of layers of the plate. A FEM model of the plate was built within the ABAQUS environment and the damping of the structure was evaluated through the IMSE method.

As it can be resumed from the state of the art, until now, the problem of designing the damping characteristics of the hybrid laminates has been stated so far considering as design variables only the thickness and orientations of the elastic plies along with the thickness and/or the material properties (shear modulus, material loss factor, density) of the viscoelastic layers. The main objective of the present work consists in determining also which are the *best number* of the constitutive layers of the hybrid laminate and the *best positions* of the elastomer layers within the stacking sequence (along with the values of orientation and thickness for each ply) in order to maximise the damping properties of the structure. Moreover, constraints on the in- and out-of-plane stiffness along with a constraint on the total mass of the hybrid plate are considered in order to avoid the degradation of the mechanical properties and the increase of the weight of the structure. The problem is formulated in the most general case: no simplifying hypotheses are made on the behaviour of the hybrid laminate and on the position of the viscoelastic plies within the stack, differently from which is usually done in literature where it is *a-priori* assumed that the positions of elastomer layers within the stack are always located between two consecutive stiffer plies. In addition, since the material properties of the elastomer plies depends on the frequency, the evaluation of the undamped eigenfrequencies and of the structural loss factors leads us to consider a non-linear modal analysis, thus the IMSE method is employed to overcome this difficulty.

As in Chapters 3 and 4 here we deal with an optimisation problem concerning modular structures. More precisely in this case the design problem concerns the hybrid laminates that can be viewed as modular systems, the modules being the layers. Again, in order to obtain a configuration that represents a global optimum and also to include the number and position of layers among the design variables we use, as optimisation tool, the genetic algorithm (GA) BIANCA (see also [142, 143]) with crossover on species. As already said in the previous Chapters, the main difficulty, when dealing with the optimisation of modular structures, is how to take into account the variable number of modules, even in the case in which the modules are non-identical, as the case of hybrid laminates with variable number of plies made of different materials. In the framework of GAs, such a problem corresponds to the search of solutions in a design space made up of individuals with variable number of chromosomes and, hence, belonging to different species.

Just like in the application considered in Chapter 3, in the case of the problem of designing the damping properties of hybrid laminates the number of modules-layers is directly related to the number of the individual's chromosomes and, hence, the optimal number of layers is an outcome of the genetic process, which automatically issues the *best*

species. Moreover, during the optimisation process, the GA is coupled with the FE code ANSYS in order to evaluate the objective and constraint functions.

The Chapter is organised as follows: firstly geometry, material properties and loading conditions along with the FE model adopted for the hybrid plate are described in Sec. 5.2, then the mathematical formulation of the design problem of the damping properties of the structure as an optimisation problem as well as the description of the numerical strategy are detailed in Sec. 5.3. In Sec. 5.4 the numerical results concerning the case of a rectangular hybrid plate are shown to validate the accuracy and the reliability of the proposed approach, and, finally, some concluding remarks end the Chapter.
This Chapter is substantially taken from the article [175].

5.2 Description of the problem: application to the design of a hybrid laminate

5.2.1 Geometry and materials

The optimisation strategy presented in this Chapter allows to find a solution for the problem of designing the damping properties of hybrid laminates and it is applied to a rectangular hybrid plate, whose dimensions are depicted in Fig. 5.1.

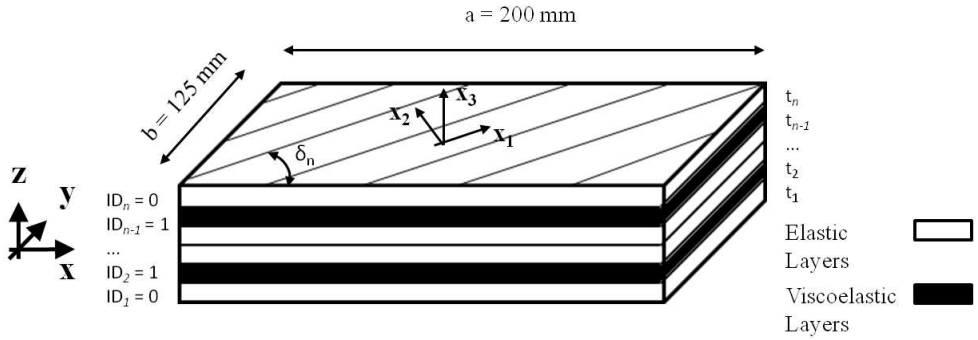

Figure 5.1: Geometry of the hybrid plate.

Concerning the typical dimensions of the plate, the thickness of each layer is constrained to remain sufficiently small compared to both width and length of the plate, in order to keep valid the assumptions of the thin plate model. Moreover, we assume that the fibre-reinforced plies have linear elastic orthotropic behaviour. Adopting the vectorial notation for strain $\boldsymbol{\varepsilon}$ and stress $\boldsymbol{\sigma}$ tensors and introducing the compliance tensor $\mathbf{S}$, the constitutive law can be stated as follows:

$$\begin{Bmatrix} \varepsilon_{11} \\ \varepsilon_{22} \\ \varepsilon_{33} \\ \gamma_{23} \\ \gamma_{13} \\ \gamma_{12} \end{Bmatrix} = \begin{bmatrix} 1/E_1 & -\nu_{12}/E_1 & -\nu_{13}/E_1 & 0 & 0 & 0 \\ -\nu_{12}/E_1 & 1/E_2 & -\nu_{23}/E_2 & 0 & 0 & 0 \\ -\nu_{13}/E_1 & -\nu_{23}/E_2 & 1/E_3 & 0 & 0 & 0 \\ 0 & 0 & 0 & 1/G_{23} & 0 & 0 \\ 0 & 0 & 0 & 0 & 1/G_{13} & 0 \\ 0 & 0 & 0 & 0 & 0 & 1/G_{12} \end{bmatrix} \begin{Bmatrix} \sigma_{11} \\ \sigma_{22} \\ \sigma_{33} \\ \sigma_{23} \\ \sigma_{13} \\ \sigma_{12} \end{Bmatrix} , \quad (5.1)$$

where ε_{ii} and γ_{ij} are the strain components and σ_{ij} are the stress components, with $i, j = 1, 2, 3$. The parameters used to describe the behaviour of the material are the technical constants of elasticity: the Young's moduli E_i, the Poisson's ratios ν_{ij} and the shear moduli G_{ij}. The subscripts $(1, 2, 3)$ correspond to the direction of the axes in the material frame of the single layer. Concerning the material of the elastic plies, a glass-epoxy lamina has been used, whose material properties are listed in Table 5.1 [153].

Young's modulus E_1 [GPa]	29.9
Young's modulus E_2 [GPa]	7.5
Young's modulus E_3 [GPa]	7.5
Shear modulus G_{12} [GPa]	2.25
Shear modulus G_{23} [GPa]	2.25
Shear modulus G_{13} [GPa]	2.25
Poisson's ratio ν_{12}	0.24
Poisson's ratio ν_{23}	0.24
Poisson's ratio ν_{13}	0.24
Density ρ [kg m^{-3}]	1500

Table 5.1: Material properties for the glass-epoxy lamina, taken from [153]

The material used for the viscoelastic layers is a rubber-like material having linear isotropic behaviour. In addition, the properties of that material are considered dependent upon the loading frequency f. Introducing the fourth-order complex viscoelasticity stiffness tensor $\mathbf{D}^v$ the constitutive law is:

$$\boldsymbol{\sigma} = \mathbf{D}^v(f) \cdot \boldsymbol{\varepsilon} , \quad (5.2)$$

with:

$$\mathbf{D}^v(f) = \mathbf{D}^v_r(f) + \mathrm{i}\mathbf{D}^v_i(f) , \quad (5.3)$$

where $\mathbf{D}^v_r(f)$ and $\mathbf{D}^v_i(f)$ are the fourth-order tensors which characterise the energy storage and the dissipative response of the material, respectively. Similarly to Eq. (5.1), the use of the vectorial notation yields:

$$\mathbf{D}_r^v = \Lambda \begin{bmatrix} 1-\nu(f) & \nu(f) & \nu(f) & 0 & 0 & 0 \\ \nu(f) & 1-\nu(f) & \nu(f) & 0 & 0 & 0 \\ \nu(f) & \nu(f) & 1-\nu(f) & 0 & 0 & 0 \\ 0 & 0 & 0 & \frac{1}{2}(1-2\nu(f)) & 0 & 0 \\ 0 & 0 & 0 & 0 & \frac{1}{2}(1-2\nu(f)) & 0 \\ 0 & 0 & 0 & 0 & 0 & \frac{1}{2}(1-2\nu(f)) \end{bmatrix} ,$$

$$\mathbf{D}_i^v = \Lambda^* \begin{bmatrix} 1-\nu(f)^* & \nu(f)^* & \nu(f)^* & 0 & 0 & 0 \\ \nu(f)^* & 1-\nu(f)^* & \nu(f)^* & 0 & 0 & 0 \\ \nu(f)^* & \nu(f)^* & 1-\nu(f)^* & 0 & 0 & 0 \\ 0 & 0 & 0 & \frac{1}{2}(1-2\nu(f)^*) & 0 & 0 \\ 0 & 0 & 0 & 0 & \frac{1}{2}(1-2\nu(f)^*) & 0 \\ 0 & 0 & 0 & 0 & 0 & \frac{1}{2}(1-2\nu(f)^*) \end{bmatrix} , \tag{5.4}$$

with:

$$\begin{aligned} \Lambda &= \frac{E(f)}{(1+\nu(f))(1-2\nu(f))} , \\ \nu(f)^* &= \eta_v(f)\nu(f) , \\ \Lambda^* &= \frac{E(f)}{(1+\nu(f)^*)(1-2\nu(f)^*)} . \end{aligned} \tag{5.5}$$

In Eq. (5.4) and (5.5), $E(f)$ and $\nu(f)$ are the frequency-dependent Young's modulus and Poisson's ratio, while $\eta_v(f)$ is the material loss factor. The material properties used for the viscoelastic layers are taken from [174]. The variation of the Young's modulus with the frequency is expressed as:

$$E(f) = E_s + E_d \log\left(\frac{f}{\overset{\frown}{f}}\right) , \tag{5.6}$$

where $E_s = 0.0041$ GPa is the steady-state value of the Young's modulus, $E_d = 0.0322$ GPa is the amplitude of the part that depends upon the frequency, while $\overset{\frown}{f} = 1$ Hz is a reference value for the frequency. The Poisson's ratio and the material loss factor are kept constants and equal to $\nu = 0.3$ and $\eta_v = 0.3$, respectively, whilst the density is $\rho = 968.1$ kg m^{-3}.

5.2.2 Loading conditions

The design of the hybrid laminate represents a compromise between its damping capability and the ability of keeping good mechanical properties in terms of stiffness, without

increasing too much the weight.

The dynamic response of the structure is evaluated through a classical free vibration analysis. Only the first $N = 5$ non-rigid modes are calculated considering free-displacement boundary conditions on the edges of the plate. It is worth noting that, since the material properties of the viscoelastic layers depend upon the frequency, the calculation of the eigenfrequencies, as well as the modal loss factors, needs an iterative procedure for each eigenfrequency.

Concerning this kind of problems, several numerical strategies are available in literature. These approaches are substantially divided in frequency-domain and time-domain-based approaches. Since in this work the dynamic response of the structure is evaluated through a free vibration analysis, we look for a numerical strategy belonging to the class of the frequency-domain-based approaches. A detailed description of the different solution strategies is available in [154]. Among all the possible frequency-domain-based approaches, the most suited for our problem are the Iterative Modal Strain Energy (IMSE) and the Iterative Complex Eigensolution (ICE) methods.

The IMSE method is an extension of the MSE method originally introduced by Ungar and Kerwin [176]. The MSE approach is based on the principle that the undamped natural modes of the viscoelastically damped structure are representative of the damped model and, thus, a frequency-independent stiffness matrix might be used. Nevertheless, this assumption is valid only for low to moderate additions of damping materials. Moreover, in order to obtain more realistic values of the modal loss factors, the variation of the stiffness matrix of the damped structure with the frequency has to be taken into account. To this purpose, a modification of the original MSE algorithm was proposed in [154, 162], by introducing an iterative approach, i.e. the IMSE approach, which more appropriately considers the dependence of the energy storage and the dissipative response of the material upon the frequency. As a consequence, an iterative calculation of the real (undamped) eigensolution is performed using the continuously iteratively updated real part of the stiffness matrix of the rubber layers. The material properties are updated according to the adopted material law, in our case the law of Eq. (5.6), at the value of frequency of the current iteration, in the neighbourhood of the considered natural mode. Once the convergence on the i^{th} undamped natural frequency is reached, the corresponding modal loss factor η_i is evaluated as:

$$\eta_i = \eta_v(f_i)\frac{W_v(f_i)}{W_{tot}(f_i)} \ , \tag{5.7}$$

where $\eta_v(f_i)$ is the material loss factor at the current frequency, while $W_v(f_i)$ and $W_{tot}(f_i)$ are the strain energy of the viscoleastic layers and the total strain energy of the structure for the i^{th} mode, respectively.

The ICE strategy appears as a sound alternative to evaluate the modal loss factors of the structure. The ICE method is exact in the sense that it does not determine the modal loss factors according to the definition of the MSE approach, but it employs directly the

evaluated complex eigenvalues to calculate the exact modal loss factors of the structure. In other words, in the framework of the IMSE approach an iterative calculation of the real eigensolution is performed, while in the context of the ICE approach an iterative calculation of the complex eigensolution is carried out. Therefore, the resultant ICE strategy can be seen as a more accurate and generally applicable method when dealing with such problems.

Nevertheless, since the FE model of the hybrid plate is built within a commercial FE code, i.e. ANSYS, we choose to employ the IMSE approach to evaluate the modal loss factors of the structure. Even though the ICE strategy is more robust than the IMSE one in evaluating the loss factors, the IMSE method is doubtless easier to implement within a commercial code. In addition, the ICE method is time-consuming and requires a higher computational effort because, for each mode, repeated complex eigensolutions have to be performed before reaching the convergence. Moreover, we recall that this non-linear process has to be included in the framework of a genetic-based optimisation process which often requires a high number of evaluations of the objective and constraint functions. Finally, the IMSE method leads to obtain a good estimation of the damping properties of the structure (for structures with low or moderate damping capabilities), in terms of natural frequencies and modal loss factors, as shown in [155, 162, 174]. The previous considerations have oriented our choice on the IMSE approach as numerical strategy used to calculate the modal loss factors of the hybrid laminated plate considered in this work. The logical flow of the IMSE approach, which we have implemented within the ANSYS environment, is shown in Fig. 5.2.

Along with the increase of damping capability, the structure must withstand to the application of static loads, i.e. the structure has to exhibit good properties in terms of stiffness. To this purpose, extension as well as bending stiffness properties are studied by considering three different static loading conditions, as shown in Fig. 5.3. In particular, two simulations are performed under uniaxial prescribed displacement in x and y directions, and in both cases the corresponding reactions R_x and R_y are evaluated, having in this way informations about the in-plane stiffness of the hybrid plate. Moreover, to have a measurement of the out-of-plane stiffness, a bending calculation is performed: a prescribed deflection is imposed along the z direction in the center of the laminate and the corresponding reaction R_z is then determined. In each one of the three considered static loading conditions, the imposed displacement is $\delta = 1$ mm.

A conclusive remark: it is worth noting that employing a different strategy to evaluate the modal loss factors of the structure (namely the use of an alternative and more accurate strategy as the ICE approach) does not imply any change in the optimisation procedure that we will describe in the next Section.

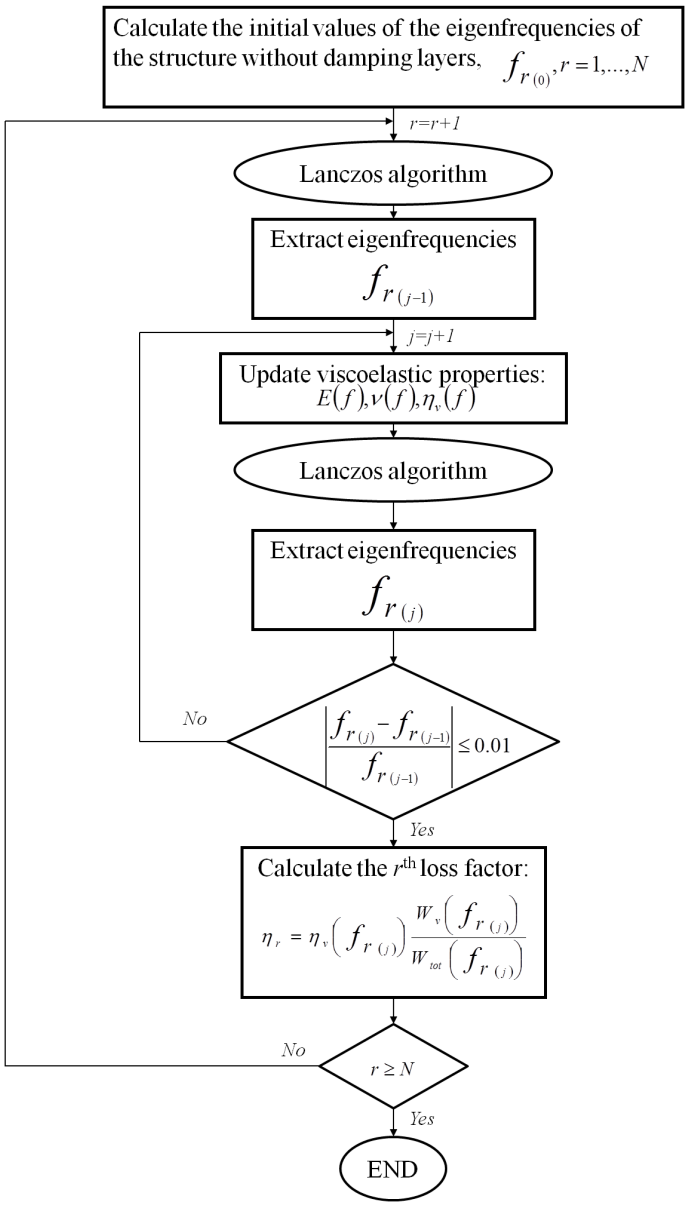

Figure 5.2: Flow of the IMSE strategy for the prediction of the loss factors of the structure.

5.2.3 Finite element model of the hybrid plate

As shown in Fig. 5.4, two different mechanisms of dissipating the vibratory energy can essentially be observed in viscoelastically damped structures, see [151]: the first dissipation phenomenon is linked to the shear strains, which are predominant in the constrained viscoelastic materials, while the second one is related to the direct normal strains, in the case of unconstrained viscoelastic materials.

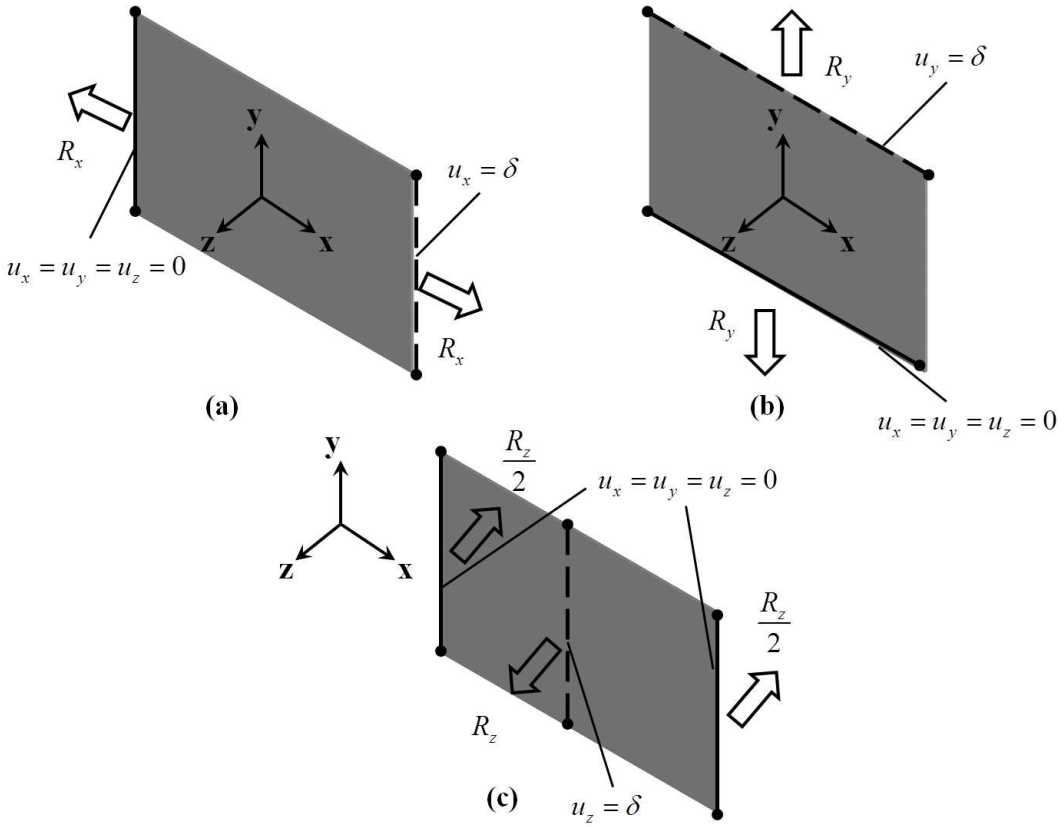

Figure 5.3: Static tests for the evaluation of the optimisation constraints: (a) uniaxial displacement along x direction, (b) uniaxial displacement along y direction and (c) uniaxial displacement along z direction.

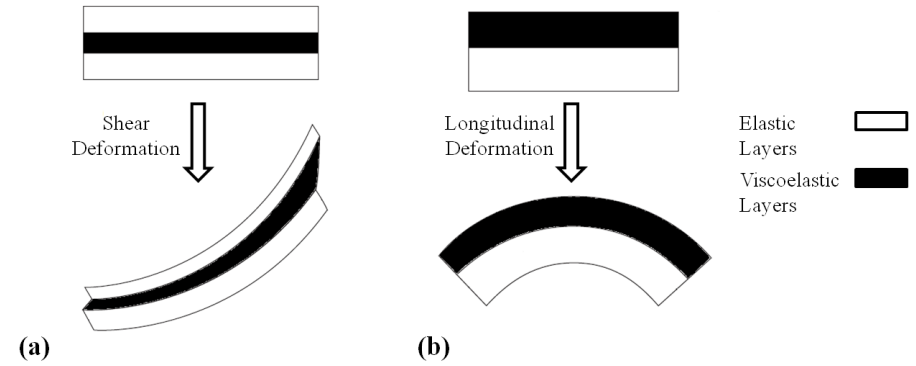

Figure 5.4: Basic mechanisms for viscoelastic damping: (a) constrained and (b) unconstrained treatment.

In order to predict these phenomena, 3D brick elements have been considered to model the rubber layers: we need to build a mathematical model able to describe (with a good level of accuracy and reliability) the mechanical response of the physical system. To this purpose the FE model of the hybrid plate has to be able to catch those aspects which normally, even with higher-order 2D theories, are not well described, e.g. the damping response associated to the shear strains through-the-thickness.

Since the model is built in ANSYS environment, we use SOLID185 elements, which are solid elements with 8 nodes and 3 degrees of freedom (DOFs) per node. Moreover, this type of element is also employed for the elastic plies.

In addition, since the FEM model is built with solid elements, the number of DOFs could be large, thus implying significant CPU time for each calculation. To this purpose, after a preliminary mesh sensitivity study, the optimal in-plane sizes of brick elements are chosen equal to 3×3 mm^2. Moreover, we have previously checked that a single element in the thickness of each layer is sufficient to capture in correct way the damping mechanisms associated to the viscoelastic plies. Finally, as we will explain in Sec. 5.3, since the number of layers is one of the design variables of the optimisation process, the total number of DOFs of the whole model will vary along with the number of plies.

5.3 Formulation of the optimal damping properties problem

In this section, the problem of designing the damping properties of a hybrid plate is stated as a constrained optimisation problem. The goal of our strategy consists in maximising the first N modal loss factors of the structure, without degrading the stiffness properties of the plate and increasing too much its weight.

The problem is stated in the most general case, thus the design variables are:

- the total number of layers (both elastic and viscoelastic), n;
- the position and the number of the viscoelastic layers within the stack, which are directly linked to the variable ID_k, $(k = 1, ..., n)$, that identifies the nature of the k^{th} ply, i.e. $\mathrm{ID}_k = 1$ if the k^{th} ply is viscoelastic, $\mathrm{ID}_k = 0$ otherwise;
- the thickness of each layer, t_k $(k = 1, ..., n)$;
- the fibre orientation of the elastic plies, δ_k $(k = 1, ..., n)$.

It is worth noting that, since the number of layers is included among the optimisation variables, the total number of design variables of the whole optimisation process can change for each possible point-solution in the design space, or, in other words, the procedure determines by itself the optimal number of design variables.

5.3.1 Mathematical statement of the problem and solving strategy

The optimisation problem can now be established. The maximisation of the first N modal factors can be expressed as the minimisation of the following objective function:

$$\Phi = -\sum_{i=1}^{N} \eta_i \ , \tag{5.8}$$

that represents the opposite of the sum of the first N modal loss factors. Moreover, the constraints on the maximum decrease of the stiffness properties and on the maximum increase of the mass of the plate have to be considered. Therefore, the constrained minimisation problem can be stated as a classical non-linear programming problem (NLPP) as follows:

$$\begin{aligned}
&\min \ \ \Phi\left(n, \mathrm{ID}_k, t_k, \delta_k\right) \quad (\text{with } k = 1, ..., n) \ , \\
&\text{subject to :} \\
&\begin{cases}
g_1(n, \mathrm{ID}_k, t_k, \delta_k) = \dfrac{{R_x}^{ref} - R_x\left(n, \mathrm{ID}_k, t_k, \delta_k\right)}{{R_x}^{ref}} - \epsilon_x \leq 0 \ , \\
g_2(n, \mathrm{ID}_k, t_k, \delta_k) = \dfrac{{R_y}^{ref} - R_y\left(n, \mathrm{ID}_k, t_k, \delta_k\right)}{{R_y}^{ref}} - \epsilon_y \leq 0 \ , \\
g_3(n, \mathrm{ID}_k, t_k, \delta_k) = \dfrac{{R_z}^{ref} - R_z\left(n, \mathrm{ID}_k, t_k, \delta_k\right)}{{R_z}^{ref}} - \epsilon_z \leq 0 \ , \\
g_4(n, \mathrm{ID}_k, t_k) = \dfrac{M\left(n, \mathrm{ID}_k, t_k\right) - M^{ref}}{M^{ref}} - \epsilon_M \leq 0 \ .
\end{cases}
\end{aligned} \tag{5.9}$$

In Eq. (5.9) R_x, R_y and R_z are the reactions of the plate, evaluated as shown in Fig. 5.3, which represent a measure of the stiffness of the structure, while M is the mass of the plate. The superscript ref stands for *reference* value. The reference values of the reactions and mass are calculated, before the optimisation process, on a reference undamped structure, i.e. a plate without elastomer layers. The quantities ϵ_x, ϵ_y, ϵ_z and ϵ_M are the user-defined tolerances on each constraint. The meaning of the constraints on the reaction forces and on the mass of the hybrid plate are the following: the maximum loss in stiffness and the maximum increase in mass of the optimised structure are superiorly bounded by the value of the corresponding tolerances.

It can be noticed that the NLPP of Eq. (5.9) is highly non-linear and non-convex in the space of design variables. In fact, for a given eigenfrequency the strain energy, and hence the loss factor of the structure, depends upon circular functions of the plies orientation. Moreover, depending on the number of layers n, the dimension of the design space, and hence the number of design variables can change. Indeed, in the objective and

constraint functions, we can enumerate three variables for each ply (the nature of the ply ID_k, the thickness t_k and the orientation δ_k), besides the variable number of layers n. Therefore, in the most general case, the overall number of design variables for the problem (5.9) is $3n + 1$.

The previous considerations on the nature and on the varying number of design variables involved into the optimisation process oriented our choice on GAs, as numerical tool, in order to search solutions for the problem (5.9).

As said in the previous Chapters, the optimisation of engineering modular systems is a difficult task since it implies the optimisation of each constitutive module composing the system, as well as the optimisation of the number of constitutive modules, as the case of the design of the hybrid plate considered here. As a matter of fact, the number of constitutive modules (the number of layers in our case) is an integer value and the design space of such optimisation problems is therefore populated by points representing structures composed of different numbers of modules (layers). As a consequence, the number of constitutive parameters (variables of the optimisation problem) is different for distinct points and the associated mathematical optimisation problem is defined over a design space of variable dimension.

Taking into account all the previous aspects, even in this Chapter we use the GA BIANCA with crossover and mutation between species as optimisation tool to perform the search of solutions for the problem at hand. Here we want to highlight the structure of the individual's genotype, and, consequently, the representation of the information for the problem (5.9) and how the GA is interfaced with the FEM code ANSYS.

Fig. 5.5 shows the genotype of the generic r^{th} individual representing the hybrid plate with n_r plies. This individual has n_r chromosomes and each chromosome is composed of 3 genes coding the design variables of each ply: the nature of the layer, ID_k, the thickness of the layer, t_k and the orientation of the layer, δ_k. An exception is the first chromosome that has 4 genes: the fourth additional gene codes the number of layers for the generic r^{th} individual. Letter e stands for empty location. It can be noticed that the variable ID_k is a discrete variable which can assume only the values 0 or 1 depending on the nature of the k^{th} ply. When the k^{th} layer is viscoelastic, i.e. $\mathrm{ID}_k = 1$, only the gene coding the thickness is treated by the GA for all genetic operations, whilst the third gene representing the orientation is ignored.

As conclusive remark, it is worth noting that for every individual at each generation, the evaluation of the objective and constraint functions is performed via a FEM analysis. Hence, also for this application the GA BIANCA is coupled with the FEM code ANSYS that we used as FEM tool to simulate the mechanical response of the hybrid plate.

ID_1	t_1	δ_1	n_r
ID_2	t_2	δ_2	
...	...	...	
ID_{n_r}	t_{n_r}	δ_{n_r}	
e	e	e	

Figure 5.5: Structure of the individual's genotype for the optimisation problem (5.9).

5.4 Studied cases and results

In order to demonstrate the capabilities of our strategy we study the optimisation of the damping properties of a rectangular hybrid plate whose in-plane dimensions are those shown in Fig 5.1. In particular we performed the optimisation process for the three following cases:

1. the case wherein the total number of layers, the orientations of the elastic laminae along with the positions and the number of viscoelastic plies are fixed *a-priori*, thus the only design variables of the problem (5.9) are the layers thickness. For this first simple case, we perform the optimisation calculations using two different GAs: the GA BIANCA and the GA available in the MATLAB Optimisation Toolbox [177], in order to compare the quality of results obtained with these two codes;

2. the case wherein we assume *a-priori* that the stacking sequence of the laminate is symmetric. In this case the total number of design variables depends upon the number of layers. Nevertheless, due to the assumption of the symmetry of the stack, the global number of variables is considerably reduced;

3. the most general case wherein no simplifying assumption on the stacking sequence of the hybrid plate is made. Even in this case the total number of design variables depends upon the number of layers.

These test cases are chosen according to the problems often treated in literature and also according to the will of testing new problems which are more general and complex than the ones often presented in literature.

It can be noticed that the design variables of the cases 2 and 3 are those discussed in Sec. 5.2. Concerning the optimisation problem of Eq. (5.9), in order to establish correct reference values for the reactions and the mass of the hybrid plate, three static

analyses have been conducted on a reference structure before starting the optimisation process, for each one of the considered cases. The undamped reference plate (without viscoelastic layers) considered here is made of 6 glass-epoxy laminae (see Table 5.1 for the material properties) with the following stacking sequence: $[90/45/0]_S$. Moreover, for the first studied case, the thickness of the elementary ply is 0.27 mm, whilst for cases 2 and 3 it is equal to 0.3 mm. Finally, the value of the reference reactions and mass for these cases are:

- ${R_x}^{ref} = -15617$ N, ${R_y}^{ref} = -40032$ N, ${R_z}^{ref} = -18.51$ N, $M^{ref} = 0.06075$ Kg for case 1;
- ${R_x}^{ref} = -17352$ N, ${R_y}^{ref} = -44480$ N, ${R_z}^{ref} = -23.06$ N, $M^{ref} = 0.0675$ Kg for cases 2 and 3.

As conclusive remark, it can be noticed that the user-defined tolerances on the constraints of the problem (5.9) are set as follows: $\epsilon_x = \epsilon_y = \epsilon_z = \epsilon_M = 0.05$, i.e. the maximum loss in stiffness and the maximum increase in mass between the optimised structure and the reference one are limited to 5% for all cases.

5.4.1 Case 1: fixed number of plies

In this first calculation we consider the simple case of the optimisation of the first modal loss factor of the structure, thus we consider only the first non-rigid mode, $N = 1$ in Eq. (5.9), in order to compare the results of the optimisation process obtained using both MATLAB and BIANCA GAs. Since the number of layers of the laminate is fixed, the new genetic operators that perform the reproduction among different species are no longer required. Moreover, we have also fixed the number and the position of the viscoelastic plies within the stacking sequence as well as the orientations of the elastic laminae. As a result of these considerations, the only design variables are the layers thickness which can vary continuously between 0.1 and 1.0 mm. In addition, the hybrid plate has 5 layers with the following stacking sequence (V stands for viscoelastic layer): [0/V/90/V/0]. For this first case, since we have only 5 layers, the number of DOFs of the FEM model of the plate is 47970.

Concerning the BIANCA GA, the structure of the individual is organised in a simpler way: the genotype is made up of 5 chromosomes, each composed of a single gene coding the thickness of the corresponding ply.

The genetic parameters of the BIANCA GA are chosen as follows: the population size is set to $N_{ind} = 30$ and the maximum number of generations is assumed equal to $N_{gen} = 80$. The crossover and mutation probability are $p_{cross} = 0.85$ and $p_{mut} = 1/N_{ind}$, respectively. Selection is performed by roulette-wheel operator and elitism is active. The ADP method is used for handling constraints. Concerning the genetic parameters of the

MATLAB GA they are the same already used for the GA BIANCA, with the exception of the mutation operator and of the method for handling constraints: in order to force the solution to belong to the feasible region we have used the @mutationadaptfeasible operator along with the standard penalty scheme developed within the MATLAB GA (for more details see [177]).

The best solutions found using BIANCA and MATLAB GAs are detailed in Table 5.2. Fig. 5.6 shows the variation of the best solution vs. generations found using these two codes. It can be noticed that the solution found using BIANCA shows better damping capabilities when compared to the one found by MATLAB. Moreover, the solution found using MATLAB converges after only 3 generations, whilst BIANCA found a better value of the objective function after about 25 generations and reaches the real global minimum after 73 generations.

Such results are mainly linked to the *biodiversity* of the population during the generations: clearly, for this kind of problem, the procedure for handling constraints, implemented within the MATLAB GA, causes a lack of diversity in the current population (we have several clone-individuals) which induces, on its turn, a premature convergence of the GA toward a local minimum. On the contrary, as it appears clearly from Fig. 5.6, BIANCA preserves a certain biodiversity through the generations and this aspect lead us to find a better solution.

	Reference	BIANCA	MATLAB
n	6	5	5
stack	$[90/45/0]_S$	[0/V/90/V/0]	[0/V/90/V/0]
t_k [mm]	$[0.27/0.27/0.27]_S$	[0.398/0.342/0.632/0.301/0.253]	[0.250/0.327/0.664/0.303/0.378]
η_1		0.00976	0.00960
f_1 [Hz]		92.30	91.13
R_x [N]	−15617	−15159 (−2.9%)	−14860 (−4.8%)
R_y [N]	−40032	−38079 (−4.9%)	−39326 (−1.8%)
R_z [N]	−18.51	−19.96 (+7.8%)	−20.21 (+9.2%)
M [Kg]	0.06075	0.06378 (+5.0%)	0.06374 (+4.9%)
Φ		−0.00976	−0.00960
g_1		−0.02066	−0.00157
g_2		−0.00120	−0.03235
g_3		−0.12843	−0.14193
g_4		−0.00014	−0.00077

Table 5.2: Best solutions found using BIANCA and MATLAB GAs for the optimisation problem (5.9), case 1 (V denotes the position of the viscoelastic ply).

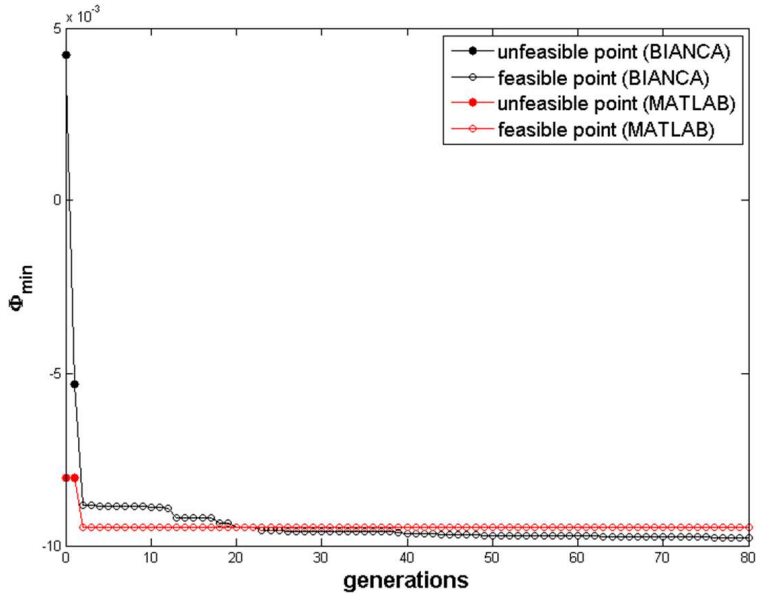

Figure 5.6: Best values of the objective function along generations for problem (5.9), case 1: comparison between BIANCA and MATLAB results.

5.4.2 Case 2: variable number of plies, symmetric stack

In this second case we assume a symmetric stack for the hybrid plate. The goal of this second calculation consists in optimising the first $N = 5$ modal loss factors of the structure for problem (5.9). The design variables, their nature and bounds are detailed in Table 5.3.

Design variable	Type	Lower bound	Upper Bound	Discretisation Step
n	integer	4	8	–
ID_k	integer	0	1	–
t_k [mm]	discrete	0.1	1.0	0.01
δ_k [deg]	discrete	-75	90	15

Table 5.3: Design variables for the optimisation problem (5.9), cases 2 and 3.

In particular, we remark that the number of layers n can vary between 4 and 8. Since the number of plies is included among the design variables, the new genetic operators that perform the crossover and mutation among species are required and the optimal value of n is an outcome of the biological selection: the most adapted species automatically issues as a natural result of the Darwinian selection. The structure of the individual's genotype

is the one discussed in Sec. 5.2 and shown in Fig. 5.5. Moreover, due to the assumption of the symmetry of the stack, the number of design variables is reduced when compared to the most general case (discussed in the next subsection): in this case the total number of design variables can vary between 7 and 13.
As said previously, the number of DOFs of the FEM model of the plate varies along with the number of plies. Indeed, for this case it varies between 39975 and 71955.

Concerning the genetic parameters, the population size is $N_{ind} = 30$, while the maximum number of generations is increased, $N_{gen} = 100$, due to the higher number of variables in the present case. The crossover and mutation probability are still $p_{cross} = 0.85$ and $p_{mut} = 1/N_{ind}$, while the shift operator and chromosomes number mutation probability are $p_{shift} = 0.5$ and $(p_{mut})_{chrom} = (n_{max} - n_{min})/N_{ind}$, where n_{max} and n_{min} are the upper and lower bounds on the number of layers, i.e. the maximum and the minimum number of chromosomes for the generic individual. Once again, we applied the roulette-wheel operator for selection, a single-individual elitism and the ADP method for handling constraints.

The best solution found by BIANCA is shown in Table 5.4. The optimal number of plies is 6. Fig. 5.7 shows the variation of the best solution and of the best species (the optimal number of plies) along the generations: the global constrained minimum has been found after 45 generations, whilst the optimal number of plies is found after only 13 generations, i.e. also in this case the best species converge faster than the best individual.

In addition, we can see that the optimal configuration of the hybrid plate, under the assumption of having a symmetric stack, shows 2 viscoelastic plies in the middle of the structure. Indeed, this is a sandwich-plate-like configuration, whose typical damping mechanism is shown in Fig. 5.8: for this configuration the damping phenomenon is associated to the shear strains through-the-thickness ε_{xz} and ε_{yz}.
As conclusive remark, it can be noticed that such a solution is equivalent to a 5 layers solution with the following stack and thickness: [0/90/V/90/0] and [0.36/0.36/0.68/0.36/0.36], respectively.

	Reference	Best solution
n	6	6
ID_k		$[0/0/1]_S$
δ_k	$[90/45/0]_S$	$[0/90/\mathrm{V}]_S$
t_k [mm]	$[0.3/0.3/0.3]_S$	$[0.36/0.36/0.34]_S$
η_1		0.01071
η_2		0.00553
η_3		0.01170
η_4		0.01042
η_5		0.01280
f_1 [Hz]		112.81
f_2 [Hz]		240.79
f_3 [Hz]		329.07
f_4 [Hz]		478.78
f_5 [Hz]		525.68
R_x [N]	-17352	-16832 (-3.0%)
R_y [N]	-44480	-43090 (-3.1%)
R_z [N]	-23.06	-23.36 ($+1.3\%$)
M [Kg]	0.0675	0.0705 ($+4.4\%$)
Φ		-0.05117
g_1		-0.02002
g_2		-0.01874
g_3		-0.06302
g_4		-0.00618

Table 5.4: Best solution found using BIANCA for the optimisation problem (5.9), case 2 (V denotes the position of the viscoelastic ply).

5.4.3 Case 3: variable number of plies, non-symmetric stack

This is the most general studied case: no simplifying hypotheses are made on the stack of the laminate. Also in this case, the goal consists in optimising the first $N = 5$ modal loss factors of the structure for problem (5.9).

The design variables, their nature and bounds are detailed in Table 4.1. Even in this case, the total number of design variables varies along with the number of plies: it can vary between 13 and 25. As the previous case, the number of DOFs varies between 39975 and 71955.

Due to the greater complexity of the optimisation process in the present case, the

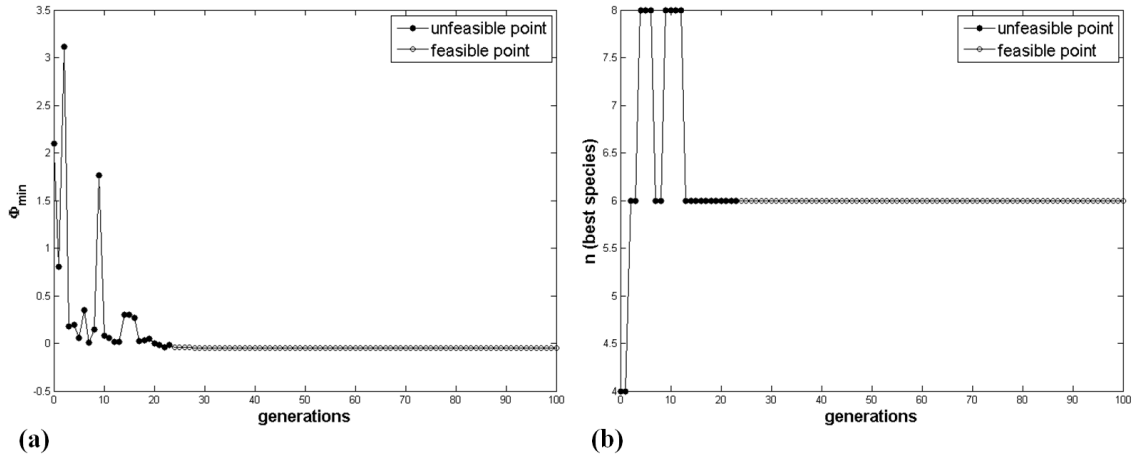

Figure 5.7: (a) Best values of the objective function and (b) number of layers along generations for problem (5.9), case 2.

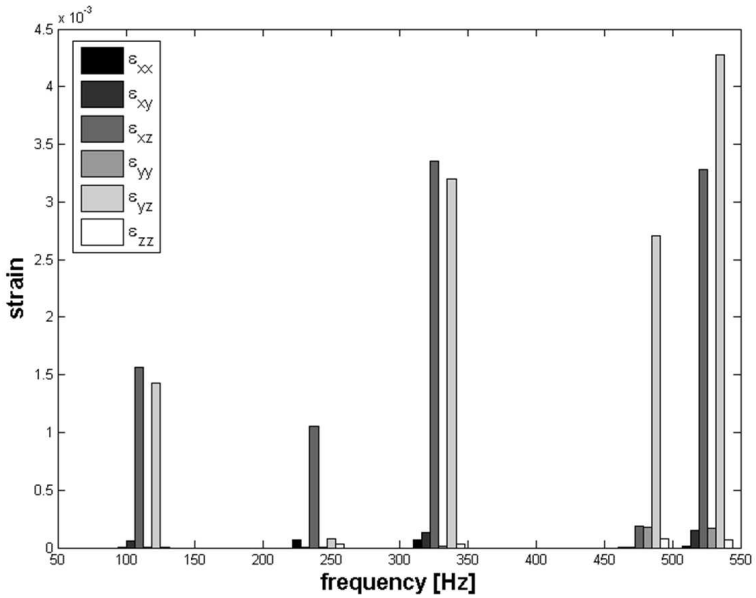

Figure 5.8: Maximum strain components in the viscoelastic plies for the optimised plate, case 2.

population size is increased up to $N_{ind} = 60$. For the rest, the genetic parameters are strictly those already used in the previous case.

The best solution found by BIANCA is shown in Table 5.5. The optimal number of plies is 6. Fig. 5.9 shows the variation of the best solution and of the best species along the generations: the global constrained minimum has been found after 62 generations,

whilst the optimal number of plies is found after only 7 generations, i.e. once again the best species converge more quickly than the best individual.

Moreover, for this case, the optimal configuration of the hybrid plate shows 2 viscoelastic plies at the top of the structure. Indeed, this is a non-conventional configuration, whose damping mechanism is shown in Fig. 5.10: for this configuration the damping phenomenon, depending on the considered eigenfrequency, involves all the strain components. As conclusive remark, it can be noticed that such a solution is equivalent to a 5 layers solution with the following stack and thickness: [V/0/90/90/0] and [0.63/0.43/0.42/0.31/0.30], respectively.

	Reference	Best solution
n	6	6
ID_k		[1/1/0/0/0/0]
δ_k	$[90/45/0]_S$	[V/V/0/90/90/0]
t_k [mm]	$[0.3/0.3/0.3]_S$	[0.32/0.31/0.43/0.42/0.31/0.30]
η_1		0.01756
η_2		0.00483
η_3		0.01228
η_4		0.01066
η_5		0.01298
f_1 [Hz]		70.09
f_2 [Hz]		164.87
f_3 [Hz]		217.90
f_4 [Hz]		317.45
f_5 [Hz]		346.97
R_x [N]	-17352	-17065 (-1.6%)
R_y [N]	-44480	-43688 (-1.7%)
R_z [N]	-23.06	-28.31 ($+22.7\%$)
M [Kg]	0.0675	0.07 ($+3.7\%$)
Φ		-0.05831
g_1		-0.03349
g_2		-0.03218
g_3		-0.27763
g_4		-0.013

Table 5.5: Best solution found using BIANCA for the optimisation problem (5.9), case 3 (V denotes the position of the viscoelastic ply).

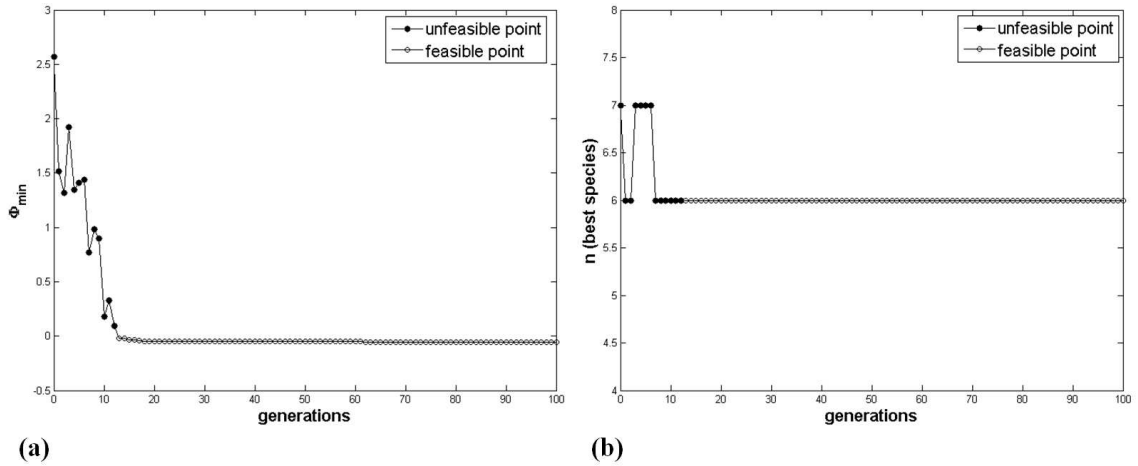

Figure 5.9: (a) Best values of the objective function and (b) number of layers along generations for problem (5.9), case 3.

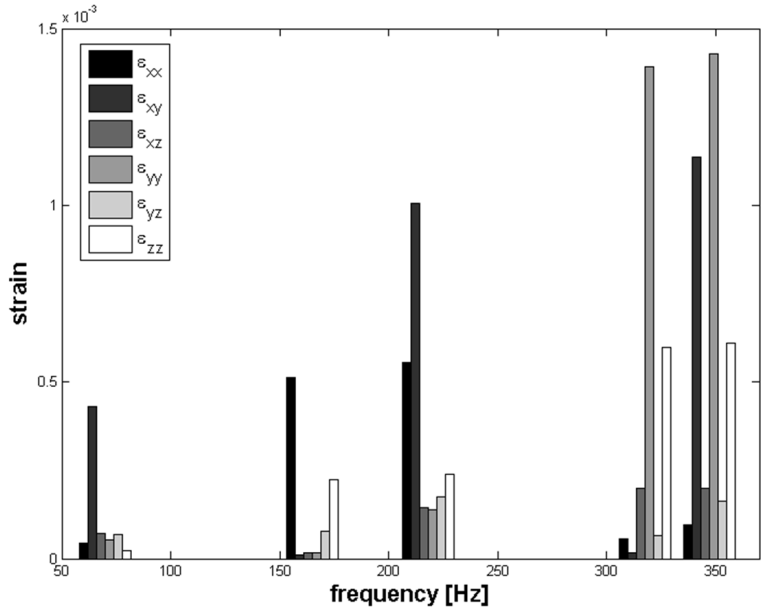

Figure 5.10: Maximum strain components in the viscoelastic plies for the optimised plate, case 3.

5.4.4 Discussion of results

Concerning the results of the first case, even though in both GAs the same size of population as well as the same probability of crossover and mutation and the same number of generations are used, the better result found by BIANCA is mainly due on one side to the

organisation and exploitation of the genetic information restrained in the population and on the other side to the ADP method for handling constraints which allows for exploring in a better way the whole domain, feasible and unfeasible regions, with respect to the classical penalty methods, like those implemented within the MATLAB GA.

For what concerns the cases 2 and 3, since the number of layers (and thus the number of optimisation variables of the whole process) is included among the design variables, standard GAs are not able to deal with this kind of problems, thus we need to use the new genetic operators for the evolution of the species implemented within BIANCA.

It can be noticed that, thanks to the genetic operators that perform the crossover and mutation among species, we do not need to perform the optimisation process discussed in Sec. 5.3 for each number of layers. Indeed, the optimal number of layers is an outcome of the genetic process, which automatically issues the *best species*.

In both cases 2 and 3 the optimal orientations of the elastic plies are equal to 0° or 90°. This result is due on one side to the choice of the static tests considered within the optimisation process and on the other side to the small range of variation of the number of layers considered in the procedure. Indeed, specifying several stiffness tests in different directions or increasing the range of the number of layers of the hybrid plate leads probably to other different orientations.

A final remark arises from the comparison of the results obtained in cases 2 and 3. Despite both plates are made of 6 layers (whereof 2 are viscoelastic plies) the better damping capabilities of the hybrid plate solution of case 3 are due to a different damping mechanism when compared to the solution of case 2. As it can be noticed from Fig. 5.8, the damping of the hybrid plate of case 2 is linked to the classical shear mechanism, i.e. since the elastomer layers are constrained by stiffer elastic plies the major mechanism for damping is due, for each eigenfrequency, to the shear strains through-the-thickness ε_{xz} and ε_{yz}. On the contrary, as shown in Fig. 5.10, for the optimised plate of case 3, depending on the considered mode, all the strain components are involved into the damping phenomenon and, in addition, the shear strains through-the-thickness ε_{xz} and ε_{yz} do not represent the major contribution for each eigenfrequency: this is due to the fact that for this configuration the viscoelastic layers are not constrained with stiffer plies. These considerations, along with the fact that in this last case we make no simplifying hypotheses on the stacking sequence of the hybrid plate, explain the better performance of the non-symmetric configuration.

5.5 Concluding remarks

In this work, an optimisation procedure for the design of damping properties of hybrid elastomer/composite laminates is presented. The goal of the procedure is to maximise the first N modal loss factors of the laminate subject to constraints on the in-plane and out-of-plane stiffness along with a constraint on the weight of the plate. The proposed

strategy relies on one hand, upon the dynamic response of the structure in terms of natural undamped frequencies and modal loss factors evaluated using the well-known Iterative Modal Strain Energy (IMSE) method, and on the other hand on the use of genetic algorithms as optimisation tool to perform the solution search.

The main key points of our strategy consist in determining which are: a) the best number of layers of the hybrid plate, and b) the best number and positions of the elastomer layers within the stacking sequence. The main difficulty, when dealing with this kind of problems, is how to take into account the variable number of layers among the optimisation variables. In order to deal with such a problem we used our improved GA BIANCA, which presents new genetic operators that perform the crossover and mutation operations among individuals of different species. Indeed, in this way the number of layers is directly related to the number of the individual's chromosomes and, hence, the optimal number of layers is an outcome of the genetic process, which automatically issues the *best species*. Due to the presence of integer and discrete variables (as the number of plies, the nature of the plies and the thickness and orientations of the elastic layers) the use of GAs appears to be particularly profitable. In particular, the use of BIANCA coupled directly with the FEM model, results to be very convenient when dealing with constrained optimisation problems of modular structures, as the one presented in this work.

The use of an evolutionary strategy along with the fact that the problem is stated in the most general case, lead us to find some non-conventional configurations, i.e. non-constrained layer configurations, which show better damping properties when compared to the classical constrained layer treatments.

Chapter 6

Optimal design of modular systems: application to hybrid elastomer/composite plates

6.1 Introduction

One of the most important challenges for automotive and aerospace industries is the reduction of noise pollution. In particular, the vibration of the structural parts composing systems represents one of the major sources of noise: when structural components moves, they produce elastic (or air) waves and hence noise. Moreover, due to their lightness and their high stiffness, composite materials are very sensitive to this phenomenon.

To this purpose, several passive solutions have been proposed in the literature: such solutions consist in bonding elastomer patches in some well-chosen regions of the structure. Even though these solutions are proved to be quiet effective [178], they are often the result of a design process made *a posteriori* which substantially modifies some fundamental properties of the structure: if on one side one can observe an increasing of the damping capabilities of the structure, contrary on the other side a degradation of its mechanical properties (in terms of reduction of the stiffness and increasing of the weight) occurs.

Recently, Le Maoût *et al.* [179] studied the problem of laminated plates damped by using rubber patches: more precisely the main goal of that work is the maximisation of the modal loss factors of the structure (in a given range of frequencies) employing a periodical pattern of viscoelastic material. They considered a three-layer plate with the following design variables: thickness and orientation angle for the elastic plies and thickness, diameter and distribution for the rubber patches (they assumed that the patches are identical and equally spaced). The modal loss factors are evaluated according to the well-known Iterative Modal Strain Energy (IMSE) method. Also in this work two different cases were considered: the case wherein the gaps between the patches are filled

by composite material and the case wherein such gaps are unfilled. The authors showed that a simultaneous design of both elastic and viscoelastic properties of the structure can lead to obtain better damping capabilities with respect to the case of employing continuous viscoelastic layers.
Even though the work of Le Maoût *et al.* is characterised by some original aspects, the optimisation problem is solved introducing several simplifying assumptions which affect the quality of the final solution. Namely, such assumptions strongly limit the search capabilities of their algorithm which converges towards a local or near-optimal solution instead of the global optimum.

The study presented in this last Chapter could be placed within the context of the works originally proposed by Le Maoût *et al.* and can be seen as a generalisation and also as an extension of those works. In particular we propose a global optimisation technique for the design of damping properties of hybrid elastomer/composite structures, i.e. composites laminated plates equipped with bonded elastomer patches. The goal of the procedure is to maximise the first N_f modal loss factors of the structure subject to constraints on the flexural stiffness and on the weight of the plate, constraints on the material design variables describing the behaviour of the composite plate and, finally, geometric constraints on the position of the patches over the composite plate.

The design problem considered in this Chapter belongs to the class of design problems of modular system. The hybrid structure studied here has two different types of modules: the modules of the first type are the patches. All the patches are modules because they have the same function and geometry, but not necessarily the same dimensions (diameter and thickness) and the same position. In addition also the number of patches is included among the design variables of the optimisation problem. The modules of the second type are the layers: all the layers, composing the composite plate, are identical, but normally they are differently oriented.

The design procedure that we propose is inspired by the radical point of view that has already inspired the works discussed in the previous Chapters: to design a modular hybrid structure by a mathematically rigorous numerical optimisation procedure that will not use any simplifying assumption. Only avoiding the use of *a priori* assumptions one can hope to obtain the true global optimum for a given problem: this is a key-point in our approach.

As in Chapter 4 we adopt a two-level procedure for the global optimum design of the hybrid structure. At the first level of the procedure, the optimal design of the hybrid structure in terms of its damping capabilities is carried out, the design variables in this phase being the constitutive parameters characterising each patch-module (number, position, thickness and diameter) along with the parameters describing the composite plate that is designed as it was composed by a single equivalent layer (namely the laminate polar parameters and the total thickness of the plate). At the second level of the procedure we look for at least one stacking sequence realising the global optimum structure found

at the first level. The proposed approach relies on one hand, upon the dynamic response of the structure in terms of natural undamped frequencies and modal loss factors which are evaluated using the IMSE method, and on the other hand on the use of the polar formalism and of the GA BIANCA as optimisation tool to perform the solution search.

The Chapter is organised as follows: the mechanical problem considered in the study as well as the optimisation strategy are introduced in Sec. 6.2. The mathematical formulation of the first-level problem is detailed in Sec. 6.3 and the problem of determining a suitable laminate is formulated in Sec. 6.4. A concise description of the FE model of the hybrid structure is given in Sec. 6.5, while in Sec. 6.6 we show the numerical results of the whole optimisation procedure. Finally, Sec. 6.7 ends the Chapter with some concluding remarks and perspectives.

6.2 Design of composite plates with bonded elastomer patches

6.2.1 Description of the problem

The optimisation procedure presented in this work is applied to the hybrid structure depicted in Fig. 6.1.

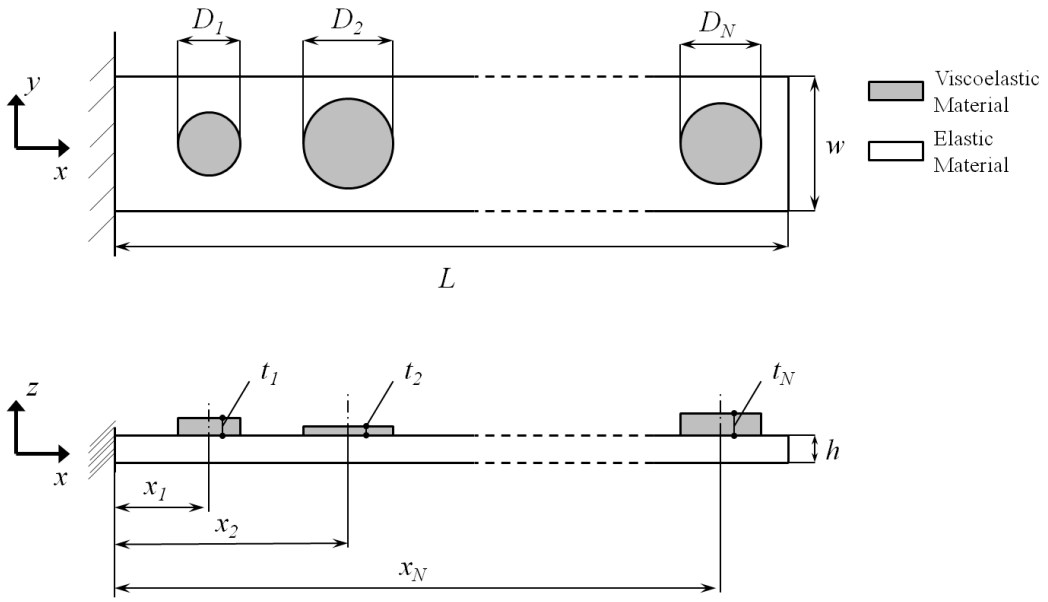

Figure 6.1: Geometry and design variables of the hybrid structure.

Such a hybrid structure is composed of a laminated plate with surface-bonded viscoelastic patches. The length of the plate sides are $L = 200$ mm and $w = 20$ mm, respectively. The plate is made of glass-epoxy laminae, whose material properties are listed in Table 6.1. For evident mechanical reasons, we assume that the laminated plate is *quasi-homogeneous* and *fully-orthotropic*, with the main orthotropy axis aligned with the x axis of the structure.

Technical moduli		**Polar parameters**	
Young's modulus E_1 [MPa]	29900	T_0 [MPa]	5412
Young's modulus E_2 [MPa]	7500	T_1 [MPa]	5200
Shear modulus G_{12} [MPa]	2250	R_0 [MPa]	3162
Poisson's ratio ν_{12}	0.24	R_1 [MPa]	2841
Density ρ [kg m^{-3}]	1500	Φ_0 [deg]	0
Thickness t_{ply} [mm]	0.125	Φ_1 [deg]	0

Table 6.1: Material properties for the glass-epoxy lamina

As previously said, no simplifying assumptions are made: indeed each patch can be different from any other, in terms of the constitutive geometrical parameters. The material used for the viscoelastic patches is a rubber-like material having linear isotropic behaviour. In addition, the material properties depend upon the loading frequency f and they are taken from [162]. The variation of the complex Young's modulus with the frequency, $E(f)$, is expressed as:

$$
\begin{aligned}
& E(f) = E^R(f) + \mathrm{i}E^I(f) \ , \\
& \text{with :} \\
& E^R(f) = {E_s}^R + {E_d}^R \log\left(\frac{f}{\breve{f}}\right) \ , \\
& E^I(f) = {E_s}^I + {E_d}^I \log\left(\frac{f}{\breve{f}}\right) \ .
\end{aligned}
\tag{6.1}
$$

The superscripts R and I stand for real and imaginary part, respectively. The subscripts s and d represent the steady-state value and the amplitude of the part that depends upon the frequency for both the real and imaginary part of the Young's modulus, while $\breve{f} = 1$ Hz is a reference value for the frequency.
In Eq. (6.1) ${E_s}^R = 4.1$ MPa and ${E_d}^R = 32.2$ MPa are the steady-state value and the amplitude of the real part, while ${E_s}^I = -7.7$ MPa and ${E_d}^I = 43.3$ MPa are the corresponding quantities for the imaginary part. The Poisson's ratio and the density are

equal to $\nu = 0.3$ and $\rho = 968.1$ kg m^{-3}, respectively, whilst the material loss factor $\eta_v(f)$ can be determined as:

$$\eta_v(f) = \frac{E^I(f)}{E^R(f)} \ . \tag{6.2}$$

6.2.2 The two-level optimisation strategy

The main aim of the optimisation strategy consists in maximising the damping capabilities of the structure (in terms of the first N_f modal loss factors) without degrading too much its stiffness and without increasing too much its weight. Concerning the organisation of the whole optimisation procedure, as already done in Chapter 4, we adopt a two-level approach. The problem of designing the damping properties of the hybrid structure is formulated into two distinct problems:

- first-level problem: the aim of this phase is the design of the structure in order to maximise the first N_f modal loss factors, satisfying, simultaneously, the constraint on the bending stiffness and on the final weight. At this stage the laminated plate is considered as an equivalent single layer, whose mechanical properties are described by means of the classical stiffness tensor **A**, **B** and **D**. We use the polar formalism to represent such tensors and we assume that the laminate is *quasi-homogeneous* and *fully-orthotropic* with the main orthotropy axis aligned with the x axis of the structure. The output of this step is, hence, the geometry of the structure, i.e. the number N of elastomer patches along with their positions over the plate and their geometrical characteristics (diameters and thickness). Further outcomes of this phase are the geometrical and the polar parameters of the laminate, i.e. its total thickness (and hence the number n of plies composing the laminate) and its anisotropic polar moduli. Thus, this is the step where the true optimal design of the structure is done, in terms of its overall properties;
- second-level problem: the goal of this phase is to find at least one stacking sequence, for the multilayer plate, giving the optimal overall elastic properties issued from the first step. At this stage, the design variables are the layers orientations.

Concerning the mathematical formulation, this will be detailed, for both the first and second step, in the next Sections.

6.3 Mathematical formulation of the first-level problem

The overall characteristics of the optimal structure have to be designed during this phase. For the problem at hand, this means that in this phase we have to determine the optimal

values of the following parameters:

- the number of viscoelastic circular patches;
- the geometrical properties of each patch;
- the thickness, and hence the number of layers, of the laminated plate;
- the mechanical properties of the laminate, namely the anisotropic polar moduli of the plate.

As in the case of the problem of the least-weight wing-box section presented in Chapter 4, we need also to determine the optimal number of modules and their mechanical characteristics, besides their dimensions. We recall, in fact, that in the most general situation, the patches share the same form but can have different sizes and positions.

It is worth noting that for the sake of simplicity, we only consider circular patches. Indeed, the aim of this study is to demonstrate the relevance of using patches to damp composite plates and not to discuss their possible geometry. More precisely, circular patches are representative of all regular polygons without the complexity of their orientation, so this choice minimises the number of geometrical characteristics of the patches.

We can immediately see that during this stage of the optimisation procedure, the design of the thickness of the plate h must be done using discrete variables, with a step equal to the thickness of the material layer used for the fabrication of the structure, see Table 6.1. Of course, this responds to a technological need and, moreover, this will give us also another important result: the number of layers to be used during the second-level design phase.

We recall that the goal of the procedure is the maximisation of the first N_f modal loss factors of the structure and this must be done satisfying on one side the mechanical constraints on the bending stiffness and on the weight of the structure, and on the other side the geometric bounds for the elastic moduli along with the geometric constraints on the position of the centre of each patch. Such aspects are described in detail in the following subsections.

6.3.1 Geometrical design variables

Before specifying the mathematical formulation of the first-level problem, we introduce the design variables. These are of two types: *geometrical* and *mechanical*. Concerning the geometrical design variables, they are shown in Fig. 6.1 and are:

- the number of patches N;
- the position of the centre of each patch x_i, $i = 1...N$;
- the diameter D_i and the thickness t_i of the generic patch, $i = 1...N$;

- the thickness of the laminated plate h;

The design variables, their nature and bounds for the first-level problem are detailed in Table 6.2.

Design variable	**Type**	**Lower bound**	**Upper Bound**	**Step**
N	discrete	1	10	1
x_i [mm]	discrete	0.1	200.0	0.1
D_i [mm]	discrete	5.0	20.0	0.1
t_i [mm]	discrete	0.5	3.0	0.05
h [mm]	discrete	1.0	4.0	0.125
$R_{0K}^{A^*}$ [MPa]	continuous	-3162.0	3162.0	–
$R_1^{A^*}$ [MPa]	continuous	0.0	2841.0	–

Table 6.2: Design space for the first-level problem.

It is worth noting that the viscoelastic patches cannot have an arbitrary distribution over the plate, but they must satisfy certain geometrical conditions in order to avoid overlapping between two consecutive patches. Moreover, we have to impose that the patches do not come outside the geometrical contour of the plate (along the direction of the x axis). Such constraints can be written as follows:

$$\begin{cases} \dfrac{D_1}{2} - x_1 \leq 0 & , \\ x_{i-1} + \dfrac{D_{i-1} + D_i}{2} - x_i \leq 0 \ , \ (i = 2, ..., N) & , \\ x_N + \dfrac{D_N}{2} - L \leq 0 & . \end{cases} \tag{6.3}$$

6.3.2 Mechanical design variables

Concerning the mechanical variables, we adopt the *polar formalism*, already introduced in Sec. 3.3 of Chapter 3, to represent the homogenised stiffness tensors $\mathbf{A}^*$, $\mathbf{B}^*$, $\mathbf{D}^*$ which describe the mechanical behaviour of the laminate in the framework of the CLPT.

The mechanical design variables are the same as the problem of the minimum-weight wing-box section: also for the problem considered in this Chapter we assume that the laminate is *quasi-homogeneous* (hence, in this way, only the extension tensor $\mathbf{A}^*$ has to be designed, the bending one $\mathbf{D}^*$ being automatically obtained) and orthotropic with the

main orthotropy axis aligned with the x axis of the plate. Thus, the conditions (4.2) and (4.21) can be applied also in this case.

Under such assumptions, as already explained in Sec. 4.4, we need only two polar quantities to completely describe the behaviour of the laminated plate, i.e. the anisotropic parameters $R_{0K}^{A^*}$ and $R_1^{A^*}$. Moreover, as discussed in Sec. 4.4 (and also in Sec. 3.3), we have to consider the geometric and feasibility constraints of Eq. (4.4) on the polar parameters which arise from the combination of the layer orientations and positions within the stack. We recall here the expression of such constraints (the quantities without the superscript A^* refer to the elementary layer):

$$\begin{cases} -R_0 \leq R_{0K}^{A^*} \leq R_0 \ , \\ 0 \leq R_1^{A^*} \leq R_1 \ , \\ 2\left(\dfrac{R_1^{A^*}}{R_1}\right)^2 - 1 - \dfrac{R_{0K}^{A^*}}{R_0} \leq 0 \ . \end{cases} \tag{6.4}$$

It is worth noting that the first two bounds of Eq. (6.4) can be easily taken into account as box-constraints, i.e. by properly setting the range of variation of the polar quantities $R_{0K}^{A^*}$ and $R_1^{A^*}$, see also Table 6.2.
All the considerations concerning the mechanical design variables made in Sec 4.4 can be repeated *verbatim* for the present case.

6.3.3 Mathematical statement of the problem

As said previously, the goal of the global structural optimisation is the maximisation of the damping capabilities of the structure without degrading too much its stiffness nor increasing too much its final weight.

The damping capabilities are estimated in terms of modal loss factors of the structure η_k, $(k = 1, ..., N_f)$ as already done for the problem of hybrid laminates presented in Chapter 5. The modal loss factors are evaluated according to Eq. (5.7) and, since the material properties of the patches depend upon the frequency, the calculation of the loss factors needs an iterative procedure: to this purpose we use the well-known IMSE approach already discussed in Sec. 5.2.

The optimisation problem can now be formulated. The maximisation of the first N_f modal factors can be expressed as the minimisation of the following objective function:

$$\Phi = -\sum_{k=1}^{N_f} \eta_k \ , \tag{6.5}$$

that represents the opposite of the sum of the first N_f modal loss factors.

Along with the increase of the damping capabilities, the structure must withstand to the application of static loads, i.e. the structure has to exhibit good properties in terms

of stiffness. Indeed, the design of the hybrid structure represents a compromise between its damping capability and the ability of keeping good mechanical properties in terms of stiffness, without increasing too much the weight. Thus, constraints on the maximum decrease of the bending stiffness and on the maximum increase of the mass of the plate have to be considered. Such constraints can be stated as follows:

$$\begin{cases} \dfrac{{M_y}^{ref} - M_y}{{M_y}^{ref}} - \epsilon_{M_y} \leq 0 \ , \\ \dfrac{M - M^{ref}}{M^{ref}} - \epsilon_M \leq 0 \ . \end{cases} \tag{6.6}$$

In Eq. (6.6) M_y is the bending moment around the y axis measured at the root section of the plate when a unitary displacement $\delta = 1$ mm is imposed at the tip. Thus, the bending moment is evaluated as shown in Fig. 6.2 and it represents a measure of the bending stiffness of the structure. In Eq. (6.6) M is the mass of the whole structure. The superscript ref stands for *reference* value. The reference values of the reaction moment and mass are calculated, before the optimisation process, on a reference undamped structure, i.e. a laminated plate without elastomer patches. The quantities ϵ_{M_y} and ϵ_M are the user-defined tolerances on each constraint. The meaning of the constraints on the reaction moment and on the mass of the hybrid structure are the following: the maximum loss in stiffness and the maximum increase in mass of the optimised structure are superiorly bounded by the value of the corresponding tolerances.

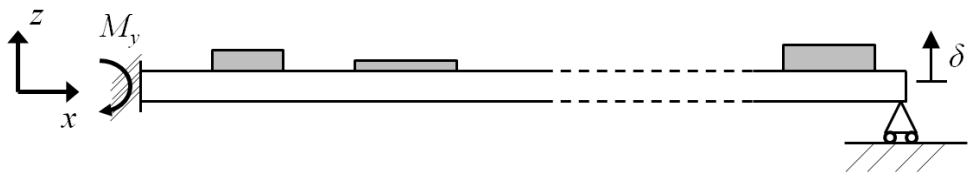

Figure 6.2: Static test for the evaluation of the bending moment: imposed unitary displacement along z direction.

To state the optimisation problem in a standard form, firstly we reorder the design variables according to the following scheme:

- the vector $\boldsymbol{\xi}$ collects the following design variables, concerning the plate and the number of patches:

$$\boldsymbol{\xi} = \left\{ \begin{array}{c} \xi_1 = N \\ \xi_2 = h \\ \xi_3 = R_{0K}^{A^*} \\ \xi_4 = R_1^{A^*} \end{array} \right\} \ , \tag{6.7}$$

- each one of the vectors $\boldsymbol{\zeta}^i$ collects the design variables of the i^{th} viscoelastic patch, $i = 1, ..., N$:

$$\boldsymbol{\zeta}^i = \left\{ \begin{array}{c} \zeta_1 = x_i \\ \zeta_2 = D_i \\ \zeta_3 = t_i \end{array} \right\} . \tag{6.8}$$

Then, we introduce the following functions:

- the objective function Φ, expressing the damping capabilities of the structure:

$$\Phi = \Phi\left(\boldsymbol{\xi}, \boldsymbol{\zeta}^i\right) , \tag{6.9}$$

- the functions expressing the two constraints (6.6) on the bending stiffness and on the weight:

$$\Psi_1\left(\boldsymbol{\xi}, \boldsymbol{\zeta}^i\right) = \frac{{M_y}^{ref} - M_y\left(\boldsymbol{\xi}, \boldsymbol{\zeta}^i\right)}{{M_y}^{ref}} - \epsilon_{M_y} , \tag{6.10}$$

$$\Psi_2\left(\boldsymbol{\xi}, \boldsymbol{\zeta}^i\right) = \frac{M\left(\boldsymbol{\xi}, \boldsymbol{\zeta}^i\right) - M^{ref}}{M^{ref}} - \epsilon_M , \tag{6.11}$$

- the functions expressing the five geometric constraints (6.4) on the polar parameters of the plate:

$$g_1\left(\xi_3\right) = -\xi_3 - R_0 , \tag{6.12}$$

$$g_2\left(\xi_3\right) = \xi_3 - R_0 , \tag{6.13}$$

$$g_3\left(\xi_4\right) = -\xi_4 , \tag{6.14}$$

$$g_4\left(\xi_4\right) = \xi_4 - R_1 , \tag{6.15}$$

$$g_5\left(\xi_3, \xi_4\right) = 2\left(\frac{\xi_4}{R_1}\right)^2 - 1 - \frac{\xi_3}{R_0} , \tag{6.16}$$

- the functions expressing the $N + 1$ geometric constraints (6.3) on the positions of the patches bonded over the plate:

$$h_1\left(\zeta_1^1, \zeta_2^1\right) = \frac{\zeta_2^1}{2} - \zeta_1^1 , \tag{6.17}$$

$$h_i\left(\zeta_1^{i-1}, \zeta_2^{i-1}, \zeta_1^i, \zeta_2^i\right) = \zeta_1^{i-1} + \frac{\zeta_2^{i-1} + \zeta_2^i}{2} - \zeta_1^i , \ (i = 2, ..., N) , \tag{6.18}$$

$$h_{N+1}\left(\zeta_1^N, \zeta_2^N\right) = \zeta_1^N + \frac{\zeta_2^N}{2} - L . \tag{6.19}$$

Finally, the problem can be stated in the standard form:

$$\begin{cases} \min \ \Phi\left(\boldsymbol{\xi}, \boldsymbol{\zeta}^1, ..., \boldsymbol{\zeta}^N\right) \ , \\ \text{s.t.} \\ \Psi_k\left(\boldsymbol{\xi}, \boldsymbol{\zeta}^1, ..., \boldsymbol{\zeta}^N\right) \leq 0 \ , & k = 1, 2 \ , \\ g_j(\boldsymbol{\xi}) \leq 0 \ , & j = 1, ..., 5 \ , \\ h_i(\boldsymbol{\zeta}^1, ..., \boldsymbol{\zeta}^N) \leq 0 \ , & i = 1, ..., N+1 \ . \end{cases} \tag{6.20}$$

Problem (6.20) is non-linear, in terms of both geometrical and mechanical variables. Its non-linearity is given not only by the objective function but also by the geometrical constraints on the laminate polar parameters as that in Eq. (6.16) and by the mechanical constraints on the bending moment and on the weight of the structure, see Eq. (6.10) and (6.11).

Finally, the dimension of the design space, i.e. the number of design variables, and the number of constraint equations depend on the number N of patches. In particular, the total number of design variables is $3N + 4$ (there are in fact 3 variables for each patch, 3 variables for the laminated plate and the number of patches, N), while the total number of constraint equations is $N+8$: the constraint on the bending moment, the constraint on the weight, 5 constraints for the laminate polar parameters and finally $N+1$ constraints for the position of the patches over the plate, see the second, third and fourth of Eq. (6.20), respectively. Moreover, unlike the case of the least-weight wing-box section problem (4.19), though the number of constraints is variable, each constraint due to the addition of a module depends also on the unknowns concerning the others modules, not only on the ones of that module, see again the fourth of Eq. (6.20) and also Eq. (6.18).

Concerning the GA BIANCA, in the case of the first-level problem we need the use of the new genetic operators of crossover and mutation between individuals belonging to different species. In fact, since the number of viscoelastic patches N is included among the design variables, the related optimisation problem is defined over a space having variable dimension (the dimension of such a space is $3N + 4$). Mathematically speaking, such a problem corresponds on one side to determine the optimal dimension of the domain (i.e. the number of patches N) and on the other side to determine the optimal values of the constitutive parameters of the patches which satisfy the requirements imposed by the optimisation problem. In addition, we use the code BIANCA interfaced with the FE code ANSYS, because for each individual at each generation, the evaluation of the objective function as well as that of the constraint function on the bending moment needs a numerical evaluation.

Fig. 6.3 shows the genotype of the generic r^{th} individual for the optimisation problem of Eq. (6.20). This individual has $N_r + 1$ chromosomes. The first chromosome is composed by 3 genes representing the design variables for the plate, i.e. thickness and polar parameters. Chromosomes from 2 to $N_r + 1$ contain 3 genes which are the design

variables for each patch: position, diameter and thickness. An exception is chromosome 2 that has 4 genes: the fourth additional gene codes the number of modules, i.e. for our problem the number of patches.

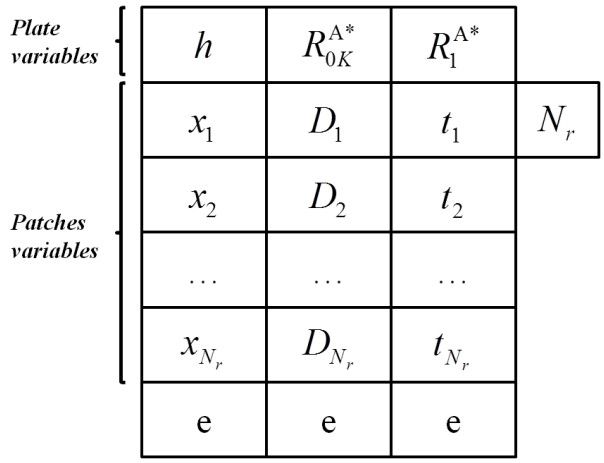

Figure 6.3: Structure of the individual genotype for the first-level optimisation problem.

6.4 Mathematical formulation of the second-level problem

The mathematical formulation of the second-level problem is exactly the same as the one discussed in Sec. 4.5, hence the reader is addressed to that Section for all the related mathematical details.

Here we recall that the main focus of the second-level phase concerns the design of the laminated plate in terms of its stacking sequence. In this phase the design of a laminate conceived to have some given properties is reduced to an unconstrained minimisation problem. Of course, this second problem depends upon the results of the first one, because the laminate to be designed must have the optimal elastic properties and thickness issued from the first-level design problem. We remind also that the design variables of this second-level problem are the layer orientations.

Concerning the code BIANCA the structure of the genotype of the individual-laminate is exactly the same discussed in Sec. 4.5 and shown in Fig. 4.4.

6.5 Finite element model of the hybrid structure

The finite element analysis is conducted in order to evaluate the objective and constraint functions for each individual, i.e. for each point in the design space at the current gener-

ation. The FE model is built in ANSYS environment, see Fig. 6.4. The need to analyse, within the same generation, different geometrical configurations (plates with different number of patches), each one corresponding to an individual, requires the creation of an ad-hoc input file for the FE code, that has to be interfaced with BIANCA. Since the number of modules is included among the decision variables, the FE model must be conceived in order to take into account for variable geometry and mesh. Indeed, for each individual at the current generation, depending on the number of chromosomes and, hence, on the number of patches the FE code has to be able to vary in a correct way the number of elements wherein the structure is discretised, thus a correct parametrisation of the model has to be done.

The structure is modelled with a combination of shell and solid elements. In particular, the laminate is modelled using ANSYS SHELL99 elements with 8 nodes and 6 degrees of freedom (DOFs) per node and its mechanical behaviour is described specifying the Cartesian components of tensors $\mathbf{A}^*$, $\mathbf{B}^*$ and $\mathbf{D}^*$ that are functions of the mechanical unknowns, i.e. the polar parameters. The viscoelastic patches are modelled using ANSYS SOLID186 elements with 20 nodes and 3 DOFs per node.

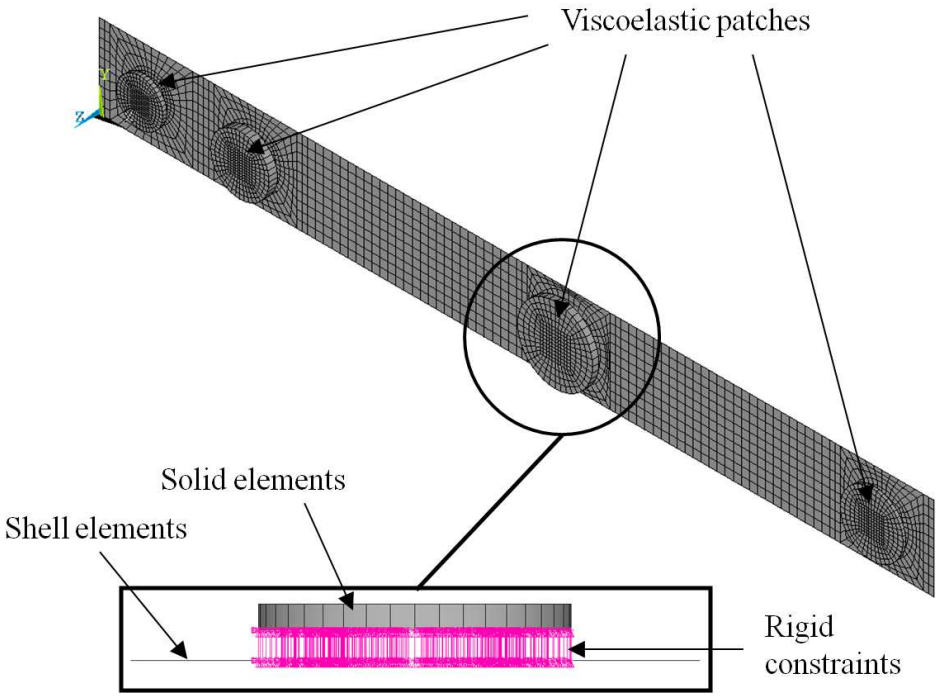

Figure 6.4: Mesh and rigid constraint equations for the FE model of the structure.

The choice of using solid elements to model the viscoelastic patches is strictly related to the main goal of our optimisation strategy: since we have to estimate the loss factors of the structure, for each natural frequency, we need to build a mathematical model able

to describe (with a good level of accuracy and reliability) the mechanical response of the physical system, i.e. the energy dissipation due to the different components of the strain tensor.

It is worth noting that, during the optimisation process, for each individual, we perform two FE calculations: a non-linear modal analysis, according to the logical flow of the IMSE method shown in Fig. 5.2, together with a linear static analysis in order to compute the reaction moment M_y, according to the scheme shown in Fig. 6.2. Concerning the boundary conditions (BCs) of the model, they can vary depending on the considered case-study as we will explain in the next Section. In any case, the extraction of the first $N_f = 5$ non-rigid modes for the FE model is carried-out.

We recall that the number of elements as well as the number of DOFs of the whole structure depends on the number of patches N. In particular, the size of the shell elements can vary over the plate surface: in the regions without the viscoelastic patches the dimensions of the shell elements are 2×2 mm^2, while a local refinement occurs in the regions where the patches are bonded. Moreover, the in-plane size of the solid elements used for the rubber patches exactly matches the one of the refinement realised for the shell elements of the laminate, see Fig. 6.4. In addition, we have previously checked that a single element in the thickness of each patch is sufficient to capture in correct way the damping mechanisms linked to the behaviour off the viscoelastic material. Finally, the number of degrees of freedom of the whole model can vary from 18006 to 56688.

Differently from what is usually done in the literature, we do not need to create fictitious elements to model the "air", which are used to fill the gaps between the elements that constitute the elastomer patches. With a correct parametrisation of the FE model, in terms of geometry and mesh, we can avoid all these difficulties and we are able to consider the exact circular geometry of the patches, without considering polygonal approximation and without introducing additional elements with fictitious properties that should alter the results of the analyses.

As conclusive remark, it can be noticed that the compatibility of the displacement field between the patches (modelled with solid elements) and the plate (modelled with shell elements) is realised by means of constraint equations on each corresponding node belonging to contiguous solid and shell elements, see Fig. 6.4. In particular, we specified rigid constraints between the nodes of the middle surface of the laminated plate and the corresponding ones of the bottom surface of the patches. Rigid constraints equations are specified according to the classical scheme implemented within the ANSYS code: the master nodes are those belonging to the middle plane of the composite plate, whilst the slave nodes are those located on the bottom surface of every patch. Through these constraint equations, the displacement of the nodes belonging to the top surface of the plate (in the region wherein the patch is bonded) is equal to that of the nodes belonging to the bottom surface of the patch.

6.6 Studied cases and results

For our optimisation problem we have considered three different examples. It is worth noting that such cases are different from a conceptual point of view. More precisely, in the first two examples the laminated plate has not to be designed and we must determine the optimal distribution of the rubber patches in order to maximise the damping capability of the system (as explained below the first two examples differ only for what concerns the BCs applied on the plate in order to study the effect of the BCs on the distribution of the patches). On the contrary, in the last one we perform the simultaneous design of both the elastic and the viscoelastic parts of the structure, namely the laminate and the patches, in order to show that we can obtain a more effective optimal configuration in terms of damping capabilities of the system. We recall that the design variables, their nature and bounds for the optimisation problem at hand are detailed in Table 6.2. Now, let us introduce the three examples.

- **Case 1**: as said previously, the goal of this example consists in maximising the first N_f modal loss factors of a given plate by simply bonding some rubber patches over the plate. Nevertheless, since the characteristics of the laminated plate (in terms of number of layers and stacking sequence and, hence, in terms of stiffness) are known *a priori*, we do not consider the constraint (6.10) on the bending stiffness as well as constraints from (6.12) to (6.16) on the laminate polar parameters. Of course, being the laminate stack given *a priori*, we do not need to solve the second-level problem of the optimisation procedure. Therefore, in this example the addition of the damping material is limited only by weight and geometrical requirements: in other words we consider only the constraint (6.11) on the weight of the plate as well as constraints from (6.17) to (6.19) on the positions of the patches for what concerns the mathematical formulation of the optimisation problem. Moreover, concerning the BCs of the FE model, in this first case the plate is clamped at the root section. We remind that the overall number of design variables depends on the number of patches N. Thus, for the present case we have $3N+1$ unknowns: since the laminated plate has not to be designed, the only design variables are the number of patches N along with their constitutive parameters, namely 3 design variables for each patch, i.e. the position x_i, the diameter D_i and the thickness t_i. In addition, for this first case, the total number of constraints is $N + 2$: 1 constraint on the weight of the structure and $N + 1$ constraints on the positions of the patches over the plate. In particular, according to the bounds on the number of patches listed in Table 6.2, the number of design variables varies between 4 and 31, while the minimum number of constraints is 3 and the maximum one is 12.

- **Case 2**: the assumptions and the considerations done for the first example are still valid for this second one. The only difference concerns the BCs applied to the

laminated plate: in the present case the plate is considered simply-supported at both root and tip sections. Therefore, our aim consists in studying the effect of the BCs of the model on the optimal distribution of the patches over the plate, and, hence, their influence on the damping capabilities of the system.

- **Case 3**: in this last example we consider the most general case where the optimum design of the system is realised simultaneously for what concerns both the elastic and viscoelastic properties of the structure: on one hand we look for the best distribution of the rubber patches and on the other hand we search for the optimal elastic properties of the laminate (in terms of its polar parameters $R_{0K}^{A^*}$ and $R_1^{A^*}$ and its thickness h) which maximise the damping capabilities of the structure satisfying, at the same time, the requirements on the weight and on the bending stiffness of the system. Therefore, for this example the first-level problem is formulated in the most general case, according to Eq. (6.20), considering all kinds of constraints. Of course, for this example we need to solve the second-level problem because the laminate stack has to be designed in order to attain the optimal elastic properties and thickness issued from the first phase of the procedure. In addition, concerning the BCs of the FE model, in this last case the plate is clamped at the root section. For the present case, the total number of design variables as well as the number of constraint equations depend on the number of patches N, as explained in Sec. 6.3: the number of unknowns can vary between 7 and 34, while the number of constraints varies between 9 and 18.

These test cases are chosen according to the problems often treated in the literature and also according to the will of testing new problems which are more general and complex than the ones often presented in the literature.

Concerning the optimisation problem of Eq. (6.20), for the first two examples the laminated plate has a quasi-homogeneous, fully-orthotropic unsymmetric stacking sequence made of 18 plies: $[-45/0/45/-45/0/45_3/0_2/-45_2/0/-45_2/45_2/0]$. The reference value for the mass of the system is evaluated considering the laminate without the rubber patches: the reference mass is $M^{ref} = 0.0135$ Kg.

Concerning the third example, in order to establish correct reference values for the reaction moment around the y axis and the mass of the hybrid plate, a static analysis is conducted on a reference structure before starting the optimisation process. The undamped reference plate, i.e. a plate without elastomer patches, considered here is made of 32 glass-epoxy laminae (see Table 6.1 for the material properties) with the following stacking sequence: $[0_2/90_2/0_2/45_2/-45_2/0_2/90_2/0_2]_S$. Finally, the reference values of the reaction moment and mass of the system for this last example are ${M_y}^{ref} = -163.0$ Nmm and $M^{ref} = 0.0240$ Kg, respectively.

As conclusive remark, it can be noticed that the user-defined tolerances on the constraints of the problem (6.20) are set as follows: $\epsilon_{M_y} = \epsilon_M = 0.05$, i.e. the relative

maximum loss in stiffness (only for the last example) and the relative maximum increase in mass (for all cases) between the optimised structure and the reference one are limited to 5%.

6.6.1 Case 1: clamped quasi-homogeneous orthotropic plate

As said previously, in this case the laminated plate is clamped at the root section. Since the number of patches is variable and they are not identical, a crossover between species is required and the optimal value of N is an outcome of the search process: the most adapted species automatically issues as a natural result of the Darwinian selection. The genotype of the individual for this case is the one shown in Fig. 6.3 without the first chromosome coding the variables of the laminated plate, i.e. the thickness and the polar parameters.

Concerning the genetic parameters, the population size is $N_{ind} = 40$ and the maximum number of generations is $N_{gen} = 100$. The crossover and mutation probability are $p_{cross} = 0.85$ and $p_{mut} = 1/N_{ind}$, while the shift operator and chromosomes number mutation probability are $p_{shift} = 0.5$ and $(p_{mut})_{chrom} = (N_{max} - N_{min})/N_{ind}$, where N_{max} and N_{min} are the upper and lower bounds on the number of patches, i.e. the maximum and the minimum number of chromosomes for the generic individual. Selection is performed by the roulette-wheel method, the elitism is active and the ADP method has been used for handling constraints.

The best solution found by BIANCA is shown in Table 6.3. The optimal number of viscoelastic patches for the damping maximisation is 3. The global constrained minimum has been found after 90 generations, see Fig. 6.5 a). Fig 6.5 b) shows the variation of the optimal number of viscoelastic patches along the generations: it can be seen that the best number of patches N varies between 2 and 3 and that the optimal value of N is reached after 80 generations.

In addition, comparing the plots in Fig. 6.5 a) and 6.5 b), one can notice that the convergence towards the best value of the number of modules (here, the number of patches) and that of the objective function are independent. They never occur at the same time, and the optimisation of the number of modules happens always before that of the objective function. Thus we can conclude that the strategy used in BIANCA for evolving simultaneously species and individuals normally let attain first the best species, and then continues to evolve individuals within the best species towards the best individual.

Fig. 6.6 shows the optimal distribution of the patches over the plate for the present case, at the first and at the last generation. We can see that the dimensions (diameter and thickness), the positions and the number of patches change during the generations.

	Best solution
N	3
x_i [mm]	$\{12.5,\ 37.5,\ 62.5\}$
D_i [mm]	$\{17.7,\ 10.1,\ 15.7\}$
t_i [mm]	$\{1.46,\ 0.66,\ 1.47\}$
η_1	0.01060
η_2	0.00846
η_3	0.00129
η_4	0.01061
η_5	0.01440
f_1 [Hz]	29.43
f_2 [Hz]	181.85
f_3 [Hz]	256.09
f_4 [Hz]	503.74
f_5 [Hz]	558.53
M [Kg]	0.014174 (+4.99%)
Φ	-0.04538

Table 6.3: Best solution found using BIANCA for the optimisation problem (6.20), case 1.

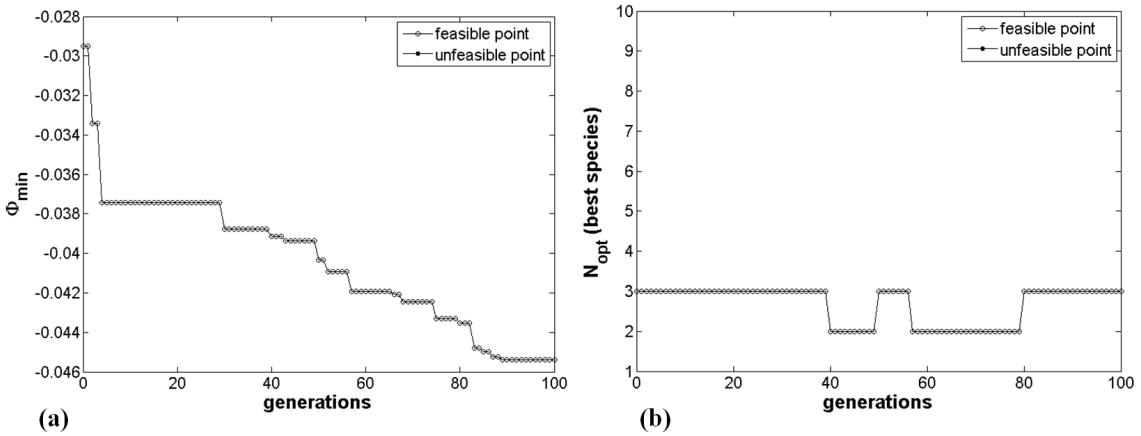

Figure 6.5: (a) Best values of the objective function and (b) optimal number of patches along generations for problem (6.20), case 1.

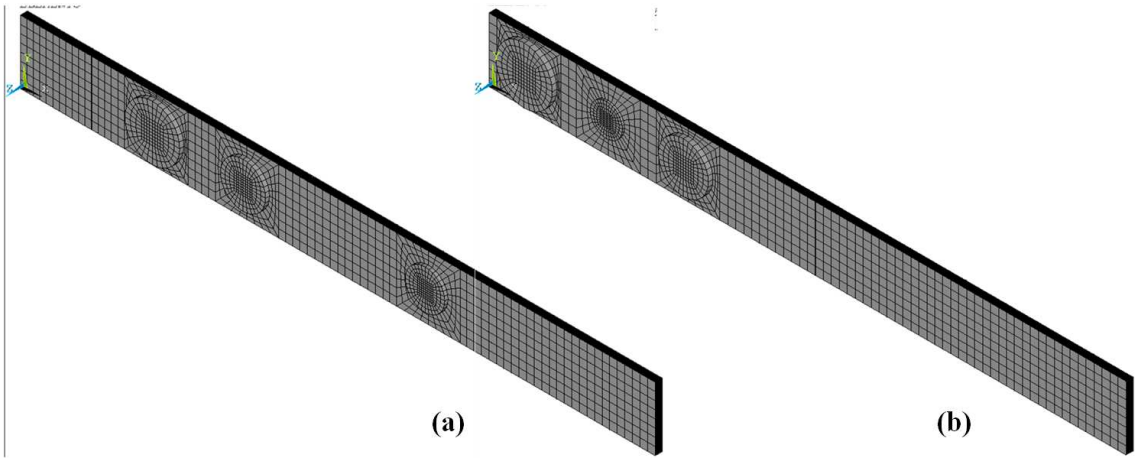

Figure 6.6: Optimal distribution of viscoelastic patches at the (a) initial and (b) final generation for problem (6.20), case 1.

6.6.2 Case 2: simply supported quasi-homogeneous orthotropic plate

In this second case the laminate is simply-supported at its ends. The aim of such an example is to study how the distribution of the viscoelastic material changes when we consider different BCs for the model. The genotype of the individual and the genetic parameters are exactly the same as the previous case.

The best solution found by BIANCA is shown in Table 6.4. For this case, the optimal number of viscoelastic patches for the damping maximisation is 2. Fig. 6.7 a) and b) show the variation of the best solution and that of the best species along the generations, respectively. We can see that the global constrained minimum was found after 73 generations, while the number of viscoelastic patches N converges to its optimal value after 13 generations. Again, the convergence towards the best value of N and that of the objective function are independent, and the convergence towards the best species is faster than the convergence towards the best individual.

Fig. 6.8 shows the optimal distribution of the patches over the plate for the present case, at the first and at the last generation. Again, according also with Fig. 6.7 b), it can be noticed that the geometry (in terms of diameter and thickness), the positions and the number of patches change during the generations.

	Best solution
N	2
x_i [mm]	$\{25.0,\ 175.0\}$
D_i [mm]	$\{17.8,\ 16.8\}$
t_i [mm]	$\{1.50,\ 1.45\}$
η_1	0.00196
η_2	0.00854
η_3	0.01563
η_4	0.01620
η_5	0.01808
f_1 [Hz]	80.78
f_2 [Hz]	319.34
f_3 [Hz]	712.52
f_4 [Hz]	1078.07
f_5 [Hz]	1268.08
M [Kg]	0.014172 (+4.98%)
Φ	−0.06041

Table 6.4: Best solution found using BIANCA for the optimisation problem (6.20), case 2.

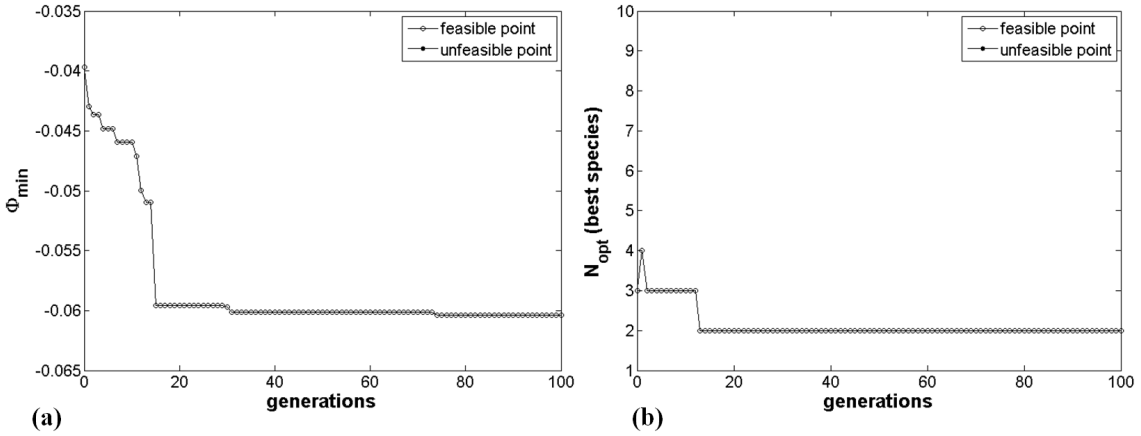

Figure 6.7: (a) Best values of the objective function and (b) optimal number of patches along generations for problem (6.20), case 2.

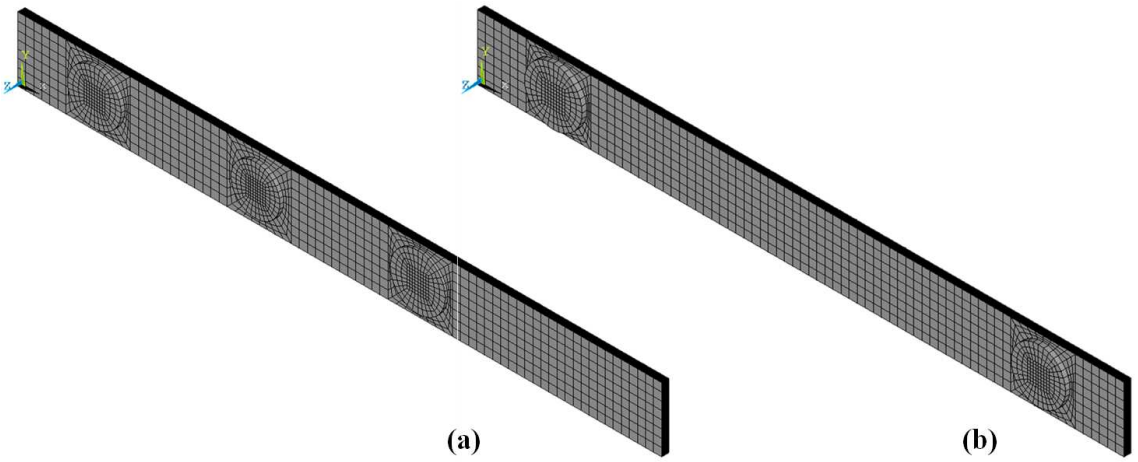

Figure 6.8: Optimal distribution of viscoelastic patches at the (a) initial and (b) final generation for problem (6.20), case 2.

6.6.3 Case 3: general case

This is the most general case where the design of both the elastic and viscoelastic parts of the structure is realised simultaneously in order to maximise its damping capabilities. We recall that in this last example also the constitutive parameters of the laminate, i.e. its total thickness and the anisotropic polar parameters, are included among the design variables. The genotype of the individual is the one discussed in Sec. 6.3 and shown in Fig. 6.3.

Due to the greater complexity of the optimisation process in the present case, the population size and the maximum number of generations are increased up to $N_{ind} = 60$ and $N_{gen} = 150$, respectively. For the rest, the genetic parameters are strictly those already used in the previous examples.

The best solution found by BIANCA is shown in Table 6.5. The optimal number of viscoelastic patches for the damping maximisation for this last case is 7. The global constrained minimum has been found after 111 generations, see Fig. 6.9 a). Fig 6.9 b) shows the variation of the optimal number of viscoelastic patches along the generations: at the first generation the best species shows 3 patches bonded over the plate. Then, one can see that the best number of patches N varies between 5 and 7 and that the optimal value of N is reached after 42 generations. Thus, as in the previous examples, the convergence towards the best value of N and that of the objective function are independent, and the convergence towards the best species is faster than the convergence towards the best individual.

Fig. 6.10 shows the optimal distribution of the patches over the plate for the present case, at the first and at the last generation. Once again, the dimensions (diameter and thickness), the positions and the number of patches change during the generations.

	Best solution
N	7
x_i [mm]	{12.5, 37.5, 62.5, 87.5, 112.5, 137.5, 162.5}
D_i [mm]	{17.0, 16.3, 16.3, 16.3, 16.1, 17.6, 17.7}
t_i [mm]	{3.00, 3.00, 3.00, 3.00, 3.00, 2.20, 2.50}
h [mm]	3.5
$R_{0K}^{A^*}$ [MPa]	3131.09
$R_1^{A^*}$ [MPa]	2768.79
η_1	0.01350
η_2	0.00298
η_3	0.01652
η_4	0.09163
η_5	0.01815
f_1 [Hz]	59.54
f_2 [Hz]	327.51
f_3 [Hz]	367.71
f_4 [Hz]	557.45
f_5 [Hz]	1022.21
M [Kg]	0.02518 (+4.93%)
M_y [Nmm]	−158.87 (−2.53%)
Φ	−0.14278

Table 6.5: Best solution found using BIANCA for the optimisation problem (6.20), case 3.

The first five non-rigid modes for the optimal configuration of whole structure are shown in Fig. 6.11. It can be noticed that we have different kinds of mode-shapes: the first, the third and the fifth mode are bending modes in the $x - z$ plane of the plate, while the second one is a bending mode in the $x - y$ plane of the plate and finally the fourth mode is a torsional mode around the x axis. Of course, the optimal distribution of the viscoealstic material, i.e. the distribution of the rubber patches over the plate, along with the elastic properties of the composite plate are influenced by all the modes and the related damping mechanisms.

Considering that the value of the ply thickness is 0.125 mm, from Table 6.5 we can notice that the laminated plate is made of 28 plies (the total optimum thickness of the laminate is $h = 3.5$ mm) and has the orthotropy with $\widehat{K}^{A^*} = 0$, because the value of the polar quantity $R_{0K}^{A^*}$ is positive.

Concerning the second-level problem, the design variables are the layers orientations,

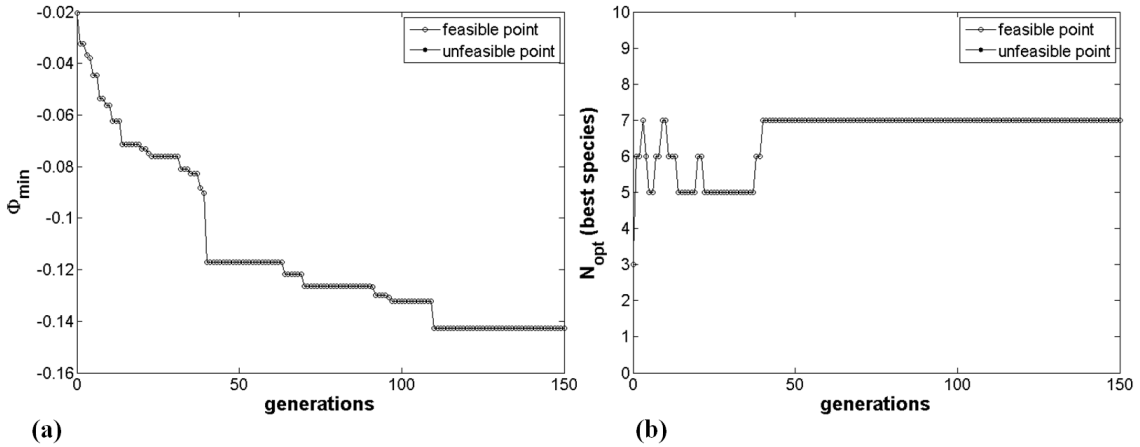

Figure 6.9: (a) Best values of the objective function and (b) optimal number of patches along generations for problem (6.20), case 3.

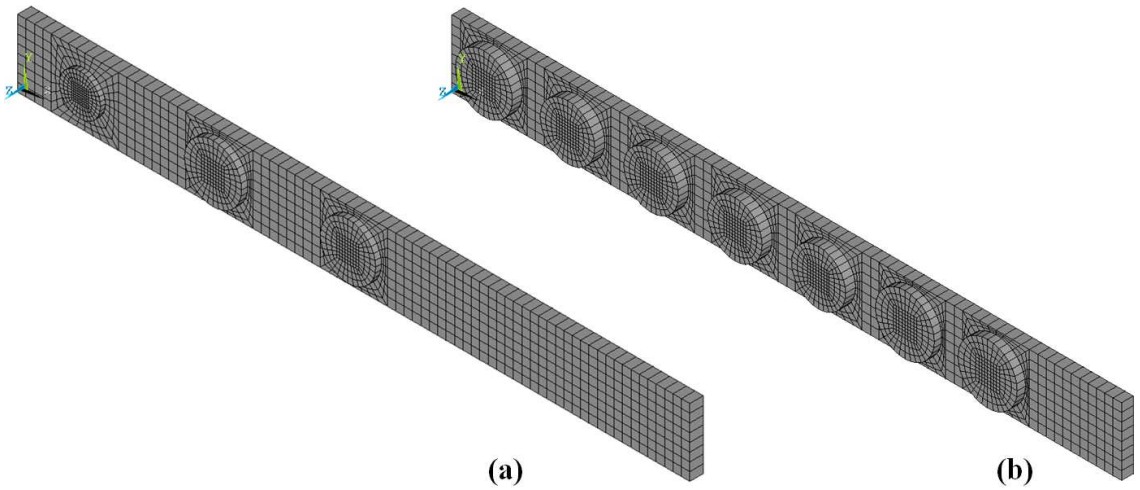

Figure 6.10: Optimal distribution of viscoelastic patches at the (a) initial and (b) final generation for problem (6.20), case 3.

which can vary between $-90°$ and $90°$ with a step of $1°$. The population size has been set to $N_{ind} = 500$ and the maximum number of generations to $N_{gen} = 500$. The crossover and mutation probability are still $p_{cross} = 0.85$ and $p_{mut} = 1/N_{ind}$, respectively. Selection is performed by the roulette-wheel operator and the elitism is active. Moreover, always concerning the second-level problem, as in each numerical technique, the quality of solutions found by BIANCA can be estimated on the basis of a numerical tolerance, that is the residual. For a discussion on the importance of the numerical residual in problems of this type, the reader is addressed to [116]. It is worth noting that, being $F(\boldsymbol{\delta})$ a

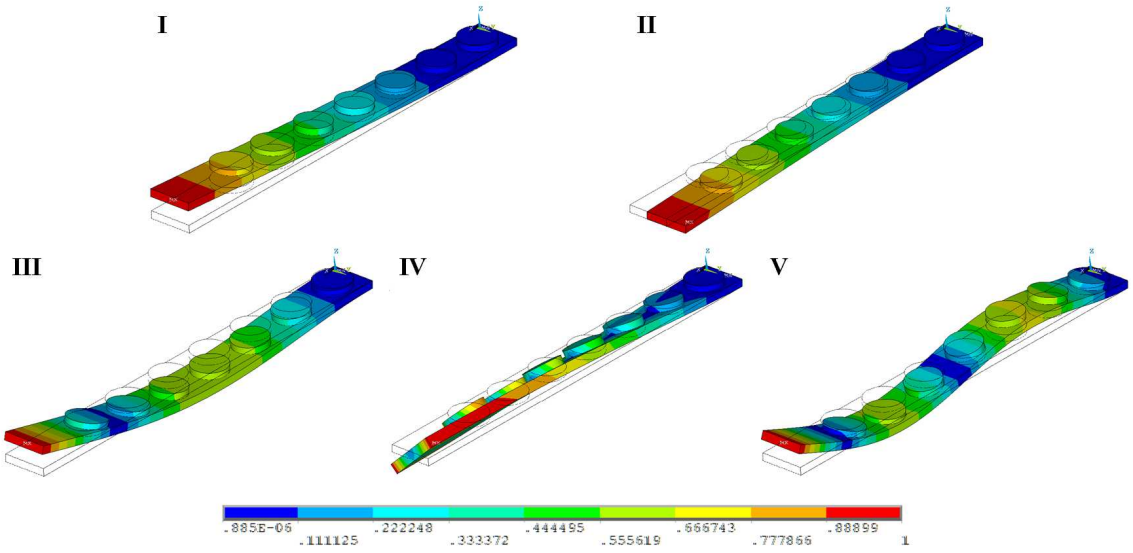

Figure 6.11: First five non-rigid modal deformed shapes of the whole structure for the optimal configuration, case 3.

non-dimensional function, the residual of the solution is a non-dimensional quantity too.

Table 6.6 shows the best stacking sequence found using BIANCA for the second-level problem. The residual in the last column is the value of the global objective function $F(\boldsymbol{\delta})$ for the solution indicated aside (we remind that exact solutions correspond to the zeroes of the objective function). Fig. 6.12 a) shows the first component of the homogenised stiffness tensors of the laminate, i.e. $\mathbf{A}^*$, $\mathbf{B}^*$ and $\mathbf{D}^*$: the solid line refers to the extension tensor, the dashed one to the bending tensor, while the dash-dotted one is linked to the coupling stiffness tensor. We can see that the laminate is uncoupled (the dash-dotted curve is reduced to a small black point in the center of the plot, because B^*_{11} is practically null), homogeneous (the solid and dashed curves are practically coincident) and orthotropic (there are two orthogonal axes of symmetry in the plane). Moreover, the main orthotropy axis is aligned with the x axis of the structure, in fact it is oriented at 0°. Similar considerations can be done for the other components of these tensors, not shown in Fig. 6.12 a) for the sake of brevity.

Fig. 6.12 b) shows the variation of the best solution during iterations: the best solution is found after 470 generations.

N. of plies	Stacking sequence (°)	Residual
28	$[0/-1/0/-2/0/0/17/-1/2/-4/0/-2/-1/-6/$ $-16/-1/-1/17/2/17/-4/-3/-1/0/0/-2/0/0]$	1.3×10^{-3}

Table 6.6: Case 3: best stacking sequences for the optimal solution.

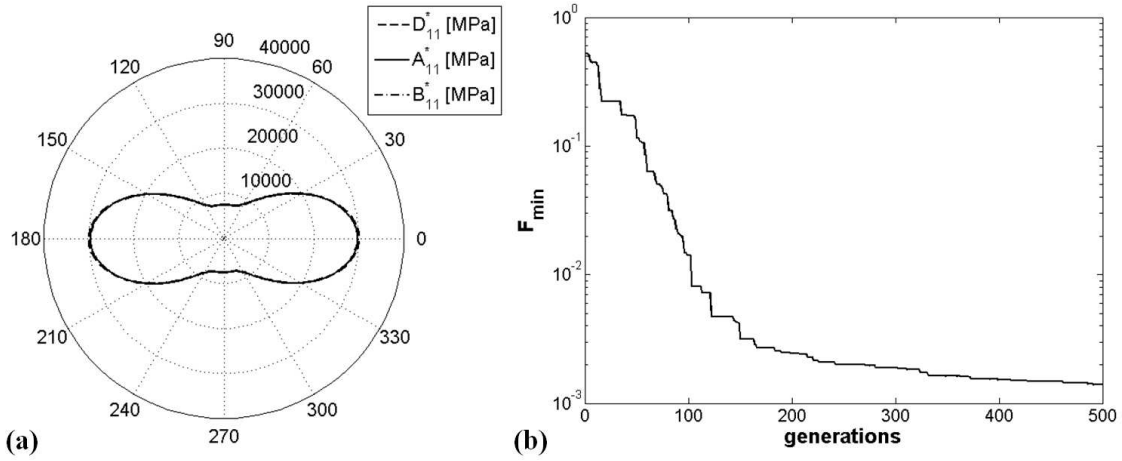

Figure 6.12: (a) First component of the homogenised stiffness tensors of the laminate and (b) best values of the objective function during iterations, case 3.

6.6.4 Discussion of results

Concerning the influence of the BCs of the model on the optimal distribution of the viscoelastic patches we can immediately see this effect by considering the results of the first and the second examples. In the first case the patches are placed near to the root section of the plate, i.e. in the region where the strains are higher and, consequently, where the damping phenomenon linked to those strain components is stronger, see also Sec 5.2 of Chapter 5 for a quick glance on the different damping mechanisms in viscoelastic materials.
The same considerations can be done also for the distribution of the patches for the second example: in this case the distribution is almost symmetric for what concerns the values of the diameters, thickness and positions, see Table 6.4. As in the previous case, also in this second example the patches are placed in the regions of the plate where the strains are higher.

Fig. 6.13 a) and b) show the maximum strain components in the rubber patches for what concerns examples 1 and 2. It can be noticed that, when we consider bending modes in the $x-z$ plane (i.e. modes n. 1, 3 and 4 for case 1 and modes n. 1, 3 and 5 for case 2) despite all the strain components are involved into the damping phenomenon, the major contribution is due to the axial strain ε_{xx} and to the shear strain through-the-thickness ε_{xz}. The same thing happens when we look at the bending modes in the $x-y$ plane, i.e. mode n. 2 for both cases 1 and 2. On the contrary, when we consider torsional modes, i.e. mode n. 5 for the first example and mode n. 4 for the second example, the major contribution to the damping mechanism of the structure is associated to the in-plane shear strains ε_{xy} and, secondly, to the shear deformations ε_{xz} and ε_{yz}, being

the effect of the longitudinal strains negligible for the torsional mode. It is worth noting that, differently from what is usually done in the literature where only bending modes are considered when studying the damping capabilities of viscoelastic materials, all the different modes, i.e. bending and torsional ones, are taken into account into the proposed optimisation procedure because they have the same influence on the damping response of the structure in terms of the values of the modal loss factors.

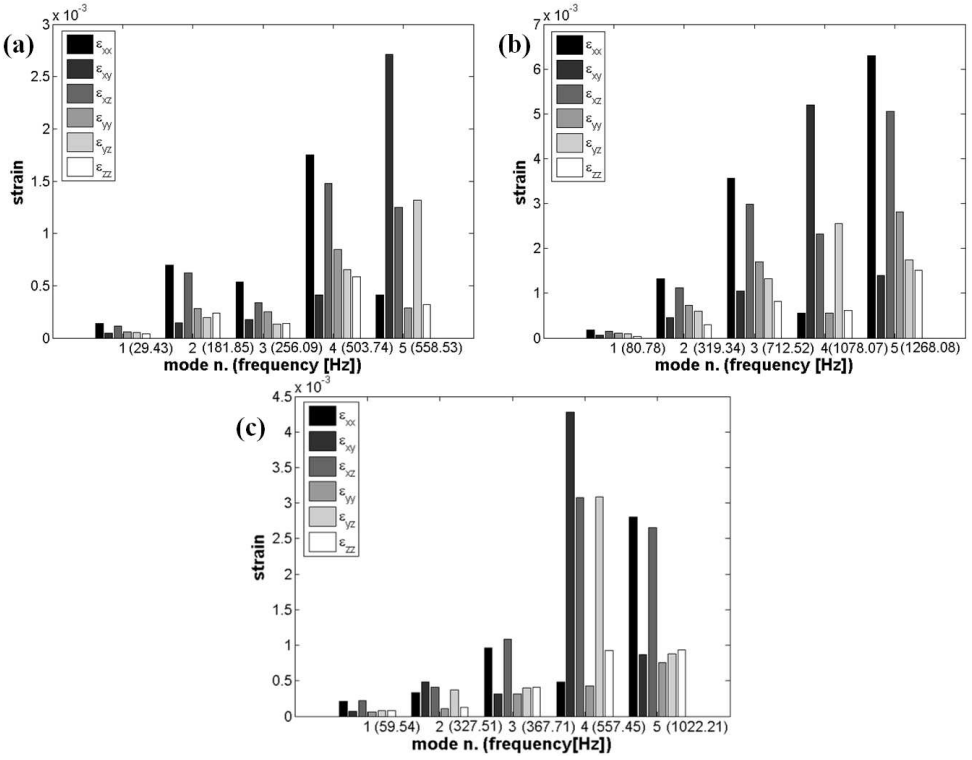

Figure 6.13: Maximum strain components in the viscoelastic patches for the optimised plate, (a) case 1, (b) case 2 and (c) case 3.

Concerning the third example, the simultaneous optimisation of the viscoelastic and elastic properties of the structure allows to find better damping capabilities when compared to the first two cases. Only by considering the overall design of the structure one can hope to find a real global optimum configuration: for this last case, in fact, the damping capability of the structure (and, hence, the values of the modal loss factors) is practically doubled with respect to that of the first two examples.

Fig. 6.13 c) shows the maximum strain components in the rubber patches for what concerns case 3. The considerations made for the first two examples can be applied also to this third case. Nevertheless, we can notice that the major contribution to the damping phenomenon of this last case is due to the torsional mode, i.e. mode n. 4 in Fig. 6.13 c):

the value of the modal loss factor associated to that mode is nine times the value of the others loss factors, see Table 6.5. This means that the torsional mode of the plate has a strong effect on the final distribution of the patches over the plate, in terms of diameters, thickness and positions.

As conclusive remark, for what concerns the third example, it can be noticed that, differently from what is usually done in the literature, we do not make any simplifying assumption on the laminate stacking sequence which is completely free, neither we use standard orientation angles for the elementary plies (like for instance $0°$, $\pm 45°$ and $90°$).

All the previous circumstances lead us to find a non-standard optimal solution which represents a real global optimum (in terms of the overall properties of the system) for the problem at hand.

6.7 Concluding remarks

The optimisation procedure presented in this work is characterised by several points that make it an innovative, effective, general method for the design of hybrid modular structures. Our motivation was to create a general procedure for the optimisation of modular systems, with the number of modules that belongs to the set of the design variables and without using special assumptions to get some results. The numerical method is, however, a fundamental part of the procedure, because it is thanks to an appropriate numerical tool that the simultaneous optimisation of the number of modules and of their characteristics is possible. We briefly recall the features of the procedure:

- no simplifying assumptions nor standard rules are used to design the laminated plate (this allows for looking for a *true global minimum*, hard to be obtained otherwise);
- the procedure is composed by two distinct but linked non-linear minimisation problems: the first one is a constrained problem that uses a *free material approach* to the design of the geometric and material properties of the system; the second step is an unconstrained problem formulated to design a laminate able to realise the overall optimal mechanical properties designed in the first step;
- quasi-homogeneous sequences are used; this allows for writing exact geometric bounds, valid for both the extension and bending behaviour and for reducing the number of mechanical design variables in the first step;
- bending orthotropy is really obtained, its type specified and the orthotropy direction directly managed, without using special sequences or orientations;
- the number of modules, i.e. the number of viscoelastic patches and of layers of the laminated plate, is directly optimised by the procedure, and this is entirely done by

a genetic approach able to select not only individuals, but also species; in practice, the algorithm determines automatically the optimal number of design variables;

- the mechanical characteristics are represented by the polar formalism, that gives several advantages, namely to explicit elastic symmetries, elastic and geometric bounds, and to eliminate from the procedure redundant mechanical properties;

- the numerical computations are carried on by a special GA, the code BIANCA, able to cross simultaneously species and individuals, to handle continuous and discrete valued variables during the same iterations and to effectively handle the constraints imposed to the problem;

- for the solution of the first-level problem, the code BIANCA has been interfaced with a FE code, in order to numerically compute some mechanical quantities, namely the modal loss factors of the structure and the bending moment around the y axis;

- the mathematical formulation of the second step problem allows for taking into account for all the possible combinations of elastic requirements and properties; it is stated as an unconstrained minimum problem of a positive semi-definite function, whose absolute minimum is equal to 0, which renders possible to know if a true global minimum has been attained.

To our best knowledge, this is the first time that the problem of maximising the damping capabilities is formulated considering a discontinuous aperiodic distribution of viscoealstic material, namely by considering elastomer patches bonded over the structure which share the same form but, at the same time, they can be characterised by different values of their constitutive geometrical parameters, i.e. diameters, thickness and positions. Moreover, this is also the first time that the optimisation problem is stated considering the geometrical requirement, in the form of constraint functions, on the position of the patches bonded over the plate. Thus, the main key points of our strategy consist in determining which are: a) the best number of rubber patches, b) their best dimensions and positions over the structure as well as c) the best values of the thickness and of the polar parameters of the laminated plate which play an important role in the determination of the damping capability of the system.

The use of an evolutionary strategy along with the fact that the problem is stated in the most general case, leads us to find some non-conventional configurations, which show better damping properties when compared to the classical constrained layer treatments, namely classical hybrid elastomer/composite laminates.

Another point deserves attention: the passive solution consisting in patches bonded over composite plates is a good alternative with respect to introducing viscoelastic layers in sandwich plates, especially in terms of manufacturing because the patches can be deposited *a posteriori* on the plate surface. Nevertheless, we can see by the example

treated in this Chapter, that such technology is relevant only if the structure is optimised *a priori*, i.e. if the simultaneous design of both elastic and viscoelastic properties of the structure is taken into account.

The proposed approach appears to be very flexible and applicable to various problems of structural engineering. Moreover, the procedure has a high level of versatility: more constraints could be easily added to the optimisation problem, e.g. constraints on the strength, yielding or de-lamination of the laminate, without reducing the power and the robustness of the proposed approach.

General conclusions and future perspectives

The main subject of this thesis is the optimal design of advanced engineering modular systems through a new genetic approach.

In particular, in the present thesis we have developed a new version of the genetic code BIANCA able to deal with optimisation problems of modular systems. Firstly, we have introduced the concept of *species*: it is linked to the number of individual's chromosomes which is, on turn, linked to the number of modules composing the system and, hence, to the overall number of design variables which uniquely defines the behaviour of the system. This has lead us to a reformulation of the structure of the individual's genotype, i.e. of the representation of the information within BIANCA, in order to properly represent its belongings to a given species.

Secondly, we developed new genetic operators allowing the reproduction between two individuals of different species. These operators have substantially changed the crossover and mutation phases of the standard GA. Thanks to such operators, BIANCA is now able to determine automatically and simultaneously the *best species* and the *best individual* within the best species.

Moreover, since very often the optimisation problems have a certain number of constraint equations (both equality and inequality constraints) to be satisfied, we developed a very general method which can handle the constraints in a very effective way: the Automatic Dynamic Penalisation (ADP) constraint-handling technique. The main advantages of such an approach (which belongs to the class of exterior penalty-based approaches) are substantially two:

- the procedure is *automatic* and problem-independent because the GA can automatically calculate the values of the penalty coefficients without the intervention of the user by simply exploiting the values of the objective and constraint functions in the current population;

- the method is *dynamic*, since the evaluation of the penalty level is updated at each generation; this allows the values of the penalty coefficients to be the most suitable to the current distribution of feasible and infeasible individuals in the population, the

expected effect being eventually to extinguish the infeasible group in the population or to limit infeasible individuals to regions close to the boundary between feasible and infeasible domains.

The ADP strategy has been tested on several benchmark problems, showing very good search capabilities compared to the best solutions provided in the literature. In addition, the ADP strategy showed to be very effective when dealing with both inequality and equality constraints, also when such constraints are expressed by non-linear, non-convex functions.

Finally, we developed a very general interface which renders BIANCA able to exchange input/output informations with mathematical models supported by external codes and also a graphical user interface for our code. Thanks to the interface with external codes BIANCA is now able to face optimisation problems where the value of the objective function and/or constraints cannot be computed analytically. Typically, this is the case of structural optimisation, where the most part of times the structural response is numerically assessed using finite element codes. In addition, thanks to the graphical user interface, BIANCA can now be easily handled and employed by any user.

The numerical strategy developed in this thesis has proved to be versatile and effective and it has been applied to a certain number of problems of different nature concerning advanced modular structures. In all the cases, the fact that the problem is every time stated in the most general case, i.e. without using any simplifying hypotheses, together with the fact that the solution search is performed by a numerical strategy which is "purely genetic" and fully problem-independent, led us to find, for each case-study, non-conventional solutions which are better than the classical ones that can be found in the literature.

The main non-classical features and results characterising each considered case can be resumed as follows:

- the identification of the electromechanical properties of piezoelectric structures (Chapter 2): the key points of this research are the estimation of the whole 3D set of electromechanical properties of the piezoelectric transducers and the use of the full set of constraints that must be imposed to the minimisation problem to ensure the positive definiteness of the stiffness tensor of the material of the patches. For such a problem, BIANCA leads us to reach, with a high precision, the reference values of the natural frequencies of the active plate for both closed and open circuit conditions;

- the design of laminates having the minimum number of layers for obtaining given elastic properties (Chapter 3): the key-point of this problem consists in reducing it to a classical unconstrained non-linear programming problem by searching the minima of a semi-definite positive function over the space of the design variables.

The numerical results obtained in this case, which are completely new and non-classical examples, show the effectiveness of the proposed approach;

- the least-weight wing box section design problem (Chapter 4): the key-point of this study is the development of a two-level procedure composed by two distinct but linked non-linear minimisation problems. The first one is a constrained problem that uses a *free material approach* for the design of the geometric and material properties of the anisotropic structure, considered as composed by a single-layer fictitious anisotropic material; the second step is an unconstrained problem formulated to design a laminate able to realise the overall optimal mechanical properties designed in the first step. The results presented in this Chapter show that when standard rules for the stacks of laminates are abandoned and the design of the optimal number of the modules composing the structure is included into the design procedure, significant savings of the weight of the structure can be obtained: up to 50%, when compared to a classical solution using an aluminium alloy, and up to 20% when compared to a solution with standard aeronautical stacking sequences;

- the design of damping capabilities of hybrid elastomer/composite laminates (Chapter 5): the key-points of our strategy consist in determining which are the best number of layers of the hybrid plate, along with the best number and positions of the elastomer layers within the stacking sequence. The fact that the problem is stated in the most general case leads us to find some non-conventional configurations, i.e. non-constrained layer configurations, which show better damping properties when compared to the classical constrained layer treatments;

- the design of damping capabilities of laminated plates with bonded viscoelastic patches (Chapter 6): the key-points of this work are, on one side, the application of the two-level procedure discussed in Chapter 4 and, on the other side, the formulation of the problem considering, for the first time, a discontinuous aperiodic distribution of viscoealstic material (the patches) and, at the same time, the geometrical requirement, in the form of constraint functions, on the position of the patches bonded over the plate. Thus, we have determined: the best number of rubber patches, their best dimensions and positions over the structure as well as the best values of the thickness and of the polar parameters of the laminated plate. Also in this case, the fact that the problem is stated in the most general case, leads us to find some non-conventional configurations, which show better damping properties when compared to classical hybrid elastomer/composite laminates.

Concerning the future perspectives, we think that our numerical approach for designing modular systems could be applied to other different problems. Further applications may occur, for example, in the case of the design of active structures actuated using piezoelectric devices (in the form of patches bonded over the structure) where we can imagine

to maximise the displacement and/or the actuated force in particular regions of the structure, satisfying simultaneously others requirements expressed in the form of constraints as, for instance, constraints on the overall weight of the system, on the positions of the piezoelectric actuators, on the energy required for the actuation and so on. The design variables of such a problem could be the number and the positions of the piezoelectric patches, their sizes, the control law which governs the electric signal transmitted to the actuators, the geometrical and material parameters of the structure where the patches are bonded and so on.
Moreover, we can imagine to extend the studied problems by considering different situations. If we consider, for instance, the problem of the least-weight wing-box section or the problem of designing the damping capabilities of laminated plates with bonded viscoelastic patches, the two-level procedure adopted to face the problem allows us to easily introduce some additional constraints both into the first and the second step of the procedure. For example, we could consider further requirements as constraints on the strength of the structure at the first step or constraints on the delamination, on the fatigue damage and so on at the second step, without changing the structure of two-level procedure.

Another possible axis of research concerns the interface of BIANCA with external codes. In particular, when it is interfaced with huge FE models or when it is used coupled with non-linear FE analyses, the time spent to find a global optimum configuration may require from several hours to several days for a complete simulation. A possible solution to reduce the computational cost is the parallelisation of the code: we can imagine to divide each population in groups of individuals which are handled by different processors, reducing in this way the time required to find the solution. Another possible alternative could consist in using metamodels as, for example, neural networks, which simulate the behaviour of the considered FE model and that provide the "same" response as that of the FE model (i.e. an approximation of the response of the FE model with a good level of accuracy) in a shorter time.

To conclude, we can assert that the works developed within this thesis led us on one hand, to find original and completely new and non-classical results for what concerns all the considered real-world engineering applications and on the other hand, to define a new genetic procedure specially conceived for the optimal design of modular systems which, on its turn, leads to explore new horizons in such a framework and whose power and effectiveness can be tested only by studying and dealing with new, more complex problems.

Bibliography

[1] A. Vincenti, M. R. Ahmadian, and P. Vannucci. BIANCA: a genetic algorithm to solve hard combinatorial optimisation problems in engineering. *Journal of Global Optimisation*, 48:399–421, 2010.

[2] A. Vincenti. *Conception et optimisation de composites par mèthode polaire et algorithmes génétiques (in French).* PhD thesis, Université de Bourgogne, France, 2002.

[3] P. Vannucci. *Un parcours de recherche multidisciplinaire en mécanique.* Université de Bourgogne, ISAT & LRMA (in French), http://tel.archives-ouvertes.fr/docs/00/62/59/58/PDF/HDR.pdf, 2002.

[4] G. Galilei. *Discorsi e dimostrazioni matematiche intorno a due nuove scienze attenenti alla meccanica e i movimenti locali.* Leiden (NL): Elsevier (in Italian), 1638.

[5] R. Hooke. On the schematisme or texture of cork, and of the cells and pores of some other such frothy bodies. *In Gabriel M. L., Fogel S., 1955: Great Experiments in biology. Prentice Hall, USA.*, 1665.

[6] P. M. L. Maupertuis. *Le système de la nature.* Paris (in French), 1751.

[7] M. Valentin. *Maupertuis, un savant oublié.* La découvrance Editions. (in French), 1998.

[8] C. Darwin. The origin of species by means of natural selection or the preservation of favored races in the struggle for life. *The Book League of America*, 1929 (originally published in 1859).

[9] A. R. Wallace. *Contributions to the theory of natural selection. A series of essays.* Macmillan & Co., London & New York, 1870.

[10] I. Rechenberg. *Evolutionsstrategie: Optimierung technischer Systeme nach Prinzipien der biologischen Evolution.* Stuttgart: Frommann-Holzboog Verlag (in German), 1973.

[11] H. P. Schwefel. *Numerical optimization for computer models*. Chichester: John Wiley, 1981.

[12] Z. Michalewicz. *Genetic algorithms + data structures = evolution programs*. Berlin: Springer, 1994.

[13] L. J. Fogel, A. J. Owens, and M. J. Walsh. *Artificial intelligence through simulated evolution*. Chichester: John Wiley, 1966.

[14] F. Glover. Heuristics for integer programming using surrogate constraints. *Decision Sciences*, 8(1):156–166, 1977.

[15] J. H. Holland. *Adaptation in natural and artificial systems*. Ann Arbor: University of Michigan Press, 1975.

[16] D. E. Goldberg. *Genetic algorithms*. New York: Addison and Wesley, 1994.

[17] B. Baudry, F. Fleurey, J. M. Jezequel, and Y. Le Traon. Automatic test case optimization: a bacteriologic algorithm. *Software IEEE*, 22(2):76–82, 2005.

[18] G. Kjellström. On the efficiency of gaussian adaptation. *Journal of Optimization Theory and Applications*, 71(3):589–597, 1991.

[19] M. Dorigo, V. Maniezzo, and A. Colorni. Ant system: Optimization by a colony of cooperating agents. *IEEE Transactions on Systems, Man, and Cybernetics-Part B*, 26(1):29–41, 1996.

[20] J. Kennedy and R. Eberhart. Particle swarm optimization. pages 1942–1945, Perth, Australia, 1995. Proceedings of the IEEE International Conference on Neural Networks.

[21] H. Shah-Hosseini. The intelligent water drops algorithm: a nature-inspired swarm-based optimization algorithm. *International Journal of Bio-Inspired Computation*, 1:71–79, 2009.

[22] S. Kirkpatrick, C. D. Gelatt Jr., and M. P. Vecchi. Optimization by simulated annealing. *Science*, 220:671–680, 1983.

[23] F. Glover and M. Laguna. *Tabu Search*. Kluwer Academic Publishers, 1998.

[24] J. M. Renders. *Algorithmes génétiques et réseaux de neurones*. Paris: Hermes (in French), 1995.

[25] J. Rechenberg. *Cybernetic solution path of an experimental problem*. Royal Aircraft Establishment, Liberty translation 1122. Farnborough, UK., 1965.

[26] C. D. Chapman, K. Saitou, and M. J. Jakiela. Genetic algorithms as an approach to configuration and topology design. *Journal of Mechanical Design ASME*, 116:1005–1012, 1994.

[27] C. Y. Lin and P. Hajela. Genetic search strategies in large scale optimization. pages 2437–2447, La Jolla, California, 1993. Proceedings of AIAA/ASME/ASCE/AHS/ASC SDM conference.

[28] C. Y. Lin and P. Hajela. Design optimization with advanced genetic search strategies. *Advances in Engineering Software*, 21:179–189, 1994.

[29] J. Ryoo and P. Hajela. Handling variable string lengths in ga-based structural topology optimization. *Struct. Multidisc. Optim.*, 26:318–325, 2004.

[30] I. Y. Kim and O. I. de Weck. Variable chromosome length genetic algorithm for progressive refinement in topology optimization. *Struct. Multidisc. Optim.*, 29:445–456, 2005.

[31] S. Abrate. Optimal design of laminated plates and shells. *Composite Structures*, 29:269–286, 1994.

[32] H. Ghiasi, D. Pasini, and L. Lessard. Optimum stacking sequence design of composite materials part i: Constant stiffness design. *Composite Structures*, 90:1–11, 2009.

[33] H. Ghiasi, D. Fayazbakhsh, D. Pasini, and L. Lessard. Optimum stacking sequence design of composite materials part ii: Variable stiffness design. *Composite Structures*, 93:1–13, 2010.

[34] R. Le Riche and R. T. Hatfka. Improved genetic algorithm for minimum thickness composite laminate design. *Composites Engineering*, 5(2):143–161, 1995.

[35] A. Todoroki and R. T. Hatfka. Stacking sequence optimization by a genetic algorithm with a new recessive gene like repair strategy. *Composites Part B*, 29:277–285, 1998.

[36] B. Liu, R. T. Hatfka, and P. Trompette. Maximization of buckling loads of composite panels using flexural lamination parameters. *Structural and Multidisciplinary Optimization*, 26:28–36, 2004.

[37] A. Muc and W. Gurba. Genetic algorithms and finite element analysis in optimization of composite structures. *Composite Structures*, 54:275–281, 2001.

[38] P.Y. Tabakov. Multi-dimensional optimisation of laminated structures using an improved genetic algorithm. *Composite Structures*, 54:349–354, 1992.

[39] S. Nagendra, D. Jestin, Z. Gürdal, R.T. Hatfka, and L.T. Watson. Improved genetic algorithm for the design of stiffened composite panels. *Computers and Structures*, 58(3):543–555, 1996.

[40] P. Kaletta and K. Wolf. Optimisation of composite aircraft panels using evolutionary computation methods. *Proceedings of ICAS 2000 Congress, Harrogate, UK, 27 August-1 September*, pages 441.1–10, 2000.

[41] M. Lillico, R. Butler, G.W. Hunt, A. Watson, D. Kennedy, and F.W. Williams. Optimum design and testing of a post-buckled stiffened panel. *American Institute of Aeronautics and Astronautics, AIAA-2000-1659*, pages 1–10, 2000.

[42] C. Bisagni and L. Lanzi. Post-buckling optimisation of composite stiffened panels using neural networks. *Composite Structures*, 58:237–247, 2002.

[43] P. Vannucci. Designing the elastic properties of laminates as an optimisation problem: a unified approach based on polar tensor invariants. *Structural and Multidisciplinary Optimisation*, 31(5):378–387, 2006.

[44] C. Julien. *Conception optimale de l'anisotropie dans les structures stratifiées à rigidité variable par la mèthode polaire-génétiques*. PhD thesis, Institut d'Alembert UMR7190 CNRS -Université Pierre et Marie Curie Paris 6 , France, 2010 (in French).

[45] T. Bäck. *Evolutionary algorithms in theory and practice*. Oxford University Press, New York, 1995.

[46] K. Bennet, M. C. Ferris, and Y. E. Ioannidis. A genetic algorithm for database query optimisation. pages 400–407. Proceedings of the Fourth International Conference on Genetic Algorithms, Morgan Kaufmann Publishers, San Mateo, CA, 1991.

[47] L. B. Booker. *Intelligent behavior as an adaptation to the task environment*. PhD thesis, University of Michigan, 1982.

[48] K. A. De Jong. Adaptive system design: a genetic approach. volume 10, pages 556–574. IEEE Transactions on Systems, Man and Cybernetics, 1980.

[49] K. A. De Jong. Genetic algorithms: a 10 year perspective. pages 169–177. Proceedings of the First International Conference on Genetic Algorithms, Lawrence Erlbaum Associates, Hillsdale, NJ, 1985.

[50] D. B. Fogel. *Evolutionary Computation: Toward a New Philosophy of Machine Intelligence*. IEEE Press, Piscataway, NJ, 1995.

[51] F. Greene. A method for utilizing diploid/dominance in genetic search. volume 1, pages 439–444, Orlando, 27-29 June 1994. Proceedings of the First IEEE International Conference on Evolutionary Computation, IEEE Service Center, Piscataway, NJ.

[52] A. Bertoni and M. Dorigo. Implicit parallelism in genetic algorithms. *Artificial Intelligence*, 61(2):307–314, 1993.

[53] C. H. Park, W. I. Lee, W. S. Han, and A. Vautrin. Multiconstraint optimisation of composite structures manufactured by resin transfer moulding process. *Journal of Composite Materials*, 39(4):347–374, 2005.

[54] D. Dasgupta and Z.(Eds.) Michalewicz. *Evolutionary Algorithms in Engineering Applications*. Springer, Berlin, 1997.

[55] Z. Michalewicz and M. Schoenauer. Evolutionary algorithms for constrained parameter optimization problems. *Evolutionary Computation*, 4(1):1–32, 1996.

[56] C. A. Coello Coello. Theoretical and numerical constraint-handling techniques used with evolutionary algorithms: a survey of the state of the art. *Computer Methods in Applied Mechanics and Engineering*, 191:1245–1287, 2002.

[57] R. Courant. Variational methods for the solution of problems of equilibrium and vibrations. *Bulletin of the America Mathematical Society*, 49:1–23, 1943.

[58] C. W. Carroll. The created response surface technique for optimizing nonlinear restrained systems. *Operations Research*, 9:169–184, 1961.

[59] A. V. Fiacco and G. P. McCormick. Extensions of sumt for nonlinear programming: Equality constraints and extrapolation. *Management Science*, 12(11):816–828, 1968.

[60] L. Davis. *Genetic Algorithms and Simulated Annealing*. Pitman, London, 1987.

[61] J. T. Richardson, M. R. Palmer, G. Liepins, and M. Hilliard. Some guidelines for genetic algorithms with penalty functions. pages 191–197, George Mason University, Morgan Kaufmann, Reading, MA, 1989. Proceedings of the Third International Conference on Genetic Algorithms.

[62] S. E. Carlson. A general method for handling constraints in genetic algorithms. pages 663–667. Proceedings of the Second Annual Joint Conference on Information Science, 1995.

[63] Z. Michalewicz. Genetic algorithms, numerical optimization, and constraints. pages 151–158, University of Pittsburgh, Morgan Kaufmann, San Mateo, CA, July 1995. Proceedings of the Sixth International Conference on Genetic Algorithms.

[64] A. Kuri Morales and C. V. Quezada. A universal eclectic genetic algorithm for constrained optimization. pages 518–522, Verlag Mainz, Aachen, Germany, September 1998. Proceedings of the 6th European Congress on Intelligent Techniques and Soft Computing, EUFIT'98.

[65] J. Joines and C. Houck. On the use of non-stationary penalty functions to solve nonlinear constrained optimization problems with gas. pages 579–584, IEEE Press, Orlando, FL, 1994. Proceedings of the First IEEE Conference on Evolutionary Computation.

[66] J. Joines and C. Houck. Varying fitness functions in genetic algorithms: Studying the rate of increase of the dynamic penalty terms. Springer, Amsterdam, Netherlands, 1998. Parallel Problem Solving from Nature V - PPSN V.

[67] A. B. Hadj-Alouane and J. C. Bean. A genetic algorithm for the multiple-choice integer program. *Operations Research*, 45:92–101, 1997.

[68] D. W. Coit and A. E. Smith. Penalty guided genetic search for reliability design optimization. *Computers & Industrial Engineering*, 30(4):895–904, 1996.

[69] D. W. Coit, A. E. Smith, and D. M. Tate. Adaptive penalty methods for genetic optimization of constrained combinatorial problems. *INFORMS Journal on Computing*, 8(2):173–182, 1996.

[70] A. E. Eiben, J. K. van der Hauw, and J. I. van Hemert. Graph coloring with adaptive evolutionary algorithms. *Journal of Heuristics*, 4(1):25–46, 1998.

[71] M. Gen and R. Cheng. Interval programming using genetic algorithms. Montpelleir, France, 1996. Proceedings of the Sixth International Symposium on Robotics and Manufacturing.

[72] F. Hoffmeister and J. Sprave. Problem-independent handling of constraints by use of metric penalty functions. pages 289–294, MIT Press, San Diego, CA, February 1996. Proceedings of the Fifth Annual Conference on Evolutionary Programming.

[73] S. S. Rao. *Engineering Optimization.* third ed., Wiley, New York, 1996.

[74] B. K. Kannan and S. N. Kramer. An augmented lagrange multiplier based method for mixed integer discrete continuous optimization and its applications to mechanical design. *Transactions of the ASME, Journal of Mechanical Design*, 116:318–320, 1994.

[75] J. S. Arora. *Introduction to Optimum Design.* McGraw-Hill, New York, 1989.

[76] A. D. Belegundu. A study of mathematical programming methods for structural optimization. *Department of Civil and Environmental Engineering, University of Iowa, Iowa City, Iowa.*, 1982.

[77] K. M. Ragsdell and D. T. Phillips. Optimal design of a class of welded structures using geometric programming. *ASME Journal of Engineering for Industries*, 98(3):1021–1025, 1976.

[78] K. Deb. Optimal design of a welded beam via genetic algorithms. *Engineering Applications of Artificial Intelligence*, 29(11):2013–2015, 1991.

[79] C. A. C. Coello and E. M. Montes. Constraint-handling in genetic algorithms through the use of dominance-based tournament selection. *Advanced Engineering Informatics*, 16:193–203, 2002.

[80] Q. He and L. Wang. An effective co-evolutionary particle swarm optimization for constrained engineering design problems. *Engineering Applications of Artificial Intelligence*, 20:89–99, 2007.

[81] Q. He and L. Wang. A hybrid particle swarm optimization with a feasibility-based rule for constrained optimization. *Applied Mathematics and Computation*, 186(2):1407–1422, 2007.

[82] J. Zhao, L. Wang, P. Zeng, and W. Fan. An effective hybrid genetic algorithm with flexible allowance technique for constrained engineering design optimization. *Expert Systems with Applications*, 39:6041–6051, 2012.

[83] K. Deb. GeneAS: a robust optimal design technique for mechanical component design. pages 497–514, Springer, Berlin, 1997. Evolutionary Algorithms in Engineering Applications.

[84] The MathWorks, Inc., 3 Apple Ill Drive, Natick, MA 01760-2098. *MATLAB version 7.12.0. (R2011a)*, September 2011.

[85] P. Tan and L. Tong. Micro-electromechanics models for piezoelectric-fiber-reinforced composite materials. *Composites science and technology*, 61(5):759–769, 2001.

[86] A. Deraemaeker, H. Nasser, A. Benjeddou, and A. Preumont. Mixing rules for the piezoelectric properties of macro fiber composites. *Journal of Intelligent Material Systems and Structures*, 20(12):1475–1482, 2009.

[87] Y. Koutsawa, F. Biscani, S. Belouettar, H. Nasser, and E. Carrera. Multi-coating inhomogeneities approach for the effective thermo-electro-elastic properties of piezoelectric composite materials. *Composite Structures*, 92(4):964–972, 2010.

[88] F. J. Sabina, R. Rodríguez-Ramos, J. Bravo-Castillero, and R. Guinovart-Díaz. Closed-form expressions for the effective coefficients of a fibre-reinforced composite with transversely isotropic constituents. II: piezoelectric and hexagonal symmetry. *Journal of the Mechanics and Physics of Solids*, 49(7):1463–1479, 2001.

[89] F. Biscani, H. Nasser, S. Belouettar, and E. Carrera. Equivalent electro-elastic properties of macro fiber composite (mfc) transducers using asymptotic expansion approach. *Composites Part B: Engineering*, 42(3):444–455, 2011.

[90] A. Deraemaeker and H. Nasser. Numerical evaluation of the equivalent properties of macro fiber composite (mfc) transducers using periodic homogenization. *International Journal of Solids and Structures*, 47(24):3272–3285, 2010.

[91] P. Pedersen. Identification techniques in composite laminates. *NATO ASI Series E Applied Sciences-Advanced Study Institute*, 361:443–452, 1999.

[92] C. M. M. Soares, M. J. M. Freitas, A.L. Arújo, and P. Pedersen. Identification of material properties of composite plate specimens. *Composite Structures*, 25:277–285, 1993.

[93] A. L. Araújo, C. M. M. Soares, J. Herskovits, and P. Pedersen. Development of a finite element model for the identification of mechanical and piezoelectric properties through gradient optimisation and experimental vibration data. *Composite Structures*, 58:307–318, 2002.

[94] A. L. Araújo, H. M. R Lopes, C. M. M. Soares, J. Herskovits, and P. Pedersen. Parameter estimation in active plate structures. *Computers and Structures*, 84:1471–1479, 2006.

[95] H. T. Banks, R. C. Smith, D. E. Brown, V. L. Metcalf, and R. J. Silcox. The estimation of material and patch parameters in a PDE-based circular plate model. *Journal of Sound and Vibration*, 199(5):777–799, 1997.

[96] R. Rikards, H. Abramovich, T. Green, J. Auzins, and A. Chate. Identification of elastic properties of composite laminates. *Mechanics of Advanced Materials and Structures*, 10:335–352, 2003.

[97] J. Chuna and J. Piranda. Application of model updating techniques in dynamics for the identification of elastic constants of composite materials. *Composites Part B: Engineering*, 30(1):79–85, 1999.

[98] K. Balasubramaniam and N. S. Rao. Inversion of composite material elastic constants from ultrasonic bulk wave phase velocity data using genetic algorithms. *Composites Part B: Engineering*, 29:171–180, 1998.

[99] G. R. Lui, W. B. Ma, and X. Han. An inverse procedure for determination of material constants of composite laminates using elastic waves. *Computer Methods in Applied Mechanics and Engineering*, 191:3543–3554, 2002.

[100] G. R. Lui, W. B. Ma, and X. Han. Determination of elastic constants of anisotropic laminated plates using elastic waves and a progressive neural network. *Journal of Sound and Vibration*, 252(2):239–259, 2002.

[101] A.L. Araújo, C.M.M. Soares, and C.A.M. Soares. Inverse techniques for the characterization of mechanical and piezoelectric properties on composite and adaptive structures: A survey. *Computational Technology Reviews, Saxe-Coburg Publications*, 2:103–123, 2012.

[102] M. Montemurro, H. Nasser, Y. Koutsawa, S. Belouettar, A. Vincenti, and P. Vannucci. Identification of electromechanical properties of piezoelectric structures through evolutionary optimisation techniques. *International Journal of Solids and Structures*, 49(13):1884–1892, 2012.

[103] J. van Randeraat and R. Setterington. *Piezoelectric Ceramics*. Mullard Ltd, London, UK, 2nd edn, 1974.

[104] W. G. Cady. *Piezoelectricity: an Introduction to the Theory and Applications of Electromechanical Phenomena in Crystals*. Mc Graw-Hill, New York, London, 1946.

[105] J. F. Nye. *Physical Properties of Crystals: Their Representation by Tensors and Matrices*. Clarendon Press, Oxford, 1957.

[106] V. Piefort. *Finite Element Modeling of Piezoelectric Active Structures*. PhD thesis, Université Libre de Bruxelles, Belgium, 2001.

[107] A. Tarantola. *Inverse Problem Theory: Methods for Data Fitting and Model Parameter Estimation*. Elsevier, New York, 1988.

[108] N-Z. Sun. *Inverse Problems in Groundwater Modelling*, volume 6 of *Theory and Applications of Transport in Porous Media.* Kluwer Academic Publishers, Boston, 1999.

[109] R. M. Jones. *Mechanics of composite materials*. McGraw-Hill, 1975.

[110] M. Montemurro, A. Vincenti, P. Vannucci, and A. Makradi. Optimisation en poids de structures composites stratifiées. Poitiers, 2011. JNC17 - Journées Nationales sur les Composites; HAL : hal-00598119.

[111] Pelletier D. Borggaard, J. and K. Vugrin. On sensitivity analysis for problems with numerical noise. In *Proceedings of the 9th AIAA/NASA/USAF/ISSMO Symposium on Multidisciplinary Analysis and Optimization. AIAA Paper 2002-5553*, 2002.

[112] J. Burman and B. Gebart. Influence from numerical noise in the objective function for flow design optimization. *International Journal of Numerical Methods for Heat & Fluid Flow*, 11(1):6–19, 2001.

[113] J.M. Fitzpatrick and J.J. Grefenstette. Genetic algorithms in a noisy environment. *Machine Learning*, 3(2):101–120, 1988.

[114] G. Verchery. Les invariants des tenseurs d'ordre 4 du type de l'élasticité. VIllard-de-Lans, (France), 1979. Proc. of colloque Euromech 115.

[115] P. Vannucci and A. Vincenti. The design of laminates with given thermal/hygral expansion coefficients: a general approach based upon the polar-genetic method. *Composite Structures*, 79:454–466, 2007.

[116] A. Vincenti, P. Vannucci, and M. R. Ahmadian. Optimization of laminated composites by using genetic algorithm and the polar description of plane anisotropy. *Mechanics of Advanced Materials and Structures*, page http://dx.doi.org/10.1080/15376494.2011.563415, 2012 (In press).

[117] F. Werren and C. B. Norris. Mechanical properties of a laminate designed to be isotropic. *US Forest Products Laboratory, report 1841*, 1953.

[118] P. Vannucci. Plane anisotropy by the polar method. *Meccanica*, 40:437–454, 2005.

[119] M. Montemurro, A. Vincenti, and P. Vannucci. Design of elastic properties of laminates with minimum number of plies. *Mechanics of Composite Materials*, 48:369–390, 2012.

[120] A. Jibawy, C. Julien, B. Desmorat, A. Vincenti, and F. Léné. Hierarchical structural optimization of laminated plates using polar representation. *International Journal of Solids and Structures*, 48:2576–2584, 2011.

[121] S. W. Tsai and N. J. Pagano. Invariant properties of composite materials. pages 233–253, Technomic, USA, 1968. Composite Materials Workshop.

[122] E. M. Wu. Fourth order tensor invariants and geometric representation. *Office of Naval Research/Advanced Research Projects Agency*, Report HPC 1970:70–123, 1970.

[123] H. T. Hahn. A derivation of invariants of fourth rank tensors. *Journal of Composite Materials*, 8:1–14, 1974.

[124] J. H. Michell. The inversion of plane stress. volume 34, pages 134–142. Proc. of the London Math. Soc., 1902.

[125] G. V. Kolosov. *On an application of complex function theory to a plane problem of the mathematical theory of elasticity.* Yuriev, Russie, 1909.

[126] N. J. Muskhelishvili. *Some basic problems of the mathematical theory of elasticity. (English translation by J. R. M. Radok, 1953).* P. Noordhoff, Gröningen, NL., 1933.

[127] A. Green and W. Zerna. *Theoretical elasticity.* Clarendon Press, Oxford, UK, 1954.

[128] P. Vannucci. A special planar orthotropic material. *Journal of Elasticity*, 67:81–96, 2002.

[129] P. Vannucci. On special anisotropy of paper. *Journal of Elasticity*, 99:75–83, 2010.

[130] P. Vannucci. Influence of invariant material parameters on the flexural optimal design of thin anisotropic laminates. *International Journal of Mechanical Sciences*, 51:192–203, 2009.

[131] N. Kandil and G. Verchery. New methods of design for stacking sequences of laminates. pages 243–257, Southampton, 1988. Proc. of CADCOMP88, - Computer Aided Design in Composite Materials.

[132] P. Vannucci and G. Verchery. Stiffness design of laminates using the polar method. *International Journal of Solids and Structures*, 38:9281–9294, 2001.

[133] P. Vannucci. A note on the elastic and geometric bounds for composite laminates. *Journal of Elasticity*, 2012 (In Press).

[134] S. W. Tsai and T. Hahn. *Introduction to composite materials.* Technomic, 1980.

[135] V. B. Hammer, M. P. Bendsoe, R. Lipton, and P. Pedersen. Parametrization in laminate design for optimal compliance. *International Journal of Solids and Structures*, 34:415–434, 1997.

[136] P. Vannucci and E. Valot. Some exact solutions for fully orthotropic laminates. *Composite Structures*, 69:157–166, 2005.

[137] R. T. Haftka and J. L. Walsh. Stacking sequence optimization for buckling of laminated plates by integer programming. *AIAA Journal*, 30:814–819, 1992.

[138] F.-X. Irisarri, D. H. Bassir, Carrere N., and J.-F. Maire. Multiobjective stacking sequence optimization for laminated composite structures. *Composites Science and Technology*, 69:983–990, 2009.

[139] T. A. Sebaey, C. S. Lopes, N. Blanco, and J. Costa. Ant colony optimization for dispersed laminated composite panels under biaxial loading. *Composite Structures*, 94:31–36, 2011.

[140] R. Butler and F.W. Williams. Optimum design using VICONOPT, a buckling and strength constraint program for prismatic assemblies of anisotropic plates. *Computers and Structures*, 43(4):699–708, 1992.

[141] J.F.M. Wiggenraad, P. Arendsen, and J.M. da Silva Pereira. Design optimisation of stiffened composite panels with buckling and damage tolerance constraints. *American Institute of Aeronautics and Astronautics, AIAA-98-1750*, pages 420–430, 1998.

[142] M. Montemurro, A. Vincenti, and P. Vannucci. A two-level procedure for the global optimum design of composite modular structures - application to the design of an aircraft wing. part 1: theoretical formulation. *Journal of Optimization Theory and Applications,*, 155(1):1–23, 2012.

[143] M. Montemurro, A. Vincenti, and P. Vannucci. A two-level procedure for the global optimum design of composite modular structures - application to the design of an aircraft wing. part 2: numerical aspects and examples. *Journal of Optimization Theory and Applications,*, 155(1):24–53, 2012.

[144] D. P. Raymer. *Aircraft Design: A Conceptual Approach*. AIAA Education Series, 2006.

[145] J. P. Foldager, J.S. Hansen, and N. Olhoff. A general approach forcing convexity of ply angle optimization in composite laminates. *Structural Optimization*, 16:201–211, 1998.

[146] P. Vannucci. A new general approach for optimising the performances of smart laminates. *Mechanics of Advanced Materials and Structures*, 18:558–568, 2011.

[147] J. L. Lagrange. Sur la figure des colonnes. *Miscellanea Taurinensia*, 1770.

[148] T. Clausen. About the shape of architectural columns. *Bull. Phys. Math. Acad. St. Petersbourg*, 9:279–294, 1851.

[149] N. V. Banichuk. *Problems and methods of optimal structural design*. Plenum Press, New York, 1983.

[150] Z. Gurdal, R. T. Haftka, and P. Hajela. *Design and optimization of laminated composite materials*. J. Wiley & Sons, New York, 1999.

[151] B. C. Nakra. Vibration control in machines and structures using viscoelastic damping. *Journal of Sound and Vibrations*, 211(3):449–465, 1998.

[152] R. Chandra, S. P. Singh, and K. Gupta. Damping studies in fiber-reinforced composites - a review. *Composite Structures*, 46:41–45, 1999.

[153] J. M. Berthelot, M. Assarar, Y. Sefrani, and A. E. Mahi. Damping analysis of composite material and structures. *Composite Structures*, 85:189–204, 2008.

[154] C. M. A. Vasques, R. A. S. Moreira, and J. Dias Rodrigues. Viscoelastic damping technologies - part I: modeling and finite element implementation. *Journal of Advanced Research in Mechanical Engineering*, 1:76–95, 2010.

[155] C. M. A. Vasques, R. A. S. Moreira, and J. Dias Rodrigues. Viscoelastic damping technologies - part II: experimental identification procedure and validation. *Journal of Advanced Research in Mechanical Engineering*, 1(2):96–110, 2010.

[156] J. M. Berthelot. Damping analysis of beams and plates using the ritz method. *Composite Structures*, 74:186–201, 2006.

[157] J. H. Yim, S. Y. Cho, Y. J. Seo, and B. Z. Jang. A study on material damping of 0° laminated composite sandwich cantilever beams with a viscoelastic layer. *Composite Structures*, 60:367–374, 2003.

[158] H. J. Wang and L. W. Chen. Vibration and damping analysis of annular plates with constrained damping layer treatments. *Journal of Sound and Vibrations*, 264:893–910, 2003.

[159] R. Rikards, A. Chate, and E. Barkanov. Finite element analysis of the damping vibrations of laminated composites. *Computers and Structures*, 47:1005–1015, 1993.

[160] J. A. Zapfe and G. A. Lesieutre. A discrete layer beam finite element for the dynamic analysis of composite sandwich beams with integral damping layers. *Computers and Structures*, 70:647–666, 1999.

[161] M. Yaman. Finite element vibration analysis of partially covered cantilever beam with concentrated tip mass. *Material & Design*, 27:243–250, 2006.

[162] S. H. Zhang and H. L. Chen. A study on the damping characteristics of laminated composites with integral viscoelastic layers. *Composite Structures*, 74:63–69, 2006.

[163] M. Ganapathi, B. P. Patel, P. Boisse, and O. Polit. Flexural loss factors of sandwich and laminated composite beams using linear and nonlinear dynamic analysis. *Composite Part B*, 30(3):245–256, 1999.

[164] K. D. Cho, J. H. Han, and I. Lee. Vibration and damping analysis of laminated plates with fully and partially covered damping layers. *Journal of Reinforced Plastics and Composites*, 19(15):1176–1200, 2000.

[165] R. F. Kristensen, K. L. Nielsen, and L. P. Mikkelsen. Numerical studies of shear damped composite beams using a constrained damping layer. *Composite structures*, 83:304–311, 2008.

[166] H. Kishi, M. Kuwata, S. Matsuda, A. Toshihiko, and M. Atsushi. Damping properties of thermoplastic-elastomer interleaved carbon fiber-reinforced epoxy composites. *Composites Science and Technology*, 64:2517–2523, 2004.

[167] M. Rao, R. Echempati, and S. Nadella. Dynamic analysis and damping of composite structures embedded with viscoelastic layers. *Composites part B*, 28:547–554, 1997.

[168] R. Lunden. Optimum distribution of damping for a vibrating beam. *Journal of Sound and Vibrations*, 66:25–37, 1979.

[169] A. K. Lall, B. C. Nakra, and N. T. Ansani. Optimum design of viscoelastically damped sandwich panels. *Engineering Optimisation*, 6:197–205, 1983.

[170] E. M. Krokosky. The ideal multifunctional constructional material. *Journal of the Structural Division, American Society of Civil Engineers*, 94:959–981, 1968.

[171] D. I. G. Jones. Temperature-frequency dependence of dynamic properties of damping materials. *Journal of Sound and Vibrations*, 33:451–470, 1974.

[172] Y. C. Chen and S. C. Huang. An optimal placement of cld treatment for vibration suppression of plates. *International Journal of Mechanical Sciences*, 44:1801–1821, 2002.

[173] A. K. Lall, B. C. Nakra, and N. T. Ansani. Optimisation of core material for a viscoelastically damped sandwich plate. pages 88–94, Institution of engineers, India, Chandigarh, 1985. Proceedings of the First National Convention on Design and Dynamics of Mechanical Systems.

[174] N. Le Maoût, E. Verron, and J. Bégué. Simultaneous geometrical and material optimal design of hybrid elastomer/composite sandwich plates. *Composite Structures*, 93:1153–1157, 2011.

[175] M. Montemurro, Y. Koutsawa, S. Belouettar, A. Vincenti, and P. Vannucci. Design of damping properties of hybrid laminates through a global optimisation strategy. *Composite Structures*, 94:3309–3320, 2012.

[176] E. E. Ungar and Jr. E. M. Kerwin. Loss factors of viscoelastic systems in terms of strain energy. *Journal of the Acoustic Society of America*, 34(2):954–962, 1962.

[177] The MathWorks, Inc., 3 Apple Ill Drive, Natick, MA 01760-2098. *Global Optimization Toolbox User's Guide*, September 2011.

[178] H. Zheng, C. Cai, and Tan X. M. Optimization of partial constrained layer damping treatment for vibrational energy minimization of vibrating beams. *Computers & Structures*, 82:2493–2507, 2004.

[179] N. Le Maoût, E. Verron, and J. Bégué. On the use of discontinuous elastomer patches to optimize the damping properties of composite sandwich plates. *Composite Structures*, 93:3057–3062, 2011.

List of Publications issued from this thesis

1. M. Montemurro, Y. Koutsawa, S. Belouettar, A. Vincenti & P. Vannucci: Design of damping properties of hybrid laminates through a global optimization strategy. *Composite Structures*, v. 94, pp. 3309-3320, 2012.
http://dx.doi.org/10.1016/j.compstruct.2012.05.003

2. M. Montemurro, H. Nasser, Y. Koutsawa, S. Belouettar, A. Vincenti & P. Vannucci: Identification of electromechanical properties of piezoelectric structures through evolutionary optimisation techniques. *International Journal of Solids and Structures*, v. 49, pp. 1884-1892, 2012.
http://dx.doi.org/10.1016/j.ijsolstr.2012.03.031

3. M. Montemurro, A. Vincenti & P. Vannucci: A two-level procedure for the global optimum design of composite modular structures - Application to the design of an aircraft wing. Part 1: theoretical formulation. *Journal of Optimization Theory and Applications*, v. 155 (1), pp. 1-23, 2012. Invited paper.
http://dx.doi.org/10.1007/s10957-012-0067-9

4. M. Montemurro, A. Vincenti & P. Vannucci: A two-level procedure for the global optimum design of composite modular structures - Application to the design of an aircraft wing. Part 2: numerical aspects and examples. *Journal of Optimization Theory and Applications*, v. 155 (1), pp. 24-53, 2012. Invited paper.
http://dx.doi.org/10.1007/s10957-012-0070-1

5. M. Montemurro, A. Vincenti & P. Vannucci: Design of elastic properties of laminates with minimum number of plies. *Mechanics of Composite Materials*, v. 48, pp. 369-390, 2012.
http://dx.doi.org/10.1007/s11029-012-9284-4

6. M. Montemurro, A. Vincenti & P. Vannucci: The Automatic Dynamic Penalisation method (ADP) for handling constraints with genetic algorithms. *Computer Methods*

in Applied Mechanics and Engineering, v. 256, pp. 70-87, 2013.
http://dx.doi.org/10.1016/j.cma.2012.12.009

7. M. Montemurro, A. Vincenti, Y. Koutsawa & P. Vannucci: A two-level procedure for the global optimisation of the damping behaviour of composite laminated plates with elastomer patches. *Journal of Vibration and Control*, (in press).